



**UNIVERSITY *of the*
WESTERN CAPE**

**RADIATION-INDUCED LEUKAEMIA IN SOUTH
AFRICA: RESPONSE OF LYMPHOCYTES AND CD34⁺
CELLS TO DIFFERENT RADIATION QUALITIES.**

MONIQUE ENGELBRECHT

2020

<http://etd.uwc.ac.za/>

**RADIATION-INDUCED LEUKAEMIA IN SOUTH AFRICA: RESPONSE OF
LYMPHOCYTES AND CD34⁺ CELLS TO DIFFERENT RADIATION QUALITIES.**

by

MONIQUE ENGELBRECHT

Submitted a thesis for the degree of

Doctor of Philosophy

in the
Department of Medical Bioscience, Faculty of Science

at the
University of the Western Cape

Bellville
UNIVERSITY of the
WESTERN CAPE
South Africa

Supervisor: Prof. M. de Kock

Co-supervisor: Dr C. Vandevoorde

Submitted: December 2020

DECLARATION

I, the undersigned, hereby declare that the work contained in this thesis titled **Radiation-induced leukaemia in South Africa: Response of lymphocytes and CD34⁺ cells to different radiation qualities** is my own work and has not previously been submitted for any degree or assessment at any university. All the sources that I have used or quoted have been indicated and acknowledged by means of complete references.



M. Engelbrecht



UNIVERSITY *of the* ^{Date}
WESTERN CAPE

ACKNOWLEDGEMENTS

Ek sal nooit weer sê: “Ek kan nie,” want “Ek is tot alles in staat deur Hom wat my krag gee.”

– Filip. 4:13

Eendag sal ek sê dat ek dit gedoen het! Vandag is daardie dag. Om 'n suksesvolle persoon te word of te word op die hoogste vlak van akademiese kwalifikasie, is nie 'n oornagproses nie. 'N Groot loopbaan, doel en geluk is die eindproduk van die voortdurende stryd, verwerping en mislukking in die PhD-lewe. Ja, 'n PhD is nie net 'n graad nie, dit is amper 'n lewe. Gedurende hierdie vier jaar het ek uiterste selfmotivering, fokus, selfvertroue, kalmte en entoesiasme teenoor die navorsingswerk vereis. Ek moes elke dag gebruik om te verbeter, beter te wees en my daaglikse of maandelikse doelwitte te bereik.

“Niks in die lewe moet gevrees word nie, dit moet net verstaan word. Dit is nou die tyd om meer te verstaan, sodat ons minder kan vrees.”

– Marie Curie

Eerstens wil ek my twee promotors, Prof de Kock en Dr Vandevoorde, opreg bedank. Dankie, Prof de Kock, vir die deurlopende ondersteuning en wyse leiding van my Honneursjaar tot Ph.D vlak. Dankie dat Prof altyd in my vermoëns en sterkpunte glo (selfs as daar selfvertroue ingesluit het). As dit nie vir Prof was nie, sou ek nooit my passie vir radiobiologie gevind het nie.

Dankie, Dr Vandevoorde, dat Dr my die geleentheid gebied het om deel te wees van hierdie ongelooflike unieke studie. As gevolg hiervan het my kennis in uiteenlopende wetenskaplike aspekte verdiep. Dr se kundige kennis hou my nooit op nie. Mag ek eendag dieselfde tipe leiding aan iemand kan gee.

Uit my hart wil ek baie dankie sê vir al die lede van die Radiation Biophysics-navorsingsgroep vir hul energie, begrip en hulp gedurende my projek, veral aan Mej Miles, Dr Ndimba en Dr Nair. Gedurende die afgelope jare het julle my vriende geword en ek is dankbaar daarvoor. Dr Ndimba, baie dankie vir jou leiding en al die hulp met die statistiese ontleding. Dankie vir jou waardevolle kommentaar en voorstelle tydens hierdie navorsing. Mej Miles, dankie vir al u ondersteuning en koffie/muffins episodes deur die koordbloedversameling. Ek sal altyd die herinneringe waardeer. Dr Nair, jou bereidwilligheid en die tyd wat jy opgeoffer het om my te help, is altyd baie waardeer. Dit was regtig 'n goeie tyd en ervaring in hierdie laboratorium.

Ek is dankbaar vir iThemba LABS dat hulle altyd my navorsing ondersteun en finansiering verskaf. Ek wil al my befonders, die Departement van Wetenskap en Innovasie (DSI), die Nasionale Navorsingstigting (NRF) van Suid-Afrika bedank in die loop van die Professionele Ontwikkelingsprogram (PDP) en die Internasionale Atoomenergie-agentskap (IAEA). In die afwesigheid van hierdie fondse sou hierdie navorsing nooit die lig gesien het nie.

'n Baie spesiale dank betuig aan al die deelnemers aan hierdie navorsing, veral die mediese personeel en donateurs in die Tygerberg- en Karl Bremer-hospitaal. Dankie dat julle altyd vriendelik was en my gehelp het om my monsters vir die dag te kry. Prof Botha en Dr Zwanepoel, julle ondersteuning en hulp word opreg waardeer. Ek hoop van harte dat hierdie werk sal bydra tot die kennis en begrip van die onderwerp wat deur bestraling veroorsaak word.

Aan al my familie en vriende: Al julle ondersteuning en aanmoediging het my aan die gang gehou deur die jare.

Aan my grootouers, Dirk en Annie Coetzee: Dankie oupa dat oupa so besorg is oor my navorsing. 'Hoe het dit vandag by die laboratorium gegaan?' 'Sal jy kan klaarmaak?' Dit is hierdie oënskynlik onbelangrike vrae oor my werk wat werklik vir my saak maak. Dankie vir ouma se ondersteuning, sowel as vir die omgee vir my studies en dat ouma altyd wil hê dat ek sukses behaal.

Aan my ouers, Eric en Madelein Engelbrecht: dankie vir AL die ondersteuning, motivering en voortdurende aanmoediging om nooit die handdoek in te gooi nie.

Aan my verloofde, die liefde van my lewe, my binnekort man, Gerhard Roberts: ek is onmeetbaar dankbaar vir jou en jou oneidige liefde. Jy het in my lewe ingestap en my perspektief op die lewe heeltemal verander. Woorde kan nie beskryf hoe gelukkig jy my maak nie. Baie dankie dat jy my geestelik ondersteun en emosionele ondersteuning gebied het deur die tyd. Ek is so geseënd om jou in my lewe te hê, jy het my altyd gedruk om my beste te doen en niks minder as uitnemendheid van my aanvaar nie. Ek is dankbaar dat God jou op my pad gestuur het en dat jy aan my sy was tydens die voltooiing van hierdie Ph.D. Jy is die een wat my gemotiveerd en positief gehou het. Ek het jou lief.

Laastens, dankie God dat U dit op my pad gestuur het en dat ek dit in u naam kon voltooi. Alle eer aan God!

"Met God is alles moontlik."

– Matteus 19:26

TRANSLATED TO ENGLISH

I can do all things because of Christ who strengthens me.

– Philippians. 4:13

One day I will say I did it! Today is that day. Being or becoming a successful person in the highest level of academic qualification is not an overnight process. A great career, purpose and happiness is the end product of facing the continues struggles, rejections, and failures in the PhD life. Yes, a PhD is not just a degree, it is almost a life. Throughout these four years, I required extreme self-motivation, focus, self-confidence, serenity and enthusiasm towards the research work. I had to use each day as an opportunity to improve, to be better and to achieve my daily or monthly goals.

“Nothing in life is to be feared, it is only to be understood. Now is the time to understand more, so that we may fear less.”

– Marie Curie

Firstly, I would like to express my sincere gratitude to my two supervisors, Prof de Kock and Dr Vandevoorde. Thank you, Prof de Kock, for the continuous support and wise guidance from my Honours year to Ph.D. Thank you for always believing in my capabilities and strengths (even when self-doubt crept in). If it wasn't for Prof, I would have never found my passion for radiobiology.

Thank you, Dr Vandevoorde, for providing me the opportunity to be a part of this incredibly unique study. As a result, my knowledge in diverse scientific aspects has deepened. Your expert knowledge never ceases to amaze me. May I be able to one day provide someone with the same type of guidance.

From the bottom of my heart I would like to say big thank you for all the Radiation Biophysics research group members for their energy, understanding and help throughout my project, especially to Ms Miles, Dr Ndimba and Dr Nair. Throughout the past years, you have become my friends and I am thankful for that. Dr Ndimba, an immense thank you for your guidance and all the assistance with the statistical analysis. Thank you for your valuable comments and suggestions during this research. Ms Miles, thank you for all your support and coffees/muffins episodes through the cord blood collections. I will always treasure the memories made. Dr Nair, your willingness and the time you sacrificed to help me was always greatly appreciated. It truly has been great time and experience in this lab.

I am grateful to iThemba LABS for always being supportive of my research and providing funding. I would like to thank all my funders, Department of Science and Innovation (DSI), the National Research Foundation (NRF) of South Africa under the Professional Development Programme (PDP) and the International Atomic Energy Agency (IAEA). In the absence of these funding's, this this research would never have seen the light of day.

A very special gratitude goes out to all the participants of this research, particularly the medical personnel and donors at Tygerberg and Karl Bremer Hospital. Thank you for always being friendly and assisting me to obtain my samples for the day. Prof Botha and Dr Zwanepoel, your support and assistance are highly appreciated. I sincerely hope that this work will add to the knowledge and understanding to the radiation-induced leukaemia topic.

To all my family and friends: All your support and encouragement kept me going.

To my grandparents, Dirk and Annie Coetzee: Thank you grandpa for being so concerned about my research. "How did it go at the lab today?" "Will you be able to finish?" It's these seemingly unimportant questions about my work that truly matters to me. Thank you for your support grandma, as well as for caring about my studies and for always wanting me to be better.

To my parents, Eric and Madelein Engelbrecht: Thank you for ALL of the support, motivation and constant encouragement to never throw in the towel.

To my fiancé, the love of my life, my soon to be husband, Gerhard Roberts: I am immeasurably grateful for you. You walked into my life and completely change my perspective on life. Words can't describe how happy how make me. Thank you for supporting spiritually and providing emotional support. I'm so very blessed to have you in my life, always pushed me to do my best and accepted nothing less than excellence from me. Forever grateful to God for sending you in my life and having you by my side while completing this Ph.D. You are the reason that kept me motivated and positive. I love you.

Lastly, thank you God for sending this on my path and that I was able to complete it in Your name. All glory to God!



“With God all things are possible.”

– Matthew 19:26

UNIVERSITY *of the*
WESTERN CAPE

DEDICATION

I dedicate my dissertation work to my family and friends – with their encouragement, affection and love is what made me able to achieve success.

“It always seems impossible until it is done.”

– Nelson Mandela

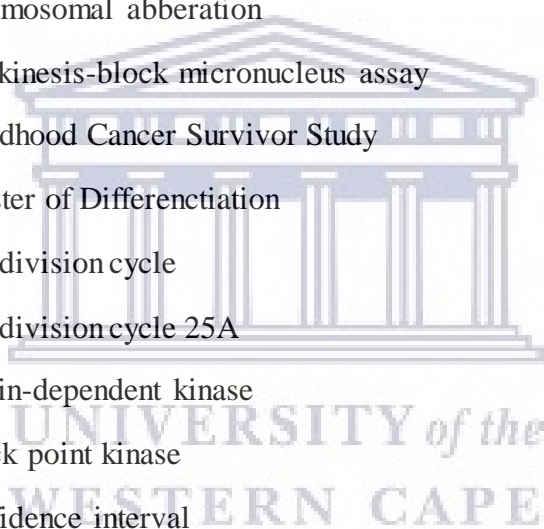


UNIVERSITY *of the*
WESTERN CAPE

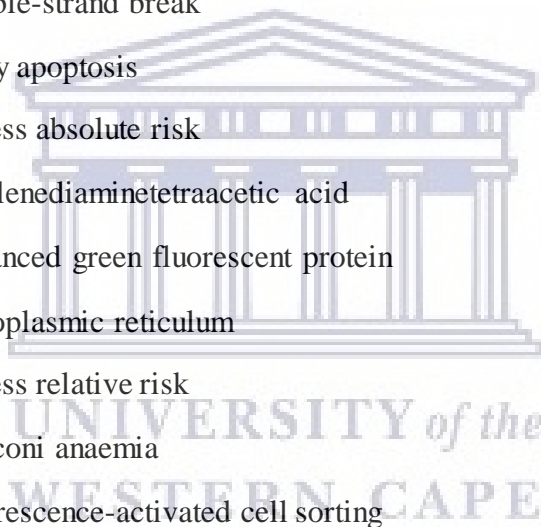
ABBREVIATIONS

α	alpha
β	beta
γ	gamma
^{60}Co γ -rays	cobalt gamma-rays
H \cdot	hydrogen radical
OH \cdot	hydroxyl radical
γ -H2AX	phosphorylated H2AX
%	percentage
$^{\circ}\text{C}$	degree Celsius
A-bomb	atomic bomb
AGM	aorta-gonad-mesonephros
AL	acute leukaemia
ALL	acute lymphoid leukaemia
AML	acute myeloid leukaemia
ANDANTE	multidisciplinary evaluation of the cancer risk from neutrons relative to photons using stem cells and the induction of second malignant neoplasms following paediatric radiation therapy
ANOVA	analysis of variance
AO	acridine orange
APAF1	apoptotic protease activating factor 1
APB	adult peripheral blood
APC	antigen-presenting cell
ATM	ataxia telangiectasia mutated
ATR	Ataxia telangiectasia and Rad3-related
Bak	Bcl-2 homologous antagonist killer

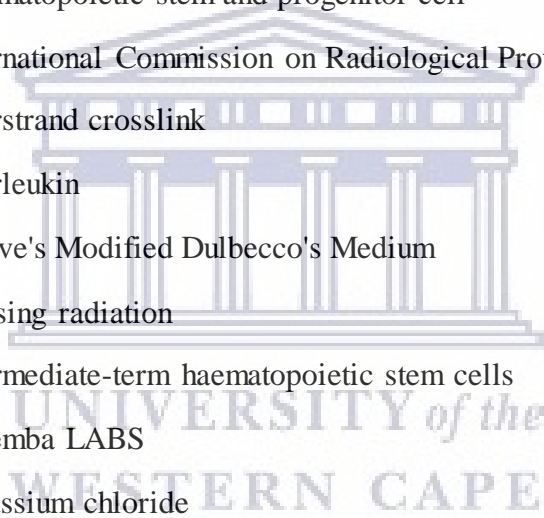
Bax	Bcl-2-associated X
Bcl-2	B-cell CLL/lymphoma 2
Be	Beryllium
BER	Base-Excision Repair
BM	bone marrow
B/M	breaks per metaphase
BMREC	Biomedical Research Ethics Committee
BN	binucleated
BSA	bovine serum albumin
c	complete
CA	chromosomal abberation
CBMN	cytokinesis-block micronucleus assay
CCSS	Childhood Cancer Survivor Study
CD	Cluster of Differentiation
Cdc	cell division cycle
Cdc25A	cell division cycle 25A
CDK	cyclin-dependent kinase
Chk	check point kinase
CI	confidence interval
CL	chronic leukaemia
CLL	chronic lymphoblastic leukaemia
CLP	common lymphoid progenitor
CML	chronic myeloid leukaemia
CMP	common myeloid progenitor
CO ₂	carbon dioxide
CPDA-1	citrate phosphate dextrose adenine-1
CSF	colony-stimulating factors
CT	computed tomography
Cyto-B	cytochalasin B



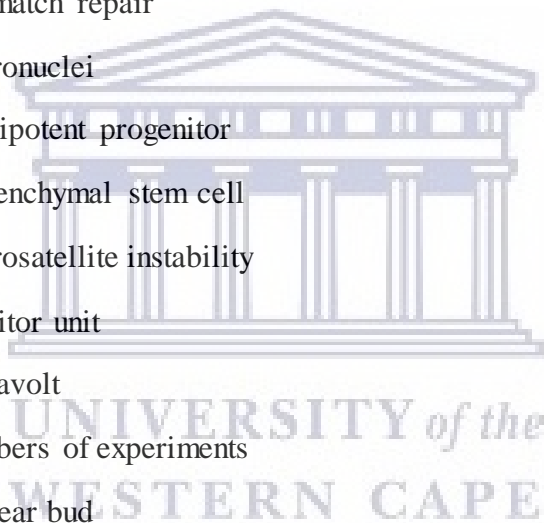
DAPI	4',6-Diamidino-2-phenylindole dihydrochloride
DC	dicentric cell
DD	death domain
DDR	DNA damage response
DDREF	dose and dose-rate effectiveness factor
DISC	death inducing signal complex
DMSO	dimethyl sulfoxide
DNA	deoxyribonucleic acid
DP	double positive
DR	death receptor
DSB	double-strand break
EA	early apoptosis
EAR	excess absolute risk
EDTA	ethylenediaminetetraacetic acid
EGFP	enhanced green fluorescent protein
ER	endoplasmic reticulum
ERR	excess relative risk
FA	Fanconi anaemia
FACS	fluorescence-activated cell sorting
FACT	Foundation for the Accreditation of Cellular Therapy
FADD	Fas-associated death domain
FBS	foetal bovine serum
Fe	iron
FITC	Fluorescein Isothiocyanate
Flt-3	Fms-like tyrosine kinase receptor
FSC-A	forward scatter-area
FSC	forward scatter
GeV	gigaelectronvolt
GG-NER	global genome nucleotide excision repair



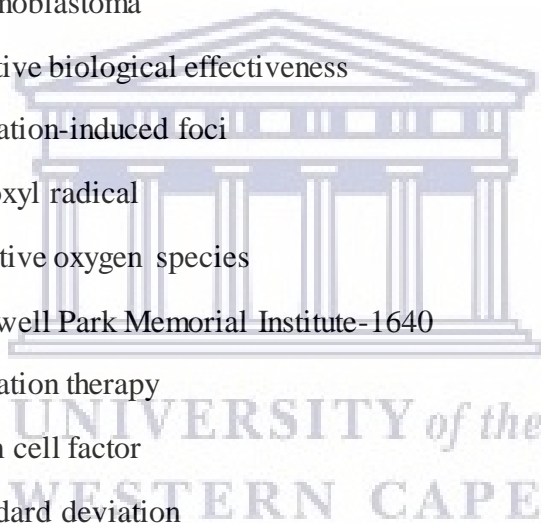
GMP	granulocyte/macrophage progenitor
Gy	Gray
h	hour(s)
H2A	Histone 2A
H2AX	Histone subtype H2A isoform X
HCl	hydrochloric acid
HDAC	Histone Deacetylase
HIV	Human immunodeficiency virus
HR	Homologous recombination
HSC	Haematopoietic stem cells
HSPC	Haematopoietic stem and progenitor cell
ICRP	International Commission on Radiological Protection
ICL	interstrand crosslink
IL	Interleukin
IMDM	Iscove's Modified Dulbecco's Medium
IR	Ionising radiation
IT-HSC	intermediate-term haematopoietic stem cells
iTL	iThemba LABS
KCl	Potassium chloride
keV	kiloelectron volts
keV/μm	kiloelectron volts/micrometer
kV	kilovoltage
kVp	peak kilovoltage
LA	late apoptosis
LAR	lifetime attributable risk
LET	linear energy transfer
LMIC	low- and middle-income
LSC	leukaemia stem cell
LSS	Life Span Study



LT-HSC	Long-term haematopoietic stem cells
mAb	monoclonal antibodies
MACS	magnetic-activated cell sorting
MEP	megakaryocyte/erythrocyte progenitor
MeV	megaelectron volt
mGy	milligray
MHC	major histocompatibility complex
min	minutes
mL	millilitre
MMC	mitomycin C
MMR	mismatch repair
MN	micronuclei
MPP	multipotent progenitor
MSC	mesenchymal stem cell
MSI	microsatellite instability
MU	monitor unit
MV	megavolt
n	numbers of experiments
NBUB	nuclear bud
NDI	nuclear division index
NER	nucleotide excision repair
NHEJ	non-homologous end joining
NK	natural killer
NMISA	National Metrology Institute of South Africa
NPB	nucleoplasmic bridge
OER	oxygen enhancement ratio
p53	tumour protein p53
PB	peripheral blood
PBL	peripheral blood lymphocytes



PBMC	peripheral blood mononuclear cell
PBT	proton beam therapy
PCD	programmed cell death
PCNA	proliferating cell nuclear antigen
Pen-Strep	penicillin-streptomycin
PFA	paraformaldehyde
PHA	phytohaemagglutinin
PI	propidium iodide
PS	phosphatidylserine
PUMA	p53-upregulated modulator of apoptosis
Rb	Retinoblastoma
RBE	relative biological effectiveness
RIF	radiation-induced foci
RO ₂	peroxyl radical
ROS	reactive oxygen species
RPMI-1640	Roswell Park Memorial Institute-1640
RT	radiation therapy
SCF	stem cell factor
SD	standard deviation
SEM	standard error of the mean
SP	single positive
SSA	single-strand annealing
SSB	single-strand break
SSC-A	side scatter-area
SSC	side scatter
SSC	Separated Sector Cyclotron
SSD	source to surface distance
ST-HSC	short-term haematopoietic stem cell
TC-NER	transcription-coupled nucleotide excision repair



TCR	T-cell receptor
TPO	thrombopoietin
UCB	umbilical cord blood
UNSCEAR	United Nations Scientific Committee on the Effects of Atomic Radiation
UV	ultraviolet
VPA	Valproic acid
WHO	World Health Organisation
w _R	radiation weighting factor



ABSTRACT

Epidemiological studies have highlighted that leukaemia can be considered as the most prominent malignancy after radiation exposure during childhood. The lifetime risk on radiation-induced leukaemia for a given dose is 3 – 5 times higher for children compared to adults. The high risk at a young age is related to the elevated sensitivity of the red bone marrow where haematopoietic stem and progenitor cells (HSPCs) are located. HSPCs self-renewal capacity and long-life span increase their susceptibility to DNA damage accumulation, making them a major target of radiation-induced carcinogenesis. Proton beam therapy (PBT) is increasingly used to treat paediatric brain tumours due to its dose sparing properties compared to conventional X-ray based radiotherapy. However, concerns regarding the carcinogenic potential of secondary neutrons produced during PBT, especially in terms of their effect on HSPCs harboured in the cranial bone marrow of paediatric patients, remain. In this study, the radiobiological differences between ^{60}Co γ -rays and p(66)/Be(40) neutron exposure was investigated to resolve the underlying mechanisms for the high radiosensitivity of HSPCs (CD34⁺ cells) isolated from umbilical cord blood (UCB). For both radiation qualities, an apparent dose-dependent increase in the frequency of radiation-induced MN was observed in CD34⁺ cells. Furthermore, increased cytogenetic damage was observed with the CBMN assay after neutron irradiation, which highlights its leukaemogenic potential. In addition, no difference was observed in the nuclear division index of the CD34⁺ cells post-irradiation between both radiation qualities. The number of DNA DSBs was assessed by microscopic scoring of γ -H2AX foci, 2 and 18 hours after radiation exposure. A significant higher number of DNA DSBs were observed 2 hours after neutron irradiation with 0.5 Gy, but decreased to similar levels for both radiation qualities after 18 hours. Different stages of apoptosis in CD34⁺ cells were studied at 18 and 42 hours numerous time points post-irradiation by flow cytometry using the Annexin/PI assay. In contrast to the γ -H2AX foci results, a significant difference in late apoptosis was observed at 18 hours and 42 hours between the two radiation qualities. The results point towards a fast error-prone DNA repair in HSPCs after neutron irradiation, which might contribute to genomic instability and leukemogenesis.

In the second phase of the PhD project, the impact of age on radiosensitivity was investigated by comparing newborn T-lymphocytes with adult peripheral blood (APB) T-lymphocytes. The major difference between UCB and APB T-lymphocytes, is their immunophenotypic profile. Since it is known that different T-lymphocyte subsets have a difference in radiosensitivity, the fraction of CD4⁺, CD8⁺, naïve (CD45RA⁺) and memory (CD45RO⁺) T-lymphocytes was determined via flow cytometry in the two groups. The cytokinesis-block micronucleus (CBMN) assay was used to determine the extent to which age influences the frequency of cytogenic damage in response to ⁶⁰Co γ -rays radiation. For both APB and UCB, an outspoken dose-dependent increase in the frequency of radiation-induced MN was observed at 0.5, 1, 3 and 4 Gy. However, no significant difference was observed at 4 Gy when comparing MN yields of APB and UCB. An increased radiosensitivity of newborn to adult donors of 34%, 42%, 29%, 26% and 16% was observed based on the MN scoring at doses of 0.5, 1, 2, 3 and 4 Gy, respectively. The lowest radiosensitivity was identified at the highest dose, which might explain the non-significant difference at 4 Gy. In addition, there was a clear trend that females were more sensitive to ⁶⁰Co γ -rays radiation than males in both adults and newborns, even though the difference was not significant. The immunophenotypic study revealed that both the CD4⁺ and CD8⁺ T-lymphocytes of newborns are mainly naïve. This is illustrated by the co-expression of CD45RA⁺ on 90.70% (range: 80.80% – 98.40%) and 95.90% (range: 89.60% – 98.80%) of CD4⁺ and CD8⁺ cells respectively. The composition of adult T-lymphocytes, in contrast, is clearly different with a more equal distribution between CD45RA⁺ and CD45RO⁺ subpopulations. This finding demonstrates that there are differences in the radiosensitivity between newborn and adult T-lymphocytes which might be linked to the immunophenotypic change of T-lymphocytes with age.

TABLE OF CONTENTS

DECLARATION	i
ACKNOWLEDGEMENTS	ii
DEDICATION	viii
ABBREVIATIONS	ix
ABSTRACT	xvi
TABLE OF CONTENTS	xviii
CHAPTER 1: LITERATURE REVIEW.....	1
1.1 Introduction.....	2
1.2 Radiation.....	7
1.2.1 Ionising Radiation (IR).....	7
1.2.2 Linear Energy Transfer (LET)	8
1.2.3 Direct and Indirect Action of Ionising Radiation on DNA	9
1.2.4 Types of Radiation-Induced DNA Damage	11
1.3 DNA Damage Response (DDR).....	14
1.3.1 Cell Cycle Arrest.....	15
1.3.2 DNA Repair.....	17
1.3.2.1 BER and NER.....	18
1.3.2.2 MMR	18
1.3.2.3 HR and NHEJ	19
1.3.2.4 Direct Chemical Reversal and ICL.....	19
1.3.3 Cell Death.....	20
1.4 Haematopoiesis	24
1.4.1 Haematopoietic Stem and Progenitor Cells (HSPCs)	24
1.4.1.1 Cell Surface Markers	26
1.4.2 T-lymphocyte Maturation and Cell Surface Markers.....	28
1.5 Quiescence	30
1.6 Leukaemia.....	31
1.6.1 Origin.....	31

1.6.2 Types of Leukaemia	32
1.7 Radiation-Sensitivity of HSPCs.....	33
1.8 Radiation-Sensitivity of T-lymphocytes	34
1.9 Biomarkers for Cellular Radiosensitivity	35
1.9.1 Cytokinesis-Block Micronucleus (CBMN) Assay	35
1.9.2 γ -H2AX Foci Assay	38
1.9.3 Apoptosis.....	39
1.10 Aims and Objectives of the Study.....	40
1.10.1 Radiation Sensitivity of Human CD34 ⁺ Cells in Response to Clinical Therapy Beams: DNA Repair and Mutagenic Effects	40
1.10.2 Age Dependence in Radiation Sensitivity	42
CHAPTER 2: MATERIALS AND METHODS	43
2.1 General Information.....	44
2.2 Collection of Peripheral Blood Mononuclear Cells (PBMCs) and CD34 ⁺ Cells	44
2.2.1 Collection of Umbilical Cord Blood (UCB)	44
2.2.2 Collection of Adult Peripheral Blood (APB)	45
2.3 Isolation of PBMCs and CD34 ⁺ Cells.....	45
2.3.1 Histopaque Isolation of PBMCs	45
2.3.2 Isolation of CD34 ⁺ Cells by Magnetic-Activated Cell Sorting (MACS)	46
2.3.3 Purity Control of CD34 ⁺ Isolation Using by Flow Cytometry	47
2.4 Storage of PBMCs and CD34 ⁺ cells.....	48
2.4.1 Freezing Process.....	48
2.4.2 Thawing of CD34 ⁺ cells	48
2.5 Immunophenotyping of Adult and Newborn PBMCs	49
2.6 <i>In vitro</i> Irradiation Experimental Set-up.....	49
2.6.1 Cobalt-60 (⁶⁰ Co) gamma (γ)-ray Irradiation.....	49
2.6.2 Fast p(66)/Be(40) Neutron Irradiations	51
2.7 Semi-automated Cytokinesis Block Micronucleus (CBMN) Assay	52
2.7.1 Cell Cultures: Adult vs Newborn PBMCs	52
2.7.2 Fixation and Semi-Automated Analysis of Adult and Newborn CBMN Assay	53
2.8 Manual Cytokinesis Block Micronucleus (CBMN) Assay for CD34 ⁺ Microcultures.....	54
2.8.1 Cell Cultures: CD34 ⁺ Cells	54
2.8.2 Nuclear Division Index (NDI).....	55
2.9 γ -H2AX Foci Assay	55
2.9.1 Cell Cultures.....	55

2.9.2 Immunocytochemistry	56
2.9.3 Automated Slide Scanning and Detection of Foci	56
2.10 Apoptosis Assay	57
2.10.1 Cell Cultures	57
2.10.2 Annexin V staining and Analysis by Flow Cytometry.....	57
2.11 Statistical Analysis	57
CHAPTER 3: RESULTS SECTION 1.....	59
3.1 DNA Damage Response of CD34 ⁺ Cells to High-LET Neutron Irradiation.....	60
3.1.1 Radiation-Induced Chromosomal Damage in CD34 ⁺ Cells.....	60
3.1.2 DNA Double-Strand Breaks (DSBs) Formation and Repair After ⁶⁰ Co-γ-rays and Neutron Irradiation	67
3.1.3 Radiation-Induced Apoptosis in CD34 ⁺ Cells.....	69
CHAPTER 3: RESULTS SECTION 2.....	78
3.2 Differences in Radiosensitivity Between Newborns and Adults	79
3.2.1 Radiation-Induced Chromosomal Damage in T-lymphocytes: APB versus UCB.....	79
3.2.2 Expression of CD45RA and CD45RO on CD4 and CD8 T-lymphocytes Subsets in UCB and APB Samples	82
CHAPTER 4: DISCUSSION	91
4.1 Radiosensitivity of CD34 ⁺ to High-LET Neutron Irradiation.....	92
4.1.1 Proton Beam Therapy (PBT) and Secondary Neutron Production	92
4.1.2 Formation and Repair of DNA DSBs in CD34 ⁺ Cells	94
4.1.3 Radiation-Induced Apoptosis in CD34 ⁺ Cells.....	97
4.1.4 Effect of Radiation Quality on the Cytogenetic Damage in CD34 ⁺ Cells	101
4.2 Age Dependence in Radiation Sensitivity	105
4.2.1 Age-dependent Variances in Radiosensitivity	105
4.2.2 Differences in Immunophenotypic Profile of Newborns and Adult T-lymphocytes	108
CONCLUSIONS	113
FUTURE PERSPECTIVES	114
REFERENCES	116
APPENDICES	150

CHAPTER 1: LITERATURE REVIEW



UNIVERSITY *of the*
WESTERN CAPE

“Science knows no country, because knowledge belongs to humanity, and is the torch which
illuminates the world.”

– Louis Pasteur

1.1 Introduction

The occurrence of childhood cancer is rare, representing 1 – 10% of all cancers reported globally (Stones *et al.*, 2014; Bray *et al.*, 2018). According to 2020 estimates, globally, 11,050 children (aged 0 – 14 years) and 5,800 adolescents (aged 15 – 19 years) will be diagnosed with cancer, and 1,190 and 540, respectively, will die from the disease (Siegel, Miller and Jemal, 2020). In developed countries, advanced treatment modalities and better healthcare systems mean that more than 80% of childhood cancer cases will be cured; however, in poorer nations, the curative rate for childhood cancers is limited to 10 – 20% (Howard *et al.*, 2018). The incidence of most childhood cancers (~60%) occur in low- and middle-income (LMIC) countries, mainly because they have younger populations and therefore a larger proportion of children with cancer (Magrath *et al.*, 2013). Therefore, the incidence rates for several childhood cancers, are higher in Africa than those in high-income countries (Stefan *et al.*, 2017). Due to poverty and a limited access to healthcare providers and therapy, the survival rates are poor in LMIC (Stones *et al.*, 2014; Gupta *et al.*, 2015; Erdmann *et al.*, 2019). In response to the vast disparity in healthcare, the World Health Organisation (WHO) launched the Global Initiative for Childhood Cancer in 2018, which aims to achieve at least a worldwide 60% survival rate for all children diagnosed with cancer by 2030 ('WHO | Global Initiative for Childhood Cancer', 2018; Atun *et al.*, 2020). Accordingly, there is a renewed sense of urgency, particularly in developing countries to prioritise the successful diagnosis and treatment of all childhood cancers.

The use of ionising radiation (IR) became indispensable in current medical practice for diagnosis and therapy (Pereira, Traughber and Muzic, 2014; Jaffray and Gospodarowicz, 2015). Radiation therapy (RT) is one example of the use of IR in modern medicine, which forms an integral part of the fight against cancer, either as a stand-alone treatment or as an addition to surgery and/or chemotherapy (Marcu, 2017). The main goal of RT is to deliver a sufficiently high dose to kill the tumour cells without damaging the surrounding healthy tissue and organs. Worldwide, about 3.6 billion medical procedures involving IR are performed each year, which is leading to significant increases in human exposure to IR (Applegate, 2015).

Unfortunately IR is also recognised as one of the most powerful clastogenic and carcinogenic agents (Mortezaee *et al.*, 2019), especially for children who are considerably more sensitive compared to adults with regards to radiation-induced malignancies (Miri-Hakimabad, Rafat-Motavalli and Akhlaghi, 2014; Kutanzi *et al.*, 2016; Antonio *et al.*, 2017). In the literature,

there are several reasons that are commonly advanced to explain the apparent increased radiosensitivity of children. Foremost amongst these, the organs and tissues of children are in an active phase of growth and development. This means that there is a higher proportion of rapidly dividing cells and stem cells within a child, in comparison to an adult, making them more sensitive to IR (Sadetzki and Mandelzweig, 2009). Secondly, children have a longer life expectancy resulting in a larger window of probability to express the radiation-induced oncogenic effects later in life (Frush, 2013; Hernanz-Schulman, 2017). It is commonly postulated that radiosensitivity varies with age – the younger the patient, the higher the radiosensitivity and the risk to develop radiation-induced malignancies (Schuster *et al.*, 2018). Additionally, because of the smaller body dimensions and age-related differences the radiation dose experienced by children can be up to 50% higher than the equivalent exposure scenario in adults (Chodick *et al.*, 2009; Almohiy, 2014). Thus, the radiation risk is greater for children and adolescents than for adults when an equal radiation dose is given. In comparison with adults, only tissues subject to high levels of cell turnover throughout the individual's life are still exposed to greater risk (Alzen and Benz-Bohm, 2011).

Radiosensitivity refers to the relative susceptibility of cells, tissues, organs and organisms to the harmful effects of IR (Britel *et al.*, 2018). In humans, IR exposure is known to cause a range of biological responses which may include mutagenesis, carcinogenesis and cell death (Sokolov and Neumann, 2012). These responses may be further classified as either stochastic or deterministic effects (Mettler, 2012). Stochastic effects, such as cancer development, are related to exposure to low doses of IR (below 100 mGy), but will also be induced at higher doses. The risk is linear from low dose to high dose (linear non-threshold hypothesis), whilst deterministic effects will only appear after a certain threshold dose (Mettler, 2012; Hamada and Fujimichi, 2014). It is noted that a range of different factors play a role in the biological consequences of human IR exposure. The most important factors include the radiation dose, radiation quality, dose rate, and protracted exposure; as well as factors related to the individual, such as age, gender, health status and genetic predisposition (Mettler, 2012; Frush, 2013). In regard to the radiosensitivity of children, a number of epidemiological studies confirm the notion that children tend to be more susceptible to radiation-induced cancer in comparison to adults (Kutanzi *et al.*, 2016; Ideguchi *et al.*, 2018; Seibold *et al.*, 2020).

The first case of radiation induced cancer was reported in 1902, which manifested as ulcerations in the skin of the exposed individual. By 1911, there were reports of leukaemia arising in radiation workers (Shah, Sachs and Wilson, 2012). Indeed, Marie Curie and her daughter Irene were both thought to have died of radiation-induced leukaemia. Since that time, many experimental and epidemiological studies have confirmed the oncogenic effects of radiation in tissues of many species (Little, 2003).

Later, the Life Span Study (LSS) cohort of the Japanese atomic bomb survivors was used to make epidemiological assessments of radiation-induced cancer risks (Shah, Sachs and Wilson, 2012; Ozasa, 2016). Radiation-induced secondary cancer risks are commonly expressed in terms of the following risk models: lifetime attributable risk (LAR), excess relative risk (ERR) or excess absolute risk (EAR) (Nguyen, Moteabbed and Paganetti, 2015; Tamura *et al.*, 2017). These risk models signify an increase in cancer mortality compared to unexposed individuals. Both ERR and EAR decrease with increasing age at exposure. However, the ERR decreases with attained age, while the EAR will increase, which is attributable to an overall increase in the background rate of cancer with aging (Ozasa, 2016). The information on the late health effects in the atomic bomb survivors can be found in epidemiological studies on three main cohorts (Ozasa, 2016): a cohort of atomic bomb survivors (LSS) (120 000), survivors exposed *in utero* (3 600) and children of atomic bomb survivors (F1) (76 800). In the untimely stage after the bombings, the leukaemia incidence among the survivors did increase, especially among the children. Based on these studies, the relative risk was ~70 times higher amongst children exposed at the age of 10, and swiftly declined with exposure at older ages. Based on the observation of the general population of Hiroshima and Nagasaki before the establishment of the LSS (Folley, Borges and Yamawaki, 1952), it became clear that the leukaemia risk increased noticeably about 2 years after the bombings and peaked at about 6 to 8 years after the bombings, especially among those exposed at young ages. The risk decreased rapidly, but remains slightly elevated almost 50 years after the exposure (Ozasa *et al.*, 2019). The increased risk of radiation-induced solid cancers manifested around 10 years subsequent to the bombings and are still present today (Ozasa, 2016; Ozasa *et al.*, 2019). The results were separately updated for solid cancers (Preston *et al.*, 2007; Grant *et al.*, 2017) and haematopoietic malignancies (Hsu *et al.*, 2013). In general, the ERR for all radiation-induced cancers was higher in those exposed at young ages (Ozasa *et al.*, 2019). [Figure 1.1](#) shows also a clear gender difference, especially at early ages, which indicates that females are more radiosensitive than

males (International Commission on Radiological Protection, 1991; Hall, 2006; Nahangi and Chaparian, 2015).

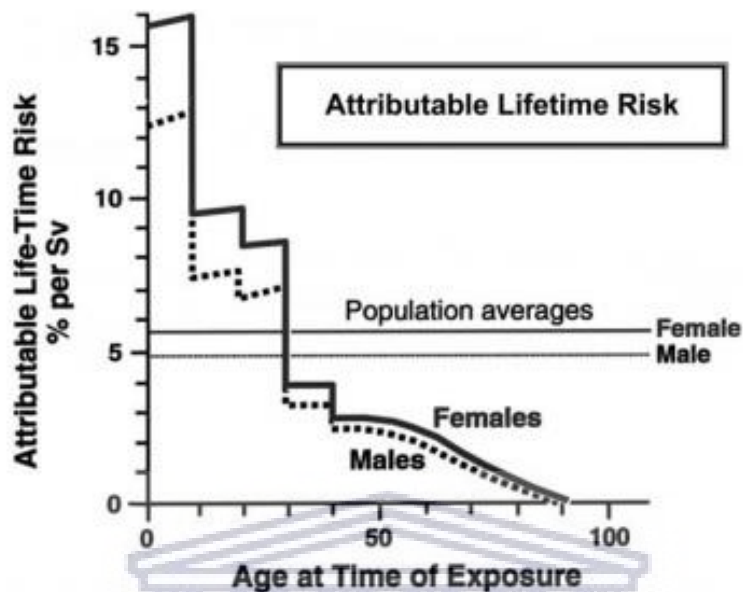


Figure 1.1. The attributable lifetime risk from a single small dose of radiation at various ages at the time of exposure. This figure represents a dramatic decrease in radiosensitivity with age. The higher risk for the younger age groups is not expressed until late in life. These estimates are based on a multiplicative model and on a dose and dose-rate effectiveness factor (DDREF) of 2 (Hall, 2006). This figure is adapted from the International Commission on Radiological Protection (ICRP) Publication 60, 1991).

In the United Nations Scientific Committee on the Effects of Atomic Radiation (UNSCEAR) 2006 Report, the committee announced that lifetime cancer risk estimates for those exposed during childhood might be a factor of 2–3 times higher than estimates for a population exposed at all ages. This verdict was based upon a lifetime projection model combining all tumour types (UNSCEAR, 2006). In the UNSCEAR 2013 report, the committee reviewed 23 different cancer types and reported the following scientific findings (UNSCEAR, 2013):

- For about 25% of cancer types, such as leukaemia and thyroid, skin, breast and brain cancer, children were clearly more radiosensitive.
- For about 15% of cancer types (e.g. colon cancer), children appear to have about the same radiosensitivity as adults.
- For about 10% of cancer types (e.g. lung cancer) children appear less sensitive to external radiation exposure than adults.

- For about 20% of cancer types (e.g. oesophagus cancer), there is insufficient evidence to make a conclusion as to any differences in risk with age at exposure.
- Finally, for about 30% of cancer types (e.g. Hodgkin's disease and prostate, rectum and uterus cancer), there is a weak relationship or none at all between radiation exposure and risk at any age of exposure.

To date, there is a lack of comprehensive epidemiological reports specifically addressing aspects of radiation exposure of children, the health effects and associated cancer risks. The commonly held belief that children might be 2 – 3 times more susceptible to radiation exposure than adults are true for certain types of cancer, but definitely not for all. Therefore, the UNSCEAR Committee is reluctant to accept an overall generalisation of the risks involved in childhood radiation exposure. The vulnerability of children after being exposed to IR has been a particular focal point, with a specific emphasis on radiation-induced leukaemia as a consequence of accidental or medical exposures, such as paediatric computed tomography (CT) scans. Numerous studies have linked the exposure from low-dose X-rays in CT scanning during childhood with the development of brain tumours and leukaemia (Brenner *et al.*, 2003; Wakeford, 2013; Meulepas *et al.*, 2014; Applegate, 2015). A study conducted by Pearce *et al.* showed that the risk of leukaemia was positively associated with estimated doses delivered by CT scans to the red bone marrow (BM) ($p = 0.0097$), as was the risk of brain tumours associated with estimated doses delivered by CT scans to the brain tissue ($p < 0.0001$) (Pearce *et al.*, 2012) (see [Figure 1.2](#)). The recently reported findings from studies of the influence of paediatric CT scans upon childhood leukaemia risk provide further evidence that low-level exposure to radiation at young age increases the risk of leukaemia. Although CT scans are very useful clinically, the potential long-term cancer risks associated with the IR exposure require proper justification of the scan, in particular for children.

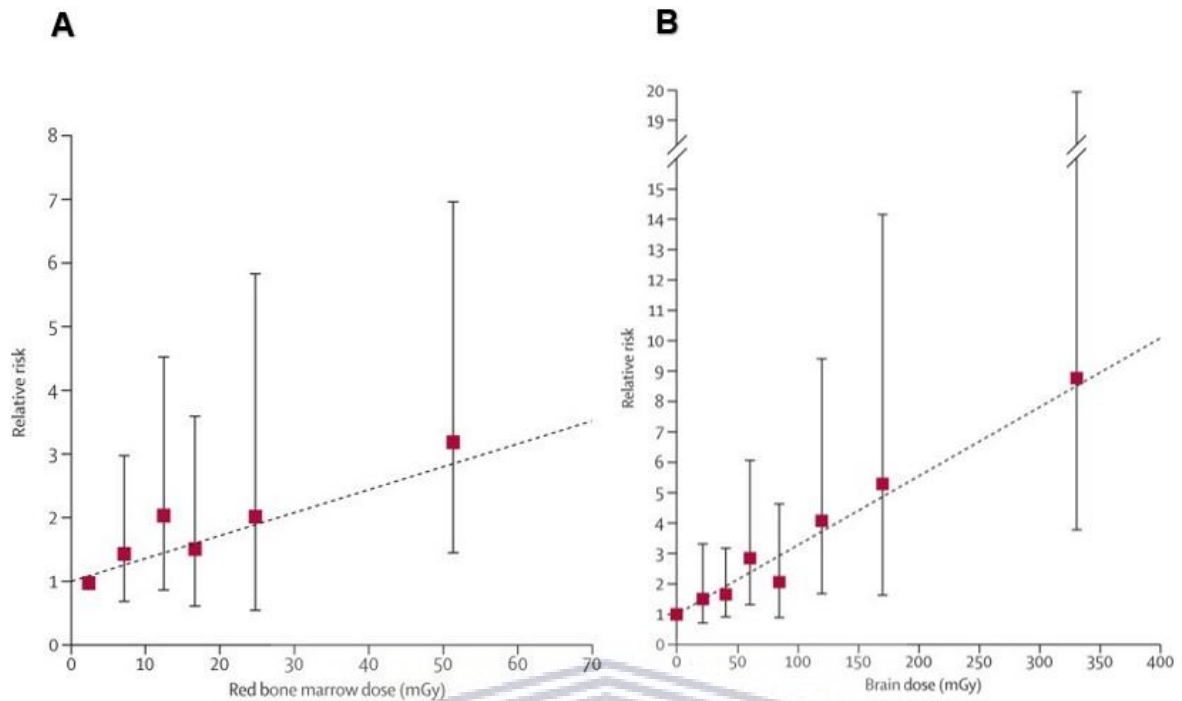
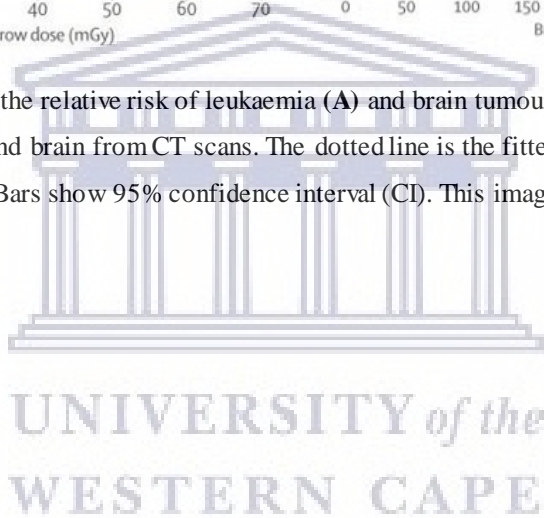


Figure 1.2. These graphs show the relative risk of leukaemia (A) and brain tumours (B) in relation to estimated radiation doses to the red BM and brain from CT scans. The dotted line is the fitted linear dose-response model (excess relative risk per mGy). Bars show 95% confidence interval (CI). This image was adapted from Pearce *et al.*, 2012.



1.2 Radiation

1.2.1 Ionising Radiation (IR)

Radiation is energy produced by matter in the form of rays or high-speed particles. IR can be categorised into electromagnetic and particle radiation with sufficient energy to eject orbital electrons from the atoms and molecules they traverse, resulting in ionisations. Electromagnetic radiations include both X-rays and γ -rays, have neither mass nor charge and are considered as waves or discrete quanta of electromagnetic energy, called photons (Hall and Giaccia, 2006). Electromagnetic radiation is the most commonly used type of IR in experimental studies and in many clinical applications (Azeemi and Raza, 2005). Particle radiation is comprised of other types of radiation like protons, α -particles, heavy charged ions, and neutrons (Figure 1.3) (De Sanctis *et al.*, 2016).

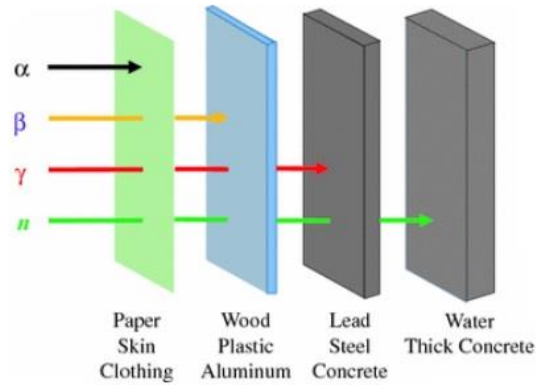


Figure 1.3. The ability of different types of radiation to pass through material is shown (De Sanctis *et al.*, 2016).

1.2.2 Linear Energy Transfer (LET)

The linear energy transfer (LET) is a physical quantity used to portray the quality of the radiation (Pradhan, 2011). The LET is defined as the average energy deposited along the track of a particle per unit length, expressed in keV/ μm . The pattern of DNA damage caused by a particle track is directly correlated to the LET and path structure of the particle beam (Nikitaki *et al.*, 2016). There are two groups of LET radiation based on their mechanism of action and biological effects, i.e. low and high-LET radiation. Low-LET radiation is sparsely ionising and results in the formation of mainly simple DNA lesions (Figure 1.4, left-side). While, clustered/complex damage is induced by high-LET radiation due to its higher ionisation density (Figure 1.4, right-side) (Bailey, 2018; Jezkova *et al.*, 2018; Hagiwara *et al.*, 2019). In other words, DNA lesions produced by high-LET radiation will be more difficult to repair, and consequently more detrimental to the cell (Fredericia, 2017). Examples of low-LET are high-energy protons, X- and γ -rays while neutrons and α -particles are examples of high-LET.

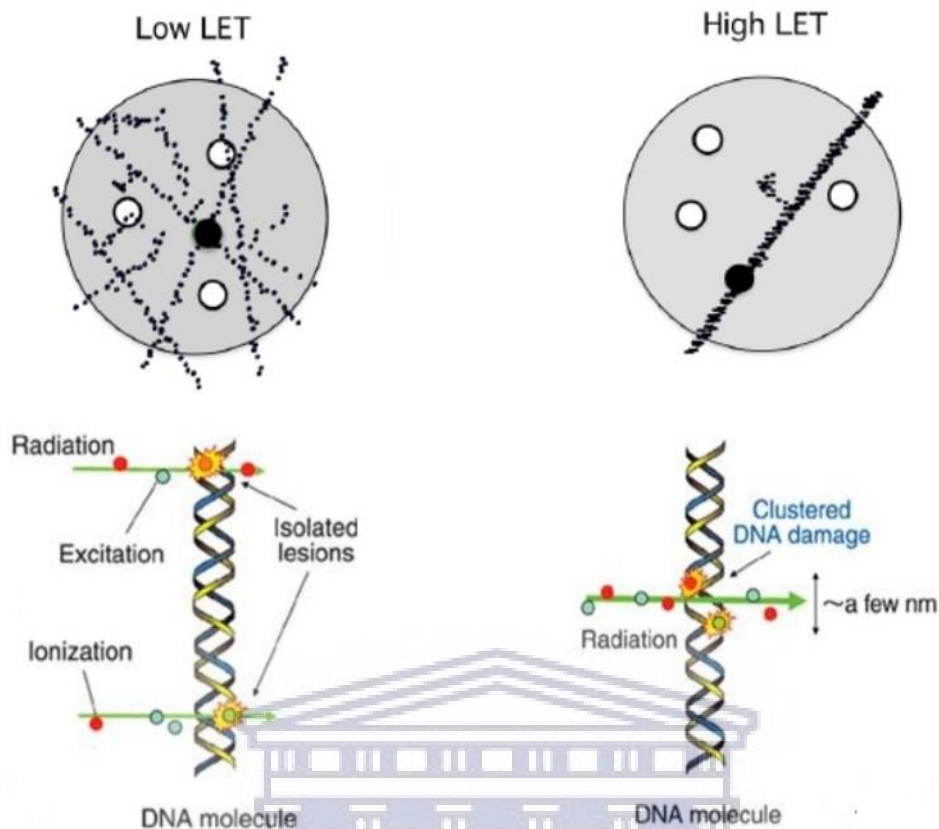


Figure 1.4. The top schematic illustration of particle tracks for low-LET (left-side) and high-LET (right-side) radiation. Low-LET requires a combination of several tracks to cause simple DNA lesions, while for high-LET radiation the impact of a single track can be lethal. (Bailey, 2018). The top illustration shows the spatial distribution of DNA damage of both low-LET (left) and high-LET (right) radiation. The bottom figure shows that both strands of DNA have 2 DNA lesions caused by 8 events (ionisations or excitations). However, the DNA lesions produced by the high-LET are in close proximity to each other, ensuing complex or clustered DNA damage (right-side), whereas the 2 lesions created by the low-LET radiation (left-side) are well separated and hence easier to repair (Fredericia, 2017).

1.2.3 Direct and Indirect Action of Ionising Radiation on DNA

IR may deposit its energy directly in the DNA, resulting in ionisation or excitation of its target or indirectly via the production of free radical species that are capable to diffuse across a distance adequate to interact with the DNA (Figure 1.5). Since 80% of cells are comprised of water, free radicals may be produced during radio-induced dissociation of the water, in a process known as water radiolysis (Alizadeh, Orlando and Sanche, 2015). During this process, the formation of hydroxyl radicals ($\text{OH}\cdot$) may be initiated. Free radicals such as $\text{OH}\cdot$ may then interact with the DNA, causing DNA damage (Pouget and Mather, 2001; Desouky, Ding and

Zhou, 2015; Tsai *et al.*, 2015). The primary free radicals are both, $\text{OH}\cdot$ and $\text{H}\cdot$, however the $\text{OH}\cdot$ radical is assumed to be the main causative agent of DNA damage via indirect action in the cell (Figure 1.5) (LaTorre Travis, 1989).

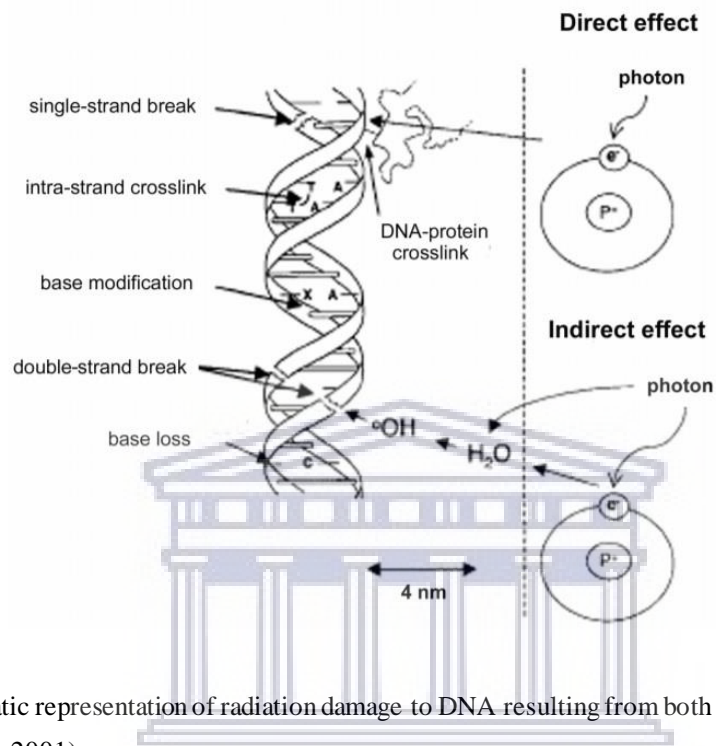


Figure 1.5. Schematic representation of radiation damage to DNA resulting from both direct and indirect effects (Pouget and Mather, 2001).

In essence, for high-LET radiation the direct action dominates, whereas for low-LET radiation the indirect action is dominant. Oxygen (O_2) is required to facilitate the radiation damage caused by indirect action and its radiosensitive effect is often explained by the oxygen fixation hypothesis. Free radicals react with O_2 transforming it to a peroxy radical (RO_2) that will lead to severe DNA damage (LaTorre Travis, 1989; Lehnert, 2007; Hall and Giaccia, 2012; Tsai *et al.*, 2015). Consequently, the O_2 status of the cell will affect the response of cells exposed to low-LET radiation more than the response of cells exposed to high-LET radiation. Under hypoxic conditions, there is less DNA damage due to a decrease of oxygen fixation and restorage of DNA damage produced by free radicals. Therefore, cell killing is greater under normoxic conditions compared to hypoxic conditions, giving rise to the concept of oxygen enhancement ratio (OER) (Valable *et al.*, 2020).

1.2.4 Types of Radiation-Induced DNA Damage

Radiation damage to DNA, resultant from both direct and indirect effects, can be categorised in different types (Nakano *et al.*, 2017) (Figure 1.5):

- Damage to the sugars
- Damage to the bases
- Intra- or inter-strand DNA crosslinks
- DNA-protein crosslinks
- DNA single-strand breaks (SSBs)
- DNA double-strand breaks (DSBs)

Among the various forms of DNA damage, DNA DSBs are considered the most genotoxic radiation-induced lesions, causing severe breakages in both strands of the double helix. DSBs can be classified as either ‘simple’ or ‘complex/clustered’ depending on the presence or absence of additional forms of DNA damage surrounding the DSBs (Rhizobium, 2013; Schipler and Iliakis, 2013; Nakano *et al.*, 2017; Xu *et al.*, 2019). The degree of the complexity will be determined by the frequency and the spatial distribution of the radiation-induced lesions within the vicinity of the damaged location (Hill, 2018; Nickoloff, Sharma and Taylor, 2020).

For low-LET radiations, approximately 20% of the DSBs are of the complex type (Mavragani *et al.*, 2019). High-LET radiation generates a denser ionising track than low-LET radiation, and likely produces more severe and complex DSBs that have a greater probability to result in lethal consequences for the cell. Therefore, the proportion of clustered damage increases with LET, reaching ~70% or higher for high-LET radiations. Table 1.1 gives an overview of the typical LET values of various types of radiation (Friedberg, Copeland and Faa, 2011).

Table 1.1. Typical LET values of various radiations (Friedberg, Copeland and Faa, 2011).

Type of radiation	LET (keV/ μm)
Cobalt-60 (Co^{60}) gamma (γ) rays	0.3
250 kVp X-radiation	2
10 MeV protons	4.7
150 MeV protons	0.5
Recoil protons from fission neutrons	45
14 MeV neutrons	12
66 MeV neutrons	20
2.5 MeV alpha (α) particles	166
2 GeV Fe nuclei	1000

Although there are a multitude of different radiation qualities available, the following description is limited to the radiation qualities that were used in this project:

- **Cobalt-60 (^{60}Co) gamma (γ) rays:** Historically 200 kV X-rays were used as reference radiation, but nowadays ^{60}Co γ -rays are often used. ^{60}Co is a synthetic radioactive isotope of cobalt with a half-life of approximately 5.3 years. ^{60}Co is used as a γ -ray source and decays to nickel-60, ($^{60}\text{Ni}_{28}$) by the emission of a beta (β) particle. The activated nickel nucleus emits two γ -ray photons with energies of 1.17 MeV and 1.33 MeV resulting in an average beam energy of 1.25 MeV (Baba *et al.*, 2013).
- **Neutrons:** A neutron is an uncharged particle with the equivalent spin as an electron and with mass somewhat greater than a proton mass. At the iThemba LABS facility (iTL, Cape Town, South Africa), fast neutrons are produced by bombarding a thick Beryllium (Be) target with 66 MeV protons generated by the separated sector cyclotron (SSC), resulting in a neutron spectrum with a fluence-weighted average energy of approximately 29.8 MeV (Jones *et al.*, 1992; Slabbert *et al.*, 2000). Routine treatment with the p(66)/Be neutron therapy unit at iThemba LABS commenced in 1989, while proton beam therapy (PBT) was first undertaken using the 200 MeV proton beam in September 1993. Studies of human exposures to neutron radiation are very limited. The

major group is the atomic bomb (A-bomb) survivors who were exposed to fission neutrons (mean energy between ~ 0.025 eV and 1 MeV) in Hiroshima and Nagasaki in August 1945 which caused appalling casualties and destruction (Heilbrom, 2015; Goodhead, 2019). In the establishment of radiation protection standards, radiation weighting factors (w_R) are used to convert the physical absorbed dose (Gy) into an equivalent dose (Sv), in order to estimate radiation-induced cancer risks (Baiocco *et al.*, 2016). Neutrons are more densely ionising and cause greater biological damage per unit absorbed dose, resulting in greater RBE than γ -rays (Rühm *et al.*, 2018; Cordova and Cullings, 2019). Thus far, neutrons in A-bomb radiation have been predictably measured by a constant RBE value of 10 (Sasaki *et al.*, 2016; Cordova and Cullings, 2019). Based on the life-span studies (LSS) and the observed differences in excess leukaemia risks between the Hiroshima and Nagasaki atomic bomb survivors, it is known that neutrons are more effective than γ -rays in causing radiation-induced leukaemia (Jordan, 2016; Ozasa, 2016). The main source for the evaluation of neutron radiation weighting factors is pooling together RBE data from different experiments which is rather old and limited for high neutron energies. As a result, substantial uncertainty remains on how the neutron RBE varies with neutron energy, but also with dose and dose rate (Baiocco *et al.*, 2016). New experimental and theoretical efforts have been recently undertaken in the framework of the European ANDANTE project (Ottolenghi *et al.*, 2015), with the main objective of determining RBE values of neutrons for specific tissues and neutron energies. The framework of ANDANTE project is to specifically evaluate the possible role of secondary neutrons in the induction of second primary neoplasms following particle therapy, particularly for paediatric patients. The difference in cancer risk between Hiroshima and Nagasaki can be readily explained by differences in the neutron component, which disappear only the neutrons are weighted by a dose-dependent variable RBE (Sasaki *et al.*, 2016). This shows that even a small dose of neutrons cannot be overlooked in cancer risk evaluation.

In the framework of this PhD project, we investigated the DNA damage response of haematopoietic stem and progenitor cells (HSPCs) to fast neutron irradiation, since secondary neutrons are produced during PBT. The clinical application of PBT is of great interest for paediatric patients due to the optimal dose distribution and the lower integral

whole-body dose compared to conventional X-ray RT, resulting in a reduction of side effects (Levin *et al.*, 2005; Liu and Chang, 2011; van de Water *et al.*, 2011; Cotter, McBride and Yock, 2012; Tian *et al.*, 2017). However, serious concerns remain around the secondary neutrons produced by nuclear interactions with the material in the beam path during PBT and in the patient's body (Kim, Chung, Shin, Lim, Shin, B. Lee, *et al.*, 2013; Trinkl *et al.*, 2017). Although it is expected that these neutron doses are only a fraction of the treatment dose, low neutron doses have been well established to have a high potential for carcinogenesis (Brenner and Hall, 2008).

1.3 DNA Damage Response (DDR)

Cells have developed intricate mechanisms to repair the many types of lesions in the DNA, caused by both endogenous and/or exogenous sources of DNA damaging agents. In order to maintain the genomic integrity of the DNA, an integrated network of signalling pathways will be activated in response to DNA damage, known as the 'DNA damage response' (DDR) (Giglia-Mari, Zotter and Vermeulen, 2011). It has been anticipated that each cell in the human body experiences approximately 100,000 spontaneous DNA damage lesions daily (Lindahl, 1993; Nickoloff, Sharma and Taylor, 2020). Endogenous DNA damage is caused by normal oxidative metabolism, where chemically active DNA engage in hydrolytic and oxidative reactions with water, leading to the production of reactive oxygen species (ROS). In addition, endogenous DNA damage can also be caused by infection and inflammation (Chan and Dedon, 2010; Chatterjee and Walker, 2017). In contrast, exogenous DNA damage occurs when environmental, physical and chemical agents damage the DNA (Chatterjee and Walker, 2017). Typical examples include ultraviolet (UV) and ionising radiation, alkylating and crosslinking agents (Kavanagh *et al.*, 2013a). As mentioned in [Section 1.2.3](#), IR is a known DNA-damaging agent and recognised for its carcinogenic potential. IR is very effective at producing DSBs, which are considered to be the most cytotoxic lesions, since misrepair or lack of repair of DSBs can lead to cell death or mutations (Kavanagh *et al.*, 2013a). As shown in [Figure 1.6](#), the DDR is a complex and highly coordinated system providing a mechanism for transducing a signal from a sensor, which recognises the damage, through a transduction cascade to a series of downstream effector proteins that determine the cellular consequence of DNA damage. These effector pathways include cell cycle arrest, DNA repair pathways that physically repair DNA

breaks or controlled cell death pathways to kill damaged cells (Harfouche and Martin, 2010; Giglia-Mari, Zotter and Vermeulen, 2011; Chatterjee and Walker, 2017; Sun, Osterman and Li, 2019; Huang and Zhou, 2020).

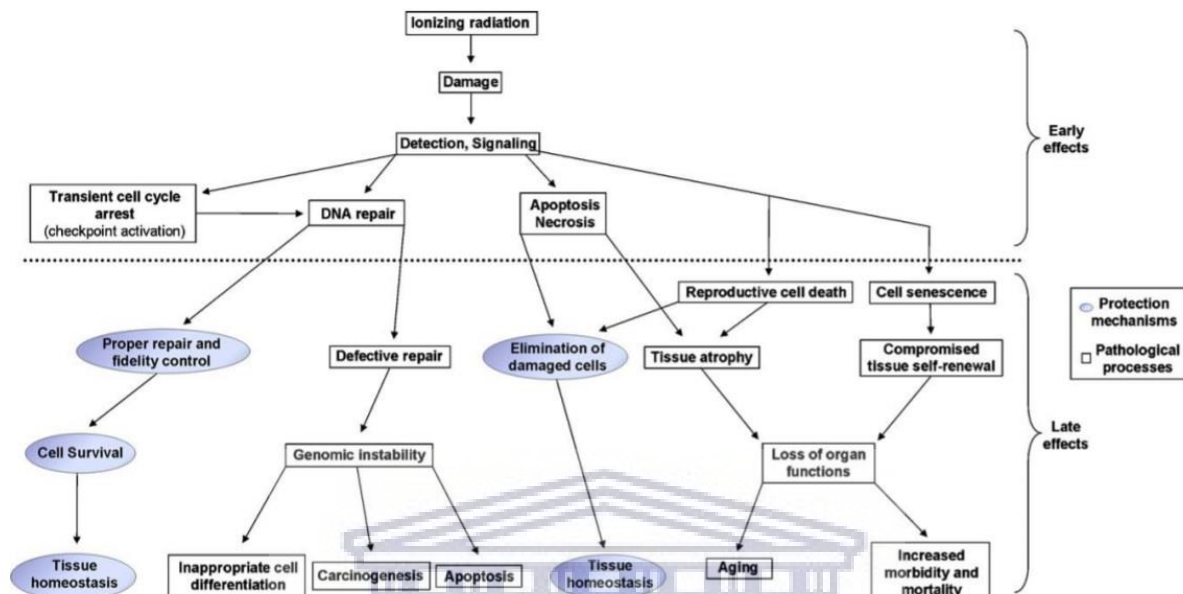


Figure 1.6. Schematic illustration of DNA response to IR. Once the cells are exposed to IR, the cells can undergo numerous fates, including cell cycle arrest and DNA repair processes, or cell death, if the damage cannot be repaired (Harfouche and Martin, 2010).

1.3.1 Cell Cycle Arrest

Cells can initiate cell cycle arrest through the activation of a cell cycle checkpoint in response to IR-induced DNA damage. This will slow or arrest cell cycle progression in order to allow time to repair the damage or to initiate cell death programs. The two key components of the checkpoint activation are based on cyclins and cyclin-dependent kinases (CDKs) complexes.

CDKs are serine/threonine kinases that can phosphorylate multiple substrates leading to the regulation of cell cycle progression (Suryadinata, Sadowski and Sarcevic, 2010; Lim and Kaldis, 2013). The molecular mechanism of cell cycle progression requires the Retinoblastoma (Rb) tumour suppressor gene family, regulatory factors namely, cyclins, CDKs and regulators of CDKs such as inhibitory kinases, activated phosphatases and non-kinase inhibitors. Cyclins are synthesised at the appropriate time for each phase and then degraded to coordinate cell cycle progression. CDKs are activated by cyclins and phosphorylate targets required for the next cell cycle phase (Gordon *et al.*, 2018). Cells that proceed past the restriction point in the

G1 phase enter S phase, while non-dividing cells can enter the G0 phase and can reversibly re-enter the cell cycle or become quiescent, losing the ability to cycle and sometimes become senescent (Nakamura-Ishizu, Takizawa and Suda, 2014). In response to DNA damage, there are four major checkpoints in the cell cycle: the G1-S checkpoint, S checkpoint, the G2-M checkpoint and the spindle assembly checkpoint. The G1-S checkpoint is activated to prevent cells that were in G1 phase at the time of DNA damage from progressing into S-phase, while the intra-S-phase checkpoint slows progression through S phase and allows time for repair of DNA damage. The G2-M checkpoint regulates entry into mitosis following DNA damage and the spindle assembly checkpoint allows alignment of delayed chromosomes on the spindle during metaphase (Cann and Hicks, 2007; Nakamura-Ishizu, Takizawa and Suda, 2014; Visconti, Della Monica and Grieco, 2016).

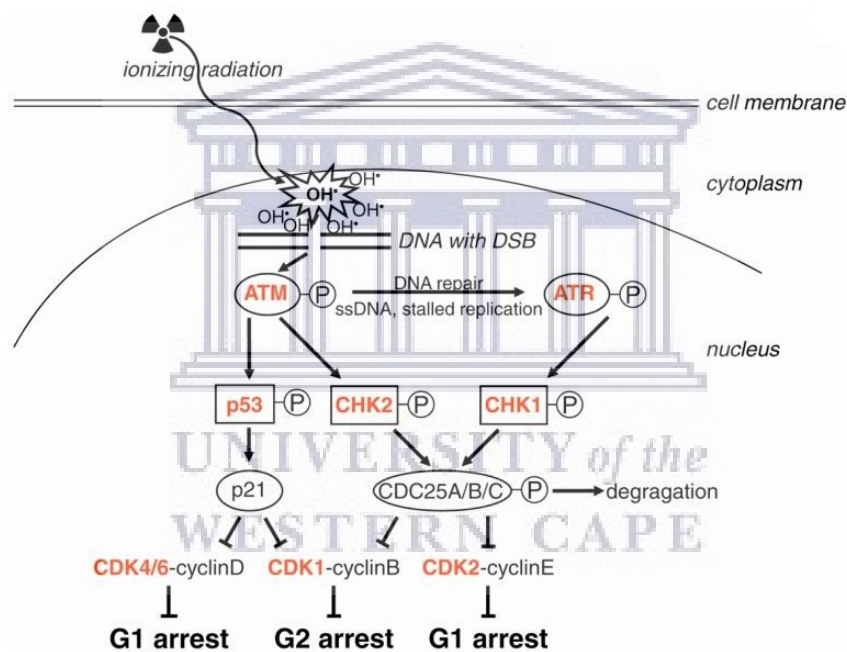


Figure 1.7. Induction of cell cycle arrest after irradiation. The hydroxyl radical induced by IR affecting the genomic integrity by induction of DSB. Next, the ataxia telangiectasia mutated (ATM) kinase is activated by phosphorylation (enclosed P) and phosphorylates p53. ATR is activated by single-stranded DNA breaks and delayed replication forks arising from the repair process. Activated p53 acts as a transcription factor and causes the expression of the CDK inhibitor, p21 which induces cell cycle arrest during the G1 and G2 phases. On the other hand, activation of checkpoint kinase 1 (Chk1) and Chk2 leads to phosphorylation of the three Cdc (cell division cycle 25) isoforms, resulting in degradation of Cdc 25. Lack of Cdc activity induce cell cycle arrest in the G1 or G2 phase, respectively. The arrows represent activation and bar-headed lines represent inhibition (Maier *et al.*, 2016).

As shown in [Figure 1.7](#), the key molecular mechanisms of checkpoint pathways that are activated in response to IR induced DNA damage is the ataxia telangiectasia mutated (ATM) and Rad3-related (ATR) pathways and subsequent downstream pathways resulting in the activation of p53 (Al-Ejeh *et al.*, 2010). DSBs activate ATM, whilst ATR is activated by either SSBs or DSBs, and both mechanisms trigger a series of phosphorylation events (Medema and Macurek, 2012). ATM phosphorylates checkpoint kinase 2 (Chk2), while ATR phosphorylates the checkpoint kinase 1 (Chk1). Chk1 and Chk2 phosphorylate Cdc25A on multiple serine residues which leads to enhanced ubiquitination and proteasome-mediated degradation of Cdc25. The destruction of Cdc25 and the activation of Wee1 by Chk1/Chk2 leads to phosphorylation on threonine 14/tyrosine 15 (Thr14/Tyr15) leading to a persistent inhibitory phosphorylation of CDK 1, 2, 4 and 6 on Thr 14/Tyr 15 or Tyr17 and thus inhibition of cyclin D-CDK4/6, E-CDK2, and cyclin A-CDK2 or cyclin A/B-CDK1 complexes and an arrest in G1/S, or S or G2/M. Inhibition of these complexes prevent the phosphorylation of Rb, which in turn prevent the release of E2F transcription factors that allow the cell by gene activation to progress through the restriction point into the following phase (Mombach, Bugs and Chaouiya, 2014; Maier *et al.*, 2016). The inhibition of CDK2 activity blocks the association of chromatin and Cdc45, a protein required for recruitment of DNA polymerase α , into assembled pre-replication complexes, thus preventing initiation of DNA synthesis (Recolin *et al.*, 2014). Activation of ATR/ATM and Chk1/Chk2 phosphorylate p53 on serine 15 and 20 respectively, leading to stabilisation through the dissociation from murine double minute 2 homolog (MDM2) and increased translation (Loughery and Meek, 2013). P53 induces the synthesis of a CDK inhibitor, p21, and proliferating cell nuclear antigen (PCNA). The interaction of p21 with PCNA facilitates a proper balancing of the DNA replication and repair machinery throughout the cell cycle (Kreis, Louwen and Yuan, 2014; Mansilla *et al.*, 2020).

1.3.2 DNA Repair

DNA damage checkpoints can only avert the transfer of mutations to daughter cells if cells possess efficient DNA repair machinery. Therefore, cells respond to DNA damage by initiating DDR pathways, which allow sufficient time for specified DNA repair to take place. There are five major DNA repair pathways: base excision repair (BER), nucleotide excision repair (NER), mismatch repair (MMR), homologous recombination (HR) and non-homologous end joining (NHEJ). In addition, uncommon specific lesions can also be removed by direct

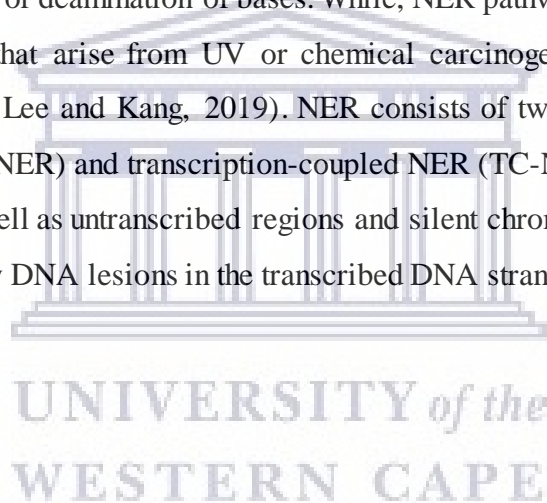
chemical reversal and interstrand crosslink (ICL) repair (Al-Ejeh *et al.*, 2010; Chatterjee and Walker, 2017).

1.3.2.1 BER and NER

Most of the induced damage is repaired using BER or NER pathways and lesions for these two repair pathways only affect one of the DNA strands. In a ‘cut-and-patch’ response, the lesion is removed, resulting in a gap and it is filled by using the intact complementary strand as a template (Hoeijmakers, 2001). Both repair pathways consist of three mutual stages, namely, lesion recognition, excision of damaged nucleotide, and lastly re-synthesis using error-free DNA polymerases (Lee and Kang, 2019). BER pathways are generally associated with the removal of small base modifications or non-bulky lesions (non-helix-distorting) induced by alkylation, DNA oxidation or deamination of bases. While, NER pathway removes bulky DNA lesions (helix-distorting) that arise from UV or chemical carcinogens (exogenous sources) (Fleck and Nielsen, 2004; Lee and Kang, 2019). NER consists of two sub-pathways, namely global genome NER (GG-NER) and transcription-coupled NER (TC-NER). GG-NER operates in the entire genome, as well as untranscribed regions and silent chromatin, whereas TC-NER identifies and repairs bulky DNA lesions in the transcribed DNA strands (Marteijn *et al.*, 2014; Kumar *et al.*, 2020).

1.3.2.2 MMR

MMR adjusts DNA mismatches generated during DNA replication and communicating signals downstream to activate a G2/M checkpoint, thereby preventing mutations from becoming permanent in dividing cells. An inactivation of the MMR machinery is associated with an increase in the spontaneous mutation rate. A defective MMR is microsatellite instability (MSI) and tumours displaying MSI are said to manifest a “mutator phenotype”, with a tendency to produce somatic mutations (Ferguson *et al.*, 2015). The MMR plays a vital role to eliminate severely damaged cells and prevents both mutagenesis in the short term and carcinogenesis in the long term (Hsieh and Yamane, 2008; Li, 2008)



1.3.2.3 HR and NHEJ

Chromatin modification is the first event that triggers the incidence of a DSB and activates a cascade of events including ATM activation, ATR activation, DNA-PKcs and targeted phosphorylation of histone H2AX (Chatterjee and Walker, 2017). Microscopically, DSBs can be observed as local dots of repair protein accumulation, also known as foci in the cell nucleus. For example, histone H2AX is phosphorylated locally around the DSB and 53BP1, RPA and RAD51 accumulate in foci after IR exposure (Brandsma and Gent, 2012). The two main distinct pathways that repair DSBs are HR and NHEJ. The main difference between these evolutionary conserved repair pathways is that HR is reliant upon DNA homology to repair the damage, whereas NHEJ ligates broken DNA ends without the use or identification of the DNA sequence homology. Even though, the HR pathway is commonly classified to be error-free and the NHEJ pathway as error-prone, both DSB repair processes play a vital role in maintaining genome stability and preventing carcinogenesis (Mao *et al.*, 2008). The relative involvement and regulation of each pathway in DSB repair rest on several factors, such as the organism, cell type, cell cycle stage, chromosomal section, radiation quality and dose (Heyer, Ehmsen and Liu, 2010). Besides homology, the location of the donor template relative to the DSB is also important as there is a distinct usage of sister chromatid donor templates in both yeast and mammalian cells (Fernandez *et al.*, 2019). The typical template for HR repair of damaged DNA sequence is the sister chromatids which are available during the S and G2 phase of the cell cycle, whereas NHEJ remains active throughout the cell cycle and does not rely on a template. Furthermore, NHEJ is considered the main pathway for repair of IR-induced DSBs in mammalian cells (Heyer, Ehmsen and Liu, 2010; Brandsma and Gent, 2012; Kavanagh *et al.*, 2013b; Takahashi *et al.*, 2014; Ferguson *et al.*, 2015; Biechonski, Yassin and Milyavsky, 2017; Zhao *et al.*, 2017).

1.3.2.4 Direct Chemical Reversal and ICL

Small subsections of DNA lesions, such as UV photolesions and alkylated bases, are purely reversed in an error-free manner. Inter-strand DNA crosslinks (ICLs) are lesions that are a covalent linkage between complementary double strands of DNA due to presence of bifunctional alkylating agents, such as the nitrogen mustards, platinum compounds and Mitomycin C (MMC) (Chatterjee and Walker, 2017). ICLs can block the progression of the DNA replication fork and transcription by inhibiting the progression of the replisome. Furthermore, ICLs may distort the structure of chromatin and prevent the access of DNA-

interacting proteins and lead to mutagenic effects (Wood, 2010). ICLs are extremely cytotoxic and can cause acute defects in DNA transcription and DNA replication (Zhu, Song and Lippard, 2013). The particular inhibitory effect of ICL agents on DNA replication is applied in both chemotherapy and phototherapy to treat various cancers and skin diseases. However, it is known that chromosome instability syndromes, such as Fanconi Anaemia (FA), make patients particularly sensitive to ICL agents (Hashimoto, Anai and Hanada, 2016). FA is a rare autosomal recessive disease with an incidence of 1:200,000 – 1:400,000 in the overall population (García and Benítez, 2008; Dong *et al.*, 2015). FA is distinguished by developmental abnormalities and early bone marrow (BM) failure leading to aplastic anaemia. In addition, FA patients are vulnerable to several types of cancer, most frequently acute myeloid leukaemia (AML). For instance, BM failure characteristic of FA patients could be initiated from a defect in ICL repair in stem cells exposed to endogenous crosslinking agents such as formaldehyde (Pontel *et al.*, 2015).

1.3.3 Cell Death

After IR exposure, an appropriate DNA damage response is the initial attempt of the cell to repair radiation-induced lesions, but if the damage is too extensive, a signalling cascade will trigger cell death. Programmed cell death can be classified into four morphologically distinct forms (Martins *et al.*, 2017; Tang *et al.*, 2019; Chen *et al.*, 2020):

- Type I apoptosis: presents cytoplasmic shrinkage, DNA fragmentation, and plasma membrane blebbing and lastly apoptotic body formation.
- Type II autophagy: is a degradation activity associated with cytoplasmic vacuolisation to form autophagosome to remove damaged or dysfunctional cells.
- Type III necrosis: manifests with permeabilisation of the cell membrane.
- Type IV entosis: exhibits ‘cell-in-cell’ cytological characteristics which is mediated by cellular engulfment to execute damaged cells.

Apoptosis is a tightly regulated ‘active’ cell death process that is associated with cell and nuclear shrinkage, nuclear fragmentation, blebbing of the cell membrane, but no early loss of membrane integrity and the formation of apoptotic bodies (Kroemer *et al.*, 2009). There are two main pathways in apoptosis, namely the extrinsic pathway and the intrinsic pathway

(Pfeffer and Singh, 2018). IR can induce either of these pathways, including the activation of sphingomyelinase responsible for catalysing the breakdown of sphingomyelin to ceramide, a second messenger, that can activate the caspase cascade (Maier *et al.*, 2016; Sia *et al.*, 2020). The intrinsic or mitochondrial pathway can be activated by active cathepsins from the lysosomal compartment, endoplasmic reticulum (ER) stress leading to calcium overload and p53-mediated transcription of genes encoding Bax, BH3 domain-only proteins (Noxa or Puma), proteins involved in ROS generation and cathepsin D (Maier *et al.*, 2016; Rahmanian, Hosseinimehr and Khalaj, 2016). P53 induces apoptosis, cell-cycle arrest, senescence and differentiation, which prevents proliferation of stressed or damaged cells (Rahmanian, Hosseinimehr and Khalaj, 2016). IR exposure and the resulting DNA damage that is picked up by ATM and ATR leads to upregulation of p53 as described in [Section 1.3.1](#) (Park *et al.*, 2016).



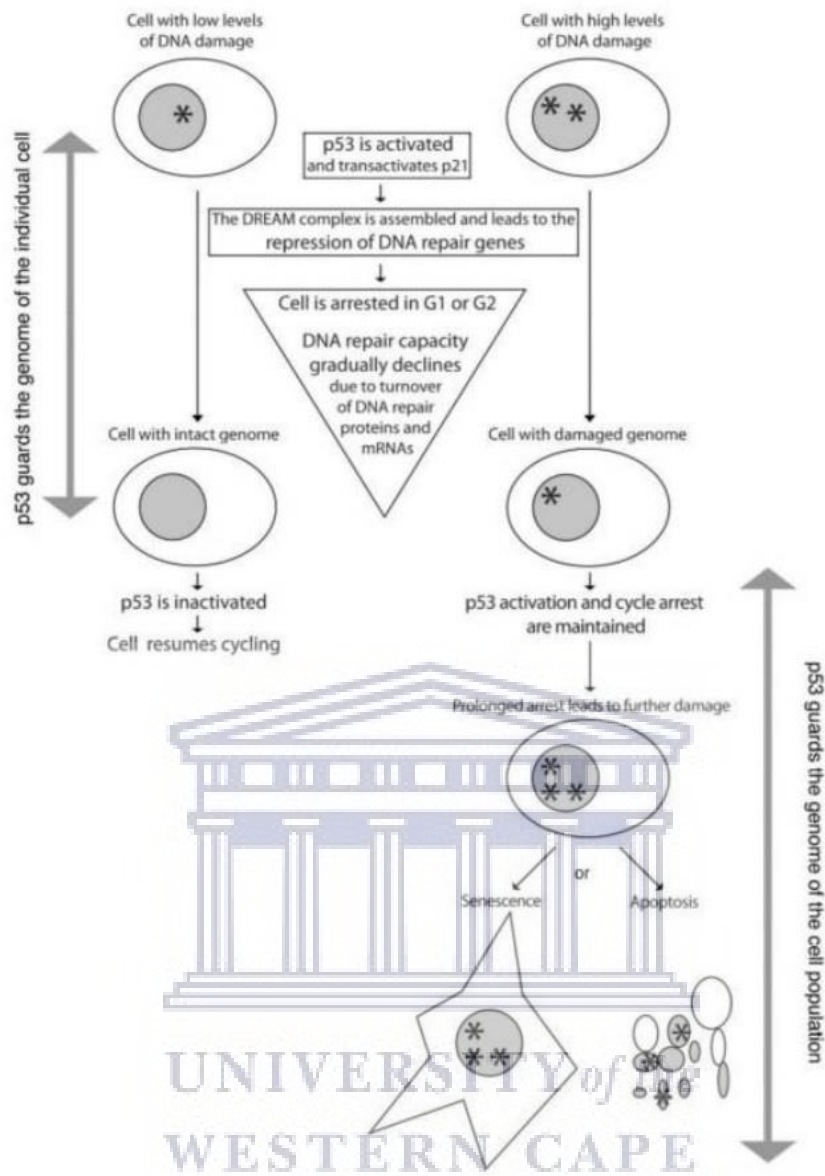


Figure 1.8. The ‘guardian of the genome’. p53 responds to DNA damage and induces a G1 or G2 arrest that might or might not lead to senescence or apoptosis. Besides this, p53 responds to a large variety of cellular stresses and promotes many different cellular responses which can be regulated differently in some tissues or tumour cells supporting pro-apoptotic response (Toufektchan and Toledo, 2018).

Evidence suggests that p53 downregulates genes that are essential to genome maintenance, however p53 acts as ‘the guardian of the genome’ (Toufektchan and Toledo, 2018). The p53-mediated downregulation of gene expression frequently depends on the activation of p21 and the recruitment of E2F4 repressive complexes at the promoter of target genes. The transcription factor, E2F4, is an important protein of the DREAM complex (DP, RB-like, E2F4 and MuvB) (Fischer *et al.*, 2016; Engeland, 2018). Subsequent to p53 activation, the DREAM complex is

recruited at the promoter of specific target genes in order to halt their transcription and induce cell cycle arrest (see Figure 1.8) (Toufekchan and Toledo, 2018). The stabilised and activated p53 can translocate into the nucleus where it activates the transcription of pro-apoptotic genes (e.g. PUMA) and suppresses the transcription of anti-apoptotic genes such as BCL-2. Cytoplasmic p53 can physically interact with members of the BCL-2 protein family, thereby promoting mitochondrial membrane permeabilization and activation of the intrinsic apoptotic pathway, resulting in the release of cytochrome c from the mitochondria into the cytoplasm to activate the intrinsic pathway-specific caspase 9 (Baig *et al.*, 2016; Brown *et al.*, 2019). As shown in Figure 1.9, extrinsic apoptotic cell death is induced by extracellular stress signals that are sensed and propagated by specific transmembrane receptors such as TNFR1 and Fas causing downstream activation of caspase 8 or 10 (Sia *et al.*, 2020). Irradiated cells can upregulate death receptors, making the cells susceptible to death through this pathway (Sheard, Uldrijan and Vojtesek, 2003).

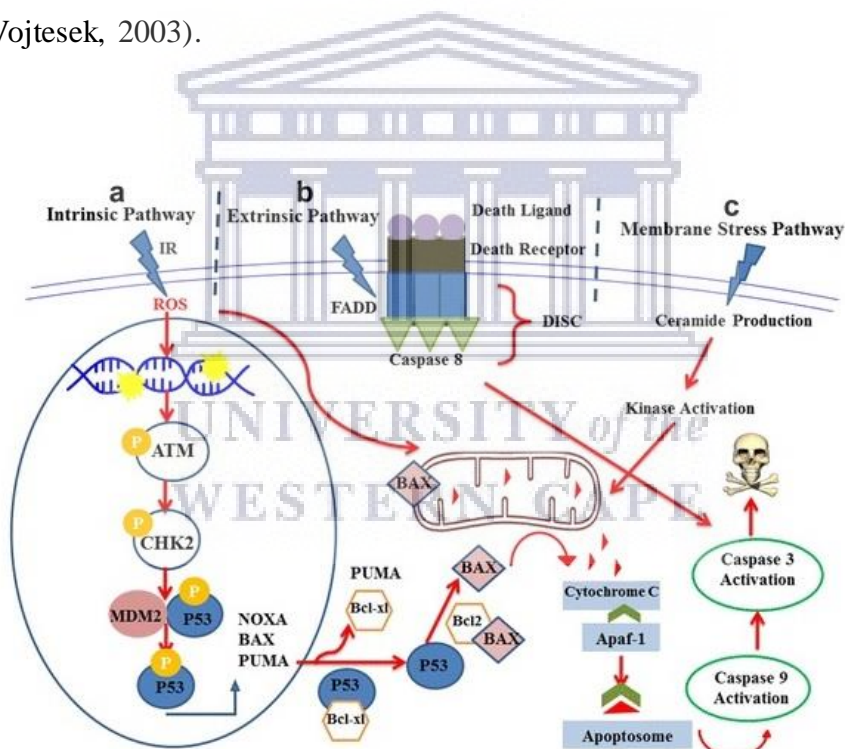


Figure 1.9. Illustration of extrinsic, intrinsic and membrane stress apoptotic pathways induced by IR. (a) DNA damage activates p53 that promotes the expression of pro-apoptotic proteins, such as BCL2 genes, PUMA (p53-upregulated modulator of apoptosis), BAX (BCL2-associated X protein) and NOXA. After its translocation to the cytoplasm, PUMA disrupts a complex by p53 and the anti-apoptotic protein BCL2L1 (BCL2-like 1 or BCL-XL). BAX then triggers cell death by permeabilisation of the outer mitochondrial membrane and subsequent release of cytochrome c (Cyt c) followed by the formation of a large multimeric complex specifically apoptosome through the contribution of cytochrome c/APAF1 (apoptotic protease activating factor 1)/caspase-9 containing apoptosome complex. (b) Radiation-induced apoptosis is also executed through the extrinsic apoptotic pathway

by signalling through death receptors (DRs). Complex formation results in receptor trimerization and consequently formation of death inducing signal complex (DISC) by participation of Fas-associated death domain (FADD) mediated by death domain (DD). (c) Apoptosis can be induced by the production of ceramide as a second messenger which is activated by DSBs and ROS and as a result activation of sphingomyelinase followed by hydrolysis of sphingomyelin and release of ceramide. Apoptosis is regulated by caspase activation which results in cell death due to production of apoptosome, DISC and ceramide in intrinsic, extrinsic and membrane stress apoptotic pathways, respectively (Rahmanian, Hosseinimehr and Khalaj, 2016).

1.4 Haematopoiesis

1.4.1 Haematopoietic Stem and Progenitor Cells (HSPCs)

Blood is a highly regenerative tissue with approximately one trillion (10^{12}) cells developing each day in the human BM. Haematopoiesis is the process of blood cell formation, which originates from a common precursor, haematopoietic stem cells (HSC) which resides in a tightly controlled BM niche that regulates the quiescence, proliferation and differentiation of HSCs (Doulatov *et al.*, 2012; Pennings, Liu and Qian, 2018). The HSCs are able to self-renew through asymmetric cell division, a process in which one daughter cell replaces the stem cell (self-renewal), and the other one is committed to differentiation (Yoo and Kwon, 2015). The self-renewal capacity of the HSCs guarantees a long-term differentiation capability by producing progeny with the same potential to differentiate into mature blood cells, without depletion of the stem cell pool (Warren and Rossi, 2009; Seita and Weissman, 2010; Julien, El Omar and Tavian, 2016; Abreu, 2018).

In mammals, haematopoiesis consist of two waves, namely the primitive wave and the definitive wave (Figure 1.10) (Jagannathan-Bogdan and Zon, 2013). The primitive wave is mainly characterised by the erythroid progenitor which leads to the differentiation of erythrocytes, needed to supply the growing embryo with oxygen (Orkin and Zon, 2008). In humans, primitive haematopoiesis begins in the yolk sac and transitions into the liver momentarily prior to the establishment of definitive haematopoiesis in the BM and thymus (Jagannathan-Bogdan and Zon, 2013; Chen *et al.*, 2014). The definitive haematopoietic wave later involves HSCs and is characterised by the generation of all blood lineages of the adult organism (Qiu *et al.*, 2014; Singh, Soman-Faulkner and Sugumar, 2019). In vertebrates,

definitive HSCs are born in the aorta-gonad-mesonephros (AGM) region of the developing embryo. They move to the foetal liver and then to the BM (Chen *et al.*, 2014).

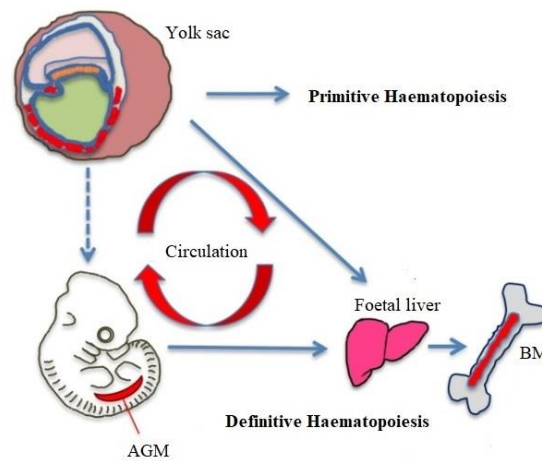


Figure 1.10. Schematic illustration of primitive and definitive haematopoiesis. Abbreviations not explained figure: aorta-gonad-mesonephros (AGM) and bone marrow (BM). Figure adapted from Chen *et al.*, 2014.

Long-term self-renewing multipotent HSCs (LT-HSC) are at the apex of a hierarchy of several progenitor cell stages with increasingly restricted lineage potentials that give rise to all blood cell lineages. As indicated in Figure 1.11, the LT-HSCs will subsequently differentiate into the short-term HSCs (ST-HSCs) and multipotent progenitors (MPPs). LT-HSCs are quiescent, but reactivate once these cells are exposed to a stress stimulus. LT-HSCs persevere for the lifespan of the organism to continuously replenish the haematopoietic system (Challen *et al.*, 2009). On the other hand, ST-HSCs have a reconstitution capability and they have the ability to sustain haematopoiesis in the short term (Yifan Zhang *et al.*, 2018). The LT-HSCs, ST-HSCs and MPPs form the haematopoietic stem and progenitor cell population (HSPCs), which further differentiate into two different lineages, namely the lymphoid and the myeloid lineage. The MPPs give rise to the common lymphoid progenitors (CLPs) and common myeloid progenitors (CMPs). CLPs produce the lymphocytes, whereas CMPs diverges into megakaryocyte and erythrocyte progenitors (MEPs), and granulocyte and macrophage progenitors (GMPs). MEPs in their turn produce megakaryocytes and erythrocytes, while GMPs generate the granulocytes, macrophages, and dendritic cells (DCs). DC can arise either from CLPs or from CMPs. As a result, all mature peripheral blood cells (Figure 1.11) are derived from the HSPCs (Kondo, 2010; Yifan Zhang *et al.*, 2018).

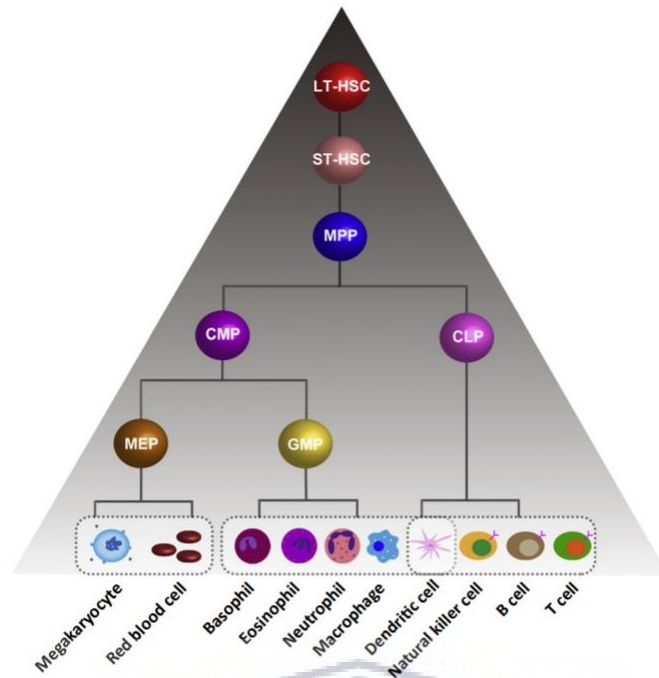


Figure 1.11. A schematic representation of the ‘classical roadmap’ of The Haematopoietic Hierarchy. The HSCs give rise to the MPPs with an accompanying reduction of self-renewal ability. Next there emerges a myeloid/lymphoid lineage segregation downstream of MPP. Abbreviations not explained figure: megakaryocyte/erythrocyte progenitor (MEP) and granulocyte/macrophage progenitor (GMP). Figure from Zhang *et al.*, 2018).

1.4.1.1 Cell Surface Markers

HSCs and their differentiated progeny can be recognised by the expression of specific cell surface lineage markers such as Cluster of Differentiation (CD) proteins and cytokine receptors (Figure 1.12). Haematopoiesis is regulated, in part, by extrinsic signalling molecules including colony-stimulating factors (CSFs) and interleukins (ILs) that activate intracellular signalling molecules (Rieger and Schroeder, 2012; Brown, 2020).

Within this PhD dissertation, the study focused on the use of HSPCs isolated from umbilical cord blood. Among HSPC markers, CD34 is well known for its sole expression on HSPCs and is the most predominant and commonly used marker for HSPC. Latent human HSPCs that are CD34 negative (CD34⁻), also recognised as the apex of the HSC compartment, become positive (CD34⁺) prior to cell division, as a result of cell cycle entry and metabolic activity (AbuSamra *et al.*, 2017). This entails that CD34⁺ cells are a heterogeneous mix of cells at various stages of differentiation. They are hierarchically categorised in LT-HSCs and ST-HSCs (Lin-

CD34⁺CD38⁻CD45RA⁻CD90⁺CD49^{f+}), and MPPs (Lin-CD34⁺CD38⁻CD45RA⁻CD90⁻CD49^{f-}) that become oligopotent progenitors (Lin-CD34⁺CD38⁺) (Seita and Weissman, 2010; Doulatov *et al.*, 2012; Rieger and Schroeder, 2012; Cimato *et al.*, 2016). Specific cell surface markers unique to human HSPC cell populations have been linked to the occurrence of certain human diseases (Cimato *et al.*, 2016). The target cell responsible for leukemogenesis still remains unidentified, but HSPCs are often considered to be a target cell for radiation-induced leukemogenesis (Taussig *et al.*, 2005; Shlush *et al.*, 2014; Verbiest *et al.*, 2018; Stouten *et al.*, 2020).

As mentioned, HSPCs are characterised by the expression of the CD34 marker and are present in placental/umbilical cord blood (UCB), BM and a small fraction in the peripheral blood (PB) (Kato *et al.*, 2013; Sidney *et al.*, 2014). Research of haematopoiesis and radiosensitivity in children is restricted, as the ethical constraints involved in the collection of blood samples from children are challenging. Therefore, a good alternative is the use of UCB. The UCB collected from the postpartum placenta and cord is a rich source of HSPCs and is used as a substitute for blood of a newborn as it is physiologically, genetically and immunologically part of the human foetus (Carroll *et al.*, 2012; Devine, 2017; Krzyzanowski *et al.*, 2019). The proportion of UCB cells expressing CD34 antigen on their surface is approximately 0.02 – 1.43%. This quantity is close to the percentage of CD34⁺ cells found in adult BM (0.5 – 5%) rather than in the PB (<0.01%). In addition, the number of CD34⁺ HLA-DR cells (analysis of the marker of mature line) and CD34⁺CD38⁻ cells in the UCB (4%) is higher than in the BM (1%) (Stojko and Witek, 2005; Hordyjewska, Popiołek and Horecka, 2015).

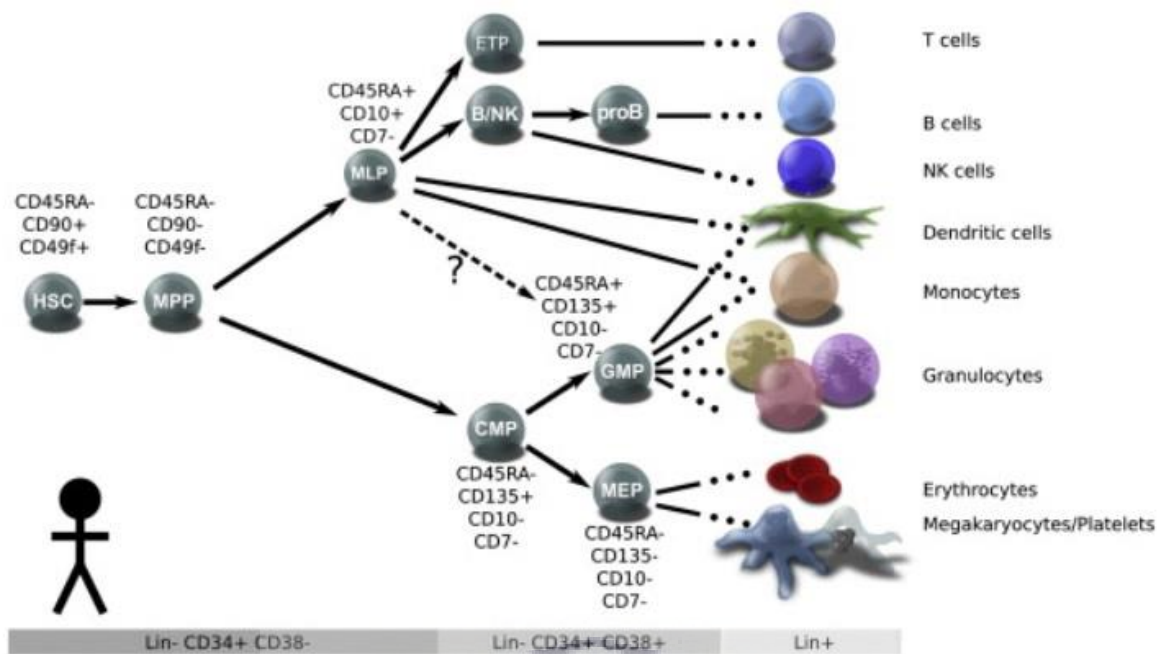


Figure 1.12. A schematic illustration of the lineage model determination in human haematopoietic hierarchies, representing major classes of stem and progenitor cells defined by cell surface phenotypes (Doulatov *et al.*, 2012).

1.4.2 T-lymphocyte Maturation and Cell Surface Markers

As previously described, T-lymphocytes originate from HSCs in the BM, which are capable of differentiating into any type of white blood cell. Immature T-lymphocytes, also known as thymocytes, migrate to the thymus to become progressively converted into fully mature and functional T-lymphocytes (Cano and Lopera, 2013). They are distinguished from other lymphocytes, such as B-lymphocytes and natural killer cells (NK cells), by the presence of a T-cell receptor (TCR) on the cell surface. T-lymphocytes can also be characterised by specific CD markers, for this reason T-lymphocytes can be either helper T-lymphocytes or cytotoxic T-lymphocytes based on whether they express CD4 (helper) or CD8 (cytotoxic) marker. The lineage-specific marker for T-lymphocytes is cytoplasmic CD3, which appears in the earliest T-lymphocyte as precursors in the thymus. During thymic maturation, the T-lymphocyte precursor undergoes rearrangements of the TCR. This process is accompanied by the appearance of other T-lymphocyte lineage-associated markers (CD5, CD4, CD8) (Young and Al-Saleem, 2008). Initially, the thymocytes express neither CD4 nor CD8, and are therefore classified as double-negative (CD4⁻CD8⁻) cells. As these cells develop, they become

double-positive T-lymphocytes ($CD4^+CD8^+$, DP) and lastly mature to single-positive ($CD4^+CD8^-$ or $CD4^-CD8^+$, SP) T-lymphocytes which are liberated from the thymus to peripheral tissues (Chan *et al.*, 1998; Geronne *et al.*, 2018). Characteristically, these mature thymocytes are still signified as either immature or naïve because they have not been presented with an antigen (Merkenschlager *et al.*, 1988; Merckenschlager and Beverley, 1989). All the above mentioned haematopoietic cells express the panhaematopoietic marker CD45, but it is usually randomly expressed or negative in immature precursors, and plasma cells are $CD45^-$ (Young and Al-Saleem, 2008).

The human immune system preserves both naïve and memory T-lymphocytes, which is characterised by the reciprocal expression of CD45RA or CD45RO isoforms (Ben-Smith *et al.*, 2008). Overall, naïve ($CD45RA^+CD45RO^-$) T-lymphocytes represent the utmost homogeneous pool of T-lymphocytes due to their deficiency in most effector functions. Naïve T-lymphocytes are maintained by Interleukin-7 (IL-7) and TCR signalling from contact with major histocompatibility complex (MHC) (Surh and Sprent, 2008; Martin *et al.*, 2017). They migrate to sites that contain secondary lymphoid organs, such as the lymph nodes and tonsils, in search of antigens presented by dendritic cells. This enables the development of antigen-specific adaptive immunity. Once they encounter antigen-presenting cell (APC) and become activated through the TCR, they proliferate and differentiate into effector T-lymphocyte that are $CD45RO^+$ with a variety of functions and that can migrate into tissues to be able to eradicate pathogens (Mackay, 1993; Alberts *et al.*, 2002; Pennock *et al.*, 2013). Once the pathogen has been eliminated, it is no longer of benefit to the host to maintain high numbers of effector cells and most of the activated T-lymphocyte die by apoptosis. However, a small fraction of these effector cells persists as memory cells which can enhance response upon a future encounter with the specific antigen. Additionally, these cells can be subdivided into central memory and effector memory T-lymphocytes with evident functions and homing abilities (Dutton, Bradley and Swain, 1998; Sallusto *et al.*, 1999). Throughout aging, individuals are exposed to new additional antigens causing the proportion of naïve T-lymphocytes population to decline as these cells shift to memory T-lymphocytes. This occurrence reveals the cumulative exposure to foreign pathogens over time (Ben-Smith *et al.*, 2008).

1.5 Quiescence

There are approximately $10^{13} - 10^{14}$ cells in our human body. At any given time, the majority of these cells are non-dividing and outside of an active cell cycle. Some of these non-dividing cells (e.g. senescent or terminally differentiated cells) are permanently arrested. Therefore, these cells can no longer re-enter the cell cycle to proliferate under normal physiological conditions. On the other hand, a population of non-dividing cells is 'reactivable' (see [Figure 1.13](#)) and can enter the proliferative cell cycle in response to physiological growth signals; these cells are called quiescent cells (Yao, 2014). Examples of quiescent cells include many stem cells, progenitor cells, lymphocytes, fibroblasts and some epithelial cells.

Most lymphocytes are short-lived, with an average life span of a week to a few months. Nonetheless, a limited amount live for years, providing a pool of long-lived T- and B-lymphocytes (De Boer and Perelson, 2012; Kumar, Connors and Farber, 2018). Under homeostatic conditions, over 80% of HSPCs remain quiescent in specific regions of bone marrow niche, assuring stemness and longevity over the lifetime of an individual (Yamada, Park and Daniel Lacorazza, 2013). Additionally, most HSPCs are maintained in the G0 phase of the cell cycle as a protective mechanism against cell damage and depletion (Nakamura-Ishizu, Takizawa and Suda, 2014). Interaction between a network of cell-intrinsic mechanisms and cell-extrinsic factors produced by the microenvironment control the re-entry of HSPCs cells into the cell cycle (Pietras *et al.*, 2011; Yamada *et al.*, 2013). The reactivation of quiescent cells (e.g. lymphocytes and stem cells) into proliferation is vital for tissue repair and regeneration and a key to the growth, development and health of advanced multicellular organisms.

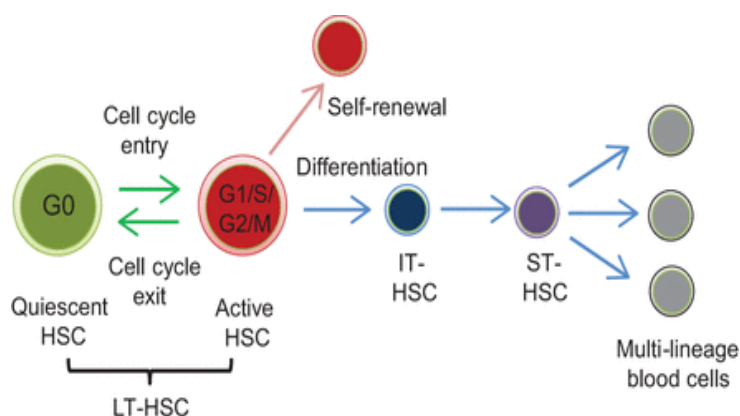


Figure 1.13. Quiescent HSCs in the G0 phase can be initiated to enter the cell cycle (G1/S/G2/M phases) and either self-renew or differentiate. Active HSCs can also exit the cell cycle and return to quiescence. During

differentiation, LT-HSCs give rise to cells with lower repopulation potential – IT-HSCs, ST-HSCs and subsequently produce multi-lineage blood cells. Next, producing multi-lineage blood cells. Abbreviations not explained in text: long-term HSCs (LT-HSCs), intermediate-term HSCs (IT-HSCs) and short-term HSCs (ST-HSCs (Nakamura-Ishizu, Takizawa and Suda, 2014).

1.6 Leukaemia

1.6.1 Origin

Leukaemia, a cancer of the bone marrow and blood, accounts for almost 1 out of 3 cancers diagnosed worldwide in children under 15 years of age, and is recognised as the most common childhood malignancy (Board, 2019). In South Africa, the leukaemia incidence rate is similar to other countries, and accounts for 25.4% malignancies diagnosed in South African children (Maree *et al.*, 2016). Similar to many other childhood cancers, the origin of childhood leukaemia is mainly unknown (WHO-ENHIS, 2009; Eden, 2010). One of the known risk factors is exposure to ionising radiation in utero and after birth (Belson, Kingsley and Holmes, 2007). Additionally, infectious diseases are expected to influence the aetiology of childhood leukaemia, especially for acute lymphoid leukaemia (ALL) (Ma *et al.*, 2009). During early infancy, a delayed exposure to common infections can lead to an increase risk of childhood leukaemia through an abnormal immune response (WHO-ENHIS, 2009; Marcotte *et al.*, 2014). Furthermore, evidence suggests that exposure to specific environmental hazardous chemicals, such as benzene, may be linked to an increase in the risk of childhood leukaemia (Carlos-Wallace *et al.*, 2016; D'Andrea and Reddy, 2018; Raaschou-Nielsen *et al.*, 2018). The incidence of childhood leukaemia has also been positively associated with socioeconomic status and risk factors, such as infection exposure (Howard *et al.*, 2008; Wiemels, 2012; Whitehead *et al.*, 2016; Greaves, 2018). The majority of human hematopoietic malignancies can be traced back to specific chromosomal translocations or somatic mutations leading in cells that make up the haematopoietic system. The alteration of transcription factors in HSPCs is a significant feature of leukaemia. Among the HSPC transcription factors are MLL (for mixed lineage-leukaemia gene), Runx1, TEL/ETV6, SCL/tal1, and LMO2 which are associated with leukaemia translocations (Orkin and Zon, 2008).

1.6.2 Types of Leukaemia

Leukaemia can be divided into multiple subtypes, namely chronic leukaemia (CL) and acute leukaemia (AL). AL is mainly characterised by the proliferation in the BM of dysfunctional and immature blast cells. In contrast, CL cases contain blast cells that are more mature and can still function normally (Shephard *et al.*, 2016). The development of CL is much slower and may take many years to become serious and noticeable, whereas AL presents with a fast, severe progression that usually requires instant treatment (Shephard *et al.*, 2016). The second approach to classifying leukaemia, denotes the condition as either myeloid or lymphoblastic. Lymphoblastic leukaemia generally develops in the lymphocytes in the BM, while myeloid leukaemia arises from erythrocytes, lymphocytes and platelets (Zhao, Wang and Ma, 2018). There are four main types of leukaemia namely, acute lymphoblastic leukaemia (ALL) acute myeloid leukaemia (AML), chronic lymphoblastic leukaemia (CLL) and chronic myeloid leukaemia (CML). Except for ALL that is the most common childhood cancer; AML, CML, and CLL are all age-dependent with the median age at diagnosis around 65 to 72 (Hao *et al.*, 2019). CLL is the most common type of leukaemia found in adults in developed countries. CLL is classified by the continuous accumulation of clonal expansion of mature CD5⁺ B-lymphocyte in the PB, BM, secondary lymphoid organ or tissues such as lymph nodes, liver, or spleen (Herishanu *et al.*, 2013; Rodrigues *et al.*, 2016; Hallek, 2017; Kipps *et al.*, 2017). The most common paediatric leukaemia subtype present in children is ALL (Whitehead *et al.*, 2016) which occurs approximately five times more often than AML and accounts for almost 78% of all childhood leukaemia diagnoses (Belson, Kingsley and Holmes, 2007). The precursor to this disease can be a T- or B-lymphocyte. The B-lymphocyte precursor leukaemia represents 80-85% of ALL (or CD19⁺, CD10⁺, B-cell cALL) cases and is most frequent in 2 – 6 years old children. Whereas the T-lymphocyte precursor leukaemia accounts for almost 15% of the cases and is more common in adolescents than in young children (Whitehead *et al.*, 2016; Terwilliger and Abdul-Hay, 2017; Raboso-Gallego *et al.*, 2019).

Several types of leukaemia are thought to originate in specific types of lineage-restricted or pluripotent cells at different stages in haematopoiesis. Childhood leukaemias are believed to originate during a subsequent stage of differentiation at either the lineage-restricted lymphoid or myeloid stem cell stage (CD34⁺CD38⁺) whereas most adult leukaemias probably originate at the pluripotent HSPC stage (CD34⁺CD38⁻) (Campos-Sanchez *et al.*, 2011; Ivanovs *et al.*, 2017; Greaves, 2018). A causative link between IR and leukaemia has been most extensively

studied amongst the Japanese A-bomb survivors (Shuryak *et al.*, 2006; Hsu *et al.*, 2013; Ozasa, 2016; Cordova and Cullings, 2019). The results of these studies have provided compelling evidence that high doses of IR lead to significant increases in the incidence of several types of leukaemia, including ALL, AML and CML subtypes, whereas CLL appeared not to be induced by IR (Kuznetsova, Labutina and Hunter, 2016). For children exposed during the Nagasaki and Hiroshima bombings, the rates of leukaemia were particularly high, especially for ALL, which is the most common type of paediatric cancer (Schmiegelow *et al.*, 2008; Whitehead *et al.*, 2016). As previously mentioned and reported in the UNSCEAR 2013 report, children are generally identified to carry a higher risk for radiation-induced malignancies, in comparison to adults, which has been quantified to be 2 – 3 times higher for solid tumours and 3 – 5 times higher for haematological malignancies, such as leukaemia (UNSCEAR, 2013). The vulnerability of children after being exposed to IR has been a particular focal point, with specific emphasis to radiation-induced leukaemia cancers as consequences of medical or accidental exposures.

1.7 Radiation-Sensitivity of HSPCs

The red BM harbours the HSPCs and is considered to be one of the most radiosensitive tissues. As previously mentioned, leukaemia has a shorter latency period than any other radiation-induced cancer (Little *et al.*, 2018).

In the study of radiation-induced leukaemia, the cells of key interest are the HSPC. These cells are characterised by an extensive self-renewal and regenerative capacity, which maintains a lifetime supply of the range of different blood cells of the haematopoietic system by producing immature progenitors that gradually and progressively, become restricted in lineage differentiation potential (Kato, Omori and Kashiwakura, 2013; Vandevoorde *et al.*, 2016). However, the unique characteristics of HSPCs, such as self-renewal capacity and long-life span, increases their susceptibility to DNA damage accumulation, making them a major target of radiation-induced carcinogenesis. Cell cycle regulation of HSPCs is extremely important to obtain a proper balance between HSPC quiescence and proliferation in order to maintain blood homeostasis. HSPCs have three different approaches to decrease endogenous DNA damage induction. Firstly, HSPCs are mainly in a quiescent phase to protect them from both metabolic-associated (such as ROS) and replication-mediated DNA damage. Secondly, HSPCs reside

inside the hypoxic areas of BM with low blood perfusion and therefore have lower O₂ levels. Thirdly, HSPCs actively transport their ROS into adjacent mesenchymal stem cells (MSCs) to further reduce their ROS levels (Rübe *et al.*, 2011; Biechonski, Yassin and Milyavsky, 2017). Regardless of these approaches, HSPCs can still accumulate DNA damage with aging (Biechonski, Yassin and Milyavsky, 2017). It is clear from literature that DNA damage repair in HSPCs is crucial for maintaining tissue homeostasis and prevent malignant transformation, as the haematopoietic system is one of the main target organs of irradiation injury. However, our understanding of the IR response of human HSPCs is still limited.

In the context of this PhD project, the radiosensitivity of CD34⁺ cells to fast neutron irradiation was specifically investigated. Radiobiology studies with this radiation quality remain scarce but are extremely relevant in the context of PBT, a RT technique that is increasingly been used to treat paediatric brain tumours. Here, CD34⁺ can be exposed to particle radiation either directly by protons, or indirectly by secondary radiation such as fast neutrons (Shao, Luo and Zhou, 2013). This is of clinical concern, since 17.5 – 27.8% of BM is located in the head of children aged 0 – 5 years old (Cristy, 1981). The radiation can induce normal tissue injury, such as myelosuppression, which has been associated with HPSC regenerative capacity loss, or leukemogenesis (Han *et al.*, 2017).

1.8 Radiation-Sensitivity of T-lymphocytes

Overall, lymphocytes (T, B and NK cells) are among the most radiosensitive cell types, followed by monocytes, macrophages and antigen-presenting cells (APCs) (Carvalho and Villar, 2018). It is well known that the lethality of T-lymphocytes arises within hours after irradiation (interphase death) and IR causes long-term adverse effects on T-lymphocyte immunity (Radford, 1994; Li *et al.*, 2015). Epidemiologic data from the A-bomb cohort found long-lasting immune dysfunction and disturbed T-lymphocyte homeostasis (Hayashi *et al.*, 2003; Kusunoki and Hayashi, 2008). Since the fraction of CD4⁺ and CD8⁺ cells in peripheral blood lymphocytes (PBL) differs among individuals, it can be expected that individual radiosensitivity might be biased by the different subset frequencies if the dose-survival curves of the CD4⁺ and CD8⁺ T-lymphocytes (Nakamura, Kusunoki and Akiyama, 1990). A study was conducted by Ozsahin *et al.* to assess *in vitro* radiation-induced CD4⁺ and CD8⁺ T-lymphocyte apoptosis. Their results showed that CD8⁺ T-lymphocytes were more sensitive

than CD4⁺ T-lymphocytes to undergo apoptosis after 8 Gy X-ray exposure (Ozsahin *et al.*, 2005). In another study, apoptosis was measured in CD4⁺ or CD8⁺ T-lymphocyte subsets after exposure to *in vitro* doses of 0, 2, 4 or 8 Gy using a ¹³⁷Cs source (661 keV). When the specific subsets of T-lymphocytes were analysed, different results were observed. CD4⁺ T-lymphocytes had less radiation-induced apoptosis than CD8⁺ T-lymphocytes at all doses (Schnarr *et al.*, 2007). Radiation-induced T-lymphocyte apoptosis can significantly predict differences in late toxicity between individuals. It could be used as a rapid screen for hypersensitive patients to RT.

1.9 Biomarkers for Cellular Radiosensitivity

In the field of radiobiology, multiple assays are available to detect radiation-induced DNA damage, (mis)repair and cellular outcomes (e.g. cell cycle arrest and cell death). In the following sections, the description will be limited to the assays used as part of this PhD thesis. The assays were used to investigate the radiosensitivity of HSPCs to different radiation qualities and compare the difference in radiosensitivity between children and adults; all linked to the increased risk of children to develop radiation-induced leukaemia.

1.9.1 Cytokinesis-Block Micronucleus (CBMN) Assay

The CBMN assay is a cytogenic technique and an appropriate biological dosimetry tool to evaluate chromosomal damage, which can also assess *in vitro* radiosensitivity, cancer susceptibility and can be used for biodosimetry (Thomas and Fenech, 2011). The micronuclei (MN) observed in binucleated (BN) cells are minute extracellular bodies, separated from the main nucleus, that consist of acentric fragments (see Figure 1.14) (Fenech, 2000, Fenech, 2007; Baeyens *et al.*, 2005; Fenech *et al.*, 2011). In addition, the CBMN assay can provide a sensitive measurement of the mis-repair of DNA DSBs (see Figure 1.15) (Fenech *et al.*, 2011). MN serve as biomarkers for radiation-induced DNA damage and originate from chromosome fragments or whole chromosomes that fail to engage with the mitotic spindle. As a result, the MN lag behind when the cell divides. Over the past decades, the CBMN assay became a well-established assay which can also serve as an indication of individual radiosensitivity (Hintzsche *et al.*, 2017).

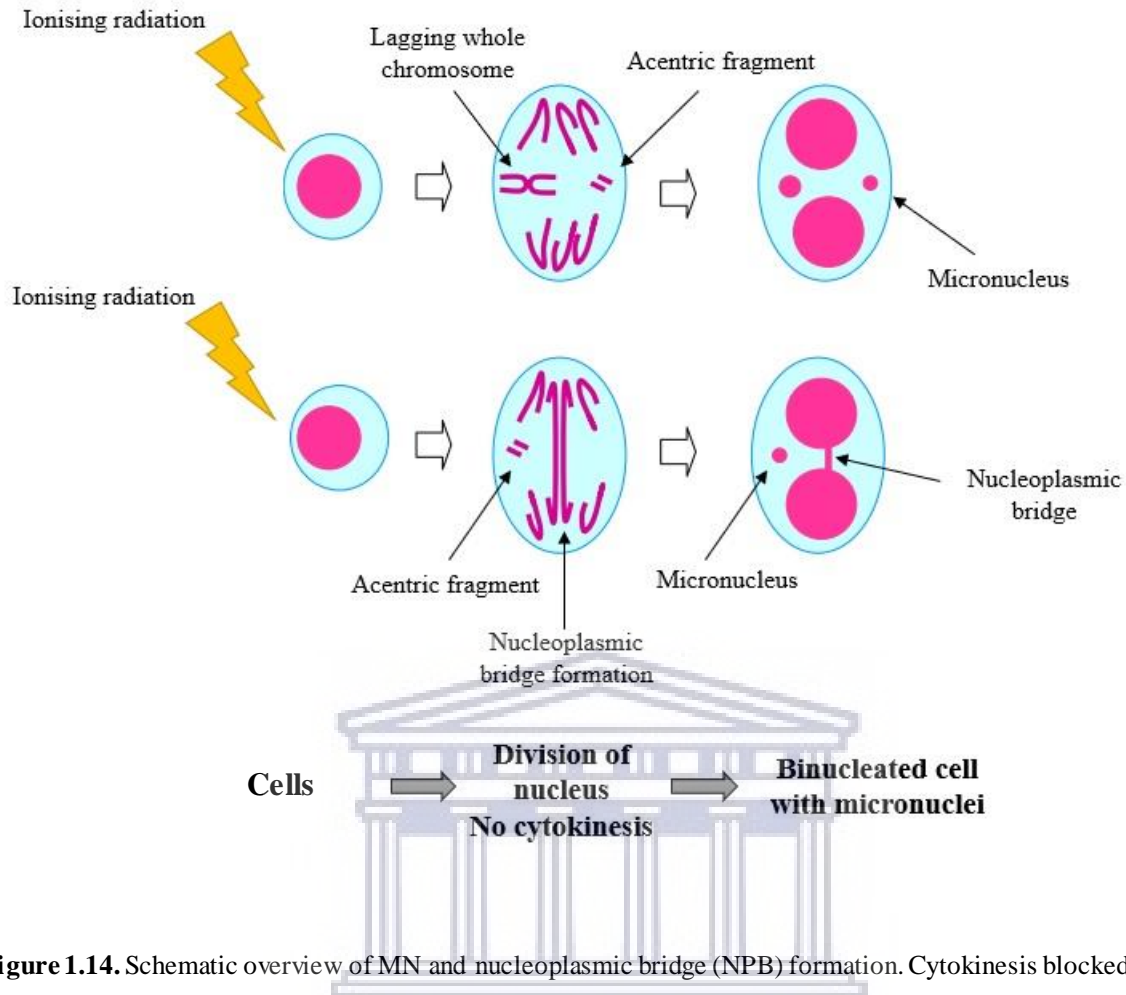


Figure 1.14. Schematic overview of MN and nucleoplasmic bridge (NPB) formation. Cytokinesis blocked cells will appear as BN cells after dividing. The acentric fragments or whole chromosomes fragments that lag during anaphase can form MN in the BN cells (Fenech *et al.*, 2011).

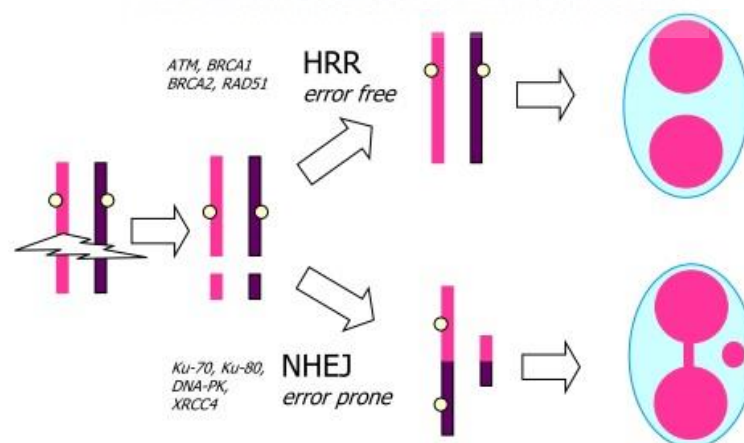


Figure 1.15. Defects in genes involved in HR pathway can be detected using the CBMN assay. Under these conditions, the cell would recourse to the NHEJ pathway that is likely to result in mis-repair of DSBs in DNA forming acentric chromosome fragments and dicentric chromosome, which is observed as NPBs and MN (Fenech *et al.*, 2011).

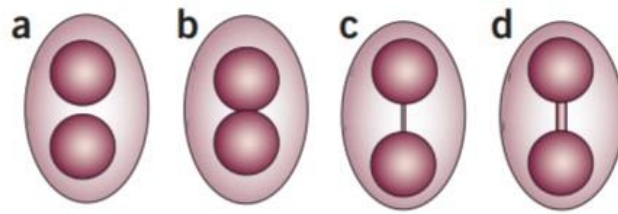


Figure 1.16. Different types of BN cells in the CBMN assay. (a) An ideal BN cell, (b) a BN cell with touching nuclei, (c) BN cell with thin NPB between nuclei and (d) BN cell with rather thick NPB (Fenech, 2007).

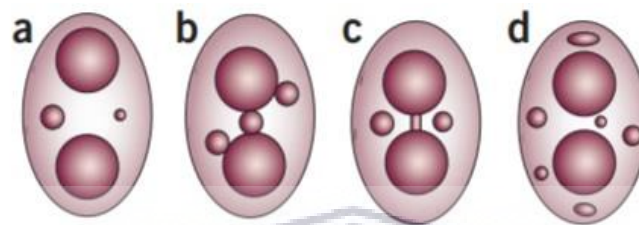


Figure 1.17. The characteristic appearance and relative size of MN in BN cells. (a) BN cell with two MN containing viable MN varying in sizes between 1/3 to 1/9 of the main nuclei. (b) BN cell with three MN touching, but not overlapping the main nuclei. (c) BN cell with NPB between main nuclei and two MN. (d) BN cell with six MN varying in sizes (Fenech, 2007).

The cytome approach in the CBMN assay is imperative because it allows genotoxic (MN, NPBs and nuclear buds in BN cells), cytotoxic (proportion of necrotic and apoptotic cells) and cytostatic (proportion and ratios of mono-, bi- and multinucleated cells (nuclear division index)) events to be captured within one assay (Fenech, 2007; Fenech *et al.*, 2011; Rodrigues *et al.*, 2018). The nuclear division index (NDI) represents the proliferation rate of the viable cells (see Figure 1.18).

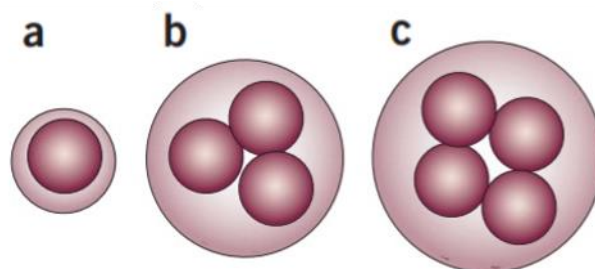


Figure 1.18. The ratios of viable mononucleated, BN cell, multinucleated cells are used to determine mitotic division rate or NDI (a measure of cytostasis). The characteristic appearance viable (a) mono-, (b) tri- and (c) quadrinuclear cells. Adapted from Fenech, 2007.

1.9.2 γ -H2AX Foci Assay

An additional way to analyse DNA damage induction and response is the γ -H2AX foci assay. Chromatin modification is the first event that registers the presence of a DSB and triggers a cascade of events including ATM activation, targeted phosphorylation of H2AX (Chatterjee and Walker, 2017). Following radiation exposure, H2AX is a variant of the core histone protein H2A; upon DNA DSB occurrence, H2AX is rapidly phosphorylated by ATM and/or DNA-PK kinases at the S139 site, which results in a modified γ -H2AX foci (Huang and Zhou, 2020). Immunostaining can be used to visualise the γ -H2AX foci post-irradiation, whereby each focus hypothetically relates to one DNA DSB. Consequently, analysis of these foci gives an estimation of the induction and repair of DNA DSBs, whereby the quantity of foci is linearly correlated with the dose given and decline in function of time post-irradiation (Rübe *et al.*, 2011; Vandevoorde *et al.*, 2016; Jakl *et al.*, 2020). When DNA repair is completed, γ -H2AX should be reverted to H2AX. The molecular mechanism of this elimination remains to be established, currently it is not clear whether dephosphorylation takes place directly in the nucleosome, or whether it requires removal of γ -H2AX from chromatin (Kinner *et al.*, 2008; Firsanov, Solovjeva and Svetlova, 2011). In contrast to γ -H2AX foci formation, the elimination is much slower. It is known that about 60% of initial radiation-induced foci (RIF) are transient with rejoining half-lives in the order of minutes, whereas the other 40% are persistent with rejoining half-lives of the order of hours (Rogakou *et al.*, 1999; Beels, Werbrouck and Thierens, 2010). In general, lymphocytes have several advantages that make them most suitable for evaluating γ -H2AX foci formation. Firstly, a considerable number of cells can be easily obtained within a short time frame before and after exposure. Secondly, the use of lymphocytes avoids cell cycle effects since unstimulated lymphocytes are of non-cycling cells (G0). The latter is also applicable to HSPCs, which are also in a quiescent state. Thirdly, the percentage of nucleosomal H2AX variant was reported to be small in lymphocytes, resulting in a low γ -H2AX background (Valdiglesias *et al.*, 2013). With the development in research and imaging, an automated platform to analyse γ -H2AX foci is available through MetaSystems' Metafer platform.

1.9.3 Apoptosis

Apoptosis, also known as programmed cell death (PCD), is a genetically regulated form of cell death, which leads to the rapid removal of the cell (Doulatov *et al.*, 2012). It plays an important role in the maintenance of tissue homeostasis. At the molecular level, apoptotic cell death is characterized by the sequential activation of different caspases. Caspase activation can be triggered by intrinsic and extrinsic apoptotic pathways, both of which may be initiated by IR. Apoptotic cells are characterised by typical morphological changes like rounding up of the cell, reduction of the cellular volume, chromatin condensation, plasma membrane blebbing and finally the complete fragmentation into compact membrane-enclosed structures, frequently referred to as 'apoptotic bodies' (Zhang *et al.*, 2018). Detection of apoptotic cells can be achieved with the Annexin V apoptosis assay (see Figure 1.19). In apoptotic cells, the membrane phospholipid phosphatidylserine (PS) is translocated from the inner to the outer layer of the plasma membrane, thereby revealing PS to the external cellular environment. The PS translocation results in the loss of membrane integrity, which accompanies the later stages of cell death resulting from either apoptotic or necrotic processes (Biosciences *et al.*, 2011). Consequently, Annexin V is generally used simultaneously with propidium iodide (PI) for identification of early and late apoptotic cells (Rieger *et al.*, 2011). Viable cells with intact membranes will not take up PI stain, while dead or damaged cells are permeable to PI. Thus, viable cells are both Annexin V and PI negative, while cells that are in early apoptosis (EA) are Annexin V positive and PI negative, and cells that are in late apoptosis (LA) or already dead are both Annexin V and PI positive.

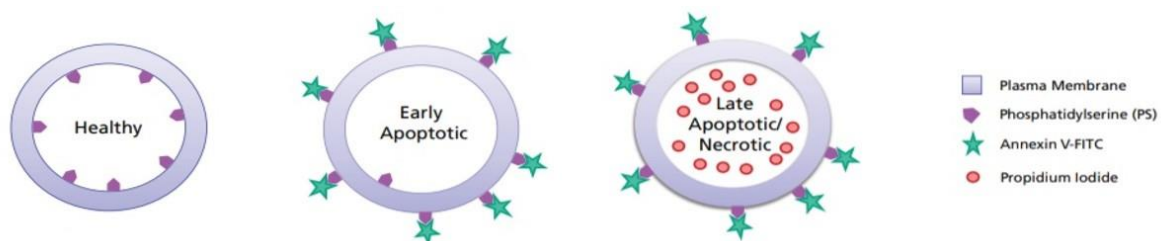


Figure 1.19. Diagram showing living, early and late apoptotic cells with markers for detection of apoptosis (Biosciences *et al.*, 2011).

1.10 Aims and Objectives of the Study

1.10.1 Radiation Sensitivity of Human CD34⁺ Cells in Response to Clinical Therapy Beams: DNA Repair and Mutagenic Effects

The primary aim of this study was to clarify the response of CD34⁺ cells, which are considered to be the target cells for radiation-induced leukaemia, to neutrons and ⁶⁰Co γ -rays at iThemba LABS. This information could be used to evaluate the radiation damage in CD34⁺ cells induced in patients treated with PBT for paediatric brain tumours, who are exposed to secondary neutrons, in order to improve secondary leukaemia risk estimation for childhood cancer survivors. As mentioned previously, PBT represents a major advance over conventional X-ray based RT, mainly due to the reduced integral dose that is delivered to non-targeted tissues, resulting in a reduction of side effects. Some degree of normal tissue injury is unavoidable and serious concerns were raised a couple of years ago regarding the secondary neutrons produced in PBT, which is particularly important for paediatric patients. Despite the fact that these secondary neutron doses are only a fraction of the proton treatment dose, low neutron doses have been well established to have a high potential for carcinogenesis. Limited information is available on the radiosensitivity of HSPCs to particle therapy beams and especially the information on fast neutron irradiation on human cells is scarce, due to a limited number of facilities which can provide this beam quality for radiobiology research. This information can provide an improved understanding of the secondary cancer risk for paediatric patients receiving PBT, but will also be relevant to other fields, such as radiation-induced leukaemia risks for astronauts who will be exposed to fast neutron irradiation during long-term interplanetary missions.

Human HSPCs are usually defined by the cell surface marker CD34⁺. However, this population represents a heterogenous mixture of cells at various stages of differentiation. Haematopoiesis involves developmental progression from HSPCs through a series of downstream progenitor cells with increasing restricted lineage potential. There is evidence that there is a difference in radiosensitivity between these hierarchically organised subsets (Heylmann *et al.*, 2014). In addition, two research groups published contradictory results on the maintenance of genomic integrity of radiation-induced DNA damage in human and murine HSPCs (Milyavsky *et al.*, 2010; Mohrin *et al.*, 2010). Therefore, human HSPCs isolated from UCB will be used in this project.

In the current study, the *in vitro* radiosensitivity of CD34⁺ cells in a South African population was investigated, in response to different radiation qualities, specifically ⁶⁰Co γ -rays irradiation and fast neutrons. In order to obtain this goal, the study consists of the following objectives:

- Objective 1: Radiation-induced chromosomal damage in CD34⁺ cells.

Limited information is available about the effects of high-LET radiation (such as neutrons) and the DNA damage repair in HSPCs. As part of this PhD project, an *in vitro* study will be undertaken with two different radiation qualities available at iThemba LABS: low-LET reference radiation (Co⁶⁰ γ -rays) and high-LET fast neutrons (average energy of 29.8 MeV). The CD34⁺ CBMN assay will be applied to compare the MN dose-response curves. In addition, the NDI will be used to provide an indication of the cytotoxic effect of the irradiation exposure on the rate of CD34⁺ cell proliferation.

- Objective 2: DNA double-strand breaks (DSBs) formation and repair after ⁶⁰Co- γ -rays and neutron irradiation.

The spectrum of complex DNA damage depends strongly on the incident radiation. High-LET particles induce DNA damage which is more complex and difficult to repair (Rall *et al.*, 2015). In addition, growing evidence suggests that DNA repair pathways could be differently activated by high-LET radiation compared to low-LET radiation (Hagiwara *et al.*, 2019). In order to investigate the induction and repair of DNA lesions induced by low-LET (Co⁶⁰ γ -rays) and high-LET (neutrons) irradiation in CD34⁺ cells, we will use immunofluorescence staining of DNA DSB repair protein γ -H2AX at two different time-points post-irradiation.

- Objective 3: Radiation-induced apoptosis in CD34⁺ cells.

Extensive radiation-induced DNA damage in the CD34⁺ cells can lead to the induction of apoptosis. In this study, the Annexin-V/PI assay will be used to assess the fraction of live (Annexin-V⁻/PI⁻), early (Annexin-V⁺/PI⁻) and late (Annexin-V⁺/PI⁺) apoptotic cells at 18 and 42 hours after ⁶⁰Co γ -rays and neutron irradiation respectively.

1.10.2 Age Dependence in Radiation Sensitivity

The second aim of this PhD dissertation, is to gain more insight in the intrinsic higher radiosensitivity of children compared to adults. As shown by epidemiological studies, there is a clear age-at-exposure effect, which makes children more vulnerable to radiation-induced malignancies compared to adults. In order to obtain this goal, the study consists of the following objectives:

- Objective 4: Radiation-induced chromosomal damage in T-lymphocytes: Adult Peripheral Blood (APB) versus UCB.

An *in vitro* study will be undertaken at iThemba LABS where isolated T-lymphocytes from APB and UCB will be irradiated with different doses (0.5, 1, 2, 3 and 4 Gy) of ^{60}Co γ -rays to obtain dose response curves. Afterwards, statistical analysis will be performed to investigate whether there is statically significant difference in radiosensitivity between the two age groups.

- Objective 5: Investigating the expression of CD45RA and CD45RO on CD4 and CD8 T-lymphocytes subsets in UCB and APB samples.

Age related immunophenotypic changes of T-lymphocytes will be taken into consideration to get a better understanding of the potential difference in radiosensitivity with age. This will be obtained through the analysis of newborn and adult T-lymphocyte subpopulations of the same donors that were used for the CBMN assay. The immunophenotypic study of the UCB and APB will focus on the fractions of CD4⁺, CD8⁺, naive CD45RA⁺ and memory CD45RO⁺ subsets.

CHAPTER 2: MATERIALS AND METHODS



UNIVERSITY *of the*
WESTERN CAPE

“I did not think; I experimented.”

– Wilhelm Rontgen

2.1 General Information

All chemicals, salts and solutions, including dimethyl sulfoxide (DMSO), hydrochloric acid (HCl) and acridine orange (AO) were of analytical grade and purchased from Sigma-Aldrich/Merck (St. Louis, Missouri, United States). Gamma irradiated foetal bovine serum (FBS) was supplied by Gibco (Dun Laoghaire, Dublin, Ireland). Iscove's Modified Dulbecco's Medium (IMDM), Roswell Park Memorial Institute (RPMI) 1640 Medium for tissue culture and penicillin-streptomycin (Pen-Strep) were obtained from Gibco (Dun Laoghaire, Dublin, Ireland). All antibodies for flow cytometry, including propidium iodine (PI) were purchased from the Scientific Group (BD Bioscience, United States). All cytokines were of analytical grade and obtained from Miltenyi Biotec Inc. (Bergisch Gladbach, Germany).

2.2 Collection of Peripheral Blood Mononuclear Cells (PBMCs) and CD34⁺ Cells

2.2.1 Collection of Umbilical Cord Blood (UCB)

Ethical approval for this study was granted by the Health Research Ethics Committee of Stellenbosch University (SU), Cape Town, South Africa (Ethics Reference #: N16/10/134, see [Appendix 1](#)). Informed consent was obtained from each mother before UCB collection, according to the NetCord-FACT International Standards for Cord Blood collection (Foundation for the Accreditation of Cellular Therapy (FACT), 2020) (see [Appendix 2](#)). The UCB collection was performed by qualified and trained persons at Tygerberg Hospital and Karl Bremer Hospital, South Africa, and universal precautions were applied to minimise risks to the health and safety of employees and volunteers. The UCB was collected after the scheduled elective Caesarean section (C-section) was performed, without impacting the normal course of the birth (Donaldson *et al.*, 2000). In total, 71 UCB samples (50 – 100 mL) were collected from full-term newborns through a needle puncture in the umbilical cord vein at the scheduled time of delivery, either at Tygerberg Hospital or at Karl Bremer Hospital, South Africa. The UCB was collected in citrate phosphate dextrose adenine (CPDA-1) JMS cord blood collection bags (SSEM Mthembu Medical (Pty) Ltd, Cape Town, South Africa). Afterwards, UCB was transported to iThemba LABS at room temperature, where CD34⁺ cells were isolated from the UCB samples as described by Vandevoorde *et al.* (2016). See [Section 2.3.1](#) of Chapter 2.

2.2.2 Collection of Adult Peripheral Blood (APB)

Ethical approval for APB collection was granted by the Biomedical Research Ethics Committee (BMREC) of the University of the Western Cape (UWC), Cape Town, South Africa (Ethics Reference #: BM20/3/5, see [Appendix 3](#)). Informed consent was obtained from each adult donor (see [Appendix 4](#)), before peripheral blood samples were collected. In total, 36 APB samples (10 – 15 mL) were collected from adult donors through a needle venepuncture at the scheduled time at the clinic at iThemba LABS. The APB collection was performed by a qualified nurse (Incon Health™) at iThemba LABS, and universal precautions were applied to minimise risks to the health and safety of volunteers. The APB was collected through venepuncture in lithium–heparin collection tubes and delivered to the Radiobiology Section of the Nuclear Medicine Department at iThemba LABS for the isolation of PBMCs.

2.3 Isolation of PBMCs and CD34⁺ Cells

2.3.1 Histopaque Isolation of PBMCs

The UCB (30 mL) or APB (15 mL) was diluted with phosphate-buffered saline (PBS) in a ratio of 1:1 and gently added onto 15 mL or 7.5 mL Histopaque-1077 (2:1, Sigma-Aldrich, St. Louis, Missouri, United States) of an angle of 45° in a 50 mL tube for UCB or APB, respectively. The layered solution was centrifuged at 2130 rpm for 15 min for APB samples and 35 min for UCB samples. After centrifugation, four layers formed and the second layer, characteristically white and cloudy, contained the mononuclear cells. This layer was carefully collected using a Pasteur pipette and P1000 micropipette. This was transferred to a 50-mL conical tube containing 30 mL PBS and was washed three times with PBS. To count the mononuclear cells, 10 µL of the cell suspension was added to 90 µL Türk solution (Gibco, Dun Laoghaire, Dublin, Ireland) and counted using a haemocytometer. The freshly isolated PBMCs were directly used to start up an experiment, whereas the UCB PBMCs were directly used to isolate CD34⁺ cells through magnetic-activated cell sorting (MACS).

2.3.2 Isolation of CD34⁺ Cells by Magnetic-Activated Cell Sorting (MACS)

After the PBMC isolation from UCB, human HSPCs were purified by using CD34⁺ immunomagnetic beads (Human CD34⁺ MicroBead Kit; Miltenyi Biotec Inc., Bergisch Gladbach, Germany) according to the manufacturer's protocol as described below (see [Figure 2.1](#)). Firstly, the PBMCs were centrifuged at 1500 rpm for 10 min. Thereafter, for 100 000 000 (10⁸) PBMCs, 300 µL MACS buffer (200 mL PBS, 4mL FBS and 800 µL ethylenediaminetetraacetic acid (EDTA)), 100 µL FcR blocking reagent (Miltenyi Biotec Inc., Bergisch Gladbach, Germany) and 100 µL CD34 MicroBeads (Miltenyi Biotec Inc., Bergisch Gladbach, Germany) were added to the pellet. After 30 min incubation at 4°C, the suspension was diluted with 10 mL MACS buffer and was centrifuged for 10 min at 1500 rpm, (4°C). The LS columns were attached to the separator magnet and rinsed three times with 3 mL ice cold MACS buffer. After centrifugation, the supernatant was removed from the cells, followed by resuspension in 3 mL ice-cold MACS buffer. Thereafter, the resuspended cells were placed on the column using a pre-separation filter. After the suspension has eluted from the column, the 50-mL conical tube was rinsed again with 3 mL cold MACS buffer in order to add the remaining cells on the filter. Subsequently, the pre-separation filter was removed, the LS column was washed three times with 3 mL ice-cold MACS buffer. The column was detached from the separation magnet and placed on top of a 15-mL conical tube. Next, 5 mL of ice-cold MACS buffer was added and the cells were then eluted from the column with a syringe. This method was repeated to increase the cell purity (>90%). After isolation, the cells were counted with a haemocytometer and trypan blue (1:1, Gibco, Dun Laoghaire, Dublin, Ireland) (Miltenyi Biotec, 2020).

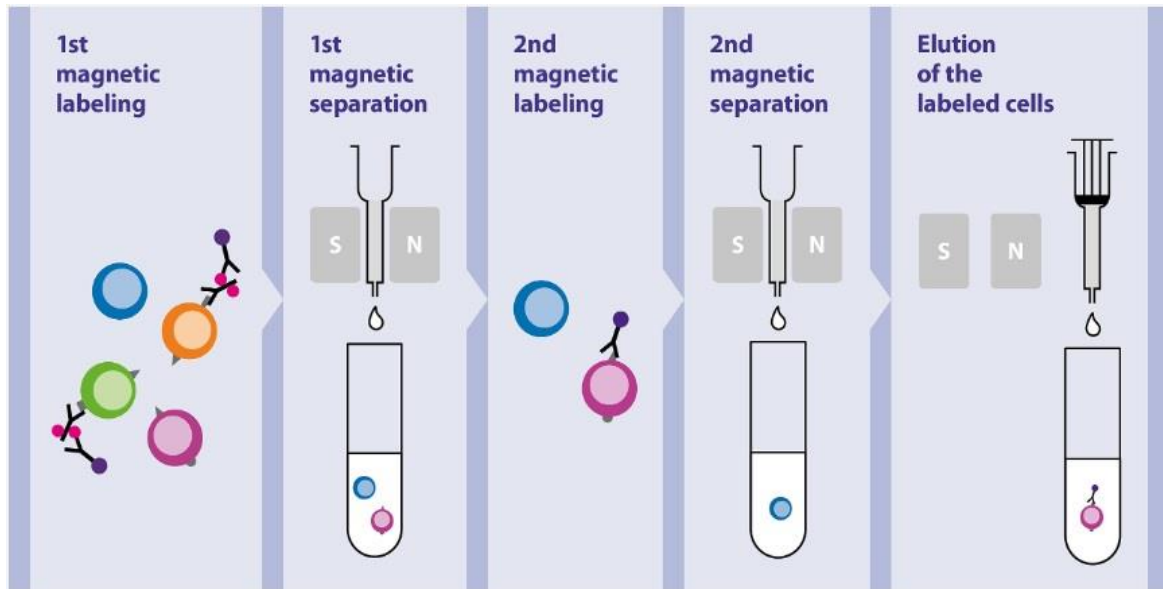


Figure 2.1. Schematic illustration of CD34⁺ cell isolation MACS, which consist of two magnetic separations to increase the cell purity (>90%) (Miltenyi Biotec, 2020).

2.3.3 Purity Control of CD34⁺ Isolation Using Flow Cytometry

After every isolation, a fraction of the final CD34⁺ samples was used to determine the purity of the isolation using the BD Accuri™ C6 flow cytometer. Briefly, 50 µL containing approximately 50 000 isolated CD34⁺ cells, were placed in a fluorescence-activated cell sorting (FACS) tube, followed by 2 µL Fc blocking reagent and 2 µL of CD34 monoclonal antibody-FITC (BD Bioscience, United States) and left to incubate for 30 min in the dark at 4°C. After the incubation period, the cells were washed with 1% bovine serum albumin (BSA, Roche diagnostics GmbH, Sigma-Aldrich/Merck, St. Louis, Missouri, United States) buffer and stained with 2 µL PI (50 µg/mL) to distinguish dead cells from the viable population. Flow cytometry analysis of CD34⁺ samples (~10 000 – 20 000 cells for each sample) revealed an average purity of $93.62 \pm 0.47\%$, as illustrated in Figure 2.2.

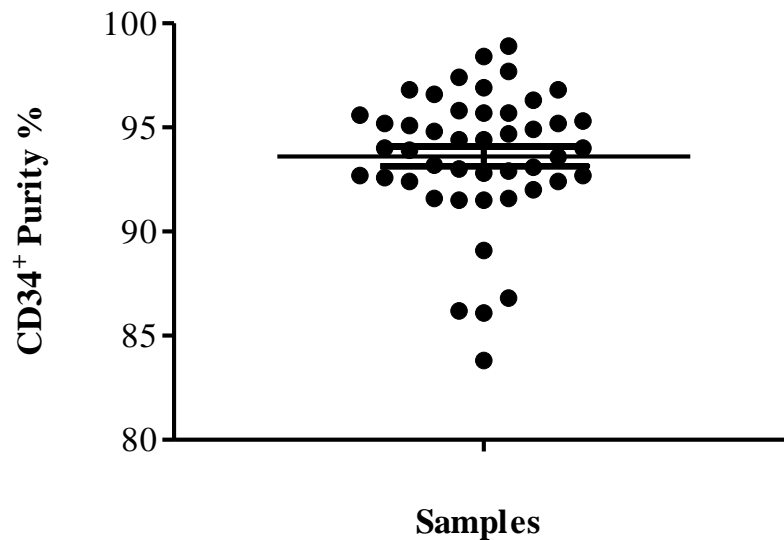


Figure 2.2. The spread in purity of the CD34⁺ samples as measured with the BD Accuri™ C6 flow cytometer. The average purity of the CD34⁺ cells was 93.62%. The error bar represents the standard error of the mean (SEM) of the different isolated samples.

2.4 Storage of PBMCs and CD34⁺ cells

2.4.1 Freezing Process

After isolation, PBMCs and CD34⁺ cells were centrifuged, the supernatant was removed and cells resuspended in ice-cold freeze media (90% FBS and 10% DMSO) and stored at -80°C. Each cryovial contained approximately 500 000 cells. The cryovials were placed in a 'Mister Frosty' which contained 100% isopropyl alcohol overnight (-80°C) and was transferred to the -80°C freezer the following day.

2.4.2 Thawing of CD34⁺ Cells

Immediately prior to irradiation, the cryovials were placed in a sterile preheated water bath (37°C) to gradually thaw. Next, each sample was transferred to a 15 mL conical tube containing approximately 7 mL complete culture medium (cRPMI, 20% FBS and 1% Pen-Strep) for PBMCs, or to 7 mL complete culture medium (cIMDM, 20% FBS and 0.5% Pen-Strep) for

CD34⁺ cells, respectively. Each cryovial was rinsed with 1 mL FBS to collect all the remaining cells. The CD34⁺ cells were centrifuged for 10 min at 1500 rpm and washed with 5 mL cIMDM or cRPMI. Finally, the cells were counted in trypan blue (1:1) with a haemocytometer. The CD34⁺ cell viability was examined, but not quantified. The CD34⁺ cells were transferred to the respective warm medium with or without growth factors and were placed in an incubator (37°C, 5% CO₂).

2.5 Immunophenotyping of Adult and Newborn PBMCs

Age related immunophenotypic changes of T lymphocytes were assessed through flow cytometric analysis of UCB (newborns) and APB (adults) T-lymphocyte subpopulations to determine the fraction of naive CD45RA⁺ and memory CD45RO⁺ subsets. The following panel of monoclonal antibodies (mAb) was used: CD3-PerCP, CD4-PE, CD8-APC, CD45RA-BB515, CD45RO-BB515 (all: BD Bioscience). Two separate FACS tubes were used in order to distinguish between naive CD45RA⁺ and memory CD45RO⁺ subsets of a donor, **tube one** contained CD3-PerCP, CD4-PE, CD8-APC, **CD45RA-BB515** antibodies and **the second tube** contained CD3-PerCP, CD4-PE, CD8-APC, **CD45RO-BB515** antibodies. Firstly, 50 µL (containing approximately 50 000 cells) mononuclear cells were transferred to the two separate FACS tubes and 2 µL of each mAb was added to the respective FACS tube. After 20 min at room temperature in the dark, cells were centrifuged (1500 rpm, 5 min) and the cell pellet was resuspended with 100 µL of PBS. Thereafter, 400 µL of PBS was added to the FACS tubes and the cell suspension was vortexed prior to the measurement. The analysis was performed with a BD Accuri™ C6 flow cytometer and approximately 50 000 – 100 000 T-lymphocyte events were measured for each sample.

2.6 *In vitro* Irradiation Experimental Set-up

2.6.1 Cobalt-60 (⁶⁰Co) gamma (γ)-ray Irradiation

In this study, ⁶⁰Co γ-rays were used as a reference radiation quality. The calibration and dosimetry for the ⁶⁰Co source was done using the IAEA TRS-398 protocol. The frozen CD34⁺

cells were thawed approximately 3 hours before irradiation and transferred to sterile 2.0 mL-cryogenic vials (NEST Biotechnology Co., Ltd., Wuxi, China) containing cIMDM, 20% FBS and 0.5% Pen-Strep (Lonza, Walkersville, MD, USA). The CD34⁺ cell suspension cultures were irradiated in sterile 2.0 mL-cryogenic vials (NEST Biotechnology Co., Ltd., Wuxi, China) with ⁶⁰Co γ -rays using a teletherapy unit (Theratron 780). Whereas, the PBMCs were aliquoted and irradiated in 5.0 mL-CELLSTAR® round-bottom polypropylene tubes (Greiner Bio-One GmbH, Frickenhausen, Germany). These round-bottom tubes were used immediately to initiate the PBMC micronucleus cultures.

The vials and round-bottom tube were placed between a 5 cm thick Perspex plate to ensure dose build-up and a 5 cm backscatter plate with a dose rate of 0.468 Gy/min for a 30 x 30 cm² field size at 75 cm Source to Surface Distance (SSD). The samples were exposed to radiation doses of 0.05 to 3 Gy depending on the specific assay performed. Sham-irradiated control samples were included for each assay. After irradiations, the samples in the vials were kept in a humidified incubator with 5% CO₂ at 37°C until termination time point.

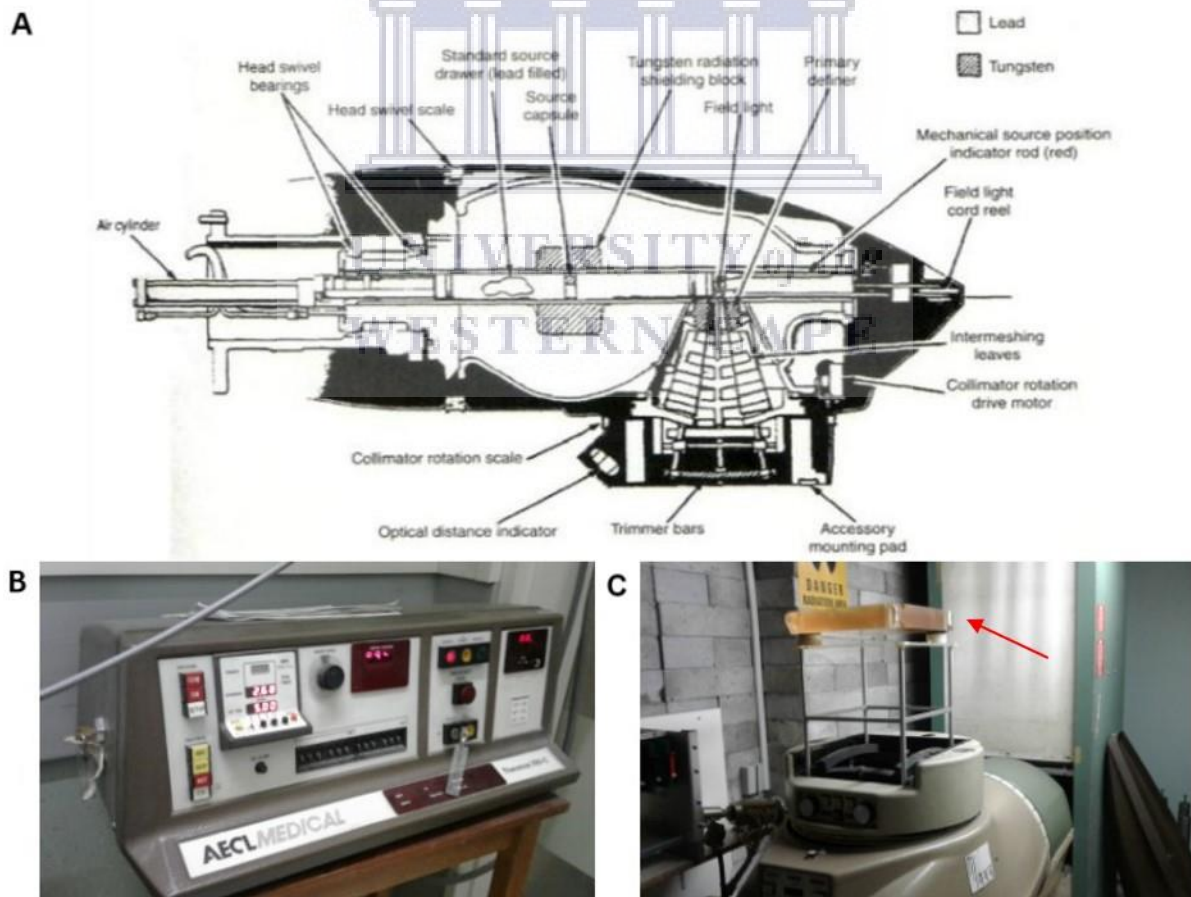


Figure 2.3. ⁶⁰Co γ -ray source. **A)** Schematic diagram of ⁶⁰Co γ -rays source (Theratron-780-source) at iThemba LABS, South Africa. **B)** Operation system of the source. **C)** Samples are placed underneath a 50 mm thick Perspex (indicated by red arrow) plate to ensure dose build-up and a 500 mm backscatter plate.

2.6.2 Fast p(66)/Be(40) Neutron Irradiations

Approximately 3 hours prior to irradiation, CD34⁺ cells were gradually thawed and resuspended in Iscove's Modified Dulbecco's Medium (Gibco, Dun Laoghaire, Dublin, Ireland) supplemented with 10% FBS (Gibco, Dun Laoghaire, Dublin, Ireland) and 0.5% Pen-Strep (Lonza, Walkersville, MD, USA). The thawed cells were transferred to sterile 2.0 mL-cryogenic vials (NEST Biotechnology Co., Ltd., Wuxi, China). The samples were exposed to a fast neutron beam using a Scanditronix clinical isocentric gantry. Here, the neutrons are produced by bombarding a thick Beryllium (Be) target with 66 MeV protons generated by the separated sector cyclotron (SSC) at the iThemba LABS Facility (iTTL, Cape Town, South Africa). The beam quality is thus inferred from the neutron energy spectrum with a fluence-weighted average energy of approximately 29.8 MeV for the 29 × 29 cm² field used (Jones *et al.*, 1992; Herbert *et al.*, 2007). A hydrogenous filter was used to reduce the contribution of thermal and epithermal neutrons. The source-to-phantom surface distance was 150 cm and irradiations were carried out at a gantry angle of 270°, resulting in a horizontal beam directed onto a water tank containing the CD34⁺ samples (depth in water tank: 5.2 cm). Samples were exposed to different doses ranging from 0.05 to 3 Gy at a dose rate of 0.400 Gy/min. Sham-irradiated control samples were included for each assay. The output factor (1.097 Gy/MU) was measured at the same position as the samples using an Exradin T2 thimble ionisation chamber, with a wall made from A-150 tissue-equivalent plastic with a 0.53 cm³ active chamber volume flushed with a propane-based tissue-equivalent gas. The ⁶⁰Co calibration factor that was used for the cross-calibration of the T2 chamber is traceable to the National Metrology Institute of South Africa (NMISA). Calibrations were performed according to the neutron dosimetry protocol as described in the ICRU Report 45 (Mijnheer *et al.*, 1989).



Figure 2.4. **A)** Entrance to the fast neutron therapy beam. **B)** Fast neutron clinical therapy beam at iThemba LABS, South Africa. **C)** CD34⁺ samples were positioned in jig for the parallel alignment of beam in a water phantom. **D)** The water phantom was pre-heated at 37°C for the samples to mimic the temperature of the human body. **E)** The source-to-phantom surface distance was 1500 mm and irradiations were carried out at a gantry angle of 270°, resulting in horizontal beam directed on a water tank containing the CD34⁺ samples. **F)** The 2 mL-cryogenic vials containing cIMDM and CD34⁺ sample which were placed in the jig. The samples were correctly positioned with aid of the lasers (green) as shown in **E**.

2.7 Semi-automated Cytokinesis Block Micronucleus (CBMN) Assay

2.7.1 Cell Cultures: Adult vs Newborn PBMCs

After PBMC isolation, approximately one million cells were diluted in 5 mL of cRPMI-1640 in culture tubes for each radiation dose. The cell viability was examined, but not quantified. The cultures were irradiated with 0.5, 1, 2, 3 and 4 Gy ⁶⁰Co γ-rays. Directly after irradiation, 100 μL phytohaemagglutinin (PHA) (25 mg/25 mL dH₂O; Sigma-Aldrich/Merck, St. Louis,

Missouri, United States) was added to each suspension culture which specifically stimulates the growth of peripheral blood T-lymphocytes at 37°C (5% CO₂) (Ocklind, 1986; Mire-Sluis *et al.*, 1987; Beinke *et al.*, 2016). After 23 h, 20 µL cytochalasin B (Cyto-B) (5 mg/3.3mL DMSO; Sigma-Aldrich/Merck St. Louis, Missouri, United States) was added to the cultures to block cytokinesis. Finally, 70 h after the initial start-up, suspension cultures were harvested (Fenech, 2007).

2.7.2 Fixation and Semi-Automated Analysis of Adult and Newborn CBMN Assay

The 5 mL suspension cultures were transferred to 15 mL conical tubes and centrifuged for 8 min at 1500 rpm. The supernatant was removed and the cell pellet was resuspended in ice cold 7 mL 0.075M KCl (5.6 g/1 L dH₂O; Sigma-Aldrich/Merck, St. Louis, Missouri, United States), added dropwise while stirred vigorously. The cold KCl induces hypotonic shock and allows cells to swell. This step was followed by centrifuging the samples for 8 min at 1500 rpm. The supernatant was removed and cells were fixed by dropwise addition of approximately 7 mL of methanol/acetic acid/ringer solution (4:1:5), while the samples were stirred vigorously. The fixed samples were stored overnight at 4°C. The following day, samples were centrifuged followed by the addition of 7 mL of the second fixation solution consisting of methanol/acetic acid (4:1). This step was repeated until the fixative was clear. The slides were prepared by removing the supernatant from each sample and adding approximately 45 µL of cell suspension onto the slides (Lasec®, Cape Town, South Africa). The slides were air dried for 30 min and were subsequently stained with mounting medium, Fluoroshield™ with DAPI (4',6-Diamidino-2-phenylindole dihydrochloride) (Sigma-Aldrich/Merck, St. Louis, Missouri, United States) and covered with a coverslip.

The Metasystems' Metafer 4 has been optimised to automatically scan the slides to detect BN T-lymphocytes and to count the number of MN in these BN cells using a classifier that was optimised in collaboration with Ghent University (Willems *et al.*, 2010; Herd *et al.*, 2016). After the automated scanning of the slides, the BN cells were then displayed in a computerised gallery where the BN cells were manually checked and false positive and negative MN scores were rectified through two scorers. At least two slides/condition were scored to provide at least 1000 scored cells per condition.

2.8 Manual Cytokinesis Block Micronucleus (CBMN) Assay for CD34⁺ Microcultures

2.8.1 Cell Cultures: CD34⁺ Cells

A main challenge was to obtain an adequate number of CD34⁺ cells per donor in order to perform different radiation doses and different radiation qualities in parallel. Therefore, we used a slightly modified version of the micro-culture method in comparison to PBMCs for which we had a large number of cells available, which was developed in a previous study (Vandevoorde *et al.*, 2016).

For the CBMN assay, the CD34⁺ cells were irradiated with 0.05, 0.5 or 1 Gy of ⁶⁰Co γ -rays or p(66)/Be(40) neutrons. After irradiation, CD34⁺ cells were cultured in a Sarstedt 48-well suspension plate (Biodex CC, Edenglen, South Africa) containing 500 μ L of cIMDM supplemented with 10% FBS and 0.5% Pen-Strep and a combination of recombinant haematopoietic cytokines, 100 ng/mL stem cell factor (SCF), 100 ng/mL FLT3 ligand and 20 ng/mL thrombopoietin (TPO) to stimulate the expansion of the CD34⁺ cells (all cytokines from Miltenyi Biotec Inc., Bergisch Gladbach, Germany). Two cultures of each condition were seeded and each well contained $\sim 10^5$ cells per 500 μ L cIMDM. The irradiated cells were kept at 37°C in a humidified 5% CO₂ atmosphere incubator for 70 h. After 23 h, Cyto-B (0.75 mg/mL) (Sigma-Aldrich/Merck Co. LLC, St. Louis, Missouri, United States) was added. Cyto-B is an inhibitor of microfilament ring assembly which is required to inhibit cytokinesis and allows to distinguish once-divided (mononucleated) cells based on their binucleated (BN) appearance (Fenech, 2007).

The CD34⁺ cells were resuspended 48h post stimulation in the 48-well suspension plate to reduce clumping of the cells. Finally, 70 h after commencement of the stimulation process, the cell suspension from each well ($\sim 500 \mu$ L) was resuspended gently to reduce cellular clumping and each well was rinsed with PBS. The cell suspension was transferred to a 2 mL Eppendorf tube followed by rinsing with 0.5 mL PBS. Subsequently, the cells were centrifuged for 8 min at 1680 rpm (Eppendorf 5810R centrifuge, Hamburg, Germany) and the supernatant was discarded. In the following steps, the cells were exposed to cold 450 μ L KCl (0.0075 M), which was added dropwise while stirred vigorously. The KCl supernatant was removed after centrifugation (8 min, 1680 rpm) and overnight fixation by adding 500 μ L of the first fixation solution (3:1:4, methanol/acetic acid/ringer solution) dropwise, while stirred vigorously. The next day, the cells were fixed by adding 500 μ L of the second fixation solution (3:1,

methanol/acetic acid) while stirred vigorously. After centrifugation (8 min, 1680 rpm), the supernatant was carefully removed (~460 µL) without disturbing the cell pellet. Thereafter, the cell pellet was resuspended in the remaining fixative and approximately 20 µL cell suspension was cautiously dropped on clean dry slides (two slides per dose). The slides were allowed to air-dry for 15 min and the samples were stained with a 0.1% aqueous solution of acridine orange (AO) (100 µL AO/ 1 mL Gurr buffer, Gibco, Dun Laoghaire, Dublin, Ireland) for 1 min followed by rinsing in Gurr buffer for 1 min. The fixed cells on the slide were then covered with a coverslip, mounted in Gurr buffer, and the MN manually scored in BN cells using a fluorescent Zeiss Axio Imager A1 microscope (Carl Zeiss AG, Oberkochen, Germany) at 200X magnification. Approximately 500 BN cells were scored per slide (two slides per sample condition).

2.8.2 Nuclear Division Index (NDI)

The nuclear division index (NDI) was calculated, which represents the proliferation rate of the cells, based on the method described by Fenech (Fenech, 2007):

$$\text{NDI} = (M_1 + 2M_2 + 3M_3 + 4M_4)/N$$

where $M_1 - M_4$ indicate the number of cells with 1 – 4 nuclei and N the total number of cells scored. For this, 500 viable cells in each sample were scored to measure the proliferation following IR exposure.

2.9 γ -H2AX Foci Assay

2.9.1 Cell Cultures

For the DNA DSB repair kinetics experiments, the CD34⁺ cells were incubated (37°C, 5% CO₂) in microcultures (~800 000 cells/cryovial) with 500 µL cIMDM for 1 – 2 h, prior to irradiations. The CD34⁺ cell suspensions were irradiated with 0.5 Gy ⁶⁰Co γ -rays or p(66)/Be(40) neutrons and incubated for 2 or 18 h post-irradiation to allow foci formation and repair. After 2 h or 18 h, the cells were placed on ice for 10 – 15 min to inhibit DDR. Next, cell suspensions of approximately 400 000 cells/250 µL were centrifuged onto coated slides (X-tra

adhesive slides, Leica Biosystems, Buffalo Grove, IL, USA) via a Cytospin funnel using a cytocentrifuge (Cellspin I, Tharmac® GmbH). Two slides were prepared for each exposure condition.

2.9.2 Immunocytochemistry

The cell containing section on each slide was encircled with a hydrophobic barrier pen (Dako pen, Diagnostech (Pty) Ltd., Johannesburg, South Africa). The cells were fixed in 3% paraformaldehyde (PFA) (Sigma-Aldrich/Merck, St. Louis, Missouri, United States) for 20 min, followed by storage overnight in PBS containing 0.5% PFA. The following day, fixed cells were washed with PBS for 5 – 10 min, followed by covering the cells on the slides with 100 μ L ice cold PBS-Triton X-100 (0.2%, Gibco, Dun Laoghaire, Dublin, Ireland) for 10 min. The cells were blocked by washing for 10 min with 1% bovine serum albumin (BSA) BSA-PBS (Roche, Sigma-Aldrich/Merck, St. Louis, Missouri, United States) for three consecutive times. Immunocytochemistry was performed using the monoclonal primary antibody (Ab) against the γ -H2AX protein (Biologend, 1 μ L anti- γ -H2AX/500 μ L blocking buffer, Biocom Africa (Pty) Ltd., Centurion, South Africa) for 1 h. After washing in blocking buffer (3 times for 10 min), cells were incubated with the polyclonal secondary antibody DAM-TRITC (1 μ L:1000 μ L in blocking buffer, DakoCytomation, Haverlee) for 1 h in the dark. After incubation, cells were washed in PBS (10 min for 3 times). Before covering the slides with a clean coverslip, a drop of Fluoroshield™ with DAPI (Sigma-Aldrich/Merck, St. Louis, Missouri, United States) (~35 μ L) was added and stained slides were left overnight at 4°C.

2.9.3 Automated Slide Scanning and Detection of Foci

The stained γ -H2AX foci slides were scanned with the Metafer 4 scanning system (MetaSystems, Altlussheim, Germany, 40X objective). The Metafer automatically scores the amount of foci in each cell as described by Vandersickel *et al.* (2010). The nuclei were captured in the DAPI channel using an optimised classifier for CD34⁺ cells. Once the nuclei were selected, the TRITC filter was used to count the number of foci/cell. These images were stored simultaneously and presented in the image gallery, which comprises an overview of the selected nuclei containing foci.

2.10 Apoptosis Assay

2.10.1 Cell Cultures

Evaluation of possible apoptosis induction in the irradiated microcultures (100 000 cells/1 mL/cryovial) were irradiated with 0.5, 1 and 3 Gy of ^{60}Co γ -rays or p(66)/Be(40) neutrons and incubated for 18 or 42 h respectively at 37°C in a humidified incubator containing 5% CO_2 . After incubation, CD34^+ cell suspensions were transferred from the cryovials to FACS tubes and, the cryovials rinsed again with 1 mL PBS to collect remaining cells. The samples in the FACS tubes were centrifuged for 10 min at 1680 rpm.

2.10.2 Annexin V Staining and Analysis by Flow Cytometry

After centrifugation, the supernatant was removed and the cell pellet was resuspended in 100 μL 1X Annexin V Binding Buffer (1:10 in dH_2O , BD Biosciences, United States). Consequently, 5 μL of FITC Annexin V and 5 μL PI was added to the tubes simultaneously for identification of early and late apoptotic cells. This was followed by vigorous stirring and incubation for 15 min at room temperature in the dark. Prior to flow cytometry analysis, 400 μL of 1X Binding Buffer (BD Biosciences, United State) was added to each tube to facilitate the binding of annexin V to phosphatidylserine and samples were analysed within 1 h.

2.11 Statistical Analysis

The results from the individual experiments were averaged and the corresponding standard error of the mean (SEM) calculated. Statistical analysis was performed using Microsoft Office Excel 2019 (Microsoft Corporation, Washington DC, USA) and GraphPad Prism Software Version 5.01 for Windows (GraphPad Software, San Diego, CA, USA). FlowJo™ v10.7 (BD Bioscience, United States) was employed to analyse flow cytometry data. The numbers of experiments (n) are indicated in each figure caption. As a result of limited availability of beamtime, not all the experiments were performed on the same day, but sham-irradiated control samples were included in each experiment. Shapiro-Wilk tests were performed to assess normality of the data. Kruskal Wallis test was performed for statistical analysis of the CBMN

(semi-automated and manual scoring), apoptosis data and CD45RA/RO fractions. Analysis of variance (ANOVA) was carried out on the NDI and γ -H2AX foci assay data. A significance level of 0.05 was used in all tests. All statistical tests were 2-sided, and p -values smaller than 0.05 (*) were considered statistically significant, $p < 0.01$ (**) highly significant and $p < 0.001$ (***) extremely significant.



CHAPTER 3: RESULTS SECTION 1

The results of this PhD dissertation are presented in two sections. **Section 1** covers the *in vitro* radiosensitivity of CD34⁺ after ⁶⁰Co γ -rays and neutron irradiation. **Section 2** entails the age dependency of cellular radiosensitivity in lymphocytes isolated from adult peripheral blood and umbilical cord blood.



UNIVERSITY *of the*
WESTERN CAPE

“I was taught that the way of progress was neither swift nor easy.”

– Marie Curie

3.1 DNA Damage Response of CD34⁺ Cells to High-LET Neutron Irradiation

3.1.1 Radiation-Induced Chromosomal Damage in CD34⁺ Cells

The CBMN assay has become a well-established standard method for measuring DNA damage in human peripheral blood lymphocytes (PBL) after IR exposure (Fenech, 2007; Vral, Fenech and Thierens, 2011). By scoring MN in BN cells that have undergone one cycle of cell division, confounding effects caused by differences in cell division kinetics can be prevented, as the inhibition of cytokinesis by Cyto-B allows one to discriminate between cells that did go into cell division and cells that did not (Fenech, 2007). For this study, a previously established micro-culture CBMN assay was adapted in order to expose isolated CD34⁺ cells of the same donors (n = 12) to ⁶⁰Co γ -rays and neutron irradiation after cryopreservation (Vandevoorde *et al.*, 2016). **Figure 3.1** shows the number of radiation-induced MN in BN CD34⁺ cells, reflecting chromosome breakage or whole chromosome loss after exposure to radiation doses of 0.05, 0.5 and 1 Gy ($p < 0.001$). For both radiation qualities, an apparent dose-dependent increase in the frequency of radiation-induced MN was observed. Although there was no statistically significant difference in MN yields at the lowest dose of 0.05 Gy between ⁶⁰Co γ -rays and neutrons ($p > 0.05$); a significantly higher MN frequency was observed at both 0.5 and 1 Gy for neutrons ($p < 0.001$). The lowest dose of 0.05 Gy resulted in an average MN frequency of 2.79 ± 0.38 MN/1000 BN cells and 3.92 ± 0.74 MN/1000 BN cells after ⁶⁰Co γ -rays and neutron irradiation respectively. This is significantly higher than the average background values (0 Gy) of 1.25 ± 0.33 MN/1000 BN cells for the ⁶⁰Co γ -ray experiments ($p < 0.01$) (**Figure 3.2, A**) and 1.46 ± 0.23 MN/1000 BN cells for neutron irradiation experiments ($p < 0.01$) (**Figure 3.2, B**). Not all the irradiation experiments could be performed on the same day, therefore separate control (0 Gy) cultures were set-up for both radiation qualities. For both ⁶⁰Co γ -rays (**Figure 3.2.1**) and neutrons (**Figure 3.2.2**), there was a significant increase in the number of MN observed in the BN cells, with an observable higher frequency of radiation-induced MN after the intermediate (**Figure 3.2.2, C**) and highest dose (**Figure 3.2.2, E**) of high-LET neutrons compared to the intermediate (**Figure 3.2.1, C**) and highest dose (**Figure 3.2.1, E**) of low-LET ⁶⁰Co γ -rays.

RBE is normally calculated at the same level of biological effect. However, the number of dose points in this study was too limited to fit a dose response curve and therefore, a biological enhancement ratio was calculated and is presented in **Table 3.1**. The biological enhancement is the ratio of the neutron induced MN over the ⁶⁰Co γ -ray induced MN mean values, ranging

between 1.61 and 2.79 for doses of 0.05 to 1 Gy, with a maximum difference between ^{60}Co γ -ray and neutron MN yields observed at 0.5 Gy (Table 3.1). As expected, these enhancement ratios indicate that fast neutrons, which are considered to be a high-LET radiation, yield a higher MN frequency compared to the reference ^{60}Co γ -ray irradiation in HSPCs at all doses.

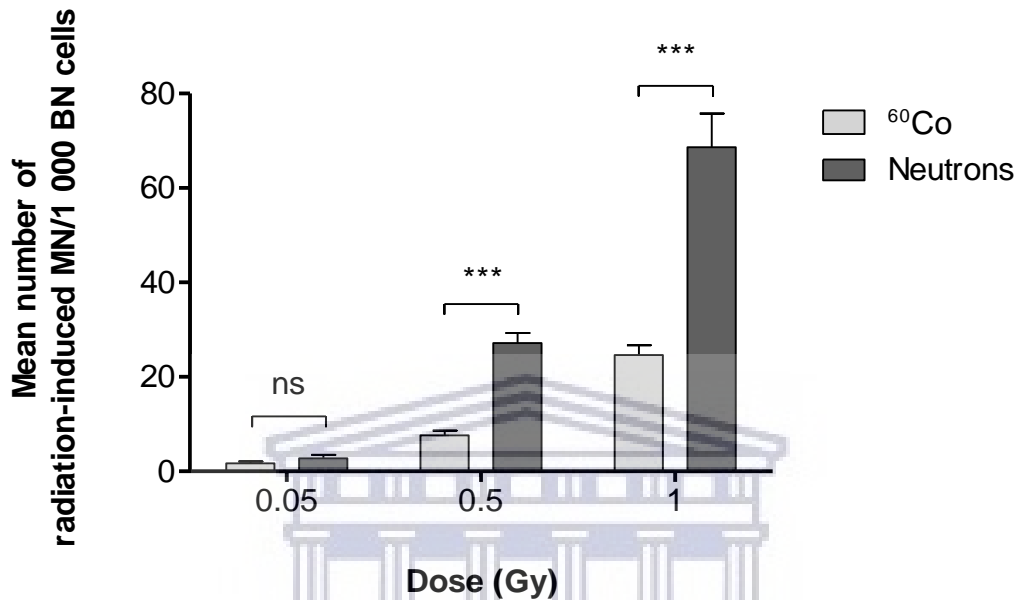


Figure 3.1. This graph shows the mean number of MN in $\text{CD}34^+$ ($n = 12$) induced by different doses (0.05, 0.5 and 1 Gy) of ^{60}Co γ -rays and $p(66)/\text{Be}(40)$ neutron irradiation. The number of MN induced by the irradiation was obtained by subtracting the mean number of MN in the non-irradiated controls (0 Gy) from the mean MN number scored in the irradiated samples. MN yields were significantly higher post-neutron irradiation compared to ^{60}Co γ -rays ($***p < 0.001$). Error bars represent the standard error of the mean (SEM) of the 12 different donors for each radiation quality. At least 1,000 BN cells were scored for each donor per condition. No statistically significant difference is indicated by ns.

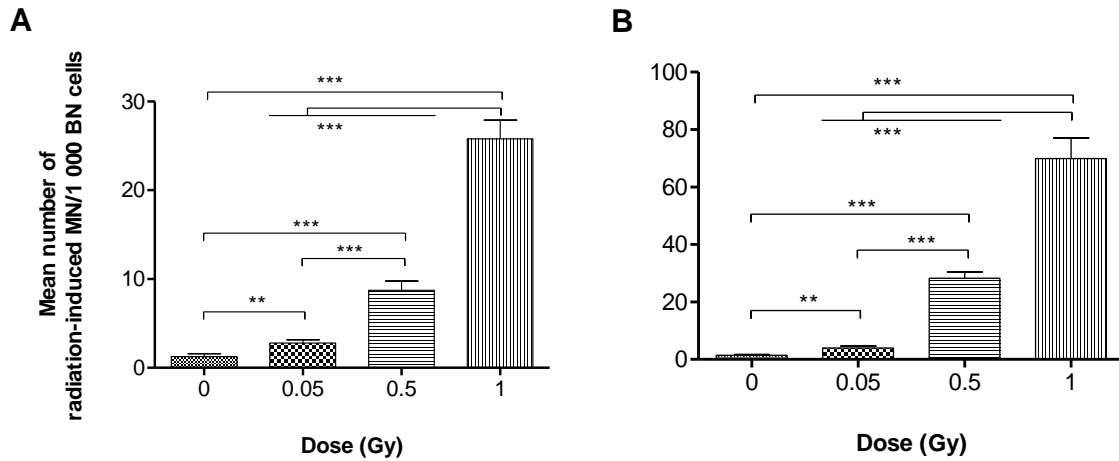


Figure 3.2. These figures show the mean number of MN in CD34⁺ (n=12) induced by different doses (0, 0.05, 0.5 and 1 Gy) of ⁶⁰Co γ-rays (A) and neutrons (B). The number of MN induced by the irradiation was obtained by scoring at least 1,000 BN cells for each donor per condition. The lowest dose of 0.05 Gy resulted in significantly higher MN frequency than the average background values (0 Gy) of 1.25 ± 0.33 MN/1000 BN cells for the ⁶⁰Co γ-ray experiments (** $p < 0.01$) (A) and for neutron irradiation samples (** $p < 0.01$) (B). For each radiation modality, the MN yields were significantly higher for 0.5 Gy (** $p < 0.001$) and 1 Gy dose (** $p < 0.001$). Error bars represent the standard error of the mean (SEM) of the 12 different donors for each radiation modality.

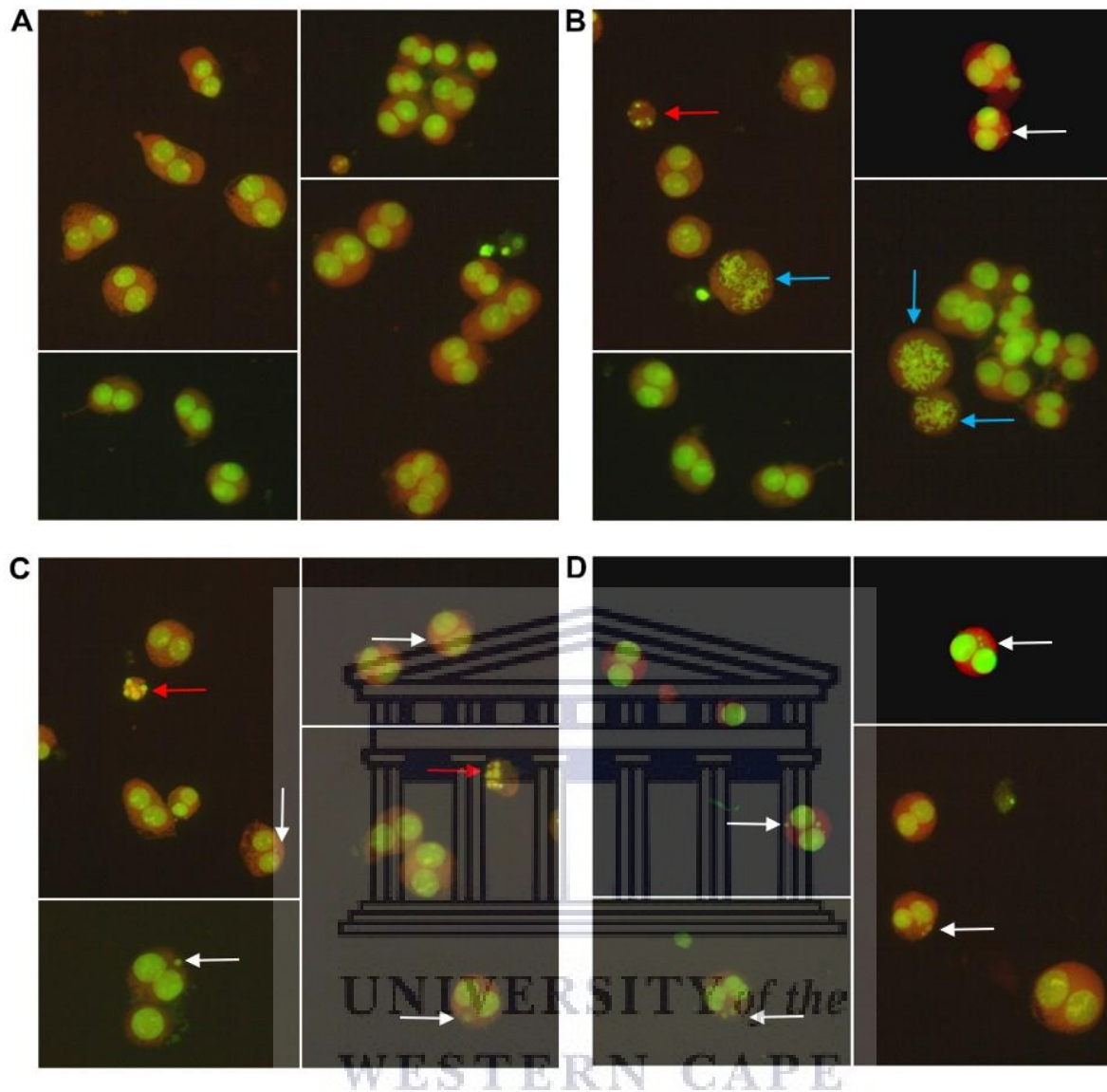


Figure 3.2.1. Sham-irradiated controls (0 Gy) with multiple BN CD34⁺ cells are shown in (A). The ⁶⁰Co-rays radiation induced MN within BN CD34⁺ cells after irradiation with lowest dose of 0.05 Gy (B), an intermediate dose of 0.5 Gy (C) and highest dose of 1 Gy (D). The intermediate dose of 0.5 Gy resulted in multiple BN cells with one MN (C), while the highest dose of 1 Gy resulted in BN cells containing two or three MN (D). White arrows indicate MN within BN cells, red arrows point out possible apoptotic cells and blue arrows indicate cell division.

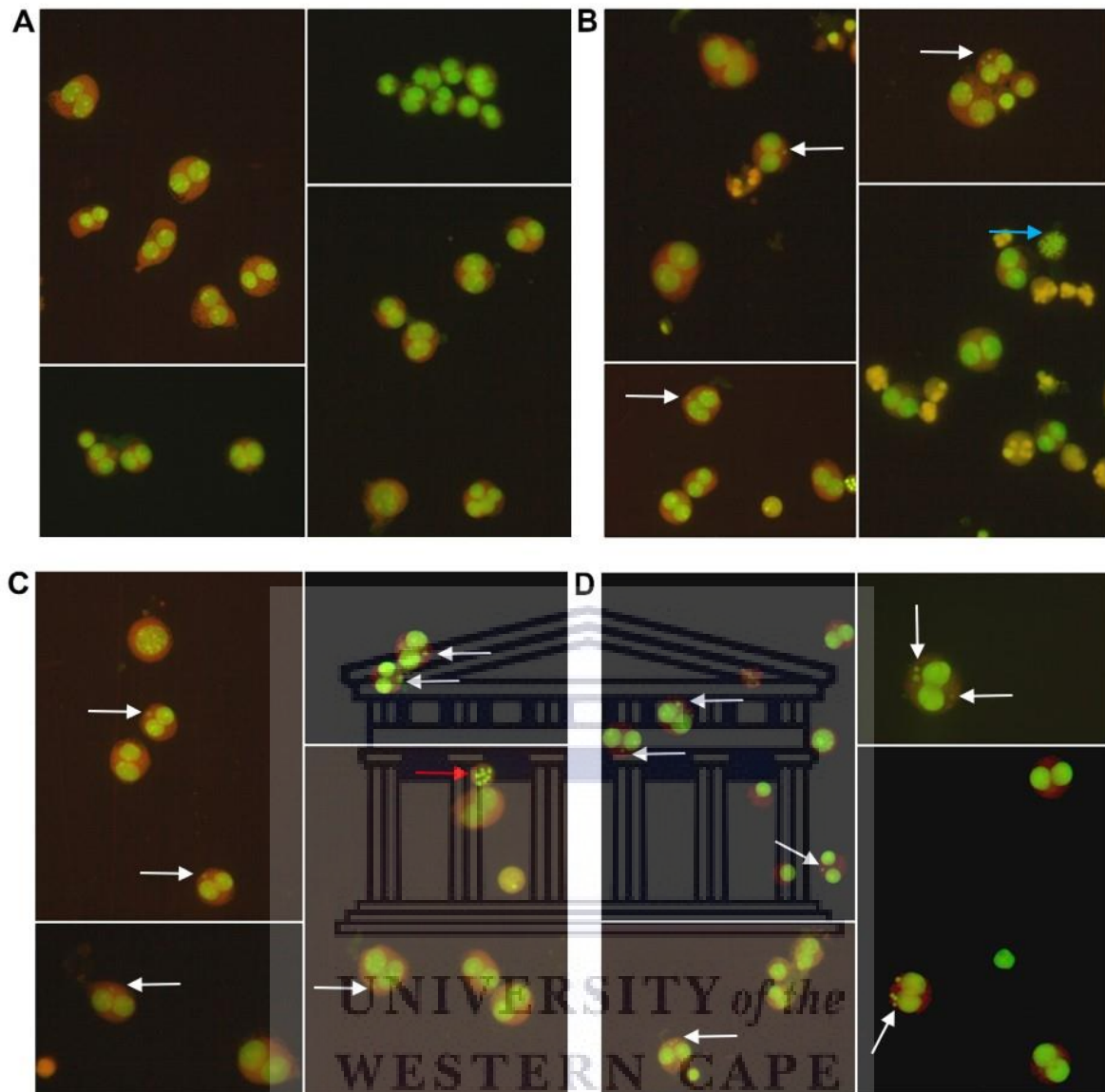


Figure 3.2.2. Sham-irradiated controls (0 Gy) of the neutron experiments with multiple BN CD34⁺ cells are shown in (A). Neutron radiation induced MN within BN CD34⁺ cells after irradiation with 0.05 Gy (B), 0.5 Gy (C) and 1 Gy (D). After irradiation with the lowest dose, the CD34⁺ cells continued cell division and BN cells with one or two MN can be observed in (B). The intermediate dose of 0.5 Gy resulted in multiple BN cells with one MN (C), whereas the highest dose of 1 Gy resulted in BN cells containing two, three or four MN shown in (D). White arrows indicate MN within BN cells, red arrows point out possible apoptotic cells and blue arrows indicate cell division.

Table 3.2. Ratio of the mean number of radiation-induced MN at different dose points (Neutrons/⁶⁰Co). The propagation of uncertainty was calculated based on the standard deviations of the induced MN values.

Dose (Gy)	0.05	0.5	1
Biological enhancement ratio	1.61 ± 1.26	3.55 ± 0.53	2.79 ± 0.47

In order to assess the impact of the two radiation qualities and the different radiation doses on the CD34⁺ cell proliferation, the nuclear division index (NDI) was calculated. Quantification of the mitotic activity of the CD34⁺ cells provides an indication of the cytotoxic effect of the irradiation exposure on the CD34⁺ cell proliferation as cells with extensive chromosomal damage will fail to undergo cell division and would not be reflected in the final number of BN cells that are scored. Although there was an apparent decreasing trend in the NDI with increasing dose for both radiation qualities, no statistically significant difference was found between ⁶⁰Co γ -ray and neutron irradiation ($p > 0.05$) (Figure 3.3). In addition, all average NDI values were between 1.0 and 2.0, illustrating that the CD34⁺ CBMN culture method was successful (Fenech, 2007). However, there was a significance decrease in the NDI of each individual donor when the absorbed dose of 1 Gy was compared to the control (0 Gy) NDI for each radiation quality ($p < 0.001$). This result suggests that the CD34⁺ cell division was affected by the exposure to 1 Gy and fewer cells went into mitosis. Overall, the average MN frequency increased with the radiation dose and was significantly higher after neutron irradiation compared to ⁶⁰Co γ -rays, while the average NDI remained consistent for both radiation qualities. Similar visual observations were seen in Figure 3.3.1 and Figure 3.3.2 after ⁶⁰Co γ -rays and neutron irradiation, respectively. This confirms optimal culture conditions and the fact that CD34⁺ cells were still undergoing mitosis post-radiation.

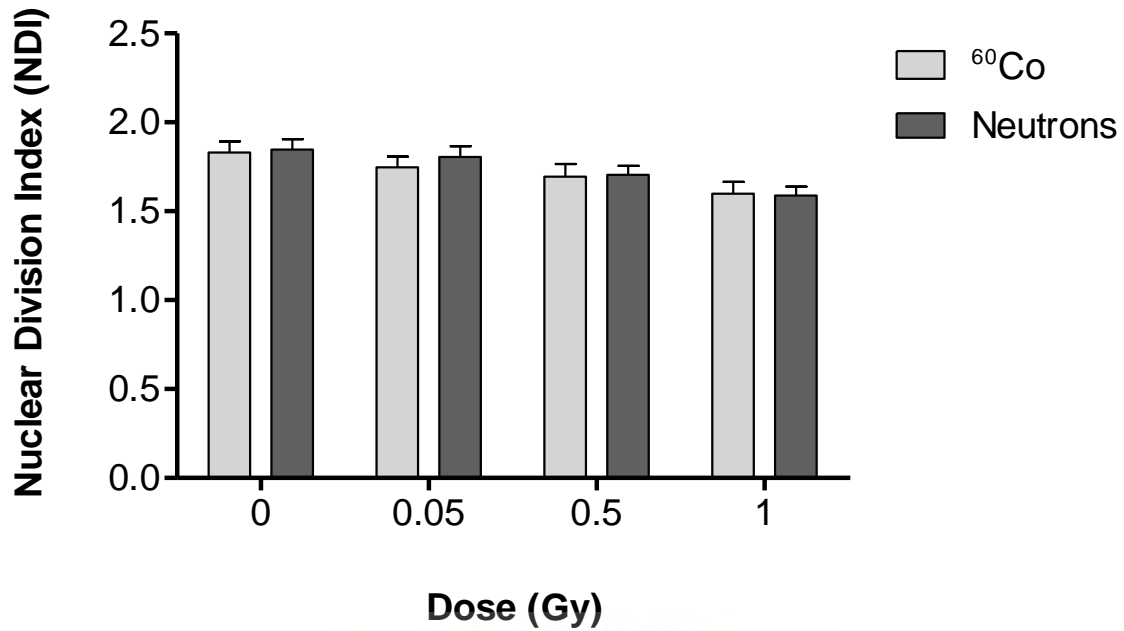


Figure 3.3. The nuclear division index (NDI) was calculated to compare the proliferation status of the micro-culture CBMN assay for the CD34⁺ samples irradiated with different radiation qualities with doses of 0, 0.05, 0.5 and 1 Gy. Error bars represent the standard error of the mean (SEM) of the 12 different donors for each radiation modality. At least 500 viable cells were scored for each donor per condition.

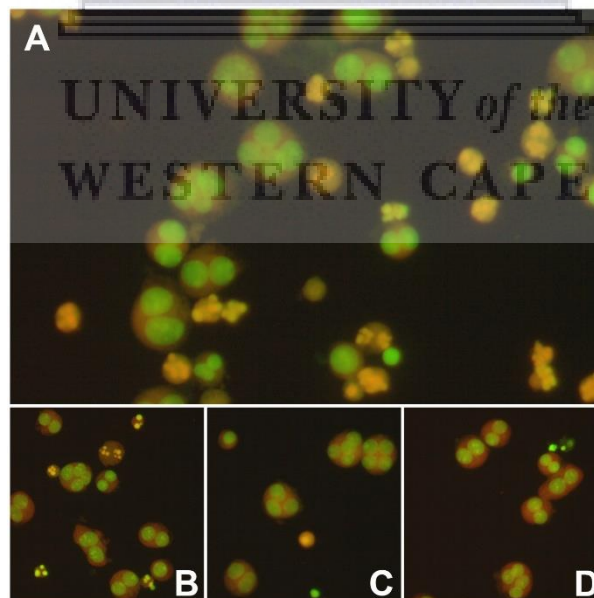


Figure 3.3.1. The nuclear division index of CD34⁺ cells post ⁶⁰Co- γ ray irradiation with sham-irradiated controls (0 Gy) (A), 0.05 Gy (B), 0.5 Gy (C) and 1 Gy (D). This figure shows only cell division following IR exposure, and not NDI quantification.

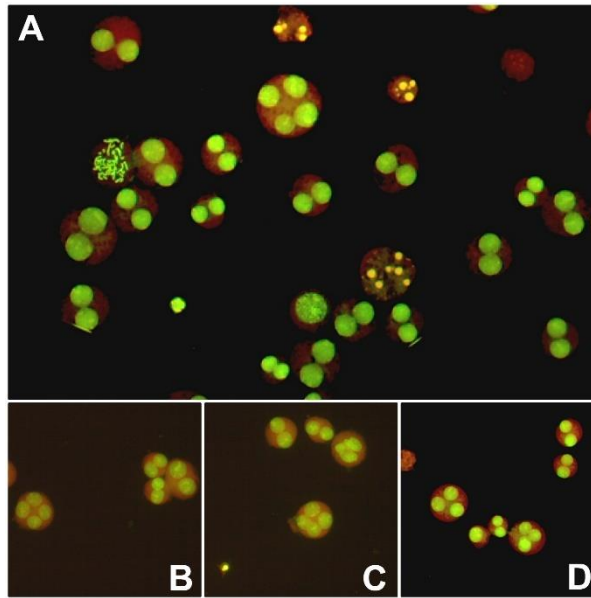


Figure 3.3.2. The nuclear division index of CD34⁺ cells post **neutron** irradiation with sham-irradiated controls (0 Gy) (A), 0.05 Gy (B), 0.5 Gy (C) and 1 Gy (D). This figure shows only cell division following IR exposure, and not NDI quantification.

3.1.2 DNA Double-Strand Breaks (DSBs) Formation and Repair After ⁶⁰Co- γ -rays and Neutron Irradiation

DNA DSBs are considered to be the most destructive and lethal form of DNA damage and the γ -H2AX foci assay is considered to be a highly sensitive technique to evaluate DNA DSB formation and repair following exposure to IR (Jakl *et al.*, 2020). In this study, the mean number of DNA DSBs was investigated in isolated CD34⁺ cells at 2 and 18 h post-irradiation (0.5 Gy) with low-LET ⁶⁰Co γ -rays and high-LET neutrons. As shown in Figure 3.4, the initial γ -H2AX foci formation after exposure to neutrons was significantly higher than after ⁶⁰Co γ -ray irradiation ($p < 0.05$). This was confirmed by images taken with the Metafer System (Figure 3.4.1, B and Figure 3.4.2, B) post-irradiation with 0.5 Gy ⁶⁰Co γ -rays and neutrons. This indicates that high-LET neutron irradiation induced a higher number of DNA DSBs at 2 h post-irradiation in CD34⁺ cells compared to ⁶⁰Co γ -rays (Figure 3.4.1 and 3.4.2). While it is expected that the repair kinetics of the more complex DNA damage induced by neutron irradiation would be slower compared to DNA DSB repair observed for ⁶⁰Co γ -rays, no statistically significant difference could be observed at 18 h post-irradiation. Furthermore, despite the fact that no difference in residual γ -H2AX foci levels could be observed between the two radiation modalities ($p > 0.05$), the residual values at 18 h were still elevated compared to sham-irradiated controls samples at 18 h (see Figure 3.4.1, D and Figure 3.4.2, D).

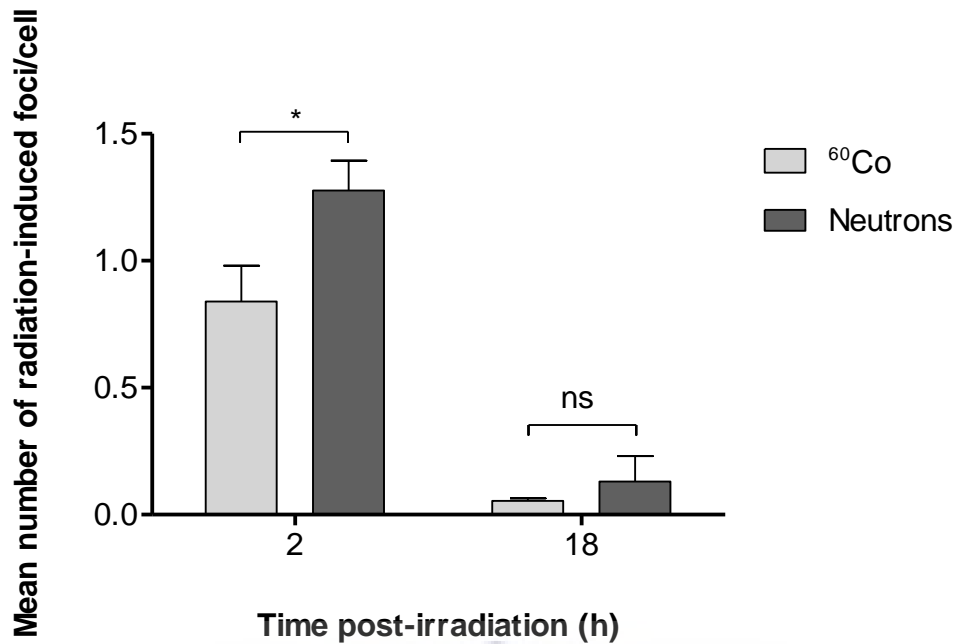


Figure 3.4. This figure shows the mean number of radiation-induced γ -H2AX foci per CD34⁺ cell at 2 and 18 h post-irradiation with 0.5 Gy. The number of radiation-induced γ -H2AX foci was obtained by subtracting the mean number of γ -H2AX foci in the non-irradiated controls from the mean γ -H2AX foci number scored in the irradiated samples. The number of radiation-induced γ -H2AX foci was significantly different between ⁶⁰Co γ -rays (n = 6) and neutron (n = 9) radiation at 2 h (* p < 0.05), but after 18 h no significant difference (p > 0.05) was observed between the two radiation qualities. Error bars represent standard error of the mean (SEM) of the different donors.

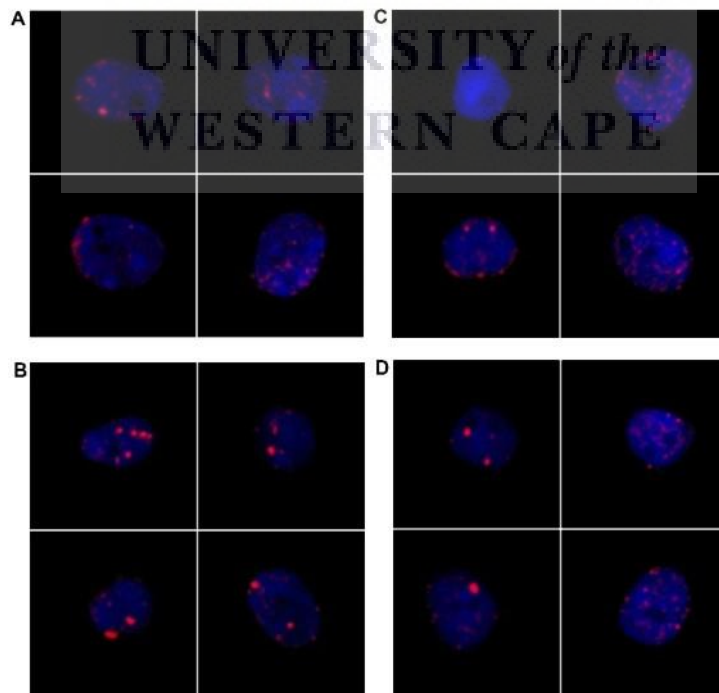


Figure 3.4.1. The images were retrieved from the Metafer automatic image analysis software system, using a 40X objective, representing γ -H2AX foci in CD34⁺ cells exposed to 0.5 Gy low-LET ⁶⁰Co γ -rays radiation after 2 h

(A; sham-irradiated controls, B; 0.5 Gy) and 18 h (C; sham-irradiated controls, D; 0.5 Gy), respectively. Red dots indicate γ -H2AX foci, while the nuclei are stained blue by using Fluoroshield™ with DAPI.

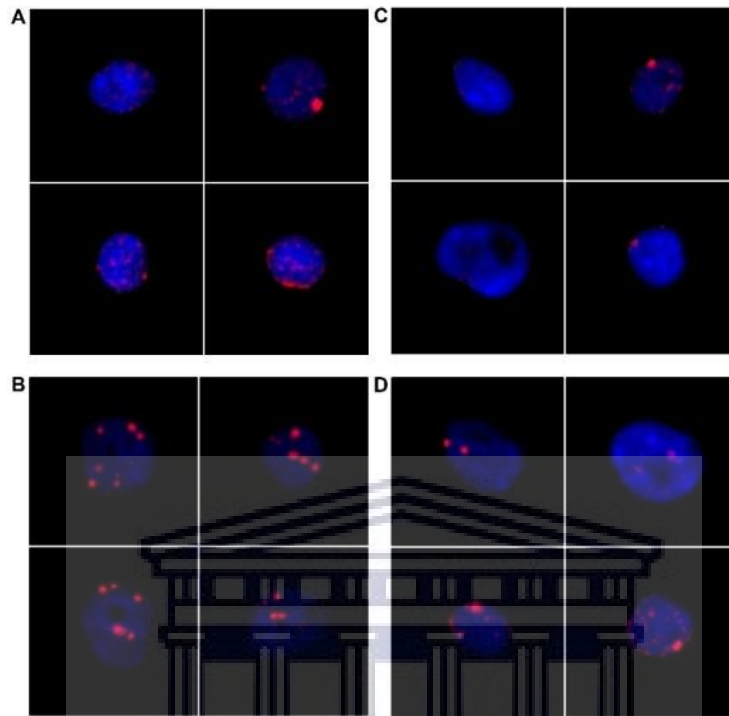


Figure 3.4.2. The images were retrieved from the Metafer automatic image analysis software system, using a 40X objective, representing γ -H2AX foci in CD34⁺ cells exposed to 0.5 Gy **high-LET neutron radiation** after 2 h (A; sham-irradiated controls, B; 0.5 Gy) and 18 h (C; sham-irradiated controls, D; 0.5 Gy), respectively. Red dots indicate γ -H2AX foci, while the nuclei are stained blue with DAPI.

3.1.3 Radiation-Induced Apoptosis in CD34⁺ Cells

When the radiation-induced DNA damage in the CD34⁺ cells is too extensive, this can lead to the induction of apoptosis. In this study, the Annexin-V/PI assay was used to assess the fraction of live (Annexin-V⁻/PI⁻), early (Annexin-V⁺/PI⁻) and late (Annexin-V⁺/PI⁺) apoptotic cells at 18 and 42 h after ⁶⁰Co γ -rays and neutron irradiation respectively. The percentage (%) of cells identified in late apoptosis is determined by gating for double positivity for Annexin V-FITC and PI. The gating strategies for flow cytometry analysis were performed using FlowJo™ v10.7 (BD Bioscience, United States) (see Figures 3.5.1 – 3.5.4) First, CD34⁺ cells were gated based on forward scatter (FSC) and side scatter (SSC) (see all Figures 3.5.1 – 3.5.4 A, D), followed by exclusion of doublets (see all Figures 3.5.1– 3.5.4 B, E). During the early stages of apoptosis, cells lose their membrane phospholipid asymmetry and expose

phosphatidylserine (PS) on the outer leaflet of the plasma membrane. This is generally considered to be an early event in apoptosis, which precedes nuclear condensation. At the onset of the externalisation of PS, the membrane integrity has not been compromised. Annexin V was shown to have a high affinity for PS and is generally accepted as a marker for early apoptosis. By combining Annexin V-FITC and DNA stain, such as PI, it was possible to identify CD34⁺ cells in late apoptosis (see all Figures 3.5.1 – 3.5.4 C, F). As clearly seen in the gating strategies, 42 h post-irradiation, the cells irradiated with 3 Gy ⁶⁰Co γ -rays (Figure 3.5.2, F) showed more cells in late apoptosis compared to cells irradiated with 3 Gy neutrons (Figure 3.5.4, F).

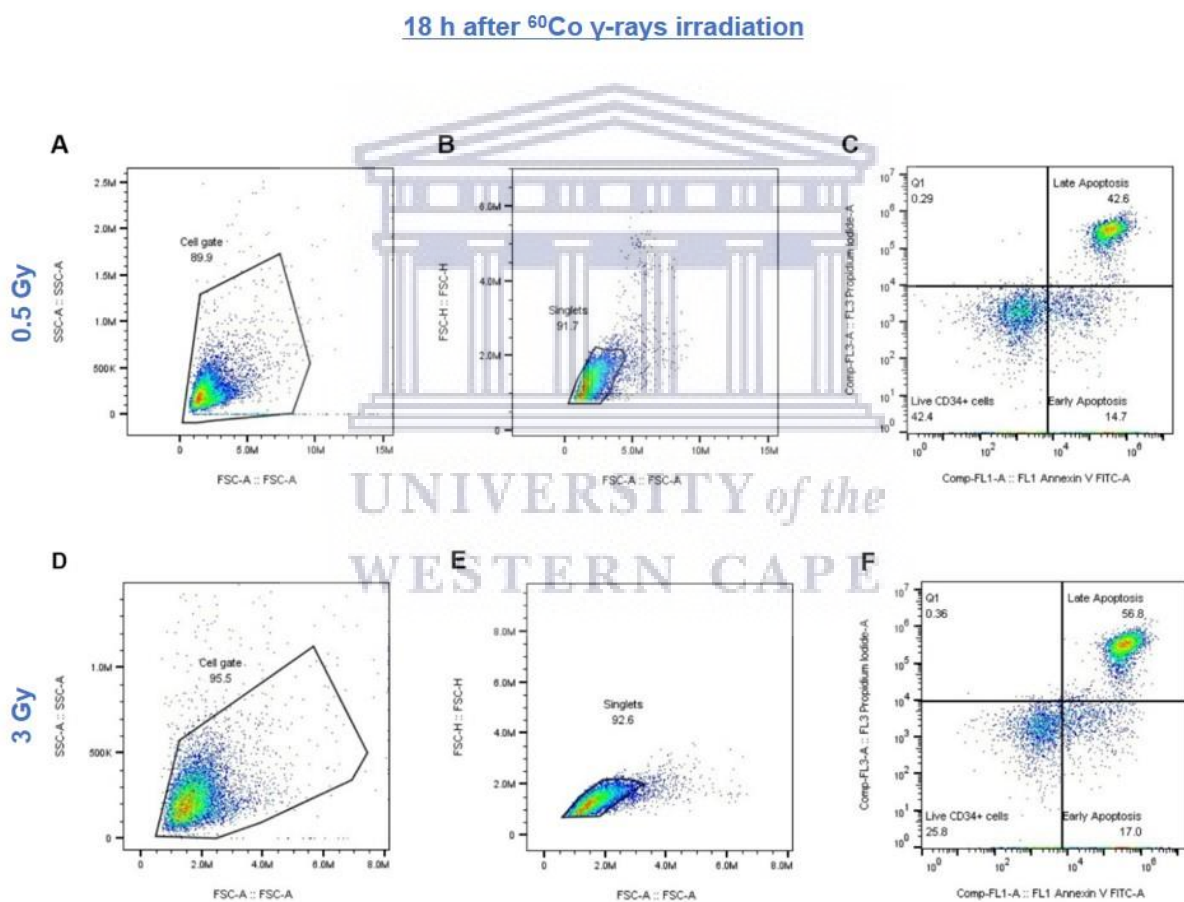


Figure 3.5.1 The gating strategy for the Annexin-V/PI apoptosis analysis. CD34⁺ cells were gated on forward (FSC) versus side scatter (SSC) to select the cell population (**A and D**). The cells were gated on FSC-Height (FSC-H) vs FSC-Area (FSC-A) to exclude all the doublets and to generate the singlets gate (**B and E**). All the subpopulations were analysed on the Annexin V-FITC versus PI scatter for live, early and late apoptosis at **18 h** after ⁶⁰Co γ -rays radiation (**C and F**). The upper part (**A – C**) represents the gating strategy of CD34⁺ cells irradiated with a low dose of ⁶⁰Co γ -rays at **0.5 Gy**; and the lower part (**D – F**) CD34⁺ cells irradiated with a high dose at **3 Gy** which resulted in a higher percentage of late apoptosis.

42 h after ^{60}Co γ -rays irradiation

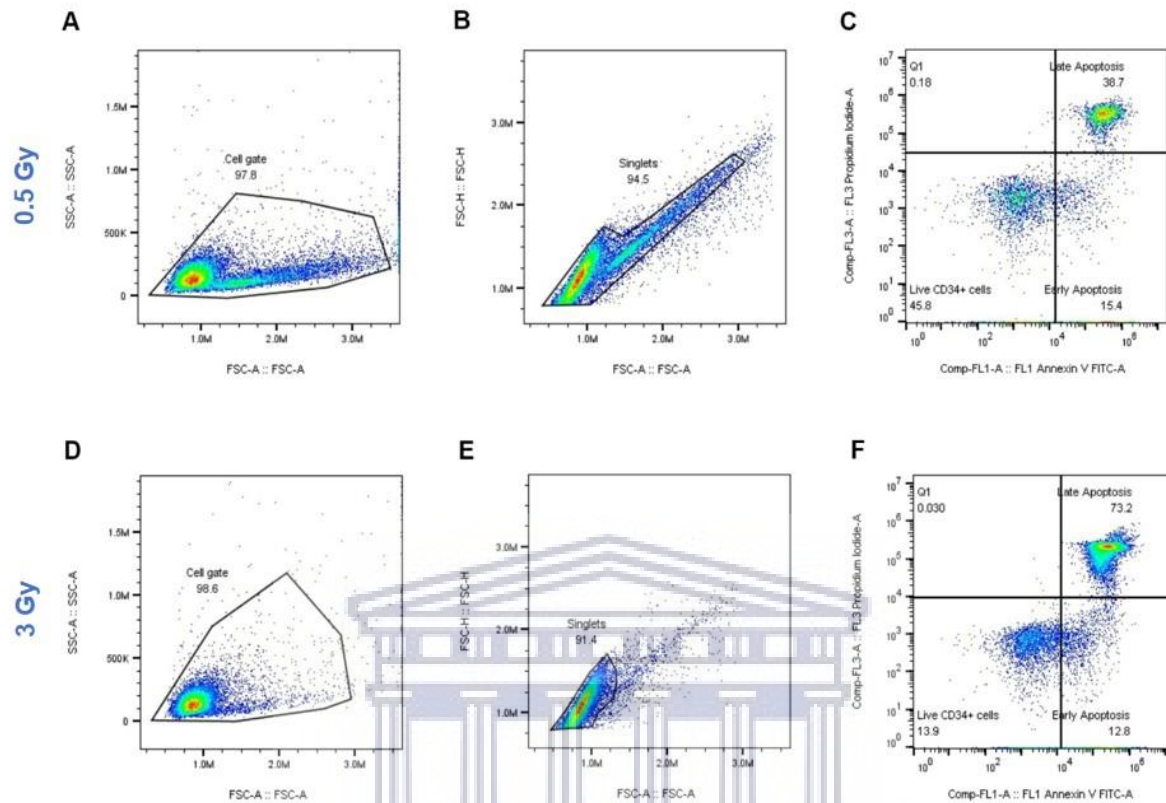


Figure 3.5.2 The gating strategy for the Annexin-V/PI apoptosis analysis. CD34^+ cells were gated on forward (FSC) versus side scatter (SSC) to select the cell population (**A and D**). The cells were gated on FSC-Height (FSC-H) vs FSC-Area (FSC-A) to exclude all the doublets and to generate the singlets gate (**B and E**). All the subpopulations were analysed on the Annexin V-FITC versus PI scatter for live, early and late apoptosis at **42 h** after ^{60}Co γ -rays radiation (**C and F**). The upper part (**A – C**) represents the gating strategy of CD34^+ cells irradiated with a low dose of ^{60}Co γ -rays at **0.5 Gy**; and the lower part (**D – F**) CD34^+ cells irradiated with a high dose at **3 Gy** which resulted in a higher percentage of late apoptosis.

18 h after neutron irradiation

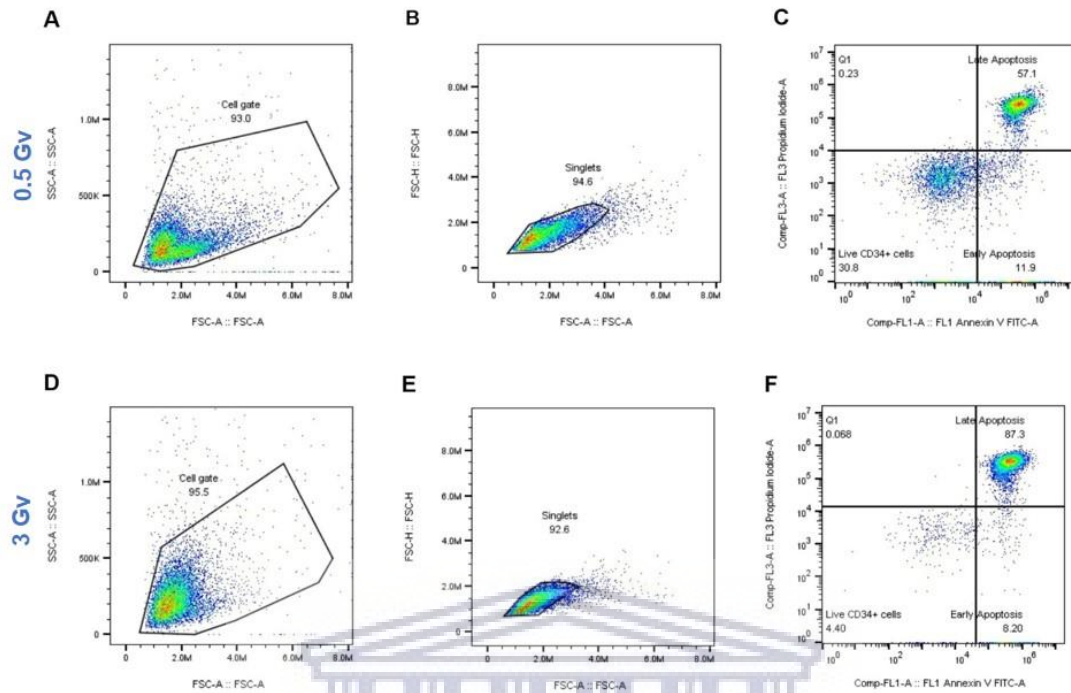


Figure 3.5.3 The gating strategy for the Annexin-V/PI apoptosis analysis. CD34⁺ cells were gated on forward (FSC) versus side scatter (SSC) to select the cell population (**A and D**). The cells were gated on FSC-Height (FSC-H) vs FSC-Area (FSC-A) to exclude all the doublets and to generate the singlets gate (**B and E**). All the subpopulations were analysed on the Annexin V-FITC versus PI scatter for live, early and late apoptosis at **18 h** after **neutron radiation** (**C and F**). The upper part (**A – C**) represents the gating strategy of CD34⁺ cells irradiated with a low dose of **neutrons** at **0.5 Gy**; and the lower part (**D – F**) CD34⁺ cells irradiated with a high dose at **3 Gy** which resulted in a higher percentage of late apoptosis.

42 h after neutron irradiation

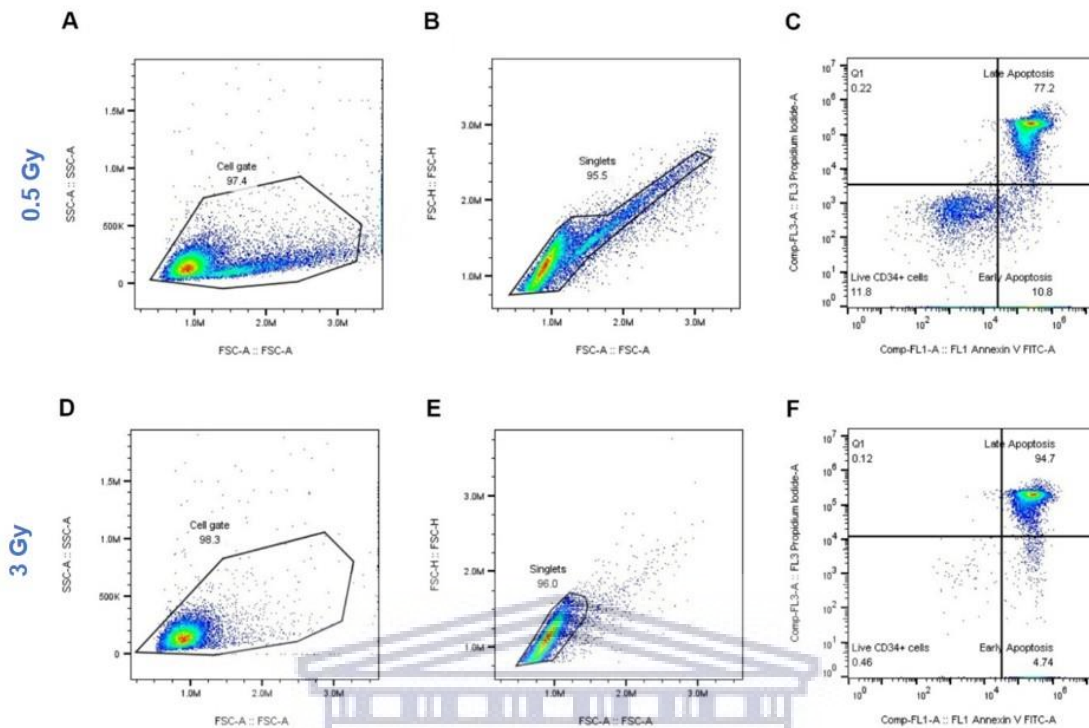


Figure 3.5.4. The gating strategy for the Annexin-V/PI apoptosis analysis. CD34⁺ cells were gated on forward (FSC) versus side scatter (SSC) to select the cell population (**A and D**). The cells were gated on FSC-Height (FSC-H) vs FSC-Area (FSC-A) to exclude all the doublets and to generate the singlets gate (**B and E**). All the subpopulations were analysed on the Annexin V-FITC versus PI scatter for live, early and late apoptosis at **42 h** after **neutron radiation** (**C and F**). The upper part (**A – C**) represents the gating strategy of CD34⁺ cells irradiated with a low dose of **neutrons** at **0.5 Gy**; and the lower part (**D – F**) CD34⁺ cells irradiated with a high dose at **3 Gy** which resulted in a higher percentage of late apoptosis.

Figures 3.6, A and 3.6, B showed a decrease in the percentage of live CD34⁺ cells over time post-irradiation ($p < 0.05$). While there was no significant difference between the percentages of live cells for both radiation modalities ($p > 0.05$), but the radiation dose did induce a significant decrease in the level of live cells compared to the sham-irradiated controls (0 Gy) at 0.5, 1 and 3 Gy ($p < 0.05$). As shown in Figure 3.6.1, B and Figure 3.6.1, E, there was a significant increase in early apoptosis from 18 to 42 h for both radiation modalities ($p < 0.01$). In addition, there was a significant decrease in early apoptosis between 0 and 3 Gy dose ($p < 0.001$) (Figure 3.6.1, B and 3.6.1, E). However, the type of radiation quality did not significantly affect the induction of early apoptosis ($p > 0.05$). In the analysis of late apoptosis, (see Figure 3.6.1, C and Figure 3.6.1, F) there was a significant increase from 18 to 42 h post-

irradiation ($p < 0.01$). Furthermore, a statistically significant difference during late apoptosis was observed between ^{60}Co γ -rays and neutron irradiations ($p < 0.05$). Overall, the late apoptosis levels after exposure to high-LET neutrons was higher in comparison to low-LET ^{60}Co γ -rays (see Table 3.2). For example, 18 h post-irradiation, the percentage of late apoptosis at a dose of 3 Gy was $43.17 \pm 6.14\%$ for ^{60}Co γ -rays and $55.55 \pm 4.87\%$ for neutron irradiation. In addition, significant difference was observed for each dose (0.5, 1 and 3 Gy) compared to sham-irradiated controls (0 Gy) ($p < 0.05$). In Figure 3.6.2, different cell morphologically changes can be observed post-irradiation which is indicative of apoptosis. Apoptosis-related morphological characteristics includes cell shrinkage, surface blebbing and the formation of apoptotic bodies.

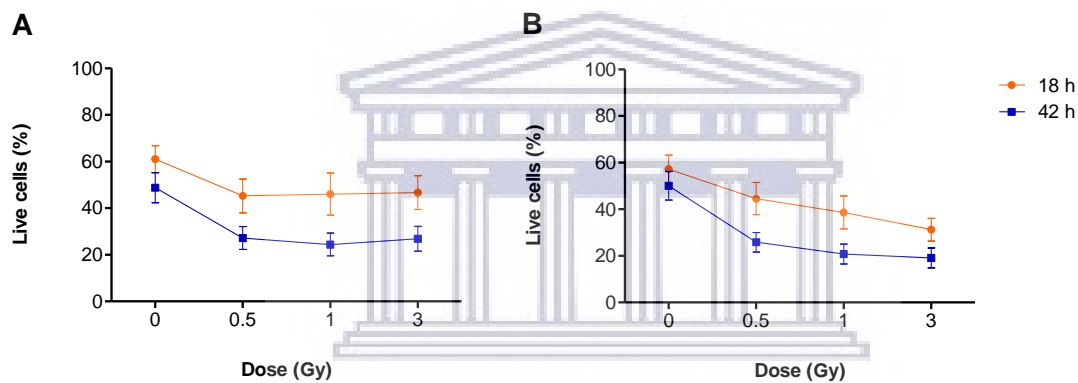


Figure 3.6. This illustration shows mean percentage of living CD34^+ cells of the same donors were irradiated with three different radiation doses of 0, 0.5, 1 and 3 Gy of ^{60}Co γ -rays (A) and neutrons (B) after 18 (orange) and 42 h (blue). The error bars represent the standard error of mean (SEM) of the different donors ($n = 13$).

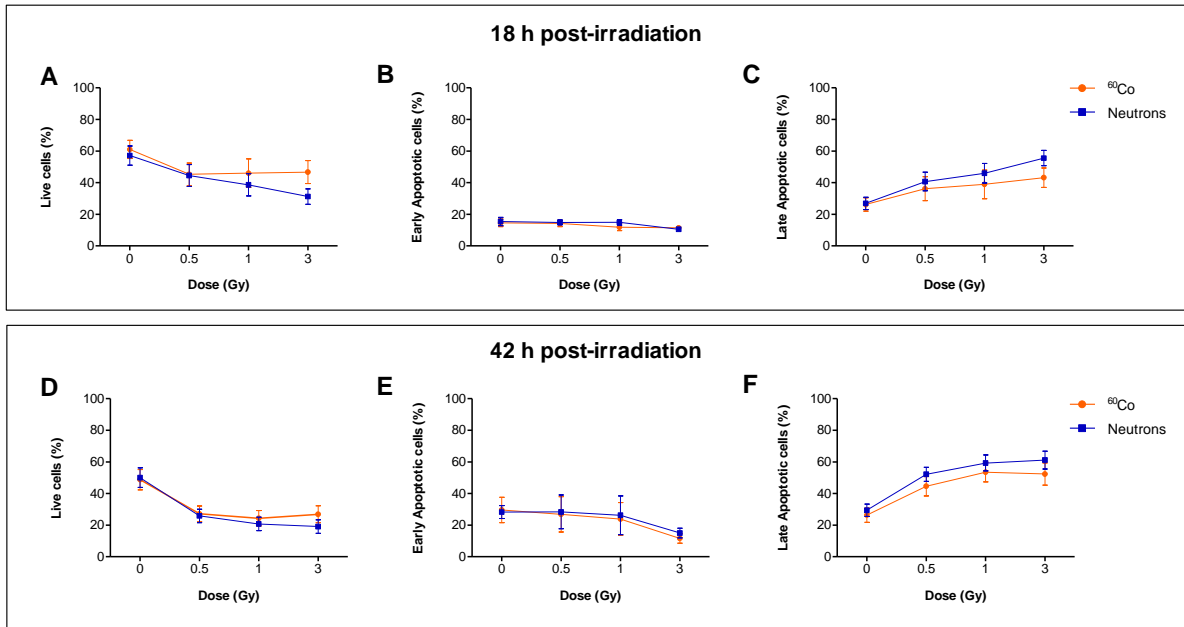


Figure 3.6.1 This illustration shows mean percentage of living, early and late apoptotic cells 18 h (A – C) and 42 h (D – F) post-irradiation with ⁶⁰Co γ -rays (orange) and neutrons (blue). The isolated CD34⁺ cells of the same donors were irradiated with three different radiation doses of 0, 0.5, 1 and 3 Gy. The error bars represent the standard error of mean (SEM) of the different donors (n = 13).

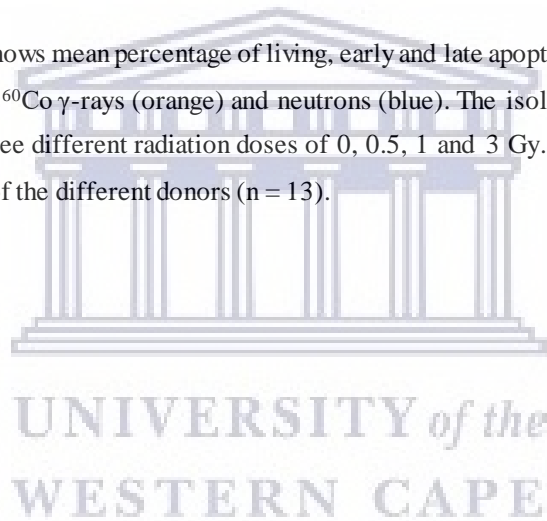


Table 3.2. This table represents mean percentage (standard error of the mean (SEM)) of living, early and late apoptotic CD34⁺ cells of the same donors were irradiated with three different radiation doses of 0, 0.5, 1 and 3 Gy of ⁶⁰Co γ -rays (orange) and neutrons (blue) after 18 and 42 h.

⁶⁰ Co γ -rays					Neutrons				
Dose (Gy)	Hours (h)	Live cells	Early apoptosis	Late apoptosis	Dose (Gy)	Hours (h)	Live cells	Early apoptosis	Late apoptosis
0	18	61.03 \pm 5.77	14.62 \pm 2.41	26.24 \pm 4.2	0	18	57.18 \pm 6.04	15.46 \pm 2.66	26.92 \pm 3.99
0.5		45.25 \pm 7.23	14.23 \pm 2.03	36.21 \pm 7.60	0.5		44.58 \pm 6.88	14.88 \pm 1.54	40.73 \pm 5.88
1		46.06 \pm 9.00	11.88 \pm 2.20	38.94 \pm 9.10	1		38.64 \pm 7.05	14.975 \pm 1.75	45.97 \pm 6.22
3		46.71 \pm 7.25	11.43 \pm 1.37	43.17 \pm 6.10	3		31.26 \pm 4.87	10.50 \pm 0.95	55.55 \pm 4.87
0	42	48.78 \pm 6.40	29.60 \pm 8.01	26.38 \pm 4.50	0	42	50.08 \pm 6.15	28.28 \pm 4.10	29.50 \pm 3.92
0.5		27.19 \pm 4.92	26.85 \pm 11.15	44.62 \pm 6.20	0.5		25.86 \pm 4.21	28.40 \pm 10.69	52.20 \pm 4.41
1		24.39 \pm 4.88	23.90 \pm 10.36	53.55 \pm 6.20	1		20.83 \pm 4.25	26.27 \pm 12.30	59.32 \pm 5.03
3		26.85 \pm 5.33	22.18 \pm 10.74	52.35 \pm 7.00	3		19.12 \pm 12.00	12.00 \pm 3.05	61.18 \pm 5.67

UNIVERSITY of the
WESTERN CAPE

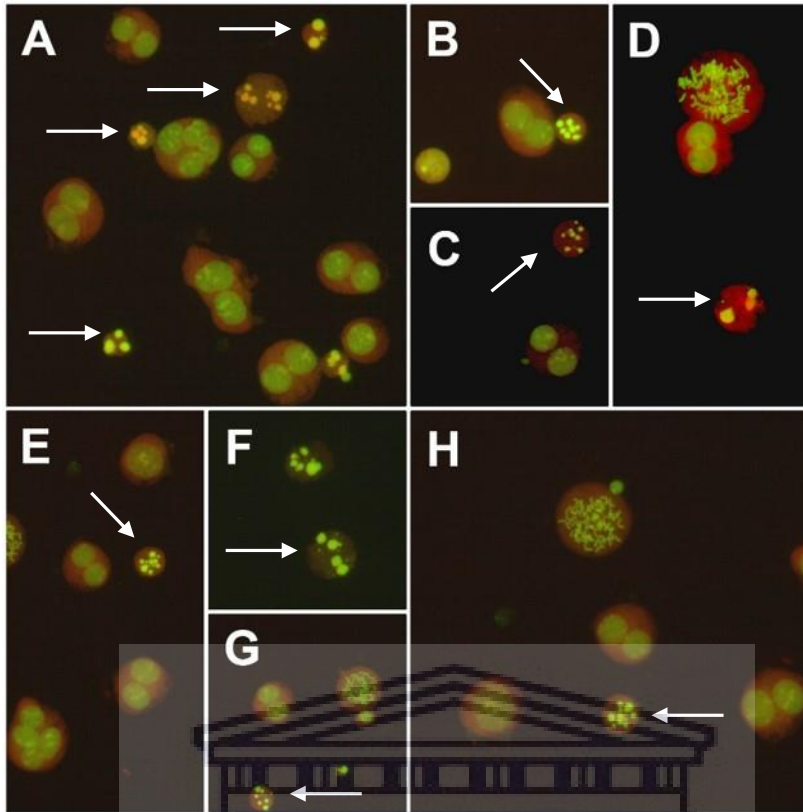


Figure 3.6.2. The images were captured from a fluorescent Zeiss Axio Imager A1 microscope, at 20X magnification after CBMN assay, are indicative of apoptosis. CD34⁺ cells in images **A – D** were exposed to low-LET ⁶⁰Co γ-rays, CD34⁺ cells in whereas images **E – H** were exposed to high-LET neutrons. White arrows show characteristic features of apoptosis.

UNIVERSITY of the
WESTERN CAPE

CHAPTER 3: RESULTS SECTION 2



UNIVERSITY *of the*
WESTERN CAPE

3.2 Differences in Radiosensitivity Between Newborns and Adults

3.2.1 Radiation-Induced Chromosomal Damage in T-lymphocytes: APB versus UCB

As described in the previous Section 1 of this Chapter 3, chromosomal radiosensitivity can be evaluated using the cytokinesis-block micronucleus (CBMN) assay. In order to determine the extent to which age influences the frequency of cytogenic damage (chromosome breakage or whole chromosome loss) in response to IR, T-lymphocytes were isolated from 27 adult donors (aged 23 – 61 years) and from the UCB of 32 newborns. The isolated lymphocytes were exposed to 0 (control), 0.5, 1, 2, 3 or 4 Gy of ^{60}Co γ -rays. Figure 3.7 shows the fitted dose response curve of radiation-induced MN in BN T-lymphocytes of adults versus newborns. For both APB and UCB, an outspoken dose-dependent increase in the frequency of radiation-induced MN was observed (see Figure 3.7). Although there was no statistically significant difference in MN yields at the highest dose of 4 Gy between APB and UCB ($p > 0.05$); a significantly higher MN frequency was observed at 0.5 and 2 Gy ^{60}Co γ -rays ($p < 0.01$), as well as at 1 and 3 Gy ^{60}Co γ -rays ($p < 0.001$) (Figure 3.7). In both APB and UCB donors, a great number of radiation-induced MN can be observed after 4 Gy exposure (Figure 3.7.1, F and Figure 3.7.2, F) in comparison with the lower doses ranging from 0 to 3 Gy. The lowest dose of 0.5 Gy yielded an average MN frequency of 14.74 ± 0.79 MN/1000 BN cells for APB and 15.94 ± 1.39 MN/1000 BN cells for UCB after ^{60}Co γ -rays irradiation, which was significantly higher than the average background values (0 Gy) of 4.19 ± 0.45 MN/1000 BN cells for APB ($p < 0.0001$) and 1.88 ± 0.28 MN/1000 BN cells for UCB ($p < 0.0001$), respectively. As not all the irradiation experiments could be performed on the same day, therefore separate control (0 Gy) cultures were set-up for both age groups. In both age groups, there was no significant difference between genders ($p > 0.05$) (Figure 3.8 and 3.9). However, there was a clear trend that females were more sensitive than males in both adults and newborns (Figure 3.8 and 3.9).

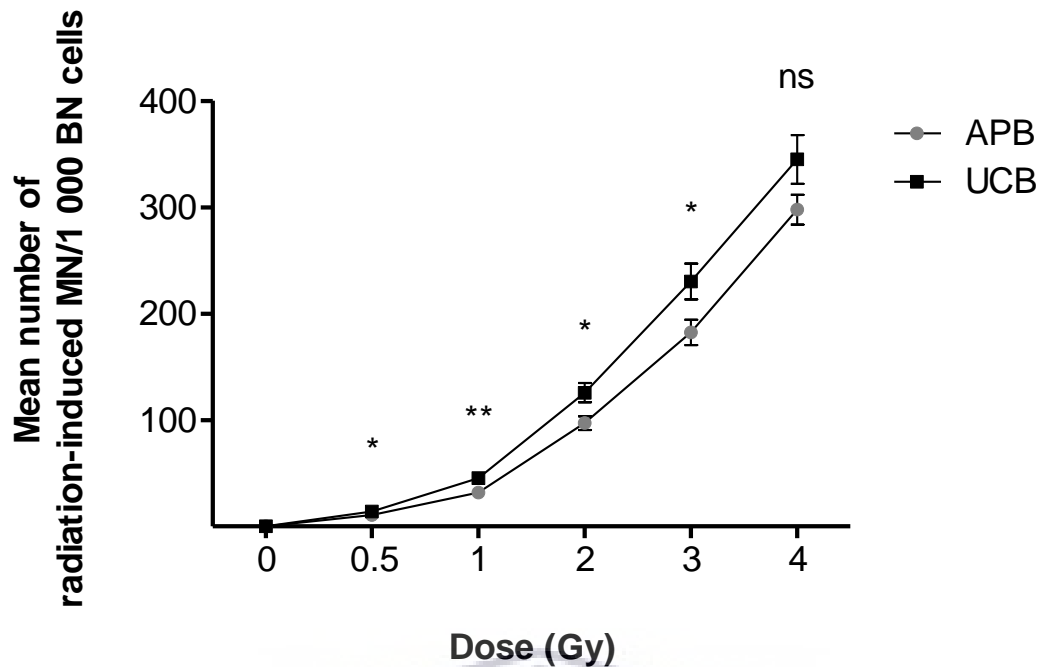


Figure 3.7. A fitted dose response curve of the mean number of MN in peripheral T-lymphocytes of adults (APB) ($n = 27$) and newborns (UCB) ($n = 32$) induced by different doses (0.5, 1, 2, 3 and 4 Gy) of ^{60}Co γ -rays irradiation. The number of MN induced by the irradiation was obtained by subtracting the mean number of MN in the non-irradiated controls (0 Gy) from the mean MN number scored in the irradiated samples. MN yields of UCB were significantly higher post-irradiation (0.5, 1, 3 and 3 Gy) compared to APB (** $p < 0.01$, * $p < 0.05$). However, after 4 Gy dose no significant (ns) difference was observed between APB and UCB ($p > 0.05$). Error bars represent the standard error of the mean (SEM). At least 1,000 BN cells were scored for each donor per condition.

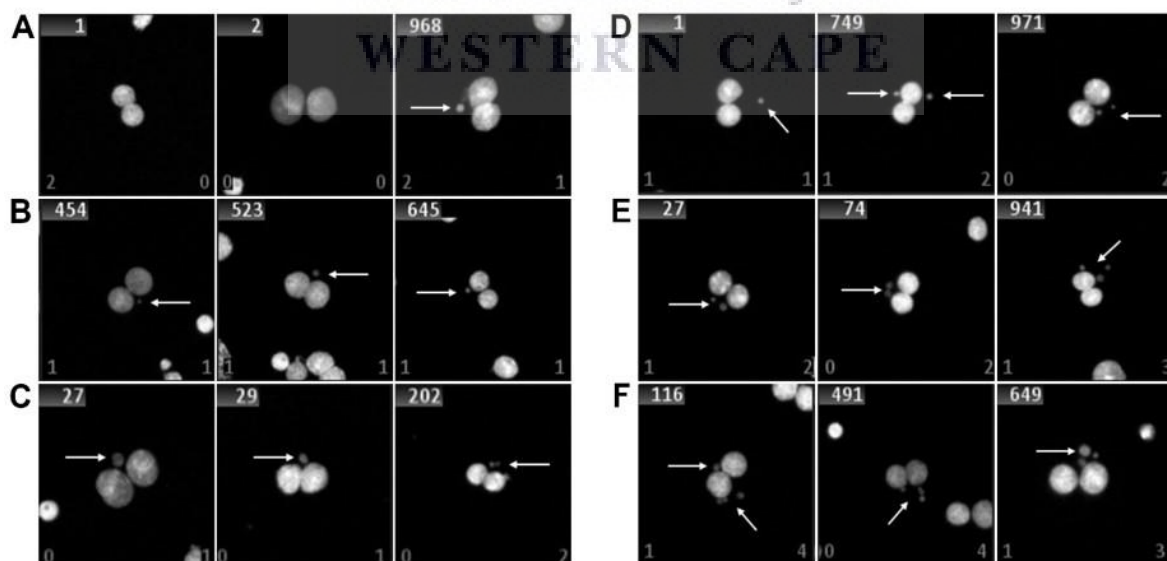


Figure 3.7.1. The selected images (A – F) in the image gallery were captured from the automated microscopic, Metafer (MetaSystems). The top left number represents the specific order of BN cells captured. In the bottom left and right corner of each image the direct MN count is from the Metafer and the MN count is the scorer's count

respectively, are depicted. APB cells were irradiated with ^{60}Co - γ rays with the following doses sham-irradiated (0 Gy) (A), 0.5 (B), 1 (C), 2 (D), 3 (E) and 4 Gy (F). All slides were scanned on the automated platform, and semi-automated scoring of MN were performed on at least two slides for each condition.

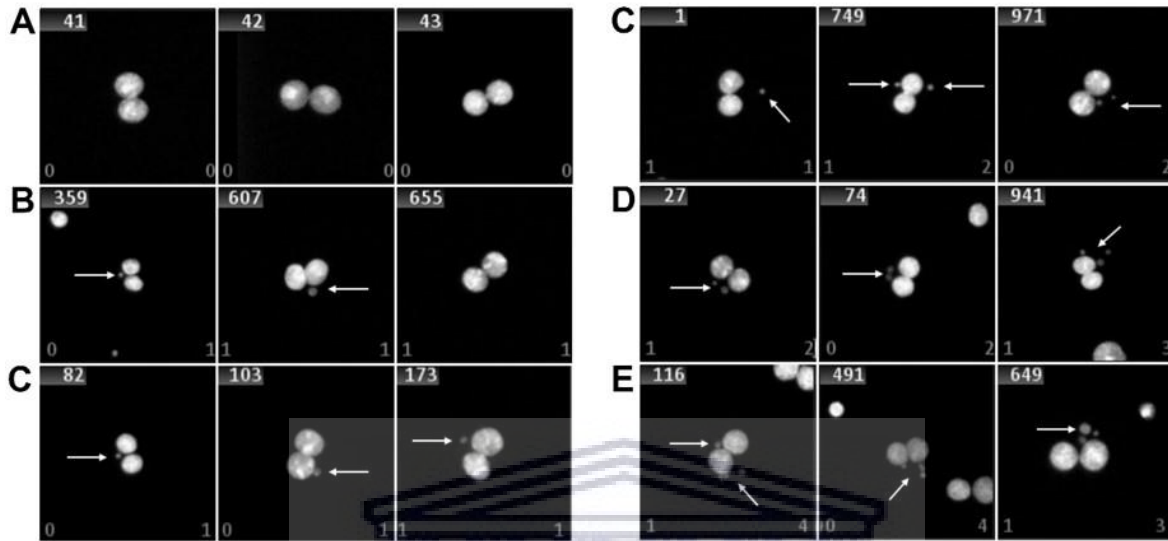


Figure 3.7.2. The T-lymphocytes of UCB were irradiated with ^{60}Co - γ rays with the following doses sham-irradiated(0 Gy) (A), 0.5 (B), 1 (C), 2 (D), 3 (E) and 4 Gy (F). All slides were scanned on the automated platform, and scoring of MN was performed on duplicate slides for each condition.

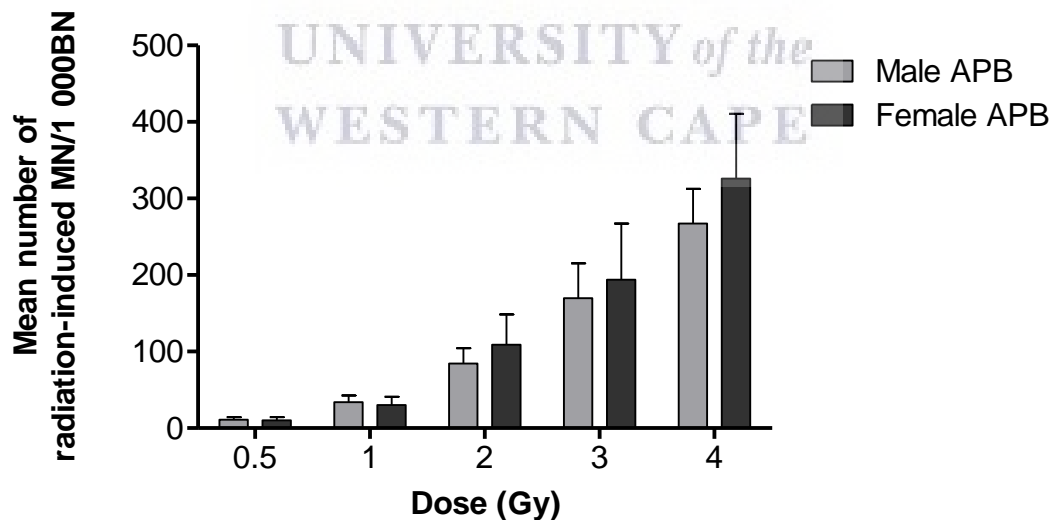


Figure 3.8. The mean number of radiation-induced MN in peripheral T-lymphocytes of male (n = 13) and female adults (n = 14) induced by different doses (0.5, 1, 2, 3 and 4 Gy) of ^{60}Co γ -rays irradiation. No significant difference was observed in MN yields between male and female adult post-irradiation ($p > 0.05$). Error bars represent the standard error of the mean (SEM). At least 1,000 BN cells were scored for each donor per condition.

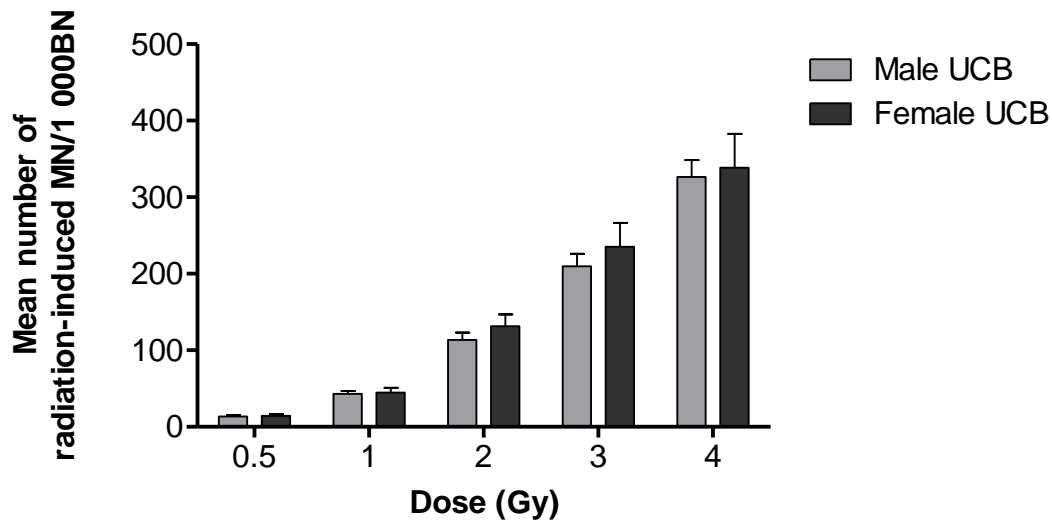


Figure 3.9. The schematic representation shows the mean number radiation-induced of MN in peripheral T-lymphocytes of male ($n = 19$) and female newborns ($n = 11$) induced by different doses (0.5, 1, 2, 3 and 4 Gy) of ^{60}Co γ -rays irradiation. No significant difference in MN yields were observed between male and female newborns post-irradiation ($p > 0.05$). Error bars represent the standard error of the mean (SEM). At least 1,000 BN cells were scored for each donor per condition.

3.2.2 Expression of CD45RA and CD45RO on CD4 and CD8 T-lymphocytes Subsets in UCB and APB Samples

The major difference between UCB T-lymphocytes and APB T-lymphocytes, is their immunophenotypic profile, which could be an underlying reason for the observed difference in cytogenetic damage between adults and newborns. An immunophenotypic study of the UCB and APB was performed to determine the percentage of T-lymphocyte subsets in the UCB and APB samples by using the BD Accuri™ C6 flow cytometer. The gating strategies for flow cytometry analysis were performed using FlowJo™ v10.7 (BD Bioscience, United States) (see [Figures 3.10.1 – 3.10.4](#)) First, the peripheral blood T-lymphocytes were gated on forward (FSC) versus side scatter (SSC) to select the T-lymphocyte population, followed by exclusion of doublets and dead cells exclusion. Thereafter, the T-lymphocytes were on gated on CD3-PerCP vs SSC-A to include all CD3⁺ cells, then gated on the CD4⁺ or CD8⁺ population. Finally, all the subpopulations were analysed on the CD4-PE-A or CD8-APC-A versus CD45RO-BB515-A or CD45RA-BB515-A. There was a significance difference between the percentage of CD4⁺ and CD8⁺ T-lymphocyte fraction in UCB ($p < 0.001$) and no significant difference in APB ($p > 0.05$) (see [Figure 3.11](#)). This figure shows a significant difference was observed in

CD4⁺ and CD8⁺ T-lymphocyte fraction between UCB ($p < 0.001$) and APB ($p < 0.01$). Table 3.3 and Table 3.4 show the expression of CD45RA and CD45RO on CD4⁺ and CD8⁺ T-lymphocytes of all individual newborn and adult donors, respectively. Table 3.5 shows the median percentage of naïve and memory CD4⁺ and CD8⁺ T-lymphocytes of newborns and adults. The results clearly show that both the CD4⁺ and CD8⁺ T-lymphocytes of newborns are mainly naïve, illustrated by the co-expression of CD45RA⁺ on 90.70% (range: 80.80% – 98.40%) and 95.90% (range: 89.60% – 98.80%) of CD4⁺ and CD8⁺ cells respectively. Whereas, the composition in adult T-lymphocytes is clearly different, with a more equal distribution between CD45RA⁺ and CD45RO⁺ subpopulations. The results show that both the CD4⁺ and CD8⁺ T-lymphocytes of adults are mainly memory T-lymphocytes, illustrated by the co-expression of CD45RO⁺ on 50.55% (range: 41.10% – 86.50%) and 42.50 (range: 31.40% – 56.90%) of CD4⁺ and CD8⁺ cells respectively. Figure 3.12 represents the mean percentage of expression of CD45RA⁺ and CD45RO⁺ on CD4⁺ and CD8⁺ T-lymphocyte subsets in UCB and APB samples. This observation demonstrates the differences between newborn and adult T-lymphocytes and there is an immunophenotypic change of T-lymphocytes with age.

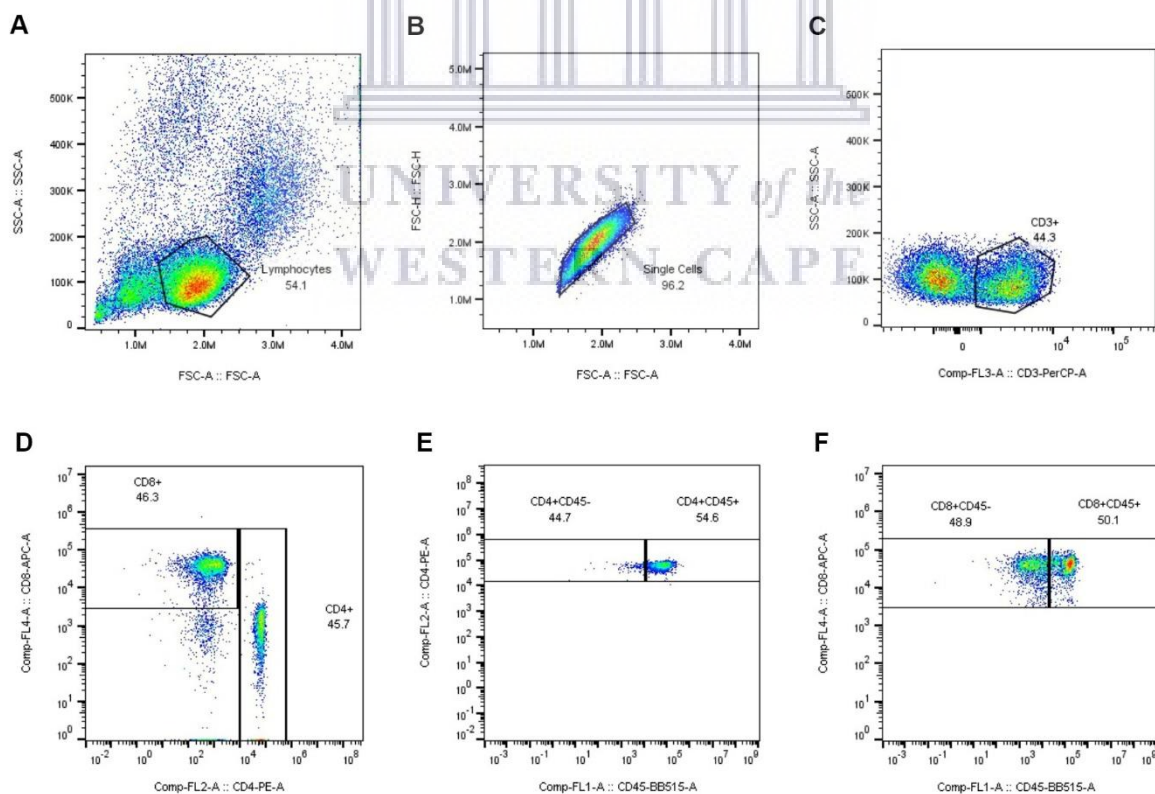


Figure 3.10.1. The gating strategy for the expression of naïve (CD45RA) markers on peripheral blood CD4⁺ and CD8⁺ T-lymphocytes in adults (APB). The peripheral blood T-lymphocytes were gated on forward (FSC) versus side scatter (SSC) to select the lymphocyte cell population (A). The cells were gated on FSC-Height (FSC-

H) vs FSC-Area (FSC-A) to exclude all the doublets and to generate the singlets gate (**B**). Subsequently, the cells were on gated on CD3-PerCP vs SSC-A to include all CD3⁺ cells (**C**), then gated on the CD4⁺ or CD8⁺ population (**D**). All the subpopulations were analysed on the CD4-PE-A (**E**) or CD8-APC-A (**F**) versus CD45-BB515-A. Data were analysed using FlowJo v10.6.1 software, and population frequencies expressed as percent of the CD4⁺ or CD8⁺ parent population.

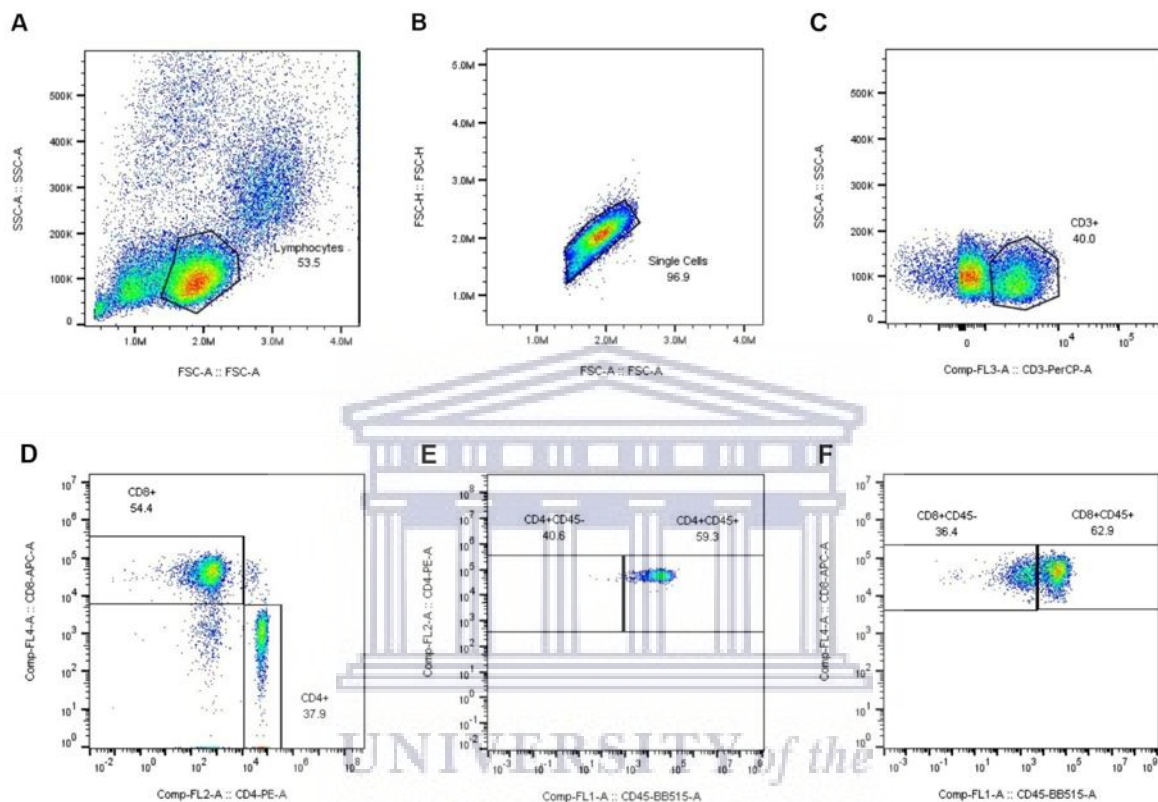


Figure 3.10.2. The gating strategy for the expression of **memory (CD45RO) markers** on peripheral blood CD4⁺ and CD8⁺ T-lymphocytes in **adults (APB)**. The peripheral blood T-lymphocytes were gated on forward (FSC) versus side scatter (SSC) to select the lymphocyte cell population (**A**). The cells were gated on FSC-Height (FSC-H) vs FSC-Area (FSC-A) to exclude all the doublets and to generate the singlets gate (**B**). Subsequently, the cells were on gated on CD3-PerCP vs SSC-A to include all CD3⁺ cells (**C**), then gated on the CD4⁺ or CD8⁺ population (**D**). All the subpopulations were analysed on the CD4-PE-A (**E**) or CD8-APC-A (**F**) versus CD45-BB515-A. Data were analysed using FlowJo v10.6.1 software, and population frequencies expressed as percent of the CD4⁺ or CD8⁺ parent population.

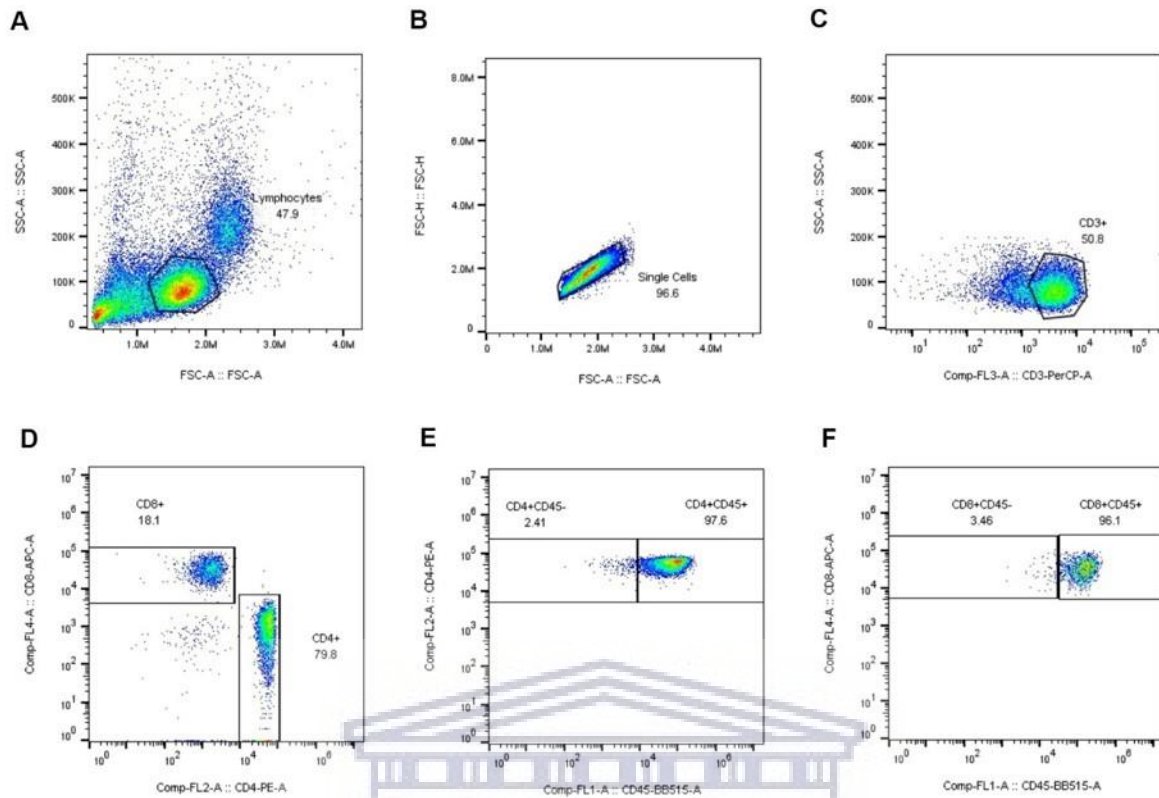


Figure 3.10.3. The gating strategy for the expression of **naïve (CD45RA) markers** on peripheral blood CD4⁺ and CD8⁺ T-lymphocytes in **newborns (UCB)**. The peripheral blood T-lymphocytes were gated on forward (FSC) versus side scatter (SSC) to select the lymphocyte cell population (A). The cells were gated on FSC-Height (FSC-H) vs FSC-Area (FSC-A) to exclude all the doublets and to generate the singlets gate (B). Subsequently, the cells were on gated on CD3-PerCP vs SSC-A to include all CD3⁺ cells (C), then gated on the CD4⁺ or CD8⁺ population (D). All the subpopulations were analysed on the CD4-PE-A (E) or CD8-APC-A (F) versus CD45-BB515-A. Data were analysed using FlowJo v10.6.1 software, and population frequencies expressed as percent of the CD4⁺ or CD8⁺ parent population.

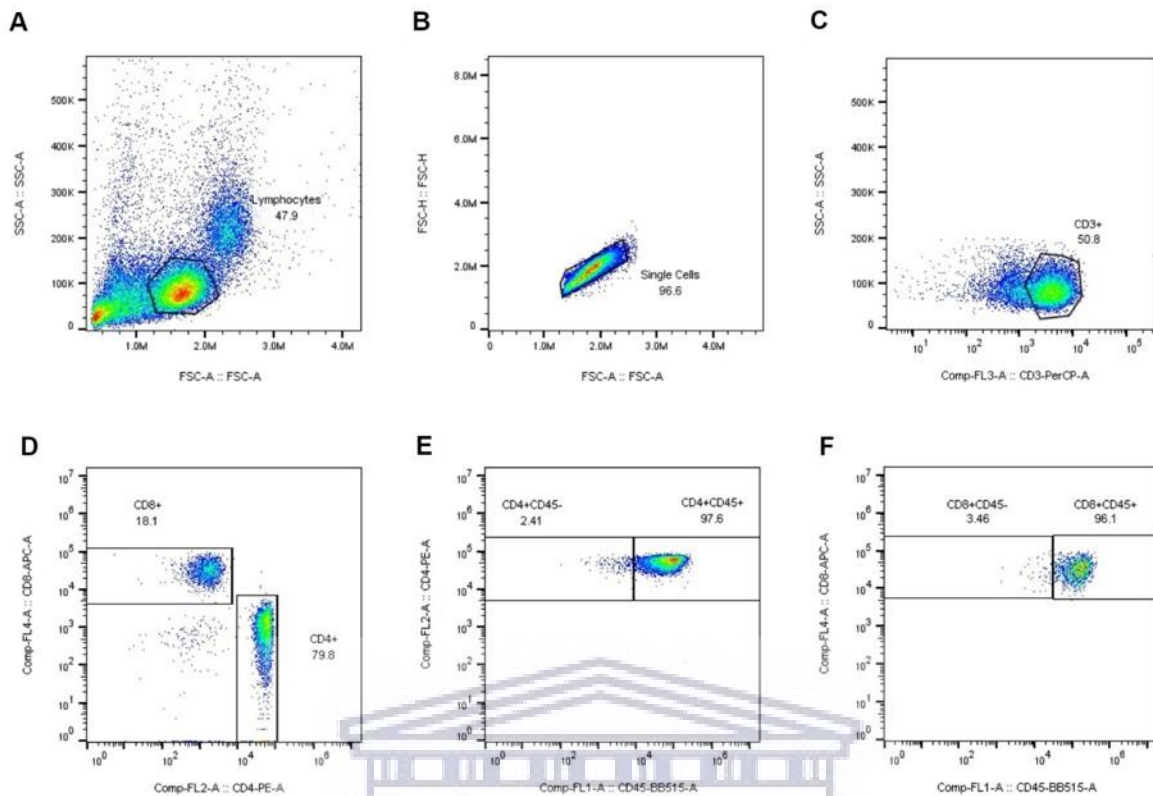


Figure 3.10.4. The gating strategy for the expression of **memory (CD45RO)** markers on peripheral blood CD4⁺ and CD8⁺ T-lymphocytes in **newborns (UCB)**. The peripheral blood T-lymphocytes were gated on forward (FSC) versus side scatter (SSC) to select the lymphocyte cell population (**A**). The cells were gated on FSC-Height (FSC-H) vs FSC-Area (FSC-A) to exclude all the doublets and to generate the singlets gate (**B**). Subsequently, the cells were on gated on CD3-PerCP vs SSC-A to include all CD3⁺ cells (**C**), then gated on the CD4⁺ or CD8⁺ population (**D**). All the subpopulations were analysed on the CD4-PE-A (**E**) or CD8-APC-A (**F**) versus CD45-BB515-A. Data were analysed using FlowJo v10.6.1 software, and population frequencies expressed as percent of the CD4⁺ or CD8⁺ parent population.

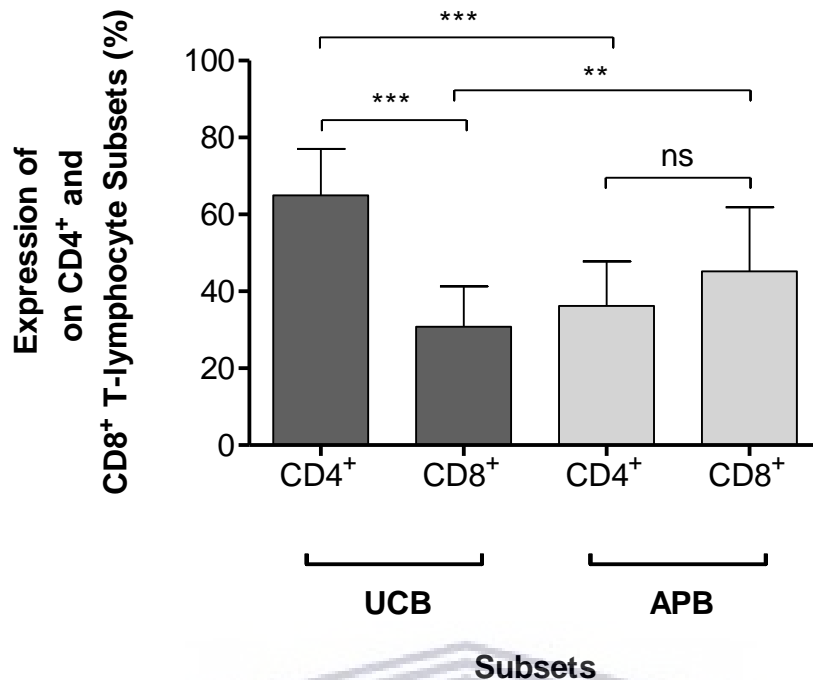


Figure 3.11. This graph shows the mean percentage of CD4 and CD8 T-lymphocyte subsets in UCB (n = 33) and APB (n = 18) samples. The fraction of CD4⁺ were significant higher compared to CD8⁺ T-lymphocyte subsets in UCB ($***p < 0.001$), whereas, no significance was observed between CD4⁺ and CD8⁺ fraction in APB ($p > 0.05$). A significant difference is noted between CD4⁺ ($***p < 0.001$) and CD8⁺ ($**p < 0.01$) fraction when comparing UCB and APB. Error bars represent the standard error of mean (SEM) of the different donors.

Table 3.3. Percentage (%) expression of CD45RA and CD45RO on CD4 and CD8 T-lymphocyte subsets in UCB samples (n = 33).

UCB or APB	Gender	HIV	SUBPOPULATIONS			
			CD4 ⁺		CD8 ⁺	
			CD4CD45 RA ⁺	CD4CD45 RO ⁺	CD8CD45 RA ⁺	CD8CD45 RO ⁺
	M	-	88.30	12.20	89.60	8.35
	M	-	91.20	8.49	96.40	2.93
	M	?	89.90	9.06	97.70	2.33
	M	+	81.80	16.70	94.20	4.27
	M	-	92.40	7.37	94.20	5.38
	M	-	90.70	0.87	97.30	0.99
	F	-	89.60	10.40	98.80	0.99
	M	-	96.30	3.54	98.60	0.38
	F	-	92.40	5.10	91.60	7.43
	M	+	89.70	6.80	90.40	7.51
	F	-	86.40	12.30	91.10	6.95
	F	-	90.70	9.20	95.10	3.47
	F	+	88.00	12.00	98.70	0.84
	F	-	91.60	8.96	89.80	8.87
	F	-	86.70	13.20	97.40	2.21
	M	-	90.10	9.65	95.30	4.32
	M	-	80.80	19.00	97.70	1.77
	M	-	86.20	13.60	92.50	6.99
	F	-	89.90	10.10	94.70	4.97
	F	-	92.20	7.71	98.70	1.02
	M	-	90.00	8.98	98.80	1.09
	M	-	94.60	5.03	95.90	4.39
	F	+	97.30	2.44	95.00	4.00
	F	-	98.40	1.50	98.00	1.96
	M	-	94.00	5.74	97.00	2.99
	M	-	97.60	2.40	95.90	3.65
	M	-	85.80	13.60	97.70	1.37
	M	-	87.80	12.20	92.70	7.82
	M	-	99.40	0.63	95.10	4.28
	M	-	95.00	4.47	96.70	3.31
	F	+	97.60	2.24	99.20	0.82
	F	-	95.60	4.39	98.20	1.75
	F	-	86.50	12.50	93.00	5.81

Abbreviations: UCB, umbilical cord blood; F, female; M, male; HIV, human immunodeficiency virus; +, positive; -, negative; ?, did not indicate.

Table 3.4. Percentage (%) expression of CD45RA and CD45RO on CD4 and CD8 T-lymphocyte subsets in APB samples (n = 18).

UCB or APB	Gender	HIV	SUBPOPULATIONS			
			CD4 ⁺		CD8 ⁺	
			CD4CD45 RA ⁺	CD4CD45 RO ⁺	CD8CD45 RA ⁺	CD8CD45 RO ⁺
	M	-	49.80	51.20	68.60	31.40
	F	-	33.40	65.80	44.40	53.30
	M	-	28.80	73.20	66.70	32.20
	F	-	12.70	86.50	43.00	55.30
	F	-	31.60	66.60	57.90	42.10
	F	-	55.30	46.70	41.80	55.10
	M	-	34.40	65.40	57.50	43.90
	M	-	34.00	66.20	43.10	56.90
	F	-	44.00	55.50	56.50	42.90
	F	-	52.80	45.70	76.10	23.20
	F	?	45.30	54.40	56.20	39.90
	F	-	30.90	69.10	64.00	31.90
	F	-	44.00	46.00	62.40	34.00
	M	-	58.90	41.10	41.20	55.80
	M	-	48.50	50.00	55.30	40.30
	M	-	28.80	71.10	46.70	51.60
	F	-	48.50	52.00	44.50	51.50
	F	-	21.80	77.30	41.30	58.10

Abbreviations: APB, adult peripheral blood; F, female; M, male; HIV, human immunodeficiency virus; +, positive; -, negative.

Table 3.5. Median percentage (%) expression of CD45RA and CD45RO on CD4 and CD8 T-lymphocyte subsets in UCB and APB samples. The percentage range is given in parenthesis.

SUBPOPULATION	T newborns (UCB)	T adult (APB)
CD4 ⁺	64.60 (44.25–88.45)	28.80 (10.94–56.00)
	CD45RA ⁺ 90.70 (80.80–98.40)	44.65 (12.70–58.90)
	CD45RO ⁺ 8.96 (0.87–16.70)	50.55 (41.10–86.50)
	CD8 ⁺ 30.30 (15.8–51.25)	55.03 (18.60–69.60)
CD8 ⁺	CD45RA ⁺ 95.90 (89.60–98.80)	56.35 (41.20–76.10)
	CD45RO ⁺ 3.47 (0.83–8.87)	42.50 (31.40–56.90)

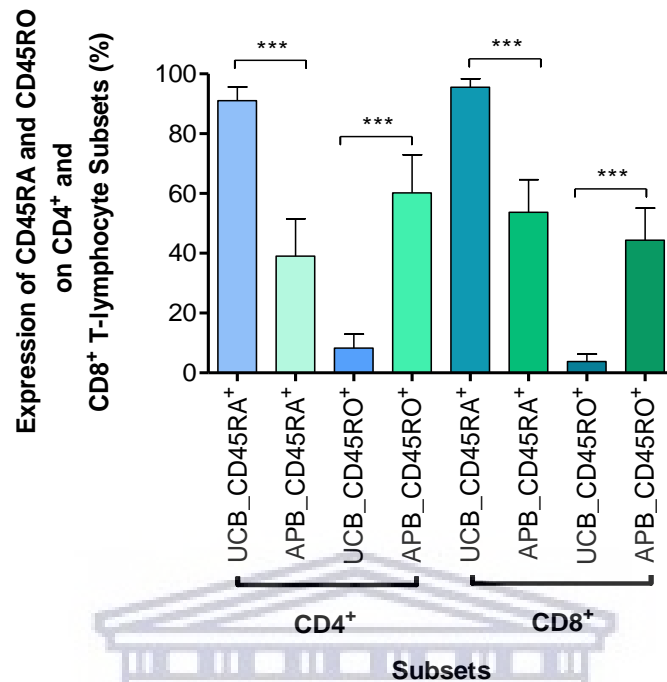


Figure 3.12. Schematic representation of the mean percentage of expression of CD45RA and CD45RO on CD4 and CD8 T-lymphocyte subsets in UCB (n = 33) and APB (n = 18) samples. The expression of CD45RA on CD4 and CD8 T-lymphocyte subsets in UCB were significantly higher compared to APB donors ($***p < 0.001$), whereas the expression of CD45RO on CD4 and CD8 T-lymphocyte subsets in APB significantly higher compared to UCB samples ($***p < 0.001$). Error bars represent the standard deviation (SD) of the different donors.

UNIVERSITY of the
WESTERN CAPE

CHAPTER 4: DISCUSSION



“The important thing is to never stop questioning or learning.”

– Albert Einstein

4.1 Radiosensitivity of CD34⁺ to High-LET Neutron Irradiation

4.1.1 Proton Beam Therapy (PBT) and Secondary Neutron Production

The clinical application of proton beam therapy (PBT) has increased significantly over the last few years. According to the Particle Therapy Co-Operative Group (PTCOG), the number of proton therapy facilities is forecast to increase from 92 facilities that are currently in operation to 153 active PBT centres by 2025 (PTCOG, 2020). This sharp increase in PBT is mainly attributable to optimal dose distribution and lower integral whole-body dose with a subsequent reduction of side effects compared to conventional X-ray based radiation therapy (RT) (van de Water *et al.*, 2011; Leroy *et al.*, 2016; Hu *et al.*, 2018; Tian *et al.*, 2018; Hill-Kayser *et al.*, 2019). The significant decrease in dose to non-target tissues is particularly important for children and PBT is now widely used to treat paediatric malignancies, specifically brain tumours (Hu *et al.*, 2018; Sardaro *et al.*, 2019). Several studies have demonstrated a correlation between the irradiated volume of normal brain tissue and the consequent impact on the neurocognitive functions, academic performances and quality of life (Merchant *et al.*, 2014). Owing to the superior sparing of normal tissue, paediatric brain tumour patients treated with PBT have improved outcomes across several neurocognitive areas (Gross *et al.*, 2019; Jalali and Goda, 2019). Although clinical data is encouraging, randomised clinical trials comparing PBT and conventional RT remain limited, particularly on secondary malignancies (SMs) and it is therefore important to investigate the existing radiobiological uncertainties related to PBT for paediatric patients (Merchant, 2013).

Some experts have expressed concerns that protons, despite their dose sparing properties, have the potential to produce unwanted doses outside the primary field due to the production of stray radiation, including secondary neutrons (Schneider and Halg, 2015). During PBT, such neutrons are inevitably produced through nuclear interactions in the components of the proton beam line, the treatment collimator and the patient's body (Kim, Chung, Shin, Lim, Shin, S. B. Lee, *et al.*, 2013; Trinkl *et al.*, 2017; Cordova and Cullings, 2019). While it is anticipated that the absorbed dose resulting from these secondary neutrons is small, the significant uncertainty on the high relative biological effectiveness (RBE) of neutrons remains a critical concern with respect to cancer induction (Liu and Chang, 2011; Schneider and Halg, 2015; Matsumoto *et al.*, 2016). Recently, a multidisciplinary approach was used to determine neutron RBEs for different tissues and neutron energies within the European ANDANTE project. This project

involves a multidisciplinary evaluation of the cancer risk from neutrons relative to photons using stem cells and the induction of second malignant neoplasms following paediatric radiation therapy (ANDANTE), to obtain a better understanding of the possible role of secondary neutrons in the induction of SMs following particle therapy (Ottolenghi *et al.*, 2015; Juerß *et al.*, 2017). The study on fast neutrons and HSPCs as part of this PhD project, are closely linked to the aim and outline of this large European consortium. However, it is important to mention that the more recent active pencil-beam scanning systems that are currently used for proton beam delivery, produce significantly less neutrons than the older passive scattering systems (Hälg and Schneider, 2020). Therefore, the risk of developing a SM from secondary neutrons produced during modern PBT for a brain lesion is small and is outweighed by the therapeutic benefit. A long-term follow-up study in our institute on patients treated for intracranial and cranial pathologies, where the older passive scattering PBT was applied, showed no out-of-field SMs in any of the age groups and only one in-field SM was reported 15 years after treatment (Vernimmen *et al.*, 2018). The results are reassuring for children and young adults, since the patient's age at treatment plays a major role in the risk for SMs. Still, the number of long-term follow-up studies on paediatric patients treated with PBT remains low. Hence, it is worth to investigate the biological effects of neutrons to improve our understanding of the possible associated risks for childhood cancer survivors, particularly for in the context of haematological malignancies, such as leukaemia. This is important in the context of PBT for paediatric brain tumours, since 17.5 – 27.8% of the red BM that harbours the HSPCs is located in the heads of children in the first 5 years of age (Cristy, 1981).

As previously mentioned in the Chapter 1, the target cells for radiation-induced leukaemia are most likely the HSPCs (Gault *et al.*, 2019). These cells mainly reside in the red bone marrow and are characterised by an extensive self-renewal and differentiation capacity, that maintain haematopoiesis and replenishment of the blood cell pool throughout life (Rieger and Schroeder, 2012). Owing to their long lifespan, the accumulation of radiation damage in HSPCs can compromise their genomic integrity and thereby potentially give rise to leukemogenesis (Verbiest *et al.*, 2018). Despite the growing number of studies on the radiosensitivity of HSPCs, definitive data regarding radiation-induced cell death, DNA repair, and genomic stability in these rare quiescent cells remain elusive (Milyavsky *et al.*, 2010; Heylmann *et al.*, 2014; Vandevoorde *et al.*, 2016; Durdik *et al.*, 2017a; Biechonski *et al.*, 2018). In particular, experiments on the DNA damage response of HSPCs to high-LET radiation, such as neutrons and carbon ions, are limited (Becker *et al.*, 2009; Kraft *et al.*, 2015; Rodman *et al.*, 2017). The

latter is not only important in the context of the growing clinical use of particle therapy, but also for upcoming long-term interplanetary space missions, where radiation-induced leukaemia represent about 15% of the total cancer risk from space radiation (Cucinotta, To and Cacao, 2017). To the best of our knowledge, this is the first study to investigate the response of HSPCs to neutron irradiation.

4.1.2 Formation and Repair of DNA DSBs in CD34⁺ Cells

A higher number of DNA DSBs in CD34⁺ cells was observed after neutron irradiation compared to ⁶⁰Co γ -rays at 2 h post-irradiation, but similar levels of residual damage after 18 h (Figure 3.4), was seen. The 2 h results contradicts a previous study performed on isolated lymphocytes, where a significantly higher number of γ -H2AX foci was observed 2 h post-irradiation with ⁶⁰Co γ -rays compared to the same p(66)/Be(40) neutrons (Vandersickel *et al.*, 2014). The answer could be the underlying differences in DNA repair processes between CD34⁺ cells and isolated lymphocytes, which is confirmed by several other studies (Rübe *et al.*, 2011; Vasilyev *et al.*, 2013; Vandevoorde *et al.*, 2016; Durdik *et al.*, 2017b; Biechonski *et al.*, 2018; Kosik *et al.*, 2020). Rübe *et al.* studied the formation and loss of γ -H2AX foci in different stem and progenitor populations exposed to IR to gain insight into changes in DSB repair capacity in age-dependent (newborns and healthy volunteers of 16 – 83 years old). They reported lower levels of endogenous DSBs in cord blood CD34⁺ cells than in adult PBL, which suggests that unrepaired DSBs accumulate continuously in the more mature CD34⁻ cells during physiological cell aging (Rübe *et al.*, 2011). Vasilyev *et al.* showed that endogenous 53BP1 levels were significantly lower in UCB of newborns than in PBL of adults. This finding is in line with previous reports that show an increase of the endogenous DSB with age. The yields of radiation-induced 53BP1 foci were always higher in CD133⁺ cells and PBL (Vasilyev *et al.*, 2013). The CD133⁺ cells have significantly and consistently higher recruitment rate of 53BP1 to the sites of DNA damage which may indicate enhanced DNA repair capacity in CD133⁺ cells as compared to mature lymphocytes. Vandevoorde *et al.* showed that residual γ -H2AX/53BP1 foci levels 24 h post-irradiation were significantly lower in CD34⁺ cells compared to newborn T-lymphocytes, while newborn T-lymphocytes showed significantly higher foci yields than adult T-lymphocytes. However, no significant differences in the radiation-induced MN yield at 2 Gy were observed between CD34⁺ cells and newborn T-lymphocytes. Nevertheless, newborn T-lymphocytes showed a significantly higher number of

MN compared to adult T-lymphocytes. These results confirm that CD34⁺ cell quiescence promotes fast error-prone DNA repair and mutagenesis after IR exposure (Vandevorde *et al.*, 2016) that could trigger leukaemia development. This study showed that the number of residual DSBs 24 h post-exposure, is significantly lower in CD34⁺ cells than in newborn T-lymphocytes, pointing to enhanced repair of DNA DSBs. The difference in DDR may be linked to differences in chromatin structure between CD34⁺ cells and T-lymphocytes, which has a major influence on the cellular response to DNA damage (Vandevorde *et al.*, 2016). Durdik *et al.* reported that lymphocytes have shown significantly higher level of γ -H2AX foci as compared to CD34⁺ cells, thereby confirming that HSPC are less prone to undergo endogenous and radiation-induced apoptosis. This might be due to higher expression of anti-apoptotic proteins in CD34⁺ cells compared to lymphocytes (Durdik *et al.*, 2017a). In another study, Biechonski *et al.* showed human HSPCs have a 2 – 6-fold lower frequency of NHEJ events relative to the fraction of committed progenitors. They observed a reduced expression of multiple DSB repair transcripts along with more persistent 53BP1 foci in irradiated HSPCs in comparison with committed progenitors, which can account for low NHEJ activity and its distinct control in HSPCs (Biechonski *et al.*, 2018). Furthermore, Kosik *et al.* showed that CD34⁺ cells are extremely radio-resistant and display a delayed time kinetics of apoptosis compared to lymphocytes. CD34⁺ cells accumulate lower levels of endogenous DNA damage/early apoptotic γ -H2AX pan-stained cells and have a higher level of radiation-induced 53BP1 and γ -H2AX/53BP1 co-localised DNA DSBs compared to lymphocytes (Kosik *et al.*, 2020). Taken together, HSPCs may indicate enhanced DNA repair capacity as compared to T-lymphocytes.

The results presented at 18 h post-irradiation here, were unexpected, since previous studies have indicated that approximately 20 – 40% of the DNA DSBs induced by low-LET radiation exposure are complex and clustered and increase to approximately ~70% for high-LET radiation (Nikjoo *et al.*, 1999; Mavragani *et al.*, 2019). Clustered DNA damage, including clustered DSB but also non-DSB lesions, are poorly repaired or even fail to be repaired and contribute to the greater mutagenic and cytotoxic effects of high-LET radiation. Therefore, one would expect a higher fraction of residual γ -H2AX foci after 18 h for high-LET neutrons compared to low-LET ⁶⁰Co γ -rays. However, the number of residual γ -H2AX foci in isolated lymphocytes was not significantly different after 24 h in the study of Vandersickel *et al.* and the repair half-life was very similar for the two radiation modalities, namely 2.8 and 3 h for ⁶⁰Co γ -rays and p(66)/Be(40) neutron respectively (Vandersickel *et al.*, 2014). The latter agrees

with the observations at 18 h post-irradiation for CD34⁺ cells, where no significant difference was observed between the two radiation qualities. Rall *et al.* evaluated γ -H2AX foci formation in stimulated CD34⁺ cells at different time-points post-irradiation with 2 Gy of X-rays and high-LET iron ions. No significant difference in residual DNA damage were observed in either the X-ray or high LET irradiated CD34⁺ cells (Rall *et al.*, 2015). However, in contrast to the current study, the CD34⁺ cells were stimulated and the LET of the iron ion beam is much higher than the neutron beam used in the study (Slabbert and Vral, 2015). To the best of our knowledge, a limited number of studies researched DNA DSB formation and repair in CD34⁺ cells after high-LET radiation. This restricts the comparison of our γ -H2AX foci results mainly to experiments with low-LET radiation.

Low endogenous γ -H2AX foci levels were detected in the isolated CD34⁺ cells. An average value of 0.319 ± 0.052 γ -H2AX foci/cell were found that is similar to findings of previous studies for CD34⁺ cells isolated from UCB (Rübe *et al.*, 2011; Vandevoorde *et al.*, 2016). Vasilyev *et al.* evaluated γ -H2AX foci levels at the same time point (18 h) post-irradiation to ⁶⁰Co γ -rays in HSPCs isolated from UCB. They observed a significantly higher number of residual DNA DSBs compared to the non-irradiated HSPCs at the same time point (Mavragani *et al.*, 2019), which agrees with the observations at 18 h for both radiation qualities. In general, low residual DNA DSB levels are observed after 24 h for low-LET radiation qualities by other groups and suggest an efficient and fast DNA damage repair capacity in CD34⁺ cells (Rübe *et al.*, 2011; Vandevoorde *et al.*, 2016).

One of the potential underlying reasons for the fast DNA repair response in HSPCs could be the chromatin structure of the cells (Schuler and Rübe, 2013; Vandevoorde *et al.*, 2016). Since the differentiation of the hematopoietic system follows a strict hierarchical pattern starting from the most primitive and pluripotent haematopoietic stem cells (HSCs), it is anticipated that epigenetic changes in the chromatin structure will play a crucial role in the control of the gradual differentiation process (Kosan and Godmann, 2016; Sharma and Gurudutta, 2016). DNA organised in loose chromatin (euchromatin) contributes to the maintenance of pluripotency, while DNA tightly packed into dense chromatin (heterochromatin) hides the genetic code effectively and becomes inconspicuous for genetic reading and transcription (Sharma and Gurudutta, 2016). The open configuration has been proposed as one of the hallmarks of stem cells and makes them readily accessible to proteins, which could facilitate DNA repair processes in damaged stem cells (Sharma and Gurudutta, 2016). Another explanation for the fast DNA repair kinetics, could be related to the heterogeneity of the CD34⁺

cells that were used in this study. The enriched CD34⁺ cells isolated from different donors present a heterogeneous population of HSPCs at different stages of differentiation, of which the majority will consist of progenitor cells (PCs) (CD34⁺CD38⁺) and only a very small fraction of primitive, pluripotent HSCs (CD34⁺CD38⁻) (Hao *et al.*, 1995; D'Arena *et al.*, 1996). Over the past few years, several studies have illustrated distinct differences between the radiosensitivity of the pluripotent HSC population compared to their progeny (Milyavsky *et al.*, 2010; Mohrin *et al.*, 2010); and reviewed in Heylmann *et al.* (Heylmann *et al.*, 2014). A study of Milyavsky *et al.* reported that the pluripotent HSCs have delayed DSB re-joining capacity, resulting in higher levels of residual γ -H2AX foci/cell relative to the committed PCs isolated from UCB (Milyavsky *et al.*, 2010). This was confirmed in the study of Biechonski *et al.*, where the pluripotent HSCs isolated from UCB had a 2 – 6-fold lower frequency of NHEJ events in relation to the portion of PCs 12 h post-irradiation (Biechonski *et al.*, 2018). The largest fraction of the HSPCs in this study is PCs. These findings confirm the hypothesis that the fast DNA repair kinetics that were observed in our study, are attributable to the error-prone NHEJ pathways. The latter is further motivated by studies using an enhanced green fluorescent protein (EGFP)-based reported system that showed a relative preference for NHEJ in HSPCs, such as MMEJ and single-strand annealing (SSA) (Rall *et al.*, 2015). In general, approximately 8 out of 10 DNA DSBs induced by low-LET radiation are repaired by the NHEJ pathway. In contrast to the high-fidelity HR DNA DSB repair pathway, NHEJ is a fast and error-prone process that doesn't depend on cell cycle stage and sequence homology. Therefore, this repair pathway can result in genomic structural variants and chromosomal aberrations in a cell, leading to subsequent genomic instability (Kakaroungkas and Jeggo, 2014).

4.1.3 Radiation-Induced Apoptosis in CD34⁺ Cells

The activation of p53 has been associated with several pathways involved in the DDR network, which include cell cycle arrest, apoptosis and senescence (Reinhardt and Schumacher, 2012). Apoptosis is necessary to maintain tissue homeostasis, but excessive apoptosis can lead to tissue atrophy and possible loss of tissue. The induction of apoptosis in HSPCs proceeds mainly via a p53-dependent pathway and is initiated by a high amount of acute or chronic genotoxic damage (Solozobova and Blattner, 2011; Biechonski, Yassin and Milyavsky, 2017). In addition to controlling the proliferation of HSCs, p53 is an essential component for maintaining the quiescent state of HSCs (Liu *et al.*, 2009). This p53 activity is controlled by two p53 target

genes that regulate the quiescent state of HSCs, Gfi-1 and Nedcin (Liu *et al.*, 2009). Moreover, damaged HSPCs by IR exposure can be sacrificed in favour of maintaining genomic integrity (Doulatov *et al.*, 2012). Additional response to DNA damage is senescence and differentiation to more lineage-restricted progenitor cells. Differentiation is an important mechanism that prevents the accumulation of damaged HSPCs by pushing them towards differentiation instead of self-renewal, which can be seen as a mechanism to suppress leukaemogenesis (Doulatov *et al.*, 2012). In the current study, it was observed that CD34⁺ cells derived from UCB are less prone to undergo apoptosis following irradiation by either high or low LET radiation. A possible explanation could be that p53 also facilitates DNA damage repair in CD34⁺ since the type of DNA damage drives the specific cellular response of p53. The transcriptional regulatory functions of p53 control the expression of its pro-apoptotic target genes such as the p53 upregulated mediator of apoptosis, Puma, that induces apoptosis in HSPCs under conditions of genotoxic stress (Zilfou, Spector and Lowe, 2005; Biechonski *et al.*, 2017) (Figure 4.1). Wu *et al.* (2005) showed that the transcription factor Slug is induced by p53 and protects HSPCs from apoptosis triggered by DNA damage. Following irradiation, Slug is induced by p53 and protects the damaged cells from apoptosis by directly repressing p53-mediated transcription of Puma (Inoue *et al.*, 2002; Wu *et al.*, 2005). The role of Slug in determining the fate of normal hematopoietic progenitors is highly relevant to cancer therapy, due to their sensitivity to genotoxic agents that limits therapeutic doses of radiation (Wu *et al.*, 2005). The results establish that the DDR of human HSCs differs in multiple ways from more mature hematopoietic populations. Primitive HSCs/MPPs exhibit delayed DSB rejoining and persistent DDR foci and undergo higher levels of p53/ASPP1-dependent apoptosis compared to progenitor population in response to IR. p53 inactivation or Bcl-2 overexpression effectively antagonised IR-induced apoptosis and provided profound rescue of HSC repopulation potential in primary transplanted mice. However, in serial transplanted mice, HSCs with disabled p53 exhibited persistently high spontaneous γ -H2AX foci in the engrafted cells and this correlated with markedly decreased HSC self-renewal capacity. By contrast, Bcl-2-overexpressing HSCs with intact p53 were able to sustain HSC self-renewal, establishing that the negative impact of disabled p53 on HSC self-renewal must be due to impairment of apoptosis-independent p53 function. Taken together, these results indicate that p53 has discrete functions in human HSCs that are balanced to facilitate genome stability and optimal self-renewal: one is apoptosis dependent and serves to negatively regulate HSCs, especially after IR, whereas, the other is apoptosis independent, positively regulating HSCs especially during serial transplantation. Alongside apoptosis regulation, p53 has additional functional roles such as regulation of HSC

self-renewal which occurs independently from the regulation of apoptosis (Milyavsky *et al.*, 2010). In addition, human HSCs are sensitised to apoptosis after γ -irradiation, sacrificing damaged HSCs in order to maintain the genomic integrity. Milyavsky *et al.* (2010) reported that the HSCs and MPP fraction show an enhanced p53-and ASPP1-dependent apoptosis and persistent γ -H2AX foci upon γ -irradiation compared to committed progenitors (Milyavsky *et al.*, 2010). This might be potential strategies to protect HSPCs from the myelosuppressive effects of RT.

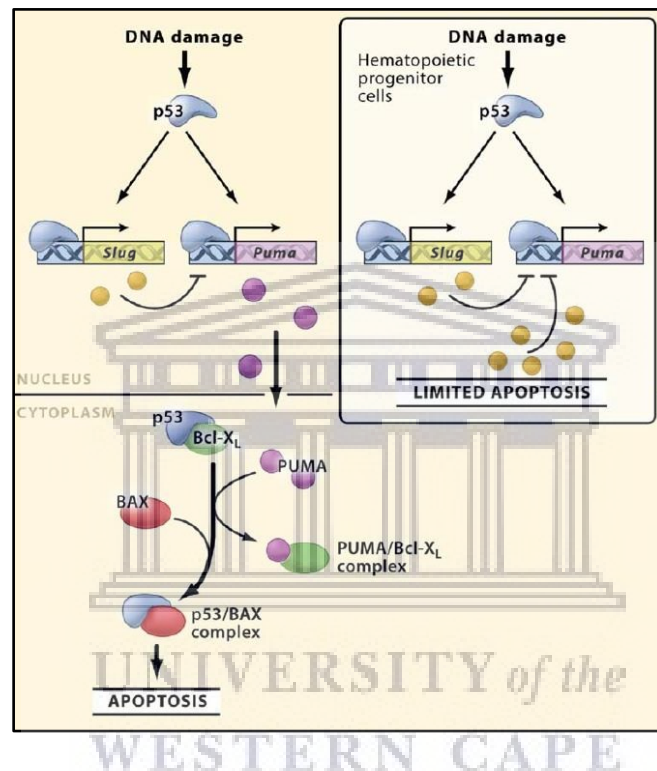


Figure 4.1. A representation of the role of Puma and Slug in modulating apoptosis mediated by p53. Once activated by DNA damage, p53 activates several target genes, including Puma (which encodes a proapoptotic BH3-only protein) and Slug (which encodes a transcription factor that represses Puma transcription). In most cells, the quantity of Slug may not be sufficient to suppress Puma and prevent apoptosis. However, in HSPCs, the endogenous amount of Slug protein is adequate to suppress Puma and limit apoptosis induced by DNA damage. Also shown in this figure is the role of Puma and p53 in coordinating cell death in the cytoplasm. Here, Puma binds Bcl-xL and displaces p53, thereby allowing p53 to directly activate Bax and induce permeabilisation of mitochondria and cell death (Zilfou *et al.*, 2005)

IR can cause long term BM injury, resulting in the induction of HSPCs senescence which will impair HSCPs self-renewal ability leading to a reduction in the HSPCs pool (Shao *et al.*, 2013; Biechonski, Yassin and Milyavsky, 2017; Chen *et al.*, 2019). In a previous study, HSCs from irradiated mice accumulated at the G2/M phase of the cell cycle and were negative for mitotic

markers, signifying activity of the G2/M checkpoint upon radiation induced DNA damage (Brown *et al.*, 2015). Unfortunately, it was not possible to include cell cycle analysis in this study in order to highlight potential cell cycle arrests after irradiation of HSPCs after low- and high-LET irradiation.

As expected, a slow decrease in the percentage of living cells was reported with increased radiation dose for both radiation qualities and this trend increased from 18 to 42 h (Figure 3.6.1, A and Figure 3.6.1, D), which corresponds to the increasing mean number of cells that undergoes early and late apoptosis. The mean number of cells remain relatively constant with increasing dose and no significant difference in early apoptosis could be observed between both radiation qualities (Figure 3.6.1, B and Figure 3.6.1, E). However, at 42 h after ^{60}Co γ -rays and neutron irradiation, a slight decrease in the number of early apoptotic cells is noticeable at 3 Gy (Figure 3.6.1, E), suggesting a higher fraction of CD34⁺ cells that are already in late apoptosis for this dose point. Furthermore, as expected from the results obtained for living cells, the levels of late apoptosis gradually increased with dose for both low- and high-LET radiation (Figure 3.6A and Figure 3.6 B).

As previously mentioned, high-LET radiation is more efficient in producing more severe and complex DNA DSBs that have a greater probability to result in a lethal event. A significant difference was observed in late apoptosis between the low-LET and high-LET radiation after 18 and 42 h ($p < 0.05$) (Figure 3.6.1, C and Figure 3.6.1, F) at 0, 0.5 and 3 Gy. This might indicate that the lack of significant difference observed in residual γ -H2AX foci between ^{60}Co γ -rays radiation and neutron treated CD34⁺ cells at 18 h could be attributable to the loss of damaged cells as expected after high-LET radiation exposure. Vral *et al.* reported that there was no significant difference in apoptosis induction for PBL exposed to ^{60}Co γ -rays and 5.5 MeV neutrons after 24 h, nor at longer incubation times of 48 – 72 h, for doses ranging from 0.05 to 5 Gy (Vral *et al.*, 1998). This contradicts the current study, where a significant increase in late apoptosis at 42 h were observed in CD34⁺ cells, which seem to be more prone to undergo apoptosis following high-LET radiation at dose 1 and 3 Gy. In a study of Kraft *et al.*, where HSPCs were isolated from peripheral blood of healthy adults, the induction of apoptosis over time was slightly higher for high-LET carbon ions with a maximum of 30 – 35% for 2 Gy carbon-ions compared to 25% for the same dose of X-rays, which is in agreement with a previous study from the same group (Becker *et al.*, 2009; Kraft *et al.*, 2015).

Several studies investigated the apoptotic response of CD34⁺ cells to low-LET radiation. Milyavsky *et al.* reported approximately 35% of late apoptosis in the PCs at 18 h post-irradiation with 3 Gy X-rays, while almost 60% of the pluripotent HSCs were in late apoptosis at the same time point. As previously mentioned, the majority of the CD34⁺ cells that were used in the current study, were PCs (CD34⁺CD38⁺). Therefore, the 43.7% of late apoptosis at 18 h post-irradiation with low-LET ⁶⁰Co γ -rays is in relatively close range to the findings of Milyavsky's group (Milyavsky *et al.*, 2010). These findings speculate that p53 possibly facilitates DNA damage repair in CD34⁺ and that the transcription factor Slug which is induced by p53 and protects HSPCs from apoptosis, is triggered by DNA damage. The results showed a 2-fold higher fraction of CD34⁺ cells in late apoptosis (36.21%) at 18 h post-irradiation with 0.5 Gy compared to Durdik's findings ($\pm 15\%$). Durdik and co-workers studied radiation-induced apoptosis at ⁶⁰Co γ -ray doses ranging from 0.05 to 2 Gy in CD34⁺ cells isolated from UCB (Durdik *et al.*, 2017a). However, it is important to take into consideration that the background levels (0 Gy) of late apoptosis at 18 h was only $\pm 10\%$ in the study of Durdik *et al.*, while the values of this study were higher at 18 h (26.24%). Durdik *et al.* observed a 2-fold increase in late apoptosis, 42 h post-irradiation with 0.5 Gy, while our results showed only a slight increase of 8.41%. In addition, the CD34⁺ cells in this study expressed only a slightly higher average in late apoptosis at 42 h irrespective of the ⁶⁰Co γ -rays radiation dose, 44.62% (0.5 Gy) and 52.35% (3 Gy) (Figure 3.6.1, F), while Durdik *et al.* observed a larger increase in late apoptosis with increasing dose from 0.5 to 2 Gy at 42 h (Durdik *et al.*, 2017a). In conclusion, the comparison with Durdik *et al.* indicated that the apoptotic response was slightly faster in this study and already reached a plateau at 42 h. However, Durdik *et al.* irradiated the CD34⁺ cells on ice, which might have influenced the DNA damage response at early time-points after irradiation. Additional studies with more intermediate time-points and different irradiation conditions are needed to clarify the observed differences.

4.1.4 Effect of Radiation Quality on the Cytogenetic Damage in CD34⁺ Cells

The CBMN assay was used in CD34⁺ cells to evaluate the cytogenetic damage induced by the low-LET ⁶⁰Co γ -rays and high-LET fast neutron irradiation, which is also a well-known biomarker for radiosensitivity (El-Zein, Vral and Etzel, 2011; Vandevoorde *et al.*, 2016). It is generally accepted that high-LET neutron irradiation is more effective in inducing cytogenetic damage than sparsely ionising low-LET radiation and this was also confirmed in the present

study (Figure 3.1). As a result of the low numbers of CD34⁺ cells after isolation per donor, a culture technique for the CBMN assay requiring low cell numbers (approximately 100,000 isolated cells per culture) with low volume of cIMDM (~200 – 500 µL) was established by Vandevoorde *et al.* (Vandevoorde *et al.*, 2016). In this study however, the isolated CD34⁺ cells were stored in -80°C before the irradiation experiments which is a slight deviation from the protocol developed by Vandevoorde *et al.* Other studies either pooled the CD34⁺ cells of different donors or expanded the CD34⁺ cells in culture. Hintzsche *et al.* pre-cultured the CD34⁺ cells upon thawing for 4 days before experimental treatment to increase cell numbers (Hintzsche, Montag and Stopper, 2018). This resulted in a 7- to 10-fold increase in the number of cells but also enhances the chance of further differentiation of the HSPCs.

In the current study, a dose-dependent induction of MN frequency was observed, which is in line with previous studies showing that the number of radiation-induced MN is strongly correlated with radiation dose and depends on the radiation quality (Lusiyanti *et al.*, 2016). Post-irradiation with the lowest dose of 0.05 Gy, a statistically significant increase in the MN frequency was observed compared to sham-irradiated controls for both ⁶⁰Co γ-rays and neutrons ($p < 0.001$). Becker *et al.* analysed the frequency in chromosomal aberrations in human CD34⁺ cells after low-LET X-ray and carbon ion (29 keV/µm) irradiation (Becker *et al.*, 2009). The effect of 29 keV/µm carbon ions was more noticeable compared to X-rays and the fraction of complex-type aberrations was higher following carbon ion exposure. The resulting RBE values ranged from 1.4 to 1.7 (Becker *et al.*, 2009). In this study, the biological enhancement ratio was found to range from 1.6 to 3.6 for neutron doses of 0.05 Gy and 0.5 Gy, respectively (Table 1.1). This is much higher than RBE values reported by Becker *et al.* and contradicts the general rule that the RBE increases at lower doses. However, as noted in the results section, this enhancement ratio is not a valid substitute for RBE and dose response curves are required to determine α and β parameters to calculate the RBE at the desired level of biological effect. Vandersickel *et al.* reported RBE values that ranged between 3.6 and 1.6 for PBL in the dose range of 0.05 Gy to 2 Gy, which supports our biological enhancement ratio (Vandersickel *et al.*, 2014). Therefore, the higher ratio reveals that a larger proportion of the induced DNA DSBs are mis-repaired after high-LET neutron irradiation. The latter radiation quality is therefore more effective than ⁶⁰Co γ-rays at inducing cytogenetic damage in human CD34⁺, even at low doses of 0.5 Gy. Rall *et al.* used premature chromosome condensation to study the rejoining of radiation-induced chromatid breaks at 9 h after 2 Gy irradiation in PBL and CD34⁺ cells (Rall *et al.*, 2015). For X-ray irradiation, more than 50% of the chromatid

breaks were repaired within 1 – 2 h post-irradiation. However, the rejoining of chromatid breaks was slower after 2 Gy of very high-LET irradiation (calcium and titanium ions, 180 and 150 keV/μm, respectively) (Rall *et al.*, 2015).

In this study, the average NDI values were determined for both irradiation modalities, which illustrates the reliability of the culturing method that was used (Figure 3.3). The NDI for PBL is presumed to be in the range of 1.3 – 2.2 (Fenech, 2007). This is in line with the results for isolated CD34⁺ cells, with a comparable NDI of 1.84 ± 0.06 for the unirradiated cultures, which is in accordance and more improved than previous publications reporting values of 1.58 ± 0.13 (Vandevoorde *et al.*, 2016) and 1.58 ± 0.10 (Roos and Kaina, 2013). In addition, even after irradiation, the NDI remained above 1.5 for each dose and both radiation modalities, which reflects good proliferation in the CBMN cultures. The lowest NDI value would be 1.0, which is the case if all of the viable CD34⁺ cells fail to divide during the cytokinesis-block period and as a result, all of them would be mononucleated. If all viable CD34⁺ cells have completed one division this would have resulted in an NDI value of 2.0. In the current findings, no significant difference could be observed in the mean NDI for the two different radiation modalities ($p > 0.05$), illustrating that the low radiation doses and difference in LET did not impact the proliferation capacity of the CD34⁺ cells and the CBMN assay provides a true reflection of the radiation-induced cytogenetic damage.

From the analyses of the results, it was noted that several limitations may have been overlooked, such as CD34⁺ cell populations are a heterogenous mix of primitive HSCs and more lineage-committed progenitor cells, which display differences in radiosensitivity. Further research is needed to elucidate the DNA damage response of the different subsets and their connection to specific types of radiation-induced leukaemias post-neutron irradiation. In addition, due to the p(66)/Be(40) neutron beam time is not available on demand CD34⁺ cells were frozen. This could have contributed to the variability and the higher level of apoptosis in non-irradiated samples, although the error bars are comparable to observations performed by other groups. In addition, the *in vitro* irradiation of isolated CD34⁺ cells from UCB is a simplified way to study the underlying mechanisms that are involved in the regulation of HSC fate after neutron irradiation. A growing number of studies illustrates the importance of the bone marrow microenvironment, also known as bone marrow niche, to support HSPC function.

Stem cells depend on their microenvironment, the stem cell niche, for regulation of self-renewal and differentiation (Schofield, 1978). In case of the bone marrow niche, there reside

two major types of multipotent stem cells: HSCs and mesenchymal stem cells (MSCs) (Vanegas and Vernet, 2017). During homeostasis, HSCs often travel from one BM compartment to another. Under stress conditions when the BM cannot sustain sufficient haematopoiesis, HSCs can even travel to the spleen or liver (Wei and Frenette, 2018). The hallmark of HSCs is their ability to implement a quiescent state and persist in the non-dividing G₀ phase of the cell cycle. It has been described that an appropriate association between HSCs and the BM niche, may influence the fate of HSCs and modulate haematopoiesis (Arai, Hirao and Suda, 2005; Cho *et al.*, 2020). This concept is known as the ‘niche hypothesis’, in which the niche forms a regulatory unit that limits the entry of HSCs into the cell cycle, thereby protecting them from exhaustion or from errors in DNA replication. Therefore, identification of molecular signals that regulate the fate of HSCs could improve knowledge of the regulation of haematopoiesis in health and disease (Boulais and Frenette, 2015).

This BM stem cell niche regulates the *in vivo* cell fate of normal HSC, as well as leukaemia stem cells (LSCs). Several studies have indicated that the regeneration of normal HSCs and the process of leukaemogenesis change with age (Carlesso and Cardoso, 2010; Henry, Marusyk and DeGregori, 2011; Lee *et al.*, 2019). However, the role of microenvironmental factors in these age-related effects are unclear. In a study conducted by Lee *et al.*, they compared the stem cell niche in neonatal and adult BM to investigate the possible differences in microenvironmental regulation of both normal and LSCs (Lee *et al.*, 2019). They observed that MSC niche in neonatal BM contained higher frequency of primitive subsets of mesenchymal stroma expressing both platelet-derived growth factor receptor and Sca-1, and higher expression levels of the niche cross-talk molecules, Jagged-1 and CXCL-12 compared to the adult BM. Thus, the normal HSCs transplanted into neonatal mice resulted in higher regeneration in BM compared to adult BM. On the other hand, the *in vivo* self-renewal of LSCs was higher in adult BM than in neonatal BM, resulting in an increased frequency of leukaemia-initiating cells. That study showed that a distinctive microenvironment influences the function of normal and LSCs that provide important insights into age-related changes in haematological disease (Lee *et al.*, 2019).

Radiation-induced damage to the bone marrow niche and the several different types of non-haematopoietic cells that compose this microenvironment, might indirectly damage or influence the DNA damage response of HSPCs (Lu *et al.*, 2020). Therefore, co-culture experiments with mesenchymal stroma cells or bone marrow derived endothelial cells as performed by Biechonski *et al.* (Biechonski *et al.*, 2018) and Cary *et al.* (Cary *et al.*, 2019),

could give a more comprehensive idea of the impact of the bone marrow niche on the radiosensitivity of HSPCs. Although much progress has been made in animal studies, it remains difficult to extrapolate findings from mice to humans, particularly since there seems to be a difference in the radiosensitivity of murine and human HSPCs (Heylmann *et al.*, 2014).

4.2 Age Dependence in Radiation Sensitivity

4.2.1 Age-dependent Variances in Radiosensitivity

Lymphocytes of the peripheral blood are commonly used for radiosensitivity and biodosimetry studies as they are easily obtainable. Furthermore, they are in the G₀-phase and therefore no cell cycle dependent difference in radiosensitivity occurs. In Section 3.2.1 of this PhD thesis, statistically significant differences were observed between newborn and adult T-lymphocytes (aged 23 – 61 years) in radiation-induced MN yields; except at the highest dose of 4 Gy ⁶⁰Co γ -rays (Figure 3.7). A high radiation-induced MN yield of 344.91 ± 22.83 MN/1000 BN cells was observed in newborns compared to a lower yield of 297 ± 14.00 MN/1000 BN cells in adults after 4 Gy ($p > 0.05$). Even though there were no significant differences observed between males and females in the radiation-induced MN yields for both age groups, there was a trend showing females are more sensitive to radiation than males (Figure 3.8 and Figure 3.9).

As early as in 1994, Floyd *et al.* investigated the intrinsic radiosensitivity of adult and cord blood lymphocytes by using the MN assay (Floyd and Cassoni, 1994). They analysed the radiation-induced MN for 10 different APB donors and 5 UCB donors. When comparing the amount of MN induced after 2 Gy X-ray irradiation (dose rate of 2.35 Gy/min), they observed that only 2 UCB donors were more radiosensitive than the mean percentage of APB samples. However, at 4 Gy irradiation, 4 out of the 5 UCB samples showed increased radiosensitivity when compared to the average radiosensitivity percentage of the APB samples. These findings are in line with the results presented here, but differs in that they scored micronucleated cells and not the micronucleus frequency, as in the study. Floyd *et al.* observed a significant difference ($p < 0.02$), once the slope of the dose-response curves of the 5 UCB donors were compared to the mean dose response of the APB donors. A higher radiosensitivity of newborns was also reported in a study of Vandevoorde *et al.*, where significant differences were observed between newborn and adult T-lymphocytes in radiation-induced MN frequencies. After 2 Gy

X-ray irradiation, a high radiation-induced MN yield of 351 ± 23 MN/1000 BN cells was observed in newborns compared to a significant lower yield of 275 ± 18 MN/1000 BN cells in adults ($p < 0.05$) (Vandevoorde *et al.*, 2016). The results showed the same trend as the Vandevoorde study but lower MN yields were seen. This might be attributable to differences in scoring technique, since a semi-automated Metafer scoring was applied in the current study, while Vandevoorde *et al.* applied manual scoring on Giemsa stained MN slides. Following 2 Gy ^{60}Co γ -rays, a high radiation-induced MN yield of 125.69 ± 9.09 MN/1000 BN cells was observed in UCB compared to a significant lower yield of 97.08 ± 6.42 MN/1000 BN cells in APB samples ($p < 0.05$). Bakhmutsky *et al.* investigated the influence of age on the frequency and types of chromosome damage in response to IR, by exposing peripheral lymphocytes 20 adults (aged 22 – 78 years) and 10 UCB samples to 0 (control), 1, 2, 3 or 4 Gy of ^{60}Co γ -rays (Bakhmutsky *et al.*, 2014). Peripheral blood lymphocytes from newborns showed statistically significant increases in the induced frequencies of translocated chromosomes, dicentrics, acentric fragments, colour junctions and abnormal cells at numerous radiation doses once compared to adult donors. In contrast, individual assessment of the adults in their study displayed no significant difference with age or gender. The increased radiosensitivity of newborn to adult donors was $37 \pm 9\%$, $18 \pm 4\%$, $12 \pm 2\%$ and $4 \pm 5\%$ formulated on the scoring of chromosomal aberrations (CA) at doses of 1, 2, 3 and 4 Gy, respectively. As previously stated, no significant difference was observed after 4 Gy irradiation between the MN yield of newborns and adults in that study. In the current study, an increased radiosensitivity of newborn to adult donors of 34%, 42%, 29%, 26% and 16% was observed, which was expressed on the MN scoring at doses of 0.5, 1, 2, 3 and 4 Gy, respectively. Once the induced CA frequencies in the irradiated samples were evaluated within each dose group, Bakhmutsky *et al.* observed decreases in the CA frequencies at 1, 2 and 3 Gy with age, with newborns ($n = 10$) having more aberrations than adults ($n = 20$, aged 22 – 78 years). At 4 Gy, the slopes of the regression lines as described by Bakhmutsky *et al.* were regularly in the same direction as the slopes at lower doses, although no statistical significance was observed between the age groups (Bakhmutsky *et al.*, 2014). These results might suggest that the cells encountered more damage at 4 Gy than cells exposed to lower doses (0.5 – 3 Gy), and would have experienced more negative selection during the 48 h (CA assay) or 72 h (MN assay) culture period, either by apoptosis or cell cycle arrest. In the current study, no significance difference was observed in the radiosensitivity of UCB and APB following 4 Gy ^{60}Co - γ -ray radiation. This observation is based on the result obtained at 4 Gy (16%) and the results obtained at the lower doses (26 – 34%) proving that newborns are more prone to radiation-induced chromosome damage than adults.

Mei *et al.*, using a colony formation assay, showed that aging did not affect the male adult population in response to 2 or 4 Gy X-ray radiation exposure (Mei *et al.*, 1996). Their results suggest that the change in sensitivity in response to IR appears to occur between birth and adulthood, rather than progressively over the years from birth to senescence. The lack of an age effect amongst adults is perhaps the result of the termination of growth and development in this age group. The findings support previous work showing that children are at higher risk of developing cancer associated with IR exposure (Kleinerman, 2006; Sadetzki and Mandelzweig, 2009). Similarly in a group of 14 individuals, no influence of age on dicentric aberrations was found (Pajic *et al.*, 2015).

An age-dependent radiosensitivity study was carried out in a cohort of healthy individuals (n = 202, mean age 50.7 years) and a cancer patient cohort (n = 393, mean age 60.4 years) (Schuster *et al.*, 2018). The lymphocytes of healthy individuals were irradiated with 2 Gy by a 6-MV linear accelerator. In the healthy individual cohort, breaks per metaphase (B/M) clearly increased with age by 0.0014 B/M per year, while no correlation of age and B/M values was found in the cancer patient cohort. In the cancer patient cohort, a substantial portion of individuals with increased radiosensitivity was expected, as individuals with impaired DDR are usually more prone to cancer. Secondly, a clear increase of the individual radiosensitivity with age was observed in the healthy individual cohort. This study shows individual radiosensitivity rises continuously with age, yet with strong inter-individual variation.

Even if an age effect was not apparent among adults, inter-individual variation due to intrinsic genetic factors may influence radiation responses. An example could be differences between ethnic groups that could assist to unravel the underlying mechanisms (Schnarr *et al.*, 2007; López, Palmer and Lawrence, 2009; Francies *et al.*, 2015). South Africa remains a complex mix of different population and ethnic groups. According to Statistics South Africa's 2020 mid-year estimations, the population consist of 80.8% Black, 8.8% Coloured, 2.6% Indian/Asian and 7.8% White citizens (Statistics South Africa, 2020). Population and ethnic differences in patients with solid and haematological malignancies have been well recognised. Epidemiological data for AL in The Western Cape Province, South Africa revealed the following (Sayers *et al.*, 1992):

- A cluster of leukaemia among white patients occurred in the Statistical Region 17 (SR17), which was significant at the 99% level.

- The prevalence of leukaemia was 50% lower than expected in coloured and black South Africans, whereas that for the white South Africans accorded with the published figures from developed countries.
- The age distribution for leukaemia was seen in the white group, but was absent in the other two groups.

However, less is known on the potential impact of ethnicity on radiosensitivity.

4.2.2 Differences in Immunophenotypic Profile of Newborns and Adult T-lymphocytes

Phenotypic and physiological differences are known to exist between APB and UCB samples. As previously stated, UCB contains HSPCs that have a much higher proliferation rate than adult stem cells in peripheral blood (Hordyjewska, Popiołek and Horecka, 2015). UCB also has almost three times as many total lymphocytes as adult blood (Beck and Lam-Po-Tang, 1994) and these lymphocytes are immunologically immature and differ in their immunophenotypes compared to lymphocytes isolated from APB (López, Palmer and Lawrence, 2009). Similar to adult naïve T-lymphocytes, most UCB T-lymphocytes express the RA⁺ isoform of the CD45 cell surface marker (Marchant and Goldman, 2005). This is likely a consequence of limited antigenic experience during pregnancy (D'Arena *et al.*, 1998; Dalal and Roifman, 2018). The immunophenotypic study determined the percentage of T-lymphocyte subsets in the UCB and APB samples by the use of flow cytometry and the results are in line with both the results of D'Arena *et al.* (D'Arena *et al.*, 1998) and Vandevoorde *et al.* (Vandevoorde, 2015). A comparison of the mean values of the three studies are presented in [Table 4.1](#).

Table 4.1. The percentage of naïve and memory CD4⁺ and CD8⁺ T-lymphocytes determined in UCB and APB in the study, compared to previous studies. Values are expressed as mean percentage (\pm SD).

Subpopulations	Umbilical cord blood (UCB)			Adult peripheral blood (APB)		
	This study	D'Arena	Vandevoorde	This study	D'Arena	Vandevoorde
CD4 ⁺ CD45RA ⁺	91.1 \pm 4.6	87.6 \pm 5.2	97.3 \pm 2.3	39.1 \pm 12.4	44.8 \pm 9.6	38.2 \pm 19.0
CD4 ⁺ CD45RO ⁺	8.3 \pm 4.1	12.3 \pm 5.2	2.5 \pm 2	60.2 \pm 12.7	55.2 \pm 9.6	58.6 \pm 17.3
CD8 ⁺ CD45RA ⁺	95.6 \pm 2.9	93.5 \pm 7.8	99.7 \pm 0.3	53.7 \pm 10.9	71.5 \pm 8.1	61.9 \pm 18.6
CD8 ⁺ CD45RO ⁺	3.8 \pm 2.5	6.4 \pm 7.8	0.3 \pm 0.3	44.4 \pm 10.8	28.5 \pm 8.1	35.6 \pm 13.8

In the study, a different distribution of CD45 isoforms was observed in newborns and adult CD4⁺ and CD8⁺ T-lymphocytes, with the CD45RA⁺ phenotype expressed at a higher level on the CD8⁺ T-lymphocyte population and a higher expression of the CD45RO⁺ phenotype on CD4⁺ T-lymphocyte, which is in line with other studies (D'Arena *et al.*, 1998; Vandevoorde *et al.*, 2016). The different cell types found in UCB as opposed to APB could be a contributing factor to the differences in sensitivity to radiation seen here (Bakhtmutsky *et al.*, 2014). Generally, naïve (CD45RA⁺/CD45RO⁻) T-lymphocytes are characterised by the furthestmost homogeneous pool of T-lymphocytes as they lack most effector functions. These lymphocytes migrate through secondary lymphoid organs in search of antigens presented by DCs. Once they encounter APCs and become activated through the T-lymphocyte receptor, they multiply and generate effector T-lymphocytes that are CD45RO⁺ with a variety of functions that can migrate into tissues (Mackay, 1993). As individuals age and encounter more new antigens, the percentage of naïve T-lymphocytes declines and that of antigen-experienced memory cells increases (Kumar, Connors and Farber, 2018). This shift away from a population of predominantly naïve T-lymphocyte obviously reflects the influences of cumulative exposure to foreign pathogens over time. It might also represent a compensatory homeostatic response to reduced numbers of naïve cells generated in the thymus, possible intrinsic cellular differential sensitivities to apoptosis and specific effects of the aged environment, which actually promote the appearance and dominance of memory cells (see Figure 4.2) (Globerson and Effros, 2000).

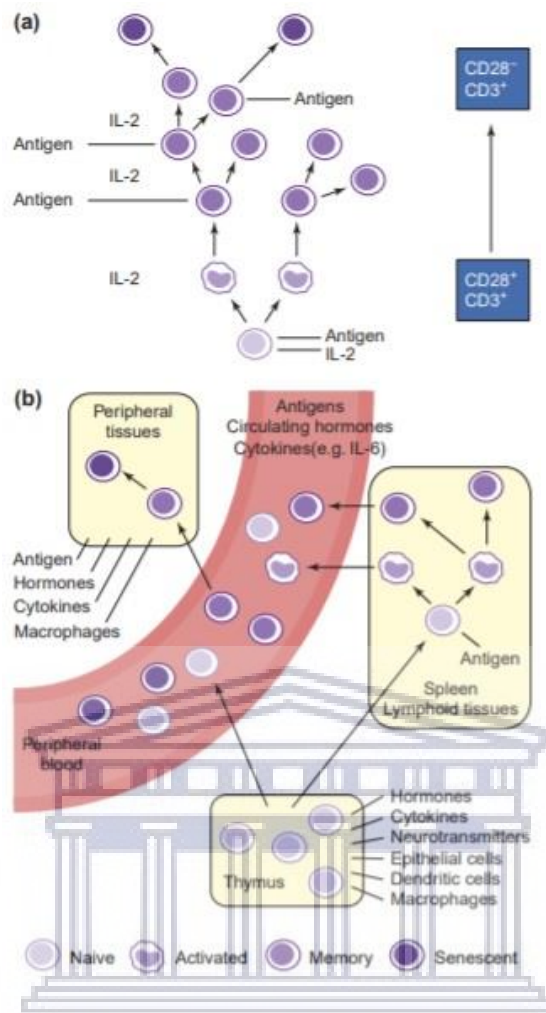


Figure 4.2. (a) This figure represents the ageing of human lymphocytes *in vitro* where naïve T-lymphocytes progress to memory T-lymphocytes and eventually reach a state of replicative senescence resulting antigen- and cytokine-driven proliferation. (b) This represents a schematic model of *in vivo* lymphocytes in the aged individual, where memory T-lymphocytes are subject to repeated encounters with antigen and other proliferative stimuli as they circulate between lymphoid organs, blood and tissues (Globerson and Effros, 2000).

Several epidemiology studies could also demonstrate that the degree of environmental antigen exposure in early life leads to changes in immune status in individuals (Messele *et al.*, 1999; Ben-Smith *et al.*, 2008; Miles *et al.*, 2019; Payne *et al.*, 2020). A study conducted by Payne *et al.* revealed a decline in the naïve/memory ratio of both CD4 and CD8 T-lymphocytes in conjunction with an increased activation markers suggesting that South African children are exposed to a wider range of environmental pathogens in early life than in children in United States (US) and Europe (Payne *et al.*, 2020). In the current study, there was a significant difference between the percentage of CD4⁺ and CD8⁺ T-lymphocyte fractions in UCB, however, no significant difference between the subsets in APB. In addition, a significant

difference was observed in CD4⁺ and CD8⁺ T-lymphocyte subsets between UCB and APB (Figure 3.12). The current results suggest that age influences the CD4⁺ and CD8⁺ T-lymphocyte subsets shift. Valiathan *et al.* (2016) investigated age-related (1 month to 92 years) changes within several subpopulations. Even though, some studies show that the number of CD8⁺ T-lymphocytes decreased with age (Klose *et al.*, 2007), the impact of age on lymphocyte subsets is not completely expounded. The current study revealed a higher percentage of CD8⁺ T-lymphocyte in newborns compared to adults, which is in line with results from Valiathan *et al.* (2016). Furthermore, Valiathan *et al.* showed that the CD8⁺ T-lymphocyte percentages decreased significantly in elderly people compared to adults. In contrast to results obtained by Valiathan *et al.* (2016), CD4⁺ T-lymphocyte percentages in this study were much lower in adults than in the newborns. Ageing has a significant impact on the circulating lymphocytes and the body's immune function and in the elderly is usually accompanied by various changes in the lymphocyte subset distribution. (Valiathan, Ashman and Asthana, 2016).

The study conducted by Vandevoorde *et al.* investigated whether the immunophenotypic differences between T-lymphocyte subsets of newborns and adults could explain the observed cellular differences in radiosensitivity by scoring residual DNA DSBs and MN after IR exposure. The CD4⁺ T-lymphocytes were selected due to the high prevalence of helper-inducer CD4⁺ cells in both UCB and APB samples (Vandevoorde *et al.*, 2016). Vandevoorde *et al.* revealed a difference in radiation sensitivity between human CD4⁺CD45RA⁺ and CD4⁺CD45RO⁺ cells. A statistically significant higher number of radiation-induced MN and residual γ -H2AX/53BP1 foci were observed in naïve CD4⁺ cells after 2 Gy X-ray exposure compared to memory CD4⁺ cells in both UCB and APB samples. This confirmed that their observed differences in foci 24 h post-irradiation and MN yields between newborn and adult T-lymphocytes are linked to the immunophenotypic changes in T-lymphocyte composition with respect to naïve and memory subsets (Vandevoorde *et al.*, 2016). The underlying mechanisms of the observed difference in radiation sensitivity of human naïve and memory T-lymphocyte subsets remains unknown and further research is necessary to elucidate these mechanisms. The observed variance in radiosensitivity between naïve and memory T-lymphocytes could be ascribed to the chromatin structure of the cells (Vandevoorde *et al.*, 2016). The DDR arises within the complex organisation of the chromatin. The chromatin structure and nucleosome organisation represent an important barrier to the efficient detection and repair of DSBs (Price and D'Andrea, 2013). Dynamic chromatin changes will ensure

accessibility to the damaged region by recruiting DNA repair proteins. The ability of repair factors to detect DNA lesions and DSBs is determined by histone modifications around the DSBs and involves dynamic chromatin changes that facilitate repair by promoting chromatin accessibility by contributing to a DSB repair pathway choice and coordination (Schuler and Rube, 2013; Aleksandrov *et al.*, 2020). Rawlings *et al.* verified that during thymocyte development, a condensation of the chromatin arises which is essential for T-lymphocyte development and maintenance of the quiescent state (Rawlings *et al.*, 2011). This mechanism ensures that cytokine driven proliferation can only occur when quiescent naïve T-lymphocytes encounter their TCR-specific antigen. Rawlings *et al.* demonstrated that TCR activation results in a decondensation of the chromatin in naïve T-lymphocytes, which permits the engagement of Stat5. This protein is crucial for peripheral T-lymphocyte proliferation which cannot enter DNA in naïve T-lymphocytes and this ability is only obtained after TCR encounter (Rawlings *et al.*, 2011). In a study conducted by Pugh *et al.*, the radiosensitivity in T-lymphocyte subpopulation in mice was investigated and demonstrated the critical role of an open chromatin state on radiosensitivity (Pugh *et al.*, 2014). The *in vivo* survival trends between the T-lymphocyte subsets were measured in mice 72 h after exposure to 1, 2 and 4 Gy Gammacell Cs¹³⁷. Following *in vivo* irradiation, the memory T-lymphocytes were more resistant to IR, while naïve T-lymphocytes were more sensitive. The upregulation of γ -H2AX was the highest in naïve T-lymphocytes which associates with the observed survival trends in radiosensitivity. The irradiated cells were incubated with or without valproic acid (VPA), a histone deacetylase inhibitor (HDAC) that opens the chromatin, for 12 and 72 h. This improved the survival of naïve T-lymphocytes, whereas memory T-lymphocyte survival remained unaffected. The existence of an open genome-wide chromatin state is a key factor of effective DNA damage repair in T-lymphocytes and a clarification for the observed variances in naïve and memory T-lymphocyte radiosensitivity. In summary, differences in radiation-induced mutagenic effects and residual DNA DSBs in human naïve and memory T-lymphocytes, suggest that radiosensitivity is strongly biased by the chromatin structure (Vandevoorde, 2015). However, further investigation is required to elucidate the observed age-dependency of radiation effects with respect to their potential link to chromosome condensation.

CONCLUSIONS

Epidemiological studies have highlighted that leukaemia can be considered as the most important malignancy after radiation exposure during childhood. The high risk is related to the high sensitivity of the red BM at young ages, which harbours HSPCs. Low-LET ^{60}Co γ -rays and high-LET $p(66)/\text{Be}(40)$ neutrons on $\text{CD}34^+$ cells (HSPCs) of newborns, the target cells for radiation-induced leukaemia, showed a dose dependent increase in apoptosis and cytogenetic damage. The CBMN results, confirms the higher mutagenic potential of neutrons compared to low-LET radiation, even after a low dose of 0.5 Gy. The results point towards a fast error-prone DNA repair in HSPCs after neutron irradiation, which might contribute to genomic instability and leukaemogenesis. The latter is particularly important in light of the growing use of PBT in the treatment of childhood cancer, where very low doses of secondary neutrons are produced. However, additional studies in the very low (out-of-field) dose range are required as well as co-culture experiments with BM-derived cells in order to investigate the potential radioprotective effect of the BM niche.

There is a clear age-dependency effect in response to IR exposure, which makes children more vulnerable to radiation-induced malignancies compared to adults. This study showed that the IR-induced MN yields of the newborn T-lymphocytes were higher compared to the MN yield of the adult T-lymphocytes. No significant difference could be observed between genders, male and female, in both age groups. The main difference between newborns and adult T-lymphocytes in these *in vitro* experiments, was their immunophenotypic profile. The flow cytometry results of this study confirm that the observed difference in radiosensitivity may be attributable to differences in the immunophenotypic profile of T-lymphocytes isolated from UCB and APB.

FUTURE PERSPECTIVES

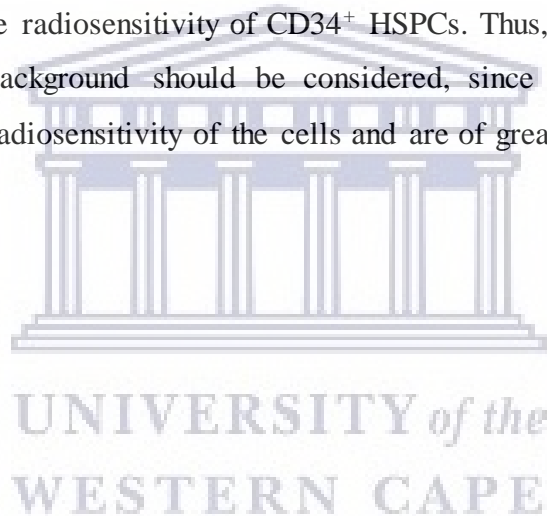
In this PhD dissertation, the radiosensitivity of the HSPCs were evaluated by using a heterogeneous population of CD34⁺ cells. In the next stage of this study, the radiosensitivity of the different primitive and more lineage-committed subsets should be investigated. As previously mentioned, the radiosensitivity of HSPCs in mice are generalised with humans. In a previous study, HSCs from irradiated mice accumulated at the G2/M phase of the cell cycle and are negative for mitotic markers, signifying activity of the G2/M checkpoint upon radiation induced DNA damage (Brown *et al.*, 2015). However, more research is needed to clarify the differences in radiation sensitivity of HSPCs in mice and humans. Therefore, *in vivo* murine models will be required to further investigate the radioprotective characteristics of the BM niche.

The results presented in the CBMN assay showed an increased chromosomal radiosensitivity in CD34⁺ HSPCs collected from UCB. This data demonstrates these CD34⁺ cells are sensitive to the mutagenic effects of ⁶⁰Co γ -rays and neutron radiation. In the next phase, the CD34⁺ HSPCs will be irradiated with PBT to further evaluate their radiosensitivity and compared to the abovementioned types of radiation (⁶⁰Co γ -rays and neutron radiation).

The results of the CBMN assay presented a significant increase in the MN yields between the T-lymphocytes of newborns compared to adult samples. However, no significant difference was observed between genders in both age categories. It would be of great interest to further evaluate the chromosomal radiosensitivity of CD34⁺ HSPCs, T-lymphocytes of newborns and adults by increasing sample numbers as well as the potential effect of ethnicity. This will require larger cohorts in the future to observed the influence of age, gender and ethnicity on radiosensitivity in South Africa.

A probable underlying mechanism of this radiosensitivity difference is the chromatin structure of naïve T-lymphocytes, which should be further investigated. Based on the clear difference observed in the immunophenotypic profile of the T-lymphocytes between the newborns and adult samples. It would be of great interest to investigate the chromatin state of the naïve and

memory T-lymphocyte subpopulations. One possible approach to determine this difference, is the use of flow cytometry to measure histone modification (for example, diAcH3 as a marker of open chromatin) in combination with lineage-specific cell surface markers (Dispirito and Shen, 2010). An additional approach to determine the influence of the condensed chromatin structure of naïve T-lymphocytes on their radiation sensitivity by using histone deacetylase inhibitor (HDAC) that opens the chromatin structure (Pugh *et al.*, 2014). Furthermore, it is known that HIV infection is associated with changes in various T-lymphocyte subsets (Messele *et al.*, 1999). Therefore, future research should investigate influence of the HIV status on the radiosensitivity of T-lymphocytes and CD34⁺ HSPCs, since previous studies have shown an increase in chromosomal radiosensitivity in HIV positive individuals (Herd *et al.*, 2016; Minnaar *et al.*, 2020). Differences in the nature and outcome of leukaemia for children of different ethnicities have been reported. It would therefore be of interest to study the influence of ethnic disparities on the radiosensitivity of CD34⁺ HSPCs. Thus, for future research, the HIV status and ethnic background should be considered, since these parameters could potentially influence the radiosensitivity of the cells and are of great relevance to the South African population.



REFERENCES

- Abreu, P. (2018) 'Bioenergetics mechanisms regulating muscle stem cell self-renewal commitment and function', *Biomedicine and Pharmacotherapy*. pp. 463–472. doi: 10.1016/j.biopha.2018.04.036.
- AbuSamra, D. B. *et al.* (2017) 'Not just a marker: CD34 on human hematopoietic stem/progenitor cells dominates vascular selectin binding along with CD44', *Blood Advances*. 1(27), pp. 2799–2816. doi: 10.1182/bloodadvances.2017004317.
- Al-Ejeh, F. *et al.* (2010) 'Harnessing the complexity of DNA-damage response pathways to improve cancer treatment outcomes.', *Oncogene*.29(46), pp. 6085–6098. doi: 10.1038/onc.2010.407.
- Alberts, B. *et al.* (2002) 'Helper T Cells and Lymphocyte Activation', in *Molecular Biology of the Cell*. 4th edn. New York: Garland Science. Available at: <https://www.ncbi.nlm.nih.gov/books/NBK26827/> (Accessed: 22 October 2020).
- Aleksandrov, R. *et al.* (2020) 'The Chromatin Response to Double-Strand DNA Breaks and Their Repair', *Cells*.. doi: 10.3390/cells9081853.
- Alizadeh, E., Orlando, T. M. and Sanche, L. (2015) 'Biomolecular damage induced by ionizing radiation: The direct and indirect effects of low-energy electrons on DNA', *Annual Review of Physical Chemistry*. 66, pp. 379–398. doi: 10.1146/annurev-physchem-040513-103605.
- Almohiy, H. (2014) 'Paediatric computed tomography radiation dose: A review of the global dilemma', *World journal of radiology*. 6(1), pp. 1–6. doi: 10.4329/wjr.v6.i1.1.
- Alzen, G. and Benz-Bohm, G. (2011) 'Radiation protection in pediatric radiology.', *Deutsches Arzteblatt International*. 108(24), pp. 407–14. doi: 10.3238/arztebl.2011.0407.
- Antonio, E. L. *et al.* (2017) 'Genotoxicity And Cytotoxicity Of X-Rays In Children Exposed To Panoramic Radiography', *Revista Paulista de Pediatria*. 35(3), pp. 296–301. doi: 10.1590/1984-0462/;2017;35;3;00010.

Applegate, K. (2015) 'Image Gently : A campaign to promote radiation protection for children worldwide', pp. 1–5. doi: 10.4102/sajr.v19i2.919.

Arai, F., Hirao, A. and Suda, T. (2005) 'Regulation of hematopoiesis and its interaction with stem cell niches', *International Journal of Hematology*, pp. 371–376. doi: 10.1532/IJH97.05100.

Atun, R. *et al.* (2020) 'Sustainable care for children with cancer: a Lancet Oncology Commission', *The Lancet Oncology*. pp. e185–e224. doi: 10.1016/S1470-2045(20)30022-X.

Azeemi, S. T. Y. and Raza, S. M. (2005) 'A critical analysis of chemotherapy and its scientific evolution.', *Evidence-based complementary and alternative medicine : 2(4)*, pp. 481–488. doi: 10.1093/ecam/neh137.

Baba, M. H., Mohib-ul-Haq, M. and Khan, A. A. (2013) 'Dosimetric Consistency of Co-60 Teletherapy Unit : A Ten Years Study', *International Journal of Health Sciences*. 7(1), pp. 15–21. doi: 10.12816/0006016.

Baeyens, A. *et al.* (2005) 'Chromosomal radiosensitivity in breast cancer patients: influence of age of onset of the disease.', *Oncology reports*. 13(2), pp. 347–353.

Baig, S. *et al.* (2016) 'Potential of apoptotic pathway-targeted cancer therapeutic research: Where do we stand', *Cell Death and Disease*. p. e2058. doi: 10.1038/cddis.2015.275.

Bailey, R. (2018) 'CAS - CERN Accelerator School: Accelerators for Medical Applications', *CERN Yellow Rep. School Proc.* CERN, 1, pp. 1–338. doi: 10.23730/CYRSP-2017-001.

Baiocco, G. *et al.* (2016) 'The origin of neutron biological effectiveness as a function of energy', *Scientific Reports*. 6. doi: 10.1038/srep34033.

Bakhtmutsky, M. V *et al.* (2014) 'Differences in cytogenetic sensitivity to ionizing radiation in newborns and adults.', *Radiation Research*, 181(6), pp. 605–16. doi: 10.1667/RR13598.1.

Beck, R. and Lam-Po-Tang, P. R. L. (1994) 'Comparison of cord blood and adult blood lymphocyte normal ranges: A possible explanation for decreased severity of graft versus host disease after cord blood transplantation', *Immunology and Cell Biology*. 72(5), pp. 440–444. doi: 10.1038/icb.1994.65.

Becker, D. *et al.* (2009) 'Response of human hematopoietic stem and progenitor cells to energetic carbon ions', *International Journal of Radiation Biology*, 85(11), pp. 1051–1059.

doi: 10.3109/09553000903232850.

Beels, L., Werbrouck, J. and Thierens, H. (2010) 'Dose response and repair kinetics of γ -H2AX foci induced by in vitro irradiation of whole blood and T-lymphocytes with X- and γ -radiation', *International Journal of Radiation Biology*. 86(9), pp. 760–768. doi: 10.3109/09553002.2010.484479.

Beinke, C. *et al.* (2016) 'Comparing seven mitogens with PHA-M for improved lymphocyte stimulation in dicentric chromosome analysis for biodosimetry', *Radiation Protection dosimetry*, 168(2), p. 235–241. doi: 10.1093/rpd/ncv286.

Belson, M., Kingsley, B. and Holmes, A. (2007) 'Risk factors for acute leukemia in children: A review', *Environmental Health Perspectives*. pp. 138–145. doi: 10.1289/ehp.9023.

Ben-Smith, A. *et al.* (2008) 'Differences between naive and memory T cell phenotype in Malawian and UK adolescents: A role for Cytomegalovirus?', *BMC Infectious Diseases*. 8(1), p. 139. doi: 10.1186/1471-2334-8-139.

Biechonski, S. *et al.* (2017) 'Quercetin alters the DNA damage response in human hematopoietic stem and progenitor cells via TopoII- and PI3K-dependent mechanisms synergizing in leukemogenic rearrangements', *International Journal of Cancer*. 140(4), pp. 864–876. doi: 10.1002/ijc.30497.

Biechonski, S. *et al.* (2018) 'Attenuated DNA damage responses and increased apoptosis characterize human hematopoietic stem cells exposed to irradiation', *Scientific Reports*. 8(1), p. 6071. doi: 10.1038/s41598-018-24440-w.

Biechonski, S., Yassin, M. and Milyavsky, M. (2017) 'DNA-damage response in hematopoietic stem cells: an evolutionary trade-off between blood regeneration and leukemia suppression', *Carcinogenesis*, 38(4), pp. 367–377. doi: 10.1093/carcin/bgx002.

Biosciences, B. D. *et al.* (2011) *Application Note Detection of Apoptosis Using the BD Annexin V FITC Assay on the BD FACSVerserTM System*.

Board, PDQ Pediatric Treatment Editorial, P. P. T. E. (2019) *Childhood Acute Lymphoblastic Leukemia Treatment (PDQ®): Health Professional Version, PDQ Cancer Information Summaries*. National Cancer Institute (US). Available at: <http://www.ncbi.nlm.nih.gov/pubmed/26389206> (Accessed: 24 July 2018).

De Boer, R. J. and Perelson, A. S. (2012) 'Quantifying T lymphocyte turnover', *Journal of*

Theoretical Biology, pp. 1–43. doi: 10.1016/j.jtbi.2012.12.025.

Boulais, P. E. and Frenette, P. S. (2015) ‘Making sense of hematopoietic stem cell niches’, *Blood*. 125(17), pp. 2621–2629. doi: 10.1182/blood-2014-09-570192.

Brandsma, I. and Gent, D. C. (2012) ‘Pathway choice in DNA double strand break repair: Observations of a balancing act’, *Genome Integrity*. p. 9. doi: 10.1186/2041-9414-3-9.

Bray, F. *et al.* (2018) ‘Global cancer statistics 2018: GLOBOCAN estimates of incidence and mortality worldwide for 36 cancers in 185 countries’, *CA: A Cancer Journal for Clinicians*. 68(6), pp. 394–424. doi: 10.3322/caac.21492.

Brenner, D. J. *et al.* (2003) ‘Cancer risks attributable to low doses of ionizing radiation: Assessing what we really know’, *Proceedings of the National Academy of Sciences of the United States of America*. 100(SUPPL. 2), pp. 13761–13766. doi: 10.1073/pnas.2235592100.

Brenner, D. J. and Hall, E. J. (2008) ‘Secondary neutrons in clinical proton radiotherapy: A charged issue’, *Radiotherapy and Oncology*, 86, pp. 165–170. doi: 10.1016/j.radonc.2007.12.003.

Britel, M., Bourguignon, M. and Foray, N. (2018) ‘The use of the term “radiosensitivity” through history of radiation: from clarity to confusion’, *International Journal of Radiation Biology*. pp. 503–512. doi: 10.1080/09553002.2018.1450535.

Brown, A. *et al.* (2015) ‘Assessing the roles of cell cycle checkpoints in HSC’, *Experimental Hematology*. 43(9), p. S54. doi: 10.1016/j.exphem.2015.06.088.

Brown, G. (2020) ‘Towards a new understanding of decision-making by hematopoietic stem cells’, *International Journal of Molecular Sciences*, 21(7). doi: 10.3390/ijms21072362.

Brown, K. *et al.* (2019) ‘Histology, Cell Death’. StatPearls Publishing, Treasure Island (FL). Available at: <http://europepmc.org/books/NBK526045>.

Campos-Sanchez, E. *et al.* (2011) ‘Acute lymphoblastic leukemia and developmental biology: a crucial interrelationship’, *Cell cycle*. 10(20), pp. 3473–3486. doi: 10.4161/cc.10.20.17779.

Cann, K. L. and Hicks, G. G. (2007) ‘Regulation of the cellular DNA double-strand break response’, *Biochemistry and Cell Biology*, pp. 663–674. doi: 10.1139/O07-135.

Cano, R. L. E. and Lopera, H. D. E. (2013) ‘Introduction to T and B lymphocytes’, in Anaya, J. M., Shoenfeld, Y., and Rojas-Villarrage, A. (eds) *Autoimmunity: From Bench to Bedside*

[Internet]. Bogota (Colombia): El Rosario University Press. Available at: <https://www.ncbi.nlm.nih.gov/books/NBK459471/> (Accessed: 21 October 2020).

Carlesso, N. and Cardoso, A. A. (2010) 'Stem cell regulatory niches and their role in normal and malignant hematopoiesis', *Current Opinion in Hematology*. pp. 281–286. doi: 10.1097/MOH.0b013e32833a25d8.

Carlos-Wallace, F. M. *et al.* (2016) 'Parental, In Utero, and Early-Life Exposure to Benzene and the Risk of Childhood Leukemia: A Meta-Analysis', *American journal of epidemiology*. 2015/11/20. 183(1), pp. 1–14. doi: 10.1093/aje/kwv120.

Carroll, P. D. *et al.* (2012) 'Umbilical cord blood as a replacement source for admission complete blood count in premature infants', *Journal of Perinatology*, 32(2), pp. 97–102. doi: 10.1038/jp.2011.60.

Carvalho, H. de A. and Villar, R. C. (2018) 'Radiotherapy and immune response: the systemic effects of a local treatment', *Clinics*. doi: 10.6061/clinics/2018/e557s.

Cary, L. *et al.* (2019) 'Bone marrow endothelial cells influence function and phenotype of hematopoietic stem and progenitor cells after mixed neutron/gamma radiation', *International Journal of Molecular Sciences*. 20(7). doi: 10.3390/ijms20071795.

Challen, G. A. *et al.* (2009) 'Mouse hematopoietic stem cell identification and analysis', *Cytometry Part A*. pp. 14–24. doi: 10.1002/cyto.a.20674.

Chan, S. *et al.* (1998) 'Visualization of CD4/CD8 T cell commitment', *Journal of Experimental Medicine*. 188(12), pp. 2321–2333. doi: 10.1084/jem.188.12.2321.

Chan, S. W. and Dedon, P. C. (2010) 'The Biological and Metabolic Fates of Endogenous DNA Damage Products', *Journal of Nucleic Acids*. 2010, p. 929047. doi: 10.4061/2010/929047.

Chatterjee, N. and Walker, G. C. (2017) 'Mechanisms of DNA damage, repair, and mutagenesis', *Environmental and Molecular Mutagenesis*. 58(5), pp. 235–263. doi: 10.1002/em.22087.

Chen, B. *et al.* (2014) 'Human Embryonic Stem Cell-Derived Primitive and Definitive Hematopoiesis', in *Pluripotent Stem Cell Biology - Advances in Mechanisms, Methods and Models*. doi: 10.5772/58628.

Chen, Y. *et al.* (2020) ‘Distinct types of cell death and the implication in diabetic cardiomyopathy’, *Frontiers in Pharmacology*. p. 42. doi: 10.3389/fphar.2020.00042.

Chen, Z. *et al.* (2019) ‘Cellular senescence in ionizing radiation (Review)’, *Oncology Reports*. pp. 883–894. doi: 10.3892/or.2019.7209.

Cho, H. J. *et al.* (2020) ‘Regulation of hematopoietic stem cell fate and malignancy’, *International Journal of Molecular Sciences*, 21(13), pp. 1–18. doi: 10.3390/ijms21134780.

Chodick, G. *et al.* (2009) ‘Radiation risks from pediatric computed tomography scanning’, *Pediatric endocrinology reviews: PER*, 7(2), pp. 29–36. Available at: <https://pubmed.ncbi.nlm.nih.gov/20118891>.

Cimato, T. R. *et al.* (2016) ‘Simultaneous measurement of human hematopoietic stem and progenitor cells in blood using multicolor flow cytometry’, *Cytometry. Part B, Clinical cytometry*. 90(5), pp. 415–423. doi: 10.1002/cyto.b.21354.

Cordova, K. A. and Cullings, H. M. (2019) ‘Assessing the Relative Biological Effectiveness of Neutrons across Organs of Varying Depth among the Atomic Bomb Survivors’, *Radiation Research*. 192(4), p. 380. doi: 10.1667/rr15391.1.

Cotter, S. E., McBride, S. M. and Yock, T. I. (2012) ‘Proton radiotherapy for solid tumors of childhood’, *Technology in Cancer Research and Treatment*. 11(3), pp. 267–278. doi: 10.7785/tcrt.2012.500295.

Cristy, M. (1981) ‘Active bone marrow distribution as a function of age in humans.’, *Physics in Medicine and Biology*. 26(3), pp. 389–400. doi: 10.1088/0031-9155/26/3/003.

Cucinotta, F. A., To, K. and Cacao, E. (2017) ‘Predictions of space radiation fatality risk for exploration missions’, *Life Sciences in Space Research*. 13, pp. 1–11. doi: 10.1016/j.lssr.2017.01.005.

D’Andrea, M. A. and Reddy, G. K. (2018) ‘Health Risks Associated With Benzene Exposure in Children: A Systematic Review’, *Global Pediatric Health*. 5, pp. 2333794X18789275-2333794X18789275. doi: 10.1177/2333794X18789275.

D’Arena, G. *et al.* (1996) ‘Human umbilical cord blood: immunophenotypic heterogeneity of CD34+ hematopoietic progenitor cells’, *Haematologica*, 81(5).

D’Arena, G. *et al.* (1998) ‘Flow cytometric characterization of human umbilical cord blood

lymphocytes: immunophenotypic features.’, *Haematologica*. 83(3), pp. 197–203.

Dalal, I. and Roifman, C. M. (2018) *Immunity of the newborn*. Available at: <https://www.uptodate.com/contents/immunity-of-the-newborn> (Accessed: 6 November 2020).

Desouky, O., Ding, N. and Zhou, G. (2015) ‘Targeted and non-targeted effects of ionizing radiation’, *Journal of Radiation Research and Applied Sciences*. 8(2), pp. 247–254. doi: 10.1016/j.jrras.2015.03.003.

Devine, K. (2017) *The Umbilical Cord Blood Controversies in Medical Law - Karen Devine - Google Books, Law*. Available at: [https://books.google.co.za/books?id=G_niDQAAQBAJ&pg=PT174&lpg=PT174&dq=umbilical+cord+blood+\(UCB\)+is+used+as+a+substitute+for+blood+of+a+newborn+as+it+is+genetically+part+of+the+foetus.&source=bl&ots=e3cRHHclYX&sig=ACfU3U0G7PMaEtxjfxekq6N31kY5VSz0iw&hl=e](https://books.google.co.za/books?id=G_niDQAAQBAJ&pg=PT174&lpg=PT174&dq=umbilical+cord+blood+(UCB)+is+used+as+a+substitute+for+blood+of+a+newborn+as+it+is+genetically+part+of+the+foetus.&source=bl&ots=e3cRHHclYX&sig=ACfU3U0G7PMaEtxjfxekq6N31kY5VSz0iw&hl=e) (Accessed: 27 February 2020).

Dispirito, J. R. and Shen, H. (2010) ‘Differentiation and Functionality T Cell + A Marker of Memory CD8 Histone Acetylation at the Single-Cell Level’, *J Immunol*, 184, pp. 4631–4636. doi: 10.4049/jimmunol.0903830.

Donaldson, C. *et al.* (2000) ‘Development of a district Cord Blood Bank: A model for cord blood banking in the National Health Service’, *Bone Marrow Transplantation*. 25(8), pp. 899–905. doi: 10.1038/sj.bmt.1702332.

Dong, H. *et al.* (2015) ‘Update of the human and mouse Fanconi anemia genes’, *Human genomics*. 9(1), p. 32.

Doulatov, S. *et al.* (2012) ‘Hematopoiesis: A human perspective’, *Cell Stem Cell*. pp. 120–136. doi: 10.1016/j.stem.2012.01.006.

Durdik, M. *et al.* (2017a) ‘Hematopoietic stem/progenitor cells are less prone to undergo apoptosis than lymphocytes despite similar DNA damage response.’, *Oncotarget*. 8(30), pp. 48846–48853. doi: 10.18632/oncotarget.16455.

Dutton, R. W., Bradley, L. M. and Swain, S. L. (1998) ‘T cell memory’, *Annual Review of Immunology*. Annu Rev Immunol, pp. 201–223. doi: 10.1146/annurev.immunol.16.1.201.

Eden, T. (2010) ‘Aetiology of childhood leukaemia’, *Cancer Treatment Reviews*. pp. 286–297. doi: 10.1016/j.ctrv.2010.02.004.

El-Zein, R., Vral, A. and Etzel, C. J. (2011) 'Cytokinesis-blocked micronucleus assay and cancer risk assessment', *Mutagenesis*, 26(1), pp. 101–106. doi: 10.1093/mutage/geq071.

Engeland, K. (2018) 'Cell cycle arrest through indirect transcriptional repression by p53: I have a DREAM.', *Cell Death and Differentiation*, 25(1), pp. 114–132. doi: 10.1038/cdd.2017.172.

Erdmann, F. *et al.* (2019) 'Social Inequalities Along the Childhood Cancer Continuum: An Overview of Evidence and a Conceptual Framework to Identify Underlying Mechanisms and Pathways', *Frontiers in Public Health*, p. 84. Available at: <https://www.frontiersin.org/article/10.3389/fpubh.2019.00084>.

Fenech, M. (2000) 'The in vitro micronucleus technique', *Mutation Research*, 455, pp. 81–95. Available at: https://ac.els-cdn.com/S0027510700000658/1-s2.0-S0027510700000658-main.pdf?_tid=39f18ac7-dd2c-4908-abbfa216d808ef4a&acdnat=1527600283_67296ced37cc446dcae534c073db2fd5 (Accessed: 29 May 2018).

Fenech, M. (2007) 'Cytokinesis-block micronucleus cytome assay', *Nature Protocols*, 2(5), pp. 1084–1104. doi: 10.1038/nprot.2007.77.

Fenech, M. *et al.* (2011) 'Molecular mechanisms of micronucleus, nucleoplasmic bridge and nuclear bud formation in mammalian and human cells', *Mutagenesis*, 26(1), pp. 125–132. doi: 10.1093/mutage/geq052.

Ferguson, L. R. *et al.* (2015a) 'Genomic instability in human cancer: Molecular insights and opportunities for therapeutic attack and prevention through diet and nutrition', *Seminars in Cancer Biology*, pp. S5–S24. doi: 10.1016/j.semcancer.2015.03.005.

Fernandez, J. *et al.* (2019) 'Chromosome preference during homologous recombination repair of DNA double-strand breaks in *Drosophila melanogaster*', *G3: Genes, Genomes, Genetics*, 9(11), pp. 3773–3780. doi: 10.1534/g3.119.400607.

Firsanov, D. V., Solovjeva, L. V. and Svetlova, M. P. (2011) 'H2AX phosphorylation at the sites of DNA double-strand breaks in cultivated mammalian cells and tissues', *Clinical Epigenetics*, pp. 283–297. doi: 10.1007/s13148-011-0044-4.

Fischer, M. *et al.* (2016) 'The p53-p21-DREAM-CDE/CHR pathway regulates G2/M cell cycle genes.', *Nucleic acids research*, 44(1), pp. 164–174. doi: 10.1093/nar/gkv927.

Fleck, O. and Nielsen, O. (2004) 'DNA repair', *Journal of Cell Science*, 117, pp. 515–517. doi:

10.1242/jcs.00952.

Floyd, D. N. and Cassoni, A. M. (1994) 'Intrinsic radiosensitivity of adult and cord blood lymphocytes as determined by the micronucleus assay', *European Journal of Cancer*, 30(5), pp. 615–620. doi: [https://doi.org/10.1016/0959-8049\(94\)90531-2](https://doi.org/10.1016/0959-8049(94)90531-2).

Folley, J. H., Borges, W. and Yamawaki, T. (1952) 'Incidence of leukemia in survivors of the atomic bomb in Hiroshima and Nagasaki, Japan.', *The American journal of medicine*. United States, 13(3), pp. 311–321. doi: 10.1016/0002-9343(52)90285-4.

Foundation for the Accreditation of Cellular Therapy (FACT) (2020) *Cord Blood Bank Standards*. Available at: <http://www.factwebsite.org/Inner.aspx?id=73&terms=umbilical+cord+blood> (Accessed: 7 July 2020).

Francies, F. Z. *et al.* (2015) 'Chromosomal radiosensitivity of lymphocytes in South African breast cancer patients of different ethnicity: An indirect measure of cancer susceptibility', *South African Medical Journal*. 105(8), pp. 675–678. doi: 10.7196/SAMJnew.8266.

Fredericia, N. P. M. (2017) 'Quantification of Radiation-induced DNA Damage following intracellular Auger-Cascades', *Ph.D Thesis*, pp. 1–207.

Friedberg, W., Copeland, K. and Faa, D. / (2011) *Ionizing Radiation in Earth's Atmosphere and in Space Near Earth Federal Aviation Administration*. Available at: www.faa.gov/library/reports/medical/oamtechreports (Accessed: 14 October 2020).

Frush, D. P. (2013) 'Radiation risks to children from medical imaging', *Revista Médica Clínica Las Condes*. Elsevier BV, 24(1), pp. 15–20. doi: 10.1016/s0716-8640(13)70124-x.

García, M. J. and Benítez, J. (2008) 'The Fanconi anaemia/BRCA pathway and cancer susceptibility. Searching for new therapeutic targets', *Clinical and Translational Oncology*. 10(2), pp. 78–84.

Gault, N. *et al.* (2019) 'Hematopoietic stem and progenitor cell responses to low radiation doses - implications for leukemia risk.', *International journal of radiation biology*. 95(7), pp. 892–899. doi: 10.1080/09553002.2019.1569777.

Gegonne, A. *et al.* (2018) 'Immature CD8 Single-Positive Thymocytes Are a Molecularly Distinct Subpopulation, Selectively Dependent on BRD4 for Their Differentiation ', *Cell Reports*, 24, pp. 117–129. doi: 10.1016/j.celrep.2018.06.007.

Giglia-Mari, G., Zotter, A. and Vermeulen, W. (2011) 'DNA damage response', *Cold Spring Harbor Perspectives in Biology*. 3(1), pp. a000745–a000745. doi: 10.1101/cshperspect.a000745.

Globerson, A. and Effros, R. B. (2000) 'Ageing of lymphocytes and lymphocytes in the aged', *Immunology Today*, pp. 515–521. doi: 10.1016/S0167-5699(00)01714-X.

Goodhead, D. T. (2019) 'Neutrons are forever! Historical perspectives', *International Journal of Radiation Biology*. pp. 957–984. doi: 10.1080/09553002.2019.1569782.

Gordon, E. *et al.* (2018) 'Cell cycle checkpoint control: The cyclin G1/Mdm2/p53 axis emerges as a strategic target for broad-spectrum cancer gene therapy - A review of molecular mechanisms for oncologists', *Molecular and Clinical Oncology*. 9(2), pp. 115–134. doi: 10.3892/mco.2018.1657.

Grant, E. J. *et al.* (2017) 'Solid Cancer Incidence among the Life Span Study of Atomic Bomb Survivors: 1958-2009.', *Radiation Research*. 187(5), pp. 513–537. doi: 10.1667/RR14492.1.

Greaves, M. (2018) 'A causal mechanism for childhood acute lymphoblastic leukaemia', *Nature Reviews Cancer*. pp. 471–484. doi: 10.1038/s41568-018-0015-6.

Gross, J. P. *et al.* (2019) 'Improved neuropsychological outcomes following proton therapy relative to X-ray therapy for pediatric brain tumor patients.', *Neuro-oncology*, 21(7), pp. 934–943. doi: 10.1093/neuonc/noz070.

Gupta, S. *et al.* (2015) 'Treating Childhood Cancer in Low- and Middle-Income Countries', in *Disease Control Priorities, Third Edition (Volume 3): Cancer*. pp. 121–146. doi: 10.1596/978-1-4648-0349-9_ch7.

Hagiwara, Y. *et al.* (2019) 'Clustered DNA double-strand break formation and the repair pathway following heavy-ion irradiation', *Journal of Radiation Research*, 60(1), pp. 69–79. doi: 10.1093/jrr/rry096.

Hälg, R. A. and Schneider, U. (2020) 'Neutron dose and its measurement in proton therapy-current State of Knowledge.', *The British Journal of Radiology*, 93(1107), p. 20190412. doi: 10.1259/bjr.20190412.

Hall, E. J. (2006) 'Intensity-modulated radiation therapy, protons, and the risk of second cancers', *International Journal of Radiation Oncology Biology Physics*, pp. 1–7. doi: 10.1016/j.ijrobp.2006.01.027.

Hall, E. J. and Giaccia, A. J. (2006) *Radiobiology for the Radiologist*. Sixth Edition. Lippincott Williams & Wilkins.

Hall, E. J. and Giaccia, A. J. (2012) *Radiobiology for the Radiologist*. Seventh. Lippincott Williams & Wilkins.

Hallek, M. (2017) 'Chronic lymphocytic leukemia: 2017 update on diagnosis, risk stratification, and treatment.', *American journal of hematology*. United States, 92(9), pp. 946–965. doi: 10.1002/ajh.24826.

Hamada, N. and Fujimichi, Y. (2014) 'Classification of radiation effects for dose limitation purposes: history, current situation and future prospects', *Journal of radiation research*. 2014/05/03. Oxford University Press, 55(4), pp. 629–640. doi: 10.1093/jrr/rru019.

Han, X. *et al.* (2017) 'Rutin-enriched extract from *Coriandrum sativum* L. Ameliorates ionizing radiation-induced hematopoietic injury', *International Journal of Molecular Sciences*. MDPI AG, 18(5). doi: 10.3390/ijms18050942.

Hao, Q. L. *et al.* (1995) 'A functional comparison of CD34 + CD38- cells in cord blood and bone marrow.', *Blood*. United States, 86(10), pp. 3745–3753.

Hao, T. *et al.* (2019) 'An emerging trend of rapid increase of leukemia but not all cancers in the aging population in the United States', *Scientific Reports*, 9(1), p. 12070. doi: 10.1038/s41598-019-48445-1.

Harfouche, G. and Martin, M. T. (2010) 'Response of normal stem cells to ionizing radiation: A balance between homeostasis and genomic stability', *Mutation Research - Reviews in Mutation Research*. pp. 167–174. doi: 10.1016/j.mrrev.2010.01.007.

Hashimoto, S., Anai, H. and Hanada, K. (2016) 'Mechanisms of interstrand DNA crosslink repair and human disorders', *Genes and Environment*, 38(1), p. 9. doi: 10.1186/s41021-016-0037-9.

Hayashi, T. *et al.* (2003) 'Radiation dose-dependent increases in inflammatory response markers in A-bomb survivors.', *International Journal of Radiation Biology*. 79(2), pp. 129–136.

Heilbronn, L. (2015) *Neutron properties and definitions (supplement)*. Available at: https://three.jsc.nasa.gov/articles/Heilbronn_Neutron_Supplement.pdf. (Accessed: 2 December 2020).

Henry, C. J., Marusyk, A. and DeGregori, J. (2011) ‘Aging-associated changes in hematopoiesis and leukemogenesis: What’s the connection?’, *Aging*. 3(6), pp. 643–656. doi: 10.18632/aging.100351.

Herbert, M. S. *et al.* (2007) ‘Determination of neutron energy spectra inside a water phantom irradiated by 64 MeV neutrons.’, *Radiation Protection Dosimetry*, 126(1–4), pp. 346–9. doi: 10.1093/rpd/ncm072.

Herd, O. *et al.* (2016) ‘Chromosomal radiosensitivity of human immunodeficiency virus positive/negative cervical cancer patients in South Africa’, *Molecular Medicine Reports*. 13(1), pp. 130–136. doi: 10.3892/mmr.2015.4504.

Herishanu, Y. *et al.* (2013) ‘Biology of chronic lymphocytic leukemia in different microenvironments: clinical and therapeutic implications’, *Hematology/Oncology Clinics of North America*, 27(2), pp. 173–206. doi: 10.1016/j.hoc.2013.01.002.

Hernanz-Schulman, M. (2017) *Pediatric CT and Image Gently*®. Nashville, TN. Available at: <https://www.imagewisely.org/-/media/ImageWisely-Files/Imaging-Physicians/IW-Hernanz-Schulman-Pediatric-CT.pdf> (Accessed: 18 August 2018).

Heyer, W.-D., Ehmsen, K. T. and Liu, J. (2010) ‘Regulation of homologous recombination in eukaryotes’, *Annual Review of Genetics*, 44, pp. 113–139. doi: 10.1146/annurev-genet-051710-150955.

Heylmann, D. *et al.* (2014) ‘Radiation sensitivity of human and murine peripheral blood lymphocytes, stem and progenitor cells’, *Biochimica et Biophysica Acta (BBA)-Reviews on Cancer*. 1846(1), pp. 121–129.

Hill-Kayser, C. E. *et al.* (2019) ‘Outcomes After Proton Therapy for Treatment of Pediatric High-Risk Neuroblastoma’, *International Journal of Radiation Oncology Biology Physics*. 104(2), pp. 401–408. doi: 10.1016/j.ijrobp.2019.01.095.

Hill, M. A. (2018) ‘Track to the future: historical perspective on the importance of radiation track structure and DNA as a radiobiological target’, *International Journal of Radiation Biology*. pp. 759–768. doi: 10.1080/09553002.2017.1387304.

Hintzsche, H. *et al.* (2017) ‘Fate of micronuclei and micronucleated cells’. doi: 10.1016/j.mrrev.2017.02.002.

Hintzsche, H., Montag, G. and Stopper, H. (2018) ‘Induction of micronuclei by four cytostatic

compounds in human hematopoietic stem cells and human lymphoblastoid TK6 cells’, *Scientific Reports*. 8(1), pp. 1–11. doi: 10.1038/s41598-018-21680-8.

Hoeijmakers, J. H. J. (2001) *A plethora of damages in DNA The consequences of DNA injury Genome maintenance mechanisms for preventing cancer*. Available at: www.nature.com (Accessed: 22 June 2020).

Hordyjewska, A., Popiołek, Ł. and Horecka, A. (2015) ‘Characteristics of hematopoietic stem cells of umbilical cord blood’, *Cytotechnology*, 67(3), pp. 387–396. doi: 10.1007/s10616-014-9796-y.

Howard, S. C. *et al.* (2008) ‘Childhood cancer epidemiology in low-income countries’, *Cancer*. John Wiley & Sons, Ltd, pp. 461–472. doi: 10.1002/cncr.23205.

Howard, S. C. *et al.* (2018) ‘The My Child Matters programme: effect of public–private partnerships on paediatric cancer care in low-income and middle-income countries’, *The Lancet Oncology*. Lancet Publishing Group, pp. e252–e266. doi: 10.1016/S1470-2045(18)30123-2.

Hsieh, P. and Yamane, K. (2008) ‘DNA mismatch repair: molecular mechanism, cancer, and ageing’, *Mechanisms of ageing and development*. 2008/03/04, 129(7–8), pp. 391–407. doi: 10.1016/j.mad.2008.02.012.

Hsu WL, Preston DL, Soda M, Sugiyama H, Funamoto S, Kodama K, Kimura A, K. N., Dohy H, Tomonaga M, Iwanaga M, Miyazaki Y, Cullings HM, Suyama A, Ozasa K, S. and RE, M. K. (2013) ‘The incidence of leukemia, lymphoma and multiple myeloma among atomic bomb survivors: 1950–2001’, *Radiation Research*, 179(3), pp. 361–382. doi: 10.1667/RR2892.1.

Hu, M. *et al.* (2018) ‘Proton beam therapy for cancer in the era of precision medicine’, *Journal of Hematology & Oncology*, 11(1), p. 136. doi: 10.1186/s13045-018-0683-4.

Huang, R. X. and Zhou, P. K. (2020) ‘DNA damage response signaling pathways and targets for radiotherapy sensitization in cancer’, *Signal Transduction and Targeted Therapy*. pp. 1–27. doi: 10.1038/s41392-020-0150-x.

Ideguchi, R. *et al.* (2018) ‘The present state of radiation exposure from pediatric CT examinations in Japan—what do we have to do?’, *Journal of Radiation Research*, 59(suppl_2), pp. ii130–ii136. doi: 10.1093/jrr/rrx095.

Inoue, A. *et al.* (2002) ‘Slug, a highly conserved zinc finger transcriptional repressor, protects

hematopoietic progenitor cells from radiation-induced apoptosis in vivo', *Cancer Cell*. 2(4), pp. 279–288. doi: 10.1016/S1535-6108(02)00155-1.

International Commission on Radiological Protection (1991) '1990 Recommendations of the International Commission on Radiological Protection', *ICRP Publication 60*, Ann. ICRP, pp. 1–3. doi: 10.1177/ANIB_21_1-3.

Ivanovs, A. *et al.* (2017) 'Human haematopoietic stem cell development: From the embryo to the dish', *Development*, 144(13), pp. 2323–2337. doi: 10.1242/dev.134866.

Jaffray, D. A. and Gospodarowicz, M. K. (2015) *Radiation Therapy for Cancer*. In: Gelband H, Jha P, Sankaranarayanan R, et al., editors. *Cancer: Disease Control Priorities, Third Edition (Volume 3)*. Washington (DC): The International Bank for Reconstruction and Development / The World Bank; 2015 Nov 1., *Cancer: Disease Control Priorities, Third Edition (Volume 3)*. The International Bank for Reconstruction and Development / The World Bank. doi: 10.1596/978-1-4648-0349-9_CH14.

Jagannathan-Bogdan, M. and Zon, L. I. (2013) 'Hematopoiesis', *Development*. Company of Biologists, 140(12), pp. 2463–2467. doi: 10.1242/dev.083147.

Jakl, L. *et al.* (2020) 'Biodosimetry of Low Dose Ionizing Radiation Using DNA Repair Foci in Human Lymphocytes', *Genes*. 11(1), p. 58. doi: 10.3390/genes11010058.

Jalali, R. and Goda, J. S. (2019) 'Proton beam therapy in pediatric brain tumor patients: Improved radiation delivery techniques improve neurocognitive outcomes', *Neuro-Oncology*, 21(7), pp. 830–831. doi: 10.1093/neuonc/noz085.

Jezkova, L. *et al.* (2018) 'Particles with similar LET values generate DNA breaks of different complexity and reparability: A high-resolution microscopy analysis of γ H2AX/53BP1 foci', *Nanoscale*. 10(3), pp. 1162–1179. doi: 10.1039/c7nr06829h.

Jones, D. T. L. *et al.* (1992) 'Neutron fluence and kerma spectra of a $p(66)/\text{Be}(40)$ clinical source', *Medical Physics*. 19(5), pp. 1285–1291. doi: 10.1118/1.596922.

Jordan, B. R. (2016) 'The Hiroshima/Nagasaki Survivor Studies: Discrepancies Between Results and General Perception', *Genetics*. 203(4), pp. 1505–1512. doi: 10.1534/genetics.116.191759.

Juerß, D. *et al.* (2017) 'Comparative study of the effects of different radiation qualities on normal human breast cells', *Radiation Oncology*, 12(1), p. 159. doi: 10.1186/s13014-017-

0895-8.

Julien, E., El Omar, R. and Tavian, M. (2016) 'Origin of the hematopoietic system in the human embryo', *FEBS Letters*. 590(22), pp. 3987–4001. doi: 10.1002/1873-3468.12389.

Kakarougkas, A. and Jeggo, P. A. (2014) 'DNA DSB repair pathway choice: an orchestrated handover mechanism', *The British Journal of Radiology*. 87(1035), p. 20130685.

Kato, K., Omori, A. and Kashiwakura, I. (2013) 'Radiosensitivity of human haematopoietic stem/progenitor cells', *Journal of Radiological Protection*. 33(1), pp. 71–80. doi: 10.1088/0952-4746/33/1/71.

Kavanagh, J. N. *et al.* (2013a) 'DNA double strand break repair: A radiation perspective', *Antioxidants and Redox Signaling*, 18(18), pp. 2458–2472. doi: 10.1089/ars.2012.5151.

Kavanagh, J. N. *et al.* (2013b) 'DNA double strand break repair: A radiation perspective', *Antioxidants and Redox Signaling*, pp. 2458–2472. doi: 10.1089/ars.2012.5151.

Kim, D. W., Chung, W. K., Shin, J., Lim, Y. K., Shin, D., Lee, B., *et al.* (2013) *Secondary neutron dose measurement for proton eye treatment using an eye snout with a borated neutron absorber*, *Radiation Oncology*. doi: 10.1186/1748-717X-8-182.

Kim, D. W., Chung, W. K., Shin, J., Lim, Y. K., Shin, D., Lee, S. B., *et al.* (2013) 'Secondary neutron dose measurement for proton eye treatment using an eye snout with a borated neutron absorber', *Radiation Oncology*. BioMed Central, 8(1), p. 182. doi: 10.1186/1748-717X-8-182.

Kinner, A. *et al.* (2008) 'Gamma-H2AX in recognition and signaling of DNA double-strand breaks in the context of chromatin.', *Nucleic acids research*. Oxford University Press, pp. 5678–5694. doi: 10.1093/nar/gkn550.

Kipps, T. J. *et al.* (2017) 'Chronic lymphocytic leukaemia', *Nature reviews. Disease primers*, 3, p. 16096. doi: 10.1038/nrdp.2016.96.

Kleinerman, R. A. (2006) 'Cancer risks following diagnostic and therapeutic radiation exposure in children', *Pediatric Radiology*. 36(2), pp. 121–125. doi: 10.1007/s00247-006-0191-5.

Klose, N. *et al.* (2007) 'Immuno-hematological reference values for healthy adults in Burkina Faso', *Clinical and Vaccine Immunology*. 14(6), pp. 782–784. doi: 10.1128/CVI.00044-07.

Kondo, M. (2010) 'Lymphoid and myeloid lineage commitment in multipotent hematopoietic

progenitors’, *Immunological Reviews*. 238(1), pp. 37–46. doi: 10.1111/j.1600-065X.2010.00963.x.

Kosan, C. and Godmann, M. (2016) ‘Genetic and Epigenetic Mechanisms That Maintain Hematopoietic Stem Cell Function’, *Stem cells international*. pp. 1–14. doi: 10.1155/2016/5178965.

Kosik, P. *et al.* (2020) ‘DNA damage response and preleukemic fusion genes induced by ionizing radiation in umbilical cord blood hematopoietic stem cells’, *Scientific Reports*. 10(1), p. 13722. doi: 10.1038/s41598-020-70657-z.

Kraft, D. *et al.* (2015) ‘Transmission of clonal chromosomal abnormalities in human hematopoietic stem and progenitor cells surviving radiation exposure’, *Mutation Research - Fundamental and Molecular Mechanisms of Mutagenesis*. 777, pp. 43–51. doi: 10.1016/j.mrfmmm.2015.04.007.

Kreis, N. N., Louwen, F. and Yuan, J. (2014) ‘Less understood issues: P21Cip1 in mitosis and its therapeutic potential’, *Oncogene*. pp. 1758–1767. doi: 10.1038/onc.2014.133.

Kroemer, G. *et al.* (2009) ‘Classification of cell death: Recommendations of the Nomenclature Committee on Cell Death 2009’, *Cell Death and Differentiation*. pp. 3–11. doi: 10.1038/cdd.2008.150.

Krzyżanowski, A. *et al.* (2019) ‘Modern ultrasonography of the umbilical cord: Prenatal diagnosis of umbilical cord abnormalities and assesment of fetal wellbeing’, *Medical Science Monitor*. pp. 3170–3180. doi: 10.12659/MSM.913762.

Kumar, B. V., Connors, T. J. and Farber, D. L. (2018) ‘Human T Cell Development, Localization, and Function throughout Life’, *Immunity*. pp. 202–213. doi: 10.1016/j.immuni.2018.01.007.

Kumar, N. *et al.* (2020) ‘Cooperation and interplay between base and nucleotide excision repair pathways: From DNA lesions to proteins’, *Genetics and Molecular Biology. Brazilian Journal of Genetics*. doi: 10.1590/1678-4685-GMB-2019-0104.

Kusunoki, Y. and Hayashi, T. (2008) ‘Long-lasting alterations of the immune system by ionizing radiation exposure: implications for disease development among atomic bomb survivors.’, *International Journal of Radiation Biology*. 84(1), pp. 1–14. doi: 10.1080/09553000701616106.

Kutanzi, K. R. *et al.* (2016) ‘Pediatric Exposures to Ionizing Radiation: Carcinogenic Considerations.’, *International Journal of Environmental Research and Public Health*. 13(11). doi: 10.3390/ijerph13111057.

Kuznetsova, I. S., Labutina, E. V. and Hunter, N. (2016) ‘Radiation Risks of Leukemia, Lymphoma and Multiple Myeloma Incidence in the Mayak Cohort: 1948–2004’, *PLOS ONE*. 11(9), p. e0162710. doi: 10.1371/journal.pone.0162710.

LaTorre Travis, E. (1989) *Primer of medical radioiology*. Mosby.

Lee, G.-Y. *et al.* (2019) ‘Age-related differences in the bone marrow stem cell niche generate specialized microenvironments for the distinct regulation of normal hematopoietic and leukemia stem cells’, *Scientific Reports*. 9(1), p. 1007. doi: 10.1038/s41598-018-36999-5.

Lee, T. H. and Kang, T. H. (2019) ‘DNA oxidation and excision repair pathways’, *International Journal of Molecular Sciences*, 20(23). doi: 10.3390/ijms20236092.

Lehnert, S. (2007) *Biomolecular Action of Ionizing Radiation*. CRC Press. doi: 10.1201/9781420011920.

Leroy, R. *et al.* (2016) ‘Proton Therapy in Children: A Systematic Review of Clinical Effectiveness in 15 Pediatric Cancers’, *International Journal of Radiation Oncology*Biophysics*Physics*. Elsevier, 95(1), pp. 267–278. doi: 10.1016/j.ijrobp.2015.10.025.

Levin, W. P. *et al.* (2005) ‘Proton beam therapy’, *British Journal of Cancer*. pp. 849–854. doi: 10.1038/sj.bjc.6602754.

Li, G. M. (2008) ‘Mechanisms and functions of DNA mismatch repair’, *Cell Research*. pp. 85–98. doi: 10.1038/cr.2007.115.

Li, H. H. *et al.* (2015) ‘Ionizing radiation impairs T cell activation by affecting metabolic reprogramming’, *International Journal of Biological Sciences*. 11(7), pp. 726–736. doi: 10.7150/ijbs.12009.

Lim, S. and Kaldis, P. (2013) ‘Cdks, cyclins and CKIs: roles beyond cell cycle regulation’, *Development*, 140(15), pp. 3079 LP – 3093. doi: 10.1242/dev.091744.

Lindahl, T. (1993) ‘Instability and decay of the primary structure of DNA’, *Nature*, 362(6422), pp. 709–715. doi: 10.1038/362709a0.

Little, J. B. (2003) ‘Ionizing Radiation’, in Kufe, D. W. *et al.* (eds) *Holland-Frei Cancer*

Medicine. 6th edn. BC Decker. Available at: <https://www.ncbi.nlm.nih.gov/books/NBK13033/> (Accessed: 2 December 2020).

Little, M. P. *et al.* (2018) 'Leukaemia and myeloid malignancy among people exposed to low doses (<100 mSv) of ionising radiation during childhood: a pooled analysis of nine historical cohort studies', *The Lancet. Haematology*. 5(8), pp. e346–e358. doi: 10.1016/S2352-3026(18)30092-9.

Liu, H. and Chang, J. Y. (2011) 'Proton therapy in clinical practice', *Chinese Journal of Cancer*. Landes Bioscience, pp. 315–326. doi: 10.5732/cjc.010.10529.

Liu, Yan *et al.* (2009) 'The p53 tumor suppressor protein is a critical regulator of hematopoietic stem cell behavior', *Cell cycle*, 8(19), pp. 3120–3124. doi: 10.4161/cc.8.19.9627.

López, M. C., Palmer, B. E. and Lawrence, D. A. (2009) 'Phenotypic differences between cord blood and adult peripheral blood', *Cytometry Part B: Clinical Cytometry*. 76B(1), pp. 37–46. doi: 10.1002/cyto.b.20441.

Loughery, J. and Meek, D. (2013) 'Switching on p53: an essential role for protein phosphorylation?', *Biodiscovery*, (7). doi: 10.7750/biodiscovery.2013.8.1.

Lu, Y. *et al.* (2020) 'The regulation of hematopoietic stem cell fate in the context of radiation', *Radiation Medicine and Protection*. 1(1), pp. 31–34. doi: 10.1016/j.radmp.2020.01.002.

Lusiyanti, Y. *et al.* (2016) 'Establishment of a dose-response curve for X-ray-induced micronuclei in human lymphocytes', *Genome Integrity*. 7(1). doi: 10.4103/2041-9414.197162.

Ma, X. *et al.* (2009) 'Infection and pediatric acute lymphoblastic leukemia', *Blood Cells, Molecules, and Diseases*. pp. 117–120. doi: 10.1016/j.bcnd.2008.10.006.

Mackay, C. R. (1993) 'Homing of naive, memory and effector lymphocytes', *Current Opinion in Immunology*. 5(3), pp. 423–427. doi: 10.1016/0952-7915(93)90063-X.

Magrath, I. *et al.* (2013) 'Paediatric cancer in low-income and middle-income countries', *The Lancet Oncology*. doi: 10.1016/S1470-2045(13)70008-1.

Maier, P. *et al.* (2016) 'Cellular pathways in response to ionizing radiation and their targetability for tumor radiosensitization', *International Journal of Molecular Sciences*. doi: 10.3390/ijms17010102.

Mansilla, S. F. *et al.* (2020) 'Cdk-independent and pcna-dependent functions of p21 in dna

replication', *Genes*, 11(6), pp. 1–17. doi: 10.3390/genes11060593.

Mao, Z. *et al.* (2008) 'Comparison of nonhomologous end joining and homologous recombination in human cells', *DNA Repair*. 7(10), pp. 1765–1771. doi: 10.1016/j.dnarep.2008.06.018.

Marchant, A. and Goldman, M. (2005) 'T cell-mediated immune responses in human newborns: Ready to learn?', *Clinical and Experimental Immunology*. pp. 10–18. doi: 10.1111/j.1365-2249.2005.02799.x.

Marcotte, E. L. *et al.* (2014) 'Exposure to infections and risk of leukemia in young children', *Cancer Epidemiology Biomarkers and Prevention*. 23(7), pp. 1195–1203. doi: 10.1158/1055-9965.EPI-13-1330.

Marcu, L. G. (2017) 'Photons - Radiobiological issues related to the risk of second malignancies', *Physica Medica*, 42, pp. 213–220. doi: 10.1016/j.ejmp.2017.02.013.

Maree, J. E. *et al.* (2016) 'The Information Needs of South African Parents of Children With Cancer', *Journal of Pediatric Oncology Nursing*. doi: 10.1177/1043454214563757.

Marteijn, J. A. *et al.* (2014) 'The integrity of DNA is constantly threatened by endo- genously formed metabolic products'. doi: 10.1038/nrm3822.

Martin, C. E. *et al.* (2017) 'Interleukin-7 Availability Is Maintained by a Hematopoietic Cytokine Sink Comprising Innate Lymphoid Cells and T Cells', *Immunity*. 47(1), pp. 171-182.e4. doi: 10.1016/j.immuni.2017.07.005.

Martins, I. *et al.* (2017) 'Entosis: The emerging face of non-cell-autonomous type IV programmed death', *Biomedical Journal*. pp. 133–140. doi: 10.1016/j.bj.2017.05.001.

Matsumoto, S. *et al.* (2016) 'Secondary neutron doses to pediatric patients during intracranial proton therapy: Monte Carlo simulation of the neutron energy spectrum and its organ doses', *Health Physics*. 110(4), pp. 380–386. doi: 10.1097/HP.0000000000000461.

Mavragani, I. V. *et al.* (2019) 'Ionizing radiation and complex DNA damage: From prediction to detection challenges and biological significance', *Cancers*. p. 1789. doi: 10.3390/cancers11111789.

Medema, R. H. and Macurek, L. (2012) 'Checkpoint control and cancer.', *Oncogene*. 31(21), pp. 2601–2613. doi: 10.1038/onc.2011.451.

Mei, N. *et al.* (1996) 'Individual Variation and Age Dependency in the Radiosensitivity of Peripheral Blood T-lymphocytes from Normal Donors', *Journal of Radiation Research*. 37(4), pp. 235–245. doi: 10.1269/jrr.37.235.

Merchant, T. E. (2013) 'Clinical controversies: proton therapy for pediatric tumors.', *Seminars in radiation oncology*, 23(2), pp. 97–108. doi: 10.1016/j.semradonc.2012.11.008.

Merchant, T. E. *et al.* (2014) 'Critical combinations of radiation dose and volume predict intelligence quotient and academic achievement scores after craniospinal irradiation in children with medulloblastoma', *International Journal of Radiation Oncology Biology Physics*. 90(3), pp. 554–561. doi: 10.1016/j.ijrobp.2014.06.058.

Merkenschlager, M. *et al.* (1988) 'Limiting dilution analysis of proliferative responses in human lymphocyte populations defined by the monoclonal antibody UCHL1: implications for differential CD45 expression in T cell memory formation', *European Journal of Immunology*. 18(11), pp. 1653–1662. doi: 10.1002/eji.1830181102.

Merkenschlager, M. and Beverley, P. C. L. (1989) 'Evidence for differential expression of CD45 isoforms by precursors for memory-dependent and independent cytotoxic responses: Human CD8 memory CTLp selectively express CD45R0 (UCHL1)', *International Immunology*. Oxford Academic, 1(4), pp. 450–459. doi: 10.1093/intimm/1.4.450.

Messele, T. *et al.* (1999) 'Reduced naive and increased activated CD4 and CD8 cells in healthy adult Ethiopians compared with their Dutch counterparts', *Clinical and Experimental Immunology*. 115(3), pp. 443–450. doi: 10.1046/j.1365-2249.1999.00815.x.

Mettler, F. A. (2012) 'Medical effects and risks of exposure to ionising radiation', *Journal of Radiological Protection*. 32(1), pp. N9–N13. doi: 10.1088/0952-4746/32/1/n9.

Meulepas, J. M. *et al.* (2014) 'Leukemia and brain tumors among children after radiation exposure from CT scans: Design and methodological opportunities of the Dutch Pediatric CT Study', *European Journal of Epidemiology*. Kluwer Academic Publishers, 29(4), pp. 293–301. doi: 10.1007/s10654-014-9900-9.

Mijnheer, B. J. *et al.* (1989) 'Report 45', *Journal of the International Commission on Radiation Units and Measurements*. os23(2), p. NP-NP. doi: 10.1093/JICRU/OS23.2.REPORT45.

Miles, D. J. C. *et al.* (2019) 'Early T Cell Differentiation with Well-Maintained Function across the Adult Life Course in Sub-Saharan Africa', *The Journal of Immunology*. 203(5), pp. 1160–

1171. doi: 10.4049/jimmunol.1800866.

Miltenyi Biotec (2020) *Cell separation strategies using MACS® Technology - USA*. Available at: <https://www.miltenyibiotec.com/US-en/products/macscell-separation/macscell-separation-strategies.html#gref> (Accessed: 8 July 2020).

Milyavsky, M. *et al.* (2010) 'A Distinctive DNA Damage Response in Human Hematopoietic Stem Cells Reveals an Apoptosis-Independent Role for p53 in Self-Renewal', *Cell Stem Cell*. 7(2), pp. 186–197. doi: 10.1016/J.STEM.2010.05.016.

Minnaar, C. A. *et al.* (2020) 'Analysis of the effects of mEHT on the treatment-related toxicity and quality of life of HIV-positive cervical cancer patients', *International Journal of Hyperthermia*. 37(1), pp. 263–272. doi: 10.1080/02656736.2020.1737253.

Mire-Sluis, A. R. *et al.* (1987) 'Human T lymphocytes stimulated by phytohaemagglutinin undergo a single round of cell division without a requirement for interleukin-2 or accessory cells', *Immunology*, 60(1), pp. 7–12. Available at: <https://pubmed.ncbi.nlm.nih.gov/3102352>.

Miri-Hakimabad, H., Rafat-Motavalli, L. and Akhlaghi, P. (2014) 'Effects of shielding the radiosensitive superficial organs of ORNL pediatric phantoms on dose reduction in computed tomography', *Journal of Medical Physics*. 39(4), p. 238. doi: 10.4103/0971-6203.144490.

Mohrin, M. *et al.* (2010) 'Hematopoietic Stem Cell Quiescence Promotes Error-Prone DNA Repair and Mutagenesis', *Cell Stem Cell*. 7(2), pp. 174–185. doi: 10.1016/J.STEM.2010.06.014.

Mombach, J. C. M., Bugs, C. A. and Chaouiya, C. (2014) 'Modelling the onset of senescence at the G1 / S cell cycle checkpoint', 15(Suppl 7), pp. 1–11.

Mortezaee, K. *et al.* (2019) 'Genomic instability and carcinogenesis of heavy charged particles radiation: Clinical and environmental implications', *Medicina (Lithuania)*. 55(9). doi: 10.3390/medicina55090591.

Nahangi, H. and Chaparian, A. (2015) 'Assessment of radiation risk to pediatric patients undergoing conventional X-ray examinations', *Radioprotection*. 50(1), pp. 19–25. doi: 10.1051/radiopro/2014023.

Nakamura-Ishizu, A., Takizawa, H. and Suda, T. (2014) 'The analysis, roles and regulation of quiescence in hematopoietic stem cells'. doi: 10.1242/dev.106575.

- Nakamura, N., Kusunoki, Y. and Akiyama, M. (1990) 'Radiosensitivity of CD4 or CD8 positive human T-lymphocytes by an in vitro colony formation assay', *Radiation Research*, 123(2), pp. 224–227. doi: 10.2307/3577549.
- Nakano, T. *et al.* (2017) 'Radiation-induced DNA–protein cross-links: Mechanisms and biological significance', *Free Radical Biology and Medicine*. pp. 136–145. doi: 10.1016/j.freeradbiomed.2016.11.041.
- Nguyen, J., Moteabbed, M. and Paganetti, H. (2015) 'Assessment of uncertainties in radiation-induced cancer risk predictions at clinically relevant doses'. doi: 10.1118/1.4903272.
- Nickoloff, J. A., Sharma, N. and Taylor, L. (2020) 'Clustered DNA double-strand breaks: Biological effects and relevance to cancer radiotherapy', *Genes*, 11(1). doi: 10.3390/genes11010099.
- Nikitaki, Z. *et al.* (2016) 'Measurement of complex DNA damage induction and repair in human cellular systems after exposure to ionizing radiations of varying linear energy transfer (LET).', *Free radical research*. 50(sup1), pp. S64–S78. doi: 10.1080/10715762.2016.1232484.
- Nikjoo, H. *et al.* (1999) 'Quantitative modelling of DNA damage using Monte Carlo track structure method', *Radiation and Environmental Biophysics*. 38(1), pp. 31–38. doi: 10.1007/s004110050135.
- Ocklind, G. (1986) 'Stimulation of human lymphocytes by phytohemagglutinin (PHA) in a new ultra-microtest plate', *Immunobiology*, 171(4), pp. 339–344. doi: [https://doi.org/10.1016/S0171-2985\(86\)80066-3](https://doi.org/10.1016/S0171-2985(86)80066-3).
- Orkin, S. H. and Zon, L. I. (2008) 'Hematopoiesis: An Evolving Paradigm for Stem Cell Biology', *Cell*. pp. 631–644. doi: 10.1016/j.cell.2008.01.025.
- Ottolenghi, A. *et al.* (2015) 'The ANDANTE project: a multidisciplinary approach to neutron RBE.', *Radiation protection dosimetry*. 166(1–4), pp. 311–315. doi: 10.1093/rpd/ncv158.
- Ozasa, K. (2016) 'Epidemiological research on radiation-induced cancer in atomic bomb survivors', *Journal of Radiation Research*, 57(S1), pp. 112–117. doi: 10.1093/jrr/rrw005.
- Ozasa, K. *et al.* (2019) 'Epidemiological studies of atomic bomb radiation at the Radiation Effects Research Foundation', *International Journal of Radiation Biology*. 95(7), pp. 879–891. doi: 10.1080/09553002.2019.1569778.

- Ozsahin, M. *et al.* (2005) ‘CD4 and CD8 T-lymphocyte apoptosis can predict radiation-induced late toxicity: A prospective study in 399 patients’, *Clinical Cancer Research*. 11(20), pp. 7426–7433. doi: 10.1158/1078-0432.CCR-04-2634.
- Pajic, J. *et al.* (2015) ‘Inter-individual variability in the response of human peripheral blood lymphocytes to ionizing radiation: comparison of the dicentric and micronucleus assays’, *Radiation and Environmental Biophysics*. 54(3), pp. 317–325. doi: 10.1007/s00411-015-0596-3.
- Park, J.-H. *et al.* (2016) ‘p53 as guardian of the mitochondrial genome’, *FEBS letters*. 2016/02/03, 590(7), pp. 924–934. doi: 10.1002/1873-3468.12061.
- Payne, H. *et al.* (2020) ‘Comparison of Lymphocyte Subset Populations in Children From South Africa, US and Europe’, *Frontiers in Pediatrics*. doi: 10.3389/fped.2020.00406.
- Pearce, M. S. *et al.* (2012) ‘Radiation exposure from CT scans in childhood and subsequent risk of leukaemia and brain tumours: A retrospective cohort study’, *The Lancet*. 380(9840), pp. 499–505. doi: 10.1016/S0140-6736(12)60815-0.
- Pennings, S., Liu, K. J. and Qian, H. (2018) ‘The Stem Cell Niche: Interactions between Stem Cells and Their Environment’, *Stem Cells International*. doi: 10.1155/2018/4879379.
- Pennock, N. D. *et al.* (2013) ‘T cell responses: Naïve to memory and everything in between’, *American Journal of Physiology - Advances in Physiology Education*. 37(4), pp. 273–283. doi: 10.1152/advan.00066.2013.
- Pereira, G. C., Traughber, M. and Muzic, R. F. (2014) ‘The Role of Imaging in Radiation Therapy Planning: Past, Present, and Future’, *BioMed Research International*. 2014, p. 231090. doi: 10.1155/2014/231090.
- Pfeffer, C. M. and Singh, A. T. K. (2018) ‘Apoptosis: A target for anticancer therapy’, *International Journal of Molecular Sciences*. p. 448. doi: 10.3390/ijms19020448.
- Pietras, E. M., Warr, M. R. and Passegué, E. (2011) ‘Cell cycle regulation in hematopoietic stem cells’, *Journal of Cell Biology*. pp. 709–720. doi: 10.1083/jcb.201102131.
- Pontel, L. B. *et al.* (2015) ‘Endogenous Formaldehyde Is a Hematopoietic Stem Cell Genotoxin and Metabolic Carcinogen.’, *Molecular cell*, 60(1), pp. 177–188. doi: 10.1016/j.molcel.2015.08.020.

Pouget, J. P. and Mather, S. J. (2001) 'General aspects of the cellular response to low- and high-LET radiation', *European Journal of Nuclear Medicine*, pp. 541–561. doi: 10.1007/s002590100484.

Pradhan, A. S. (2011) 'Optically stimulated luminescence: fundamentals and applications', *Radiation Protection Dosimetry*, 147(4), pp. 619–622. doi: 10.1093/rpd/ncr357.

Preston, D. L. *et al.* (2007) 'Solid cancer incidence in atomic bomb survivors: 1958-1998.', *Radiation research*. 168(1), pp. 1–64. doi: 10.1667/RR0763.1.

Price, B. D. and D'Andrea, A. D. (2013) 'Chromatin remodeling at DNA double-strand breaks', *Cell*. NIH Public Access, pp. 1344–1354. doi: 10.1016/j.cell.2013.02.011.

PTCOG (2020) *Particle Therapy Co-Operative Group - Particle Therapy Centers*. Available at: <https://www.ptcog.ch/> (Accessed: 2 July 2020).

Pugh, J. L. *et al.* (2014) 'Histone Deacetylation Critically Determines T Cell Subset Radiosensitivity', *The Journal of Immunology*. 193(3), pp. 1451–1458. doi: 10.4049/jimmunol.1400434.

Qiu, J. *et al.* (2014) 'Divisional history and hematopoietic stem cell function during homeostasis', *Stem Cell Reports*. 2(4), pp. 473–490. doi: 10.1016/j.stemcr.2014.01.016.

Raaschou-Nielsen, O. *et al.* (2018) 'Ambient benzene at the residence and risk for subtypes of childhood leukemia, lymphoma and CNS tumor', *International Journal of Cancer*. 143(6), pp. 1367–1373. doi: 10.1002/ijc.31421.

Raboso-Gallego, J. *et al.* (2019) 'Epigenetic Priming in Childhood Acute Lymphoblastic Leukemia', *Frontiers in Cell and Developmental Biology*. 7, p. 137. doi: 10.3389/fcell.2019.00137.

Radford, I. R. (1994) 'Radiation response of mouse lymphoid and myeloid cell lines. Part I. Sensitivity to killing by ionizing radiation, rate of loss of viability, and cell type of origin.', *International journal of radiation biology*. 65(2), pp. 203–215. doi: 10.1080/09553009414550241.

Rahmanian, N., Hosseinimehr, S. J. and Khalaj, A. (2016) 'The paradox role of caspase cascade in ionizing radiation therapy', *Journal of Biomedical Science*. 23(1), p. 88. doi: 10.1186/s12929-016-0306-8.

- Rall, M. *et al.* (2015) 'Impact of Charged Particle Exposure on Homologous DNA Double-Strand Break Repair in Human Blood-Derived Cells', *Frontiers in Oncology*. 5, p. 250. doi: 10.3389/fonc.2015.00250.
- Rawlings, J. S. *et al.* (2011) 'Chromatin condensation via the condensin II complex is required for peripheral T-cell quiescence', *EMBO Journal*, 30(2), pp. 263–276. doi: 10.1038/emboj.2010.314.
- Recolin, B. *et al.* (2014) 'Molecular mechanisms of DNA replication checkpoint activation', *Genes*, 5(1), p. 147—175. doi: 10.3390/genes5010147.
- Rhizobium, G. E. (2013) 'Complete Genome Sequence of the Sesbania Symbiont and Rice', *Nucleic acids research*. 1(1256879), pp. 13–14. doi: 10.1093/nar.
- Rieger, A. M. *et al.* (2011) 'Modified annexin V/propidium iodide apoptosis assay for accurate assessment of cell death', *Journal of visualized experiments : JoVE*. (50), p. 2597. doi: 10.3791/2597.
- Rieger, M. A. and Schroeder, T. (2012) 'Hematopoiesis', *Cold Spring Harbor Perspectives in Biology*. 4(12). doi: 10.1101/cshperspect.a008250.
- Rodman, C. *et al.* (2017) 'In vitro and in vivo assessment of direct effects of simulated solar and galactic cosmic radiation on human hematopoietic stem/progenitor cells', *Leukemia*. 31(6), pp. 1398–1407. doi: 10.1038/leu.2016.344.
- Rodrigues, C. A. *et al.* (2016) 'Diagnosis and treatment of chronic lymphocytic leukemia: recommendations from the Brazilian Group of Chronic Lymphocytic Leukemia', *Revista Brasileira de Hematologia e Hemoterapia*. 38(4), pp. 346–357. doi: 10.1016/j.bjhh.2016.07.004.
- Rodrigues, M. A. *et al.* (2018) 'The potential for complete automated scoring of the cytokinesis block micronucleus cytome assay using imaging flow cytometry', *Mutation Research - Genetic Toxicology and Environmental Mutagenesis*. pp. 53–64. doi: 10.1016/j.mrgentox.2018.05.003.
- Rogakou, E. P. *et al.* (1999) 'Megabase chromatin domains involved in DNA double-strand breaks in vivo', *Journal of Cell Biology*. 146(5), pp. 905–915. doi: 10.1083/jcb.146.5.905.
- Roos, W. P. and Kaina, B. (2013) 'DNA damage-induced cell death: from specific DNA lesions to the DNA damage response and apoptosis.', *Cancer letters*. 332(2), pp. 237–248. doi: 10.1016/j.canlet.2012.01.007.

- Rübe, Claudia E. *et al.* (2011) 'Accumulation of DNA damage in hematopoietic stem and progenitor cells during human aging', *PLoS ONE*. 6(3). doi: 10.1371/journal.pone.0017487.
- Rühm, W. *et al.* (2018) 'Typical doses and dose rates in studies pertinent to radiation risk inference at low doses and low dose rates', *Journal of Radiation Research*. pp. ii1–ii10. doi: 10.1093/jrr/rrx093.
- Sadetzki, S. and Mandelzweig, L. (2009) 'Childhood exposure to external ionising radiation and solid cancer risk.', *British Journal of Cancer*, 100(7), pp. 1021–1025. doi: 10.1038/sj.bjc.6604994.
- Sallusto, F. *et al.* (1999) 'Two subsets of memory T lymphocytes with distinct homing potentials and effector functions', *Nature*. 401(6754), pp. 708–712. doi: 10.1038/44385.
- De Sanctis, E., Monti, S. and Ripani, M. (2016) 'Radioactivity and Penetrating Power of Nuclear Radiation' pp. 39–87. doi: 10.1007/978-3-319-30651-3_2.
- Sardaro, A. *et al.* (2019) 'Proton therapy in the most common pediatric non-central nervous system malignancies: an overview of clinical and dosimetric outcomes', *Italian Journal of Pediatrics*. BioMed Central, 45(1), p. 170. doi: 10.1186/s13052-019-0763-2.
- Sasaki, M. S. *et al.* (2016) 'Neutron relative biological effectiveness in Hiroshima and Nagasaki atomic bomb survivors: A critical review', *Journal of Radiation Research*. pp. 583–595. doi: 10.1093/jrr/rrw079.
- Sayers, G. M. *et al.* (1992) 'Epidemiology of acute leukaemia in the Cape Province of South Africa', *Leukemia Research*, 16(10), pp. 961–966. doi: 10.1016/0145-2126(92)90074-H.
- Schipler, A. and Iliakis, G. (2013) 'DNA double-strand-break complexity levels and their possible contributions to the probability for error-prone processing and repair pathway choice', *Nucleic acids research*. 2013/06/26. 41(16), pp. 7589–7605. doi: 10.1093/nar/gkt556.
- Schmiegelow, K. *et al.* (2008) 'Etiology of common childhood acute lymphoblastic leukemia: The adrenal hypothesis', *Leukemia*. pp. 2137–2141. doi: 10.1038/leu.2008.212.
- Schnarr, K. *et al.* (2007) 'Individual Radiosensitivity and its Relevance to Health Physics', *Dose-Response*. 5(4), p. dose-response.0. doi: 10.2203/dose-response.07-022.schnarr.
- Schneider, U. and Hälgl, R. (2015) 'The impact of neutrons in clinical proton therapy', *Frontiers in Oncology*. 5(OCT). doi: 10.3389/fonc.2015.00235.

Schofield, R. (1978) 'The relationship between the spleen colony-forming cell and the haemopoietic stem cell. A hypothesis', *Blood Cells*. 4(1–2), pp. 7–25.

Schuler, N. and Rube, C. E. (2013) 'Accumulation of DNA Damage-Induced Chromatin Alterations in Tissue-Specific Stem Cells: The Driving Force of Aging?', *PLoS ONE*. Public 8(5), pp. 1–12. doi: 10.1371/journal.pone.0063932.

Schuster, B. *et al.* (2018) 'Rate of individuals with clearly increased radiosensitivity rise with age both in healthy individuals and in cancer patients', *BMC Geriatrics*. 18(1), p. 105. doi: 10.1186/s12877-018-0799-y.

Seibold, P. *et al.* (2020) 'Clinical and epidemiological observations on individual radiation sensitivity and susceptibility', *International Journal of Radiation Biology*. 96(3), pp. 324–339. doi: 10.1080/09553002.2019.1665209.

Seita, J. and Weissman, I. L. (2010) 'Hematopoietic stem cell: Self-renewal versus differentiation', *Wiley Interdisciplinary Reviews: Systems Biology and Medicine*. pp. 640–653. doi: 10.1002/wsbm.86.

Shah, D. J., Sachs, R. K. and Wilson, D. J. (2012) 'Radiation-induced cancer: A modern view', *British Journal of Radiology*. p. e1166. doi: 10.1259/bjr/25026140.

Shao, L. *et al.* (2013) 'Hematopoietic stem cell senescence and cancer therapy-induced long-term bone marrow injury', *Translational Cancer Research*, 2(5), pp. 397–411. doi: 10.3978/j.issn.2218-676X.2013.07.03.

Shao, L., Luo, Y. and Zhou, D. (2013) 'Hematopoietic Stem Cell Injury Induced by Ionizing Radiation', *Antioxidants & Redox Signaling*. 20(9), pp. 1447–1462. doi: 10.1089/ars.2013.5635.

Sharma, S. and Gurudutta, G. (2016) 'Epigenetic Regulation of Hematopoietic Stem Cells', *International Journal of Stem Cells*. 9(1), pp. 36–43. doi: 10.15283/ijsc.2016.9.1.36.

Sheard, M. A., Uldrijan, S. and Vojtesek, B. (2003) 'Role of p53 in regulating constitutive and X-radiation-inducible CD95 expression and function in carcinoma cells.', *Cancer research*. 63(21), pp. 7176–7184.

Shephard, E. A. *et al.* (2016) 'Symptoms of adult chronic and acute leukaemia before diagnosis: Large primary care case-control studies using electronic records', *British Journal of General Practice*. 66(644), pp. e182–e188. doi: 10.3399/bjgp16X683989.

Shlush, L. I. *et al.* (2014) 'Identification of pre-leukaemic haematopoietic stem cells in acute leukaemia', *Nature*, 506(7488), pp. 328–333. doi: 10.1038/nature13038.

Shuryak, I. *et al.* (2006) 'Radiation-Induced Leukemia at Doses Relevant to Radiation Therapy: Modeling Mechanisms and Estimating Risks', *JNCI: Journal of the National Cancer Institute*, 98(24), pp. 1794–1806. doi: <https://doi.org/10.1093/jnci/djj497>.

Sia, J. *et al.* (2020) 'Molecular Mechanisms of Radiation-Induced Cancer Cell Death: A Primer', *Frontiers in Cell and Developmental Biology*. doi: 10.3389/fcell.2020.00041.

Sidney, L. E. *et al.* (2014) 'Concise review: evidence for CD34 as a common marker for diverse progenitors.', *Stem cells*. 32(6), pp. 1380–9. doi: 10.1002/stem.1661.

Siegel, R. L., Miller, K. D. and Jemal, A. (2020) 'Cancer statistics, 2020', *CA: A Cancer Journal for Clinicians*. 70(1), pp. 7–30. doi: 10.3322/caac.21590.

Singh, R., Soman-Faulkner, K. and Sugumar, K. (2019) *Embryology, Hematopoiesis, StatPearls*. Available at: <http://www.ncbi.nlm.nih.gov/pubmed/31334965> (Accessed: 30 July 2020).

Slabbert, J. P. *et al.* (2000) 'A comparison of the potential therapeutic gain of p(66)/Be neutrons and d(14)/Be neutrons', *International Journal of Radiation Oncology*Biophysics*Physics*. 47(4), pp. 1059–1065. doi: 10.1016/S0360-3016(00)00508-3.

Slabbert, J. and Vral, A. (2015) 'Potential for Therapeutic Gain - 29 MeV Neutrons versus 6 MeV Neutrons', *Advanced Materials Research*, 1084, pp. 559–566. doi: 10.4028/www.scientific.net/amr.1084.559.

Sokolov, M. V and Neumann, R. D. (2012) 'Human embryonic stem cell responses to ionizing radiation exposures: current state of knowledge and future challenges.', *Stem Cells International*, 2012, p. 579104. doi: 10.1155/2012/579104.

Solozobova, V. and Blattner, C. (2011) 'p53 in stem cells', *World Journal of Biological Chemistry*. 2(9), pp. 202–214. doi: 10.4331/wjbc.v2.i9.202.

Statistics South Africa (2020) *2020 Mid-year population estimates*. Available at: <http://www.statssa.gov.za/publications/P0302/P03022020.pdf> (Accessed: 5 November 2020).

Stefan, C. *et al.* (2017) 'Cancer of childhood in sub-Saharan Africa', *ecancermedicalscience*. Cancer Intelligence, 11. doi: 10.3332/ecancer.2017.755.

- Stojko, R. and Witek, A. (2005) ‘Umbilical cord blood--a perfect source of stem cells?’, *Ginekologia polska*. 76(6), pp. 491–497.
- Stones, D. K. *et al.* (2014) ‘Childhood cancer survival rates in two South African units’, *South African Medical Journal*, 104(7), pp. 501–504. doi: 10.7196/SAMJ.7882.
- Stouten, S. *et al.* (2020) ‘Modeling low-dose radiation-induced acute myeloid leukemia in male CBA/H mice’, *Radiation and Environmental Biophysics*. 1, p. 3. doi: 10.1007/s00411-020-00880-9.
- Sun, S., Osterman, M. D. and Li, M. (2019) ‘Tissue specificity of DNA damage response and tumorigenesis’. doi: 10.20892/j.issn.2095-3941.2019.0097.
- Surh, C. D. and Sprent, J. (2008) ‘Homeostasis of Naive and Memory T Cells’, *Immunity*. Cell Press, pp. 848–862. doi: 10.1016/j.immuni.2008.11.002.
- Suryadinata, R., Sadowski, M. and Sarcevic, B. (2010) ‘Control of cell cycle progression by phosphorylation of cyclin-dependent kinase (CDK) substrates.’, *Bioscience reports*. 30(4), pp. 243–255. doi: 10.1042/BSR20090171.
- Takahashi, A. *et al.* (2014) ‘Nonhomologous End-Joining Repair Plays a More Important Role than Homologous Recombination Repair in Defining Radiosensitivity after Exposure to High-LET Radiation’, *Radiation Research*. 182(3), pp. 338–344. doi: 10.1667/rr13782.1.
- Tamura, M. *et al.* (2017) ‘Lifetime attributable risk of radiation-induced secondary cancer from proton beam therapy compared with that of intensity-modulated X-ray therapy in randomly sampled pediatric cancer patients’, *Journal of Radiation Research*, 58(3), pp. 363–371. doi: 10.1093/jrr/rrw088.
- Tang, D. *et al.* (2019) ‘The molecular machinery of regulated cell death’, *Cell Research*. pp. 347–364. doi: 10.1038/s41422-019-0164-5.
- Taussig, D. C. *et al.* (2005) ‘Hematopoietic stem cells express multiple myeloid markers: Implications for the origin and targeted therapy of acute myeloid leukemia’, *Blood*. 106(13), pp. 4086–4092. doi: 10.1182/blood-2005-03-1072.
- Terwilliger, T. and Abdul-Hay, M. (2017) ‘Acute lymphoblastic leukemia: a comprehensive review and 2017 update’, *Blood cancer journal*. 7(6), pp. e577–e577. doi: 10.1038/bcj.2017.53.

Thomas, P. and Fenech, M. (2011) 'Cytokinesis-block micronucleus cytome assay in lymphocytes', *Methods in Molecular Biology*, 682, pp. 217–234. doi: 10.1007/978-1-60327-409-8_16.

Tian, X. *et al.* (2017) 'The evolution of proton beam therapy: Current and future status (Review)', *Molecular and Clinical Oncology*. 8(1), p. 15. doi: 10.3892/mco.2017.1499.

Tian, X. *et al.* (2018) 'The evolution of proton beam therapy: Current and future status.', *Molecular and clinical oncology*. 8(1), pp. 15–21. doi: 10.3892/mco.2017.1499.

Toufektchan, E. and Toledo, F. (2018) 'The Guardian of the Genome Revisited: p53 Downregulates Genes Required for Telomere Maintenance, DNA Repair, and Centromere Structure', *Cancers.*, 10(5), p. 135. doi: 10.3390/cancers10050135.

Trinkl, S. *et al.* (2017) 'Systematic out-of-field secondary neutron spectrometry and dosimetry in pencil beam scanning proton therapy', *Medical physics*. 44(5), pp. 1912–1920. doi: 10.1002/mp.12206.

Tsai, J.-Y. *et al.* (2015) 'Effects of indirect actions and oxygen on relative biological effectiveness: estimate of DSB induction and conversion induced by gamma rays and helium ions', *Journal of radiation research*. 2015/04/22. 56(4), pp. 691–699. doi: 10.1093/jrr/rrv025.

UNSCEAR (2006) *United Nations Scientific Committee on the Effects of Atomic Radiation: Effects of ionizing radiation*. New York.

UNSCEAR (2013) *United Nations Scientific Committee on the Effects of Atomic Radiation: Sources, Effects and Risks of Ionizing Radiation*. New York.

Valable, S. *et al.* (2020) 'Impact of hypoxia on carbon ion therapy in glioblastoma cells: Modulation by let and hypoxia-dependent genes', *Cancers*. 12(8), pp. 1–15. doi: 10.3390/cancers12082019.

Valdiglesias, V. *et al.* (2013) 'γH2AX as a marker of DNA double strand breaks and genomic instability in human population studies', *Mutation Research - Reviews in Mutation Research*, pp. 24–40. doi: 10.1016/j.mrrev.2013.02.001.

Valiathan, R., Ashman, M. and Asthana, D. (2016) 'Effects of Ageing on the Immune System: Infants to Elderly', *Scandinavian Journal of Immunology*. 83(4), pp. 255–266. doi: 10.1111/sji.12413.

Vandersickel, V. *et al.* (2010) 'Early Increase of Radiation-induced γ H2AX Foci in a Human Ku70/80 Knockdown Cell Line Characterized by an Enhanced Radiosensitivity', *Journal of Radiation Research*. 51(6), pp. 633–641. doi: 10.1269/jrr.10033.

Vandersickel, V. *et al.* (2014) 'Induction and disappearance of γ H2AX foci and formation of micronuclei after exposure of human lymphocytes to ^{60}Co γ -rays and $p(66)+\text{Be}(40)$ neutrons', *International Journal of Radiation Biology*. 90(2), pp. 149–158. doi: 10.3109/09553002.2014.860252.

Vandevoorde, C. (2015) *Biomarker investigation of the health effects of ct x-ray exposure in children*. Ghent University. Faculty of Medicine and Health Sciences. Available at: <http://hdl.handle.net/1854/LU-7248708> (Accessed: 6 November 2020).

Vandevoorde, C. *et al.* (2016) 'Radiation Sensitivity of Human CD34⁺ Cells Versus Peripheral Blood T Lymphocytes of Newborns and Adults: DNA Repair and Mutagenic Effects', *Radiation Research*, 185(6), pp. 580–590. doi: 10.1667/RR14109.1.

Vanegas, N. D. P. and Vernot, J. P. (2017) 'Loss of quiescence and self-renewal capacity of hematopoietic stem cell in an in vitro leukemic niche', *Experimental Hematology and Oncology*. 6(1), p. 2. doi: 10.1186/s40164-016-0062-1.

Vasilyev, S. A. *et al.* (2013) 'DNA damage response in CD133⁺ stem/progenitor cells from umbilical cord blood: Low level of endogenous foci and high recruitment of 53BP1', *International Journal of Radiation Biology*. 89(4), pp. 301–309. doi: 10.3109/09553002.2013.754555.

Verbiest, T. *et al.* (2018) 'Tracking preleukemic cells in vivo to reveal the sequence of molecular events in radiation leukemogenesis', *Leukemia*. 32(6), pp. 1435–1444. doi: 10.1038/s41375-018-0085-1.

Vernimmen, F. *et al.* (2018) 'Long-Term Follow-up of Patients Treated at a Single Institution Using a Passively Scattered Proton Beam; Observations Around the Occurrence of Second Malignancies', *International Journal of Radiation Oncology*Biophysics*, 103. doi: 10.1016/j.ijrobp.2018.10.022.

Visconti, R., Della Monica, R. and Grieco, D. (2016) 'Cell cycle checkpoint in cancer: A therapeutically targetable double-edged sword', *Journal of Experimental and Clinical Cancer Research*, p. 153. doi: 10.1186/s13046-016-0433-9.

Vral, A. *et al.* (1998) 'Apoptosis induced by fast neutrons versus ⁶⁰Co gamma -rays in human peripheral blood lymphocytes', *International Journal of Radiation Biology*. 73(3), pp. 289–295. doi: 10.1080/095530098142383.

Vral, A., Fenech, M. and Thierens, H. (2011) 'The Micronucleus Assay as a Biological Dosimeter of in Vivo Ionising Radiation Exposure', *Mutagenesis*. 26(1). doi: 10.1093/MUTAGE/GEQ078.

Wakeford, R. (2013) 'The risk of childhood leukaemia following exposure to ionising radiation - A review', *Journal of Radiological Protection*, pp. 1–25. doi: 10.1088/0952-4746/33/1/1.

Warren, L. A. and Rossi, D. J. (2009) 'Stem cells and aging in the hematopoietic system', *Mechanisms of Ageing and Development*. 130(1–2), pp. 46–53. doi: 10.1016/j.mad.2008.03.010.

van de Water, T. A. *et al.* (2011) 'The Potential Benefit of Radiotherapy with Protons in Head and Neck Cancer with Respect to Normal Tissue Sparing: A Systematic Review of Literature', *The Oncologist*. 16(3), pp. 366–377. doi: 10.1634/theoncologist.2010-0171.

Wei, Q. and Frenette, P. S. (2018) 'Niches for Hematopoietic Stem Cells and Their Progeny', *Immunity*. Cell Press, pp. 632–648. doi: 10.1016/j.immuni.2018.03.024.

Whitehead, T. P. *et al.* (2016) 'Childhood Leukemia and Primary Prevention', *Current Problems in Pediatric and Adolescent Health Care*. Mosby Inc., 46(10), pp. 317–352. doi: 10.1016/j.cppeds.2016.08.004.

WHO-ENHIS (2009) *Incidence of Childhood Leukemia*. Available at: www.euro.who.int/ENHIS (Accessed: 24 July 2018).

'WHO | Global Initiative for Childhood Cancer' (2018) WHO. World Health Organization. Available at: <http://www.who.int/cancer/childhood-cancer/en/> (Accessed: 24 November 2020).

Wiemels, J. (2012) 'Perspectives on the causes of childhood leukemia.', *Chemico-biological interactions*. 196(3), pp. 59–67. doi: 10.1016/j.cbi.2012.01.007.

Willems, P. *et al.* (2010) 'Automated micronucleus (MN) scoring for population triage in case of large scale radiation events', *International Journal of Radiation Biology*. 86(1), pp. 2–11. doi: 10.3109/09553000903264481.

- Wood, R. D. (2010) ‘Mammalian nucleotide excision repair proteins and interstrand crosslink repair’, *Environmental and molecular mutagenesis*, 51(6), pp. 520–526. doi: 10.1002/em.20569.
- Wu, W. S. *et al.* (2005) ‘Slug antagonizes p53-mediated apoptosis of hematopoietic progenitors by repressing puma’, *Cell*. 123(4), pp. 641–653. doi: 10.1016/j.cell.2005.09.029.
- Xu, X. *et al.* (2019) ‘Direct observation of damage clustering in irradiated DNA with atomic force microscopy’, *Nucleic Acids Research*, 48(3), pp. e18–e18. doi: 10.1093/nar/gkz1159.
- Yamada, T., Park, C. S. and Daniel Lacorazza, H. (2013) ‘Genetic control of quiescence in hematopoietic stem cells’, *Cell Cycle*. pp. 2376–2383. doi: 10.4161/cc.25416.
- Yao, G. (2014) ‘Modelling mammalian cellular quiescence’, *Interface Focus*. doi: 10.1098/rsfs.2013.0074.
- Yoo, Y. D. and Kwon, Y. T. (2015) ‘Molecular mechanisms controlling asymmetric and symmetric self-renewal of cancer stem cells’, *Journal of Analytical Science and Technology*. doi: 10.1186/s40543-015-0071-4.
- Young, N. A. and Al-Saleem, T. (2008) ‘Lymph Nodes: Cytomorphology and Flow Cytometry’, in *Comprehensive Cytopathology*. pp. 671–711. doi: 10.1016/B978-141604208-2.10024-7.
- Zhang, Yifan *et al.* (2018) ‘Hematopoietic Hierarchy – An Updated Roadmap’, *Trends in Cell Biology*. pp. 976–986. doi: 10.1016/j.tcb.2018.06.001.
- Zhang, Yingying *et al.* (2018) ‘Plasma membrane changes during programmed cell deaths’, *Cell research*. 2017/10/27. 28(1), pp. 9–21. doi: 10.1038/cr.2017.133.
- Zhao, X. *et al.* (2017) ‘Cell cycle-dependent control of homologous recombination’, *Acta Biochimica et Biophysica Sinica*. Oxford Academic, 49(8), pp. 655–668. doi: 10.1093/ABBS/GMX055.
- Zhao, Y., Wang, Y. and Ma, S. (2018) ‘Racial Differences in Four Leukemia Subtypes: Comprehensive Descriptive Epidemiology’, *Scientific Reports*. 8(1), pp. 1–10. doi: 10.1038/s41598-017-19081-4.
- Zhu, G., Song, L. and Lippard, S. J. (2013) ‘Visualizing inhibition of nucleosome mobility and transcription by cisplatin-DNA interstrand crosslinks in live mammalian cells’, *Cancer*

Research. 73(14), pp. 4451–4460. doi: 10.1158/0008-5472.CAN-13-0198.

Zilfou, J. T., Spector, M. S. and Lowe, S. W. (2005) ‘Slugging it out: Fine tuning the p53-PUMA death connection’, *Cell*. pp. 545–548. doi: 10.1016/j.cell.2005.11.003.



APPENDICES

APPENDIX 1

Ethical approval certificate for this study was granted by the Health Research Ethics Committee of Stellenbosch University (SU), Cape Town, South Africa.

APPENDIX 2

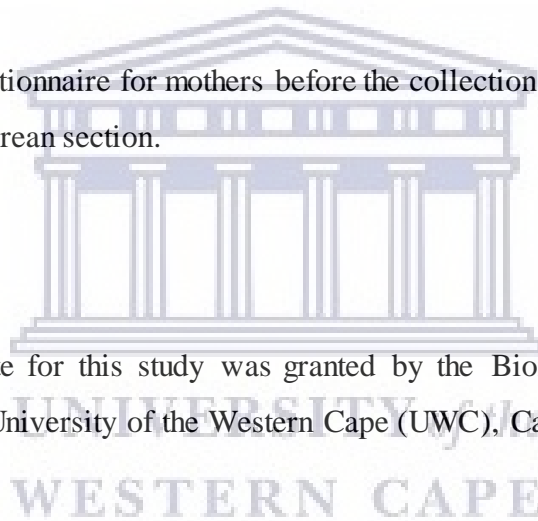
Informed consent and questionnaire for mothers before the collection of the UCB samples after a scheduled elective Caesarean section.

APPENDIX 3

Ethical approval certificate for this study was granted by the Biomedical Research Ethics Committee (BMREC) of University of the Western Cape (UWC), Cape Town, South Africa.

APPENDIX 4

Informed consent and questionnaire for adult donors.



APPENDIX 1



UNIVERSITEIT-STELLENBOSCH-UNIVERSITY
jou kennisvoort • your knowledge partner

Ethics Letter

09-Apr-2018

HREC Reference #: N16/10/134

Title: Radiation-induced leukaemia: response of CD34+ haematopoietic stem cells to clinical therapy beams

Dear Dr Charlot Vandevoorde,

Your request for extension/annual renewal of ethics approval dated 14 March 2018 refers.

The Health Research Ethics Committee reviewed and approved the annual progress report you submitted through an expedited review process.

The approval of the research project is extended for a further year.

Approval Date: 09 April 2018

Expiry Date: 08 April 2019

Kindly be reminded to submit progress reports two (2) months before expiry date.

Where to submit any documentation

Kindly note that the HREC uses an electronic ethics review management system, *Infonetica*, to manage ethics applications and ethics review process. To submit any documentation to HREC, please click on the following link: <https://applyethics.sun.ac.za>. Please note that you will first need to "update" the form in order to submit any annual progress report. Once the form has been updated, you can "create a sub-form" by selecting "HREC Progress/Final Report". You should also sign the form electronically in order for the form to be submitted for review.

Please remember to use your **Ethics Reference Number (N16/10/134)** on any documents or correspondence with the HREC concerning your research protocol and when you log into the *Infonetica* system.

National Health Research Ethics Council (NHREC) Registration Numbers: REC-130408-012 for HREC1 and REC-230208-010 for HREC2

Federal Wide Assurance Number: 00001372



Fakulteit Geneeskunde en Gesondheidswetenskappe
Faculty of Medicine and Health Sciences



Afdeling Navorsingsontwikkeling en -Steun • Research Development and Support Division

Posbus/PO Box 241 • Cape Town 8000 • Suid-Afrika/South Africa
Tel: +27 (0) 21 938 9677

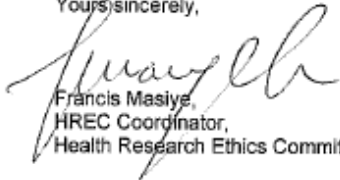


UNIVERSITEIT-STELLENBOSCH-UNIVERSITY
jou kennisentrum • your knowledge partner

Institutional Review Board (IRB) Number: IRB0005240 for HREC1
Institutional Review Board (IRB) Number: IRB0005239 for HREC2

The Health Research Ethics Committee complies with the SA National Health Act No. 61 of 2003 as it pertains to health research and the United States Code of Federal Regulations Title 45 Part 46. This committee abides by the ethical norms and principles for research, established by the Declaration of Helsinki and the South African Medical Research Council Guidelines as well as the Guidelines for Ethical Research: Principles, Structures and Processes 2015 (Department of Health).

Yours sincerely,


Francis Masiye,
HREC Coordinator,
Health Research Ethics Committee 2.



UNIVERSITY *of the*
WESTERN CAPE



UNIVERSITEIT-STELLENBOSCH-UNIVERSITY
Jan kennisvennoot • your knowledge partner

Ethics Letter

11-Apr-2019

HREC Reference #: N16/10/134

Title: Radiation-induced leukaemia: response of CD34+ haematopoietic stem cells to clinical therapy beams

Dear Dr Charlot Vandevoorde,

Your request for extension/annual renewal of ethics approval dated 25 March 2019 refers.

The Health Research Ethics Committee reviewed and approved the annual progress report you submitted through an expedited review process.

The approval of the research project is extended for a further year.

Approval date: 11 April 2019

Expiry date: 10 April 2020

Kindly be reminded to submit progress reports two (2) months before expiry date.

Where to submit any documentation

Kindly note that the HREC uses an electronic ethics review management system, *Infonetica*, to manage ethics applications and ethics review process. To submit any annual progress report to HREC for continuing review, please click on the following link: <https://applyethics.sun.ac.za>. Please note that you will first need to "update" the form in order to submit any annual progress report. Once the form has been updated, you can "create a sub-form" by selecting "HREC Progress/Final Report". You should also sign the form electronically in order for the form to be submitted for review.

Please remember to use your **Ethics Reference Number [N16/10/134]** on any documents or correspondence with the HREC concerning your research protocol.

National Health Research Ethics Council (NHREC) Registration Numbers: REC-130408-012 for HREC1 and REC-230208-010 for HREC2

Federal Wide Assurance Number: 00001372

Institutional Review Board (IRB) Number: IRB0005240 for HREC1

Institutional Review Board (IRB) Number: IRB0005239 for HREC2



STELLENBOSCH UNIVERSITY
Fakulteit Gesondheids- en Gesondheidswetenskappe
Health Research Ethics Committee

Faculty of Medicine and Health Sciences

11 APR 2019



Afdeling Navorsing en Opleiding: **STELLENBOSCH UNIVERSITY** Development and Support Division
Gesondheidsnavorsing Erekkomitee

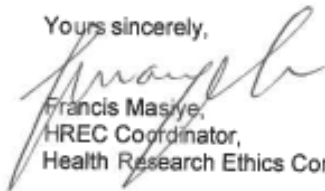
Postbus/PO Box 241 • Cape Town • 8000 • Suid-Afrika/South Africa
Tel: +27 (0) 21 938 9677



UNIVERSITEIT-SELLENBOSCH-UNIVERSITY
jou kennisvenoot • your knowledge partner

The Health Research Ethics Committee complies with the SA National Health Act No. 61 of 2003 as it pertains to health research and the United States Code of Federal Regulations Title 45 Part 46. This committee abides by the ethical norms and principles for research, established by the Declaration of Helsinki and the South African Medical Research Council Guidelines as well as the Guidelines for Ethical Research: Principles, Structures and Processes 2015 (Department of Health).

Yours sincerely,



Francis Masuye,
HREC Coordinator,
Health Research Ethics Committee 2.



UNIVERSITY of the
WESTERN CAPE



Fakulteit Geneeskunde en Gesondheidswetenskappe
Faculty of Medicine and Health Sciences



APPENDIX 2

PARTICIPANT INFORMATION LEAFLET AND CONSENT FORM

TITLE OF THE RESEARCH PROJECT: Radiation-induced leukaemia: response of CD34+ haematopoietic stem cells to clinical therapy beams

REFERENCE NUMBER: N16/10/134

PRINCIPAL INVESTIGATOR: Dr Charlot Vandevoorde

POSTAL ADDRESS:

P. O. Box 510

Somerset mall

7137

CONTACT NUMBER: 021 8431028

You are being invited to take part in a research project. Please take some time to read the information presented here, which will explain the details of this project. Please ask the study staff or doctor any questions about any part of this project that you do not fully understand. It is very important that you are fully satisfied that you clearly understand what this research entails and how you could be involved. Also, your participation is **entirely voluntary** and you are free to decline to participate. If you say no, this will not affect you negatively in any way whatsoever. You are also free to withdraw from the study at any point, even if you do agree to take part.

This study has been approved by the **Health Research Ethics Committee at Stellenbosch University** and will be conducted according to the ethical guidelines and principles of the international Declaration of Helsinki, South African Guidelines for Good Clinical Practice and the Medical Research Council (MRC) Ethical Guidelines for Research.

What is this research study all about?

This study will mainly be conducted at iThemba LABS, Faure. Umbilical cord blood samples collected at Tygerberg Hospital and Karl Bremer Hospital will be transported to iThemba LABS for the isolation of stem cells. In the first year of the project, 60 umbilical cord blood samples will be collected. The stem cells used in this project are blood forming stem cells that

give rise to all blood cells. In this research project we will study the biological response of the stem cells exposed to different types of radiation in order to gain a better insight in the origin radiation-induced blood cancer, also known as leukaemia.

Several studies have shown that radiation exposure increases the risk in both leukaemia incidence and mortality. Particularly children are at high risk. Since most leukaemias originate from the blood forming stem cells, we will use this type of stem cells present in umbilical cord blood to unravel the origin of radiation-induced leukaemia and to gain a better insight in the radiation response of the stem cells to different types of clinical therapy beams. This will help us to understand risk factors for radiation-induced leukaemia after childhood radiation exposure. However, the results will not only be valuable for children who undergo radiotherapy, it will also help us to establish a ratio of effectiveness of a specific type of radiation compared to a standard type of radiation known as gamma rays. This data will be used to optimize the protection of radiotherapy patients, but also astronauts and radiation workers. In this project, we will also investigate the influence of ethnicity and HIV status on the radiosensitivity of stem cells.

Why have you been invited to participate?

Currently, little is known about the radiosensitivity of stem cells and the origin of radiation-induced leukaemia. In order to obtain a better understanding of the underlying mechanisms and the biological response of stem cells exposed to different types of radiation, we would like to encourage you to participate in this study and donate umbilical cord blood for stem cell isolation. When the cord blood is not donated for this study, it will be considered as a leftover by-product of the birth process and be discarded as biological waste.

What will your responsibilities be?

After signing this informed consent form, you will donate 50 – 100 mL umbilical cord blood shortly after delivery of your baby. The collection will be performed by a well-trained individual and causes minimal risks. The umbilical cord blood sample will be transported to iThemba LABS, where stem cells will be isolated in the radiobiology laboratory. The stem cells will be stored at -80°C after isolation (for maximum 6 months) until beam time is available to perform the irradiations, followed by the radiosensitivity tests.

Will you benefit from taking part in this research?

If you participate in this study, the radiosensitivity of the stem cells of your child will be calculated by using sophisticated laboratory methods. Should you wish to be informed about the radiosensitivity of the cells of your child compared to the other study participants during the course of this project, this information will be given to you. The results of this study will help us to make better estimations of leukaemia risks for children exposed to radiation and to optimize radiotherapy treatment strategies.

Are there in risks involved in your taking part in this research?

Umbilical cord blood donation implies a minimal or no risk to the health of the mother and child. Cord blood will be collected just after delivery. In the first 24 h following childbirth, there is a risk of bleeding. Absolute priority and full attention will be given to the health of the mother and the child. In case there would be complications, the umbilical cord blood collection process will be interrupted and immediately stopped. The collection process will be performed by well trained personnel, in order to minimise the logistic burden of collection.

If you do not agree to take part, what alternatives do you have?

As previously stated, participation in this study is voluntary. If you decide not to participate in the study, the umbilical cord blood will be discarded as biological waste.

Who will have access to your medical records?

The information collected in this study will be protected and treated confidential. At the moment of cord blood collection, the sample will be coded in order to protect the identity of the participants. By applying a randomised coding procedure in which each identifying name is linked to a specific code, confidentiality will be ensured. The same code will be used to label all data samples in future experiments.

Only the principal investigator will have access to the list with codes, in order to consult the medical records to obtain the required information on ethnicity and HIV status.

What will happen in the unlikely event that some form injury occurred as a direct result of your participation in this research study?

The cord blood collection process will be performed by well trained personnel in a hospital environment, hence it involves minimal risks. The hospital is covered for malpractice and the

insurer will compensate you if the clinic or its staff is at fault.

Will you be paid to take part in this study and are there any costs involved?

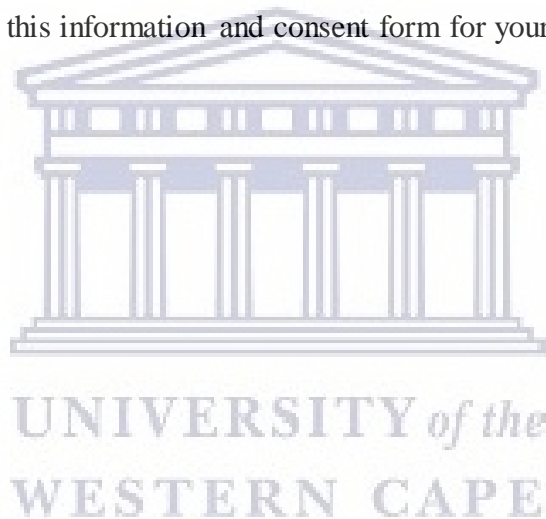
No, you will not be paid to take part in the study. There will be no costs involved for you if you take part in this study.

Is there anything else that you should know or do?

You can contact Dr Vandevoorde (iThemba LABS) at telephone number 021 843 1028 or Prof Botha, head of the Department of Obstetrics and Gynaecology at telephone number 021 9389209, if you have any further queries or encounter any problems.

You can contact the Health Research Ethics Committee at 021 9389075 if you have any concerns or complaints that have not been adequately addressed by your study doctor.

You will receive a copy of this information and consent form for your own records.



Declaration by participant

By signing below, I agree to take part in a research study entitled ‘Radiation-induced leukaemia: response of stem cells to clinical therapy beams’.

I declare that:

- I have read or had read to me this information and consent form. The document is written in a language which I understand and feel comfortable with.
- I have had a chance to ask questions and all my questions have been adequately answered.
- I understand that taking part in this study is **voluntary** and I have not been pressurised to take part.
- I may choose to leave the study at any time and will not be penalised or prejudiced in any way.
- I may be asked to leave the study before it has finished, if the study doctor or researcher feels it is in my best interests.

Signed at (*place*) on (*date*)

Signature of investigator

Signature of witness

Declaration by investigator

I (*name*) declare that:

- I explained the information in this document to
- I encouraged him/her to ask questions and took adequate time to answer them.
- I am satisfied that he/she adequately understands all aspects of the research, as discussed above
- I did/did not use an interpreter (*If an interpreter is used then the interpreter must sign*

the declaration below).

Signed at (*place*) on (*date*)

Signature of investigator

Signature of witness

Declaration by interpreter

I (*name*) declare that:

- I assisted the investigator (*name*) to explain the information in this document to (*name of participant*) using the language medium of Afrikaans/Xhosa.
- We encouraged him/her to ask questions and took adequate time to answer them.
- I conveyed a factually correct version of what was passed on to me.
- I am satisfied that the participant fully understands the content of this informed consent document and has had all his/her question satisfactorily answered.

Signed at (*place*) on (*date*)

Signature of interpreter

Signature of witness

PARTICIPANT SHORT QUESTIONNAIRE

TITLE OF THE RESEARCH PROJECT: Radiation-induced leukaemia: response of CD34⁺ haematopoietic stem cells to clinical therapy beams

REFERENCE NUMBER: N16/10/134

**PRINCIPAL INVESTIGATOR: Dr Charlot Vandevoorde
Ms Monique Engelbrecht**

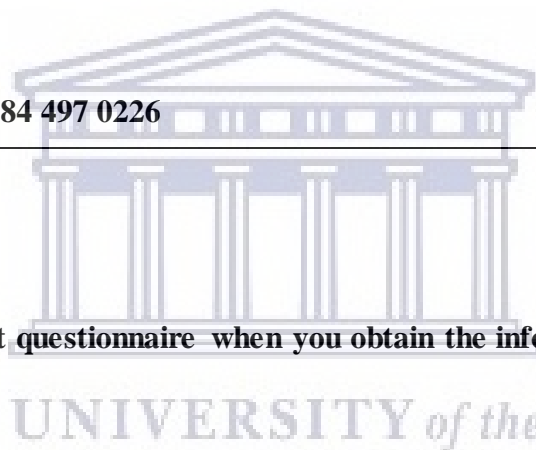
POSTAL ADDRESS:

**P. O. Box 510
Somerset mall
7137**

CONTACT NUMBER: 084 497 0226

Label:

Please complete this short questionnaire when you obtain the informed consent from the participant.



- **Race:** Black / White / Coloured / Indian / Other:.....

- **Age of the mother:**

- **Caesarean section:** Yes / No

- **HIV status** (only if the mother feels comfortable to reveal this):

Positive (+) or Negative (-)

- **Other communicable diseases?**

.....
.....
.....

- **Additional comments?**

.....
.....
.....

APPENDIX 3



UNIVERSITY of the
WESTERN CAPE



06 May 2020

Ms M Engelbrecht
Medical Biosciences
Faculty of Natural Sciences

Ethics Reference Number: BM20/3/5

Project Title: Radiation response of peripheral blood lymphocytes from healthy adult volunteers to different radiation qualities

Approval Period: 05 May 2020 – 05 May 2023

I hereby certify that the Biomedical Science Research Ethics Committee of the University of the Western Cape approved the scientific methodology and ethics of the above mentioned research project.

Any amendments, extension or other modifications to the protocol must be submitted to the Ethics Committee for approval.

Please remember to submit a progress report annually by 30 November for the duration of the project.

Permission to conduct the study must be submitted to BMREC for record-keeping.

The Committee must be informed of any serious adverse event and/or termination of the study.

A handwritten signature in black ink, appearing to read 'Josias'.

Ms Patricia Josias
Research Ethics Committee Officer
University of the Western Cape

Director: Research Development
University of the Western Cape
Private Bag X 17
Bellville 7535
Republic of South Africa
Tel: +27 21 959 4111
Email: research-ethics@uwc.ac.za

NHREC Registration Number: BMREC-130416-050

FROM HOPE TO ACTION THROUGH KNOWLEDGE.

APPENDIX 4



UNIVERSITY *of the* WESTERN CAPE

DEPARTMENT OF MEDICAL BIOSCIENCES
Private bag X 17, Bellville 7535, South Africa,
Telephone: (021) 959-2242/2433; Fax: (021) 9593125

BIOMEDICAL RESEARCH ETHICS COMMITTEE

BMREC, UWC, Tel: 021 959 4111, email: research-ethics@uwc.ac.za

Donor consent form

TITLE OF RESEARCH PROJECT:

Radiation response of peripheral blood lymphocytes from adult volunteers to different radiation qualities

Reference number: BM20/3/5

Principal Investigator: M. Engelbrecht

Address: iThemba LABS, P. O. Box 510, Somerset mall, 7137

Contact Number: 0218431028 or 0218431224

You are being invited to take part in a research project. Please ask the study staff or doctor any questions about any part of this project that you do not fully understand. It is very important that you are fully satisfied that you clearly understand what this research entails and how you could be involved. Also, your participation is entirely voluntary and you are free to decline to participate. You are also free to withdraw from the study at any point, even if you do agree to take part.

- Donation of blood for research or teaching is voluntary and you should not be placed under any pressure to donate.
- You do not have to agree to give a blood sample nor explain if you choose not to.
- Research participants have the right to refuse to participate because this study is voluntary.
- You will be explained what your blood will be used for before it is taken.

- Any personal information provided by you in connection with the donation will be held confidential.

What is this research study all about?

This study will mainly be conducted at iThemba LABS, Faure. Adults will donate blood voluntarily at the clinic at iThemba LABS by qualified nurse: Sr Yvette McDonald based at the iThemba LABS. The blood sample will be taken to the Radiobiology Section of the Nuclear Medicine Department at iThemba LABS for the isolation of lymphocytes. In the first year of the project, 60 blood samples will be collected. In this research project we will study the biological response of the lymphocytes isolated from adults exposed to different types of radiation in order to gain a better insight in the origin radiation-induced blood cancer in comparison with children (ethics approval: N16/10/134). Several studies have shown that radiation exposure increases the risk in both leukemia incidence and mortality. Particularly children are at high risk. This will help us to understand risk factors for radiation-induced leukemia after childhood radiation exposure.

Why have I been invited to participate?

In order to obtain a better understanding of the underlying mechanisms and the biological response of lymphocytes exposed to different types of radiation, we would like to encourage you to participate in this study and donate blood for lymphocyte isolation.

Who will contacted me to participate voluntarily?

An email will be distributed to ask employees at iThemba LABS to voluntarily participate in our study.

What will my responsibilities be?

After signing this informed consent form, you will donate 10 – 16 mL of blood. The lymphocytes will be stored at -80°C after isolation (for maximum 6 months) until beam time is available to perform the irradiations, followed by the radiosensitivity tests.

Are there in risks involved in taking part in this research?

Blood donation implies a minimal or no risk to the health of the volunteer. Absolute priority and full attention will be given to the health of volunteer. In case there would be complications, the blood collection process will be interrupted and immediately stopped. The collection

process will be performed by well trained personnel, in order to minimise the logistic burden of collection.

If I do not agree to take part, what alternatives do you have?

As previously stated, participation in this study is voluntary.

Who will have access to my medical records?

The information collected in this study will be protected and treated confidential. At the moment of blood collection, the sample will be coded in order to protect the identity of the participants. By applying a randomised coding procedure in which each identifying name is linked to a specific code, confidentiality will be ensured. The same code will be used to label all data samples in future experiments. Only the principal investigator will have access to the list with codes, in order to consult the medical records to obtain the required information on ethnicity and HIV status.

Will I be paid to take part in this study and are there any costs involved?

No, you will not be paid to take part in the study. There will be no costs involved for you if you take part in this study.

For reasons of safety, you should not donate if you:

- know you are, or think you might be, infected with Hepatitis B or Hepatitis C
- are unwell at the moment
- are anaemic or receiving treatment for anaemia or iron deficiency
- have given a blood donation in the last month (e.g. Western Province Blood Transfusion Services), if more than 100 mL is requested.

What should I do if I have questions about this research?

If you have any questions about the research project you can contact Prof Maryna de Kock (UWC), Tel +27 21 959 2242; email: mdekock@uwc.ac.za or Dr Charlot Vandevoorde at iThemba LABS Radiobiology lab +27 21 843 1028; email: cvandevoorde@tlabs.ac.za.

Who should I contact to report any problems that I encounter with this research besides the researcher?

You can contact the UWC secretary to Science Administrative Forum, Tel +27 21 959 3136, email: nisaacs@uwc.ac.za and request to contact the members of the Ethics and Research Committee of UWC; or UWC Research Office, tel +27 21 959 2949.





UNIVERSITY of the WESTERN CAPE

**DEPARTMENT OF MEDICAL BIOSCIENCES
Private bag X 17, Bellville 7535, South Africa,
Telephone: (021) 959-2242/2433; Fax: (021) 9593125**

BIOMEDICAL RESEARCH ETHICS COMMITTEE

BMREC, UWC, Tel: 021 959 4111, email: research-ethics@uwc.ac.za

Donor consent form

TITLE OF RESEARCH PROJECT:

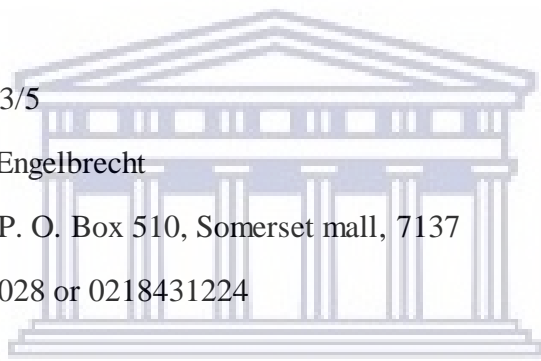
Radiation response of peripheral blood lymphocytes from adult volunteers to different radiation qualities

Reference number: BM20/3/5

Principal Investigator: M. Engelbrecht

Address: iThemba LABS, P. O. Box 510, Somerset mall, 7137

Contact Number: 0218431028 or 0218431224



**UNIVERSITY of the
DONOR DETAILS:
WESTERN CAPE**

UNIVERSITY of the DONOR DETAILS: WESTERN CAPE					
Name & Surname:					
Sex: (Please circle)		Male		Female	
Date of Birth:					
HIV Status (only if you feel comfortable to reveal this):		Positive		Negative	
Other communicable diseases/chronic medication?					
Additional comments? History of cancer/radiotherapy?					

<p>.....</p> <p>.....</p>	
I have been informed of the following:	
The quantity of blood to be taken (10ml)	
The frequency of blood donations (once only)	
The radiosensitivity tests that will be performed on my blood sample	YES / NO
I agree that the samples can be stored for possible further use in future	YES / NO
<p>By signing below, I agree to take part in a radiobiology research study.</p> <p>I declare that:</p> <p><input type="checkbox"/> I have had a chance to ask questions and all my questions have been adequately answered.</p> <p><input type="checkbox"/> I understand that taking part in this study is voluntary and I have not been pressurised to take part.</p> <p><input type="checkbox"/> I may choose to leave the study at any time and will not be penalised or prejudiced in any way.</p>	
Donor signature:	Date:
Signature of person taking blood:	Date:
Signature of researcher:	Date: